MONASH University

Development of chitosan/ alginate/ AgNP membrane for decentralized greywater treatment

Oh Kai Siang
Bachelor (Hons) of Engineering

A thesis submitted for the degree of *Doctor of Philosophy* at
Monash University in *2016*

Doctor of Philosophy

Copyright notice

Abstract

Rapid development and worldwide industrialization have caused severe impact to the fresh water bodies. Cases of water scarcity and pollutions reported worldwide drew attention of researchers to reduce water stress and seek for alternative water sources. Thus, greywater recycling is gaining impetus as the solution to curb this issue. However, greywater treatment is essential to remove pollutants and pathogens prior reuse as these will pose health risks to those in contact with greywater. In this study, membrane technology that is simple and compact was investigated as a process for application in a decentralized greywater recycling system to encourage wider implantation in Malaysia. A membrane comprising of anti-microbial biopolymers (chitosan and alginate) and a heavy metal biocide (AgNP) was developed and tested to conduct greywater treatment and disinfection in a single membrane filtration unit. The formation of polyelectrolyte complex (PEC) between the two biopolymers reduced the membrane molecular weight cut-off (MWCO) of a 242 kDa chitosan membrane to 3800 Da in the 2A1CP polyelectrolyte bilayer membrane (PCBM). However, the dense layer of alginate formed on the chitosan membrane and decline of MWCO caused the ultrapure water flux of the dense PCBM to be severely reduced. Therefore, 2A1CP was further modified with porogen on the alginate layer to improve the water flux. The modification caused the water flux of porous 2AP1CP PCBM to increase by 60% as compared to the dense 2A1CP PCBM. The 2AP1CP PCBM was capable of removing 99.8% turbidity, 99.5% total suspended solid (TSS), 81.5% chemical oxygen demand (COD), 96.9% 5-days biological oxygen demand (BOD_5), 2.6-log of Escherichia coli (E. coli) and

2.93–log of other coliforms in greywater. In addition, the disinfection efficiency of 2AP1CP membrane was enhanced when increasing concentration of AgNP was incorporated into the membrane. The membrane can remove up to 3.6-log Escherichia coli (E. coli) and 3.7-log other coliforms with 1.5 ppm AgNP loaded into the alginate layer. The increase in the bacteria removal efficiency was found to be attributed to the additional contact-killing mechanism of AgNP in the membrane structure. The 1.5 ppm AgNP PCBM was subsequently installed in a decentralized greywater treatment system to evaluate its long-term treatment performance in a greywater treatment system. The fresh 1.5 AgNP PCBM could produce 1125 L $m^{-2}day^{-1}$ at 3 bar (g) and 446 L $m^{-2}day^{-1}$ without pumping. The membrane flux reduced over two weeks of operating the system. The analysis on flux profiles showed that flux decline was mainly due to intermediate pore blocking and cake formation mechanisms. However, flux decline could be resolved with proper maintenance and membrane cleaning. In conclusion, this research contributes to the development of a membrane specialized for greywater treatment and the decentralized greywater treatment system could help to conserve freshwater, especially in arid countries. Furthermore, development of a biopolymeric membrane helps to reduce secondary waste generation from the disposal of used membranes from greywater treatment. In the future, the application of such system could be extended to treat other sources of wastewater to further increase the recycling capacity and reduce freshwater consumption.

Declaration

This thesis contains no material which has been accepted for the award of any other degree or diploma at any university or equivalent institution and that, to the best of my knowledge and belief, this thesis contains no material previously published or written by another person, except where due reference is made in the text of the thesis.

Publications during enrolment

Journals

Oh, K.S., Poh, P., Chong, M.N., Gouwanda, D., Lam, W. and Chee, C. (2015) Optimizing the in-line ozone injection and delivery strategy in a multistage pilot-scale greywater treatment system: System validation and cost-benefit analysis. Journal of Environmental Chemical Engineering 3(2), 1146-1151.

Oh, K.S., Poh, P.E., Chong, M.N., Chan, E.S., Lau, E.V. and Saint, C.P. (2016) Bathroom greywater recycling using polyelectrolyte-complex bilayer membrane: Advanced study of membrane structure and treatment efficiency. Carbohydrate Polymers 148, 161-170.

Oh, K.S., Poh, P.E., Chong, M.N. 'PEG-modified chitosan membrane for bathroom greywater treatment'. (Submitted to Chemical Engineering Journal)

Oh, K.S., Poh, P.E., Chong, M.N. 'Enhancement of a Polyelectrolyte Complex Bilayer Membrane (PCBM) with polyethylene glycol for effective greywater treatment and recycling'. (Submitted to Water Research)

Oh, K.S., Janet Leong, Y.C., Poh, P.E., Chong, M.N., Lau, E.V. 'Towards a Sustainable Urban Greywater Management: A review on greywater recycling and reuse issues in Malaysia'. (Submitted to Journal of Environmental Management)

Oh, K.S., Poh, P.E., Chong, M.N., 'Silver nanoparticle (AgNP) Polyelectrolyte Complex Bilayer Membrane (PCBM) for greywater recycling system' (Under preparation)

Patent

Poh, P.E., Oh, K.S., Chong, M.N. TEEIP:2016/UI/P2.18/OP: "A System for Treatment of Greywater", Application number: UI 2016703927. (Application filed in Intellectual Property Corporation of Malaysia on 26 October 2016)

Book chapter

Oh, K.S., Poh, P.E., Chong, M.N., 'Greywater treatment and disinfection technology. Alternative Water Supplies: An integrated approach'. Springer Publishing - Water Resources Management Series (Under preparation)

Conference abstract

Oh, K.S., Poh, P.E., Chong, M.N. (2014) 'Effect of Polyethylene Glycol (PEG) Concentration on Filtration Performance of Chitosan Membrane for Decentralized Greywater Treatment'. In: IWA 7th International Young Water Professional (YWP) Conference, 2014, Taipei, Taiwan. (From 7-11 December 2014)

Oh, K.S., Poh, P.E., Chong, M.N. (2016) 'Greywater treatment using alginate/chitosan membrane: Effect of alginate/ PEG concentration on treatment performance'. In: 9th International Conference on Fiber and Polymer Biotechnology (IFPB), 2016, Osaka, Japan. (From 7-9 September 2016)

Acknowledgement

First of all, I would like to sincerely thank my main supervisor, Dr. Poh Phaik Eong for her guidance and supervision throughout my studies. I would also like to express my deepest gratitude for her effort to review and comment on my thesis write-up. This research work would not be completed on time without her great support and supervision.

I would also like to extend my gratitude to my co-supervisor, Dr. Chong Meng Nan, for his contribution in this research project by providing guidance and advice in publishing research papers and providing me an opportunity to contribute in a book chapter.

Also, appreciation goes to Monash University Malaysia for providing full financial support to fund my research project. The lab technicians also played an important role in my PhD studies to provide assistance and training while experimental studies were conducted in the lab.

I would like to also thank my friends, for their endless love, understanding, encouragement and companion during my PhD studies. Last but not least, this thesis is dedicated to my family. A big thank you to my parents and siblings for their unconditional love and support in my life.

Table of Contents

List of tables

List of figures

List of symbols

Symbols	Description	Unit
A	Cross-sectional area of the membrane	m^2
A_e	Effective area of membrane	m^2
C_f	Final concentration	mg L^{-1}
C_i	Initial concentration	mg L^{-1}
DO_f	Final dissolved oxygen concentration	mg L^{-1}
DO_i	Initial dissolved oxygen concentration	mg L^{-1}
F_l	Maximum force required to break the membrane sample	N
J	Flux of solution	L m^{-2} hr^{-1}
J_o	Initial flux	L m^{-2} hr^{-1}
k	Mass transfer coefficient	ms^{-1}
LRV	Log removal value	Log
$M_{permeate}$	Mass of permeate collected	grams
P	Fraction of sample volume divided by total volume	Dimensionless
t	Duration of the filtration	hours

Symbols	Description	Unit
$V_{permeate}$	Volume of permeate collected	L
W_{dry}	Weight of dry membrane	g
W_{wet}	Weight of wet membrane	g

List of abbreviation

Abbreviation	Full name
Ac	Acetic acid
AgNP	Silver nanoparticle
Alg	Sodium alginate
Alg/ PEG	Alginate + PEG
BAF	Biological Aerator Floatation
BOD	Biological oxygen demand
COD	Chemical oxygen demand
COD vials	COD digestion vials (LR) and (HR)
CS	Chitosan
CS/ PEG	Chitosan + PEG
DGTS	Decentralized greywater treatment system
DI	De-ionized
DNA	Deoxyribonucleic acid
E. coli	*Escherichia coli*
EMC	Equilibrium Moisture Content
FA	Formic acid

Abbreviation	Full name
FO	Forward osmosis
FTIR	Fourier transform infrared spectroscopy
FU	Functional unit
GA	Glutaraldehyde
GWP	Global warming potential
HDPE	High density polyethylene
HRT	Hydraulic retention time
LCA	Life cycle assessment
LDPE	Low density polyethylene
LRV	Log removal value
MBR	Membrane bioreactor
MCC	Microcrystallized Cellulose
MF	Microfiltration
MWCO	Molecular weight cut-off
NaOH	Sodium hydroxide
NCC	Nanocrystallized Cellulose
NF	Nanofiltration

Abbreviation	Full name
P-1000	Poly (ethylene) glycol, Mw = 1000
P-10000	Poly (ethylene) glycol, Mw = 10000
P-100000	Poly (ethylene) oxide, Mw = 100,000
P-350000	Poly (ethylene) oxide, Mw = 350,000
P-200	Poly (ethylene) glycol, Mw = 200
P-2000	Poly (ethylene) glycol, Mw = 2000
P-3000	Poly (ethylene) glycol, Mw = 3000
P-400	Poly (ethylene) glycol, Mw = 400
P-600	Poly (ethylene) glycol, Mw = 600
P-6000	Poly (ethylene) glycol,Mw = 6000
PCBM	Polyelectrolyte complex bilayer membrane
PE	Polyethylene
PEC	Polyelectrolyte complex
PES	Polyether-sulphone
PFD	Process flow diagram
PI	Propedium iodide
PP	Polypropylene

Abbreviation	Full name
PS	Polystyrene
PVA	Polyvinyl alcohol
PVC	Polyvinyl chloride
PVDF	Polyvinylidene fluoride
RBC	Rotary Biological Contactor
RNA	Ribonucleic acid
RO	Reverse osmosis
SEM	Scanning electron microscope
TEM	Transmission electron microscopy
TGA	Thermagravimetry analysis
TOC	Total organic carbon
TPP	Sodium tripolyphosphate
TSS	Total suspended solid
UF	Ultrafiltration
UK	The United Kingdom
UP water	Ultrapure water
US EPA	United States Environmental Protection Agency

Abbreviation	Full name
USA	The United States
UV	Ultraviolet

CHAPTER 1

1 Introduction

Water is vital to sustain life on earth. Over the past decades, rapid industrialization and development have led to several environmental issues including climate change, severe water pollution and shortage issues (Chen & Ngo et al., 2013; Jury & Vaux, 2007). The problem becomes more apparent in arid regions in the world, where freshwater source is limited. In addition, urban areas with dense population and area of houses with large gardens are usually associated with high freshwater demand (Domene & Saurí, 2006). This is mainly attributed to the high volume of freshwater consumption for daily usage and huge area of garden watering (Domene & Saurí, 2006) . Likewise, Malaysia has undergone rapid developments in recent years (Chan, 2005). The water level of many river beds in Malaysia have risen due to extensive drainage basin development for large-scale projects, resulting in a higher likelihood of flooding and reduced volumes of clean water (Ho, 1996). Therefore, large amounts of freshwater were lost due to vast urbanization with limited clean water sources for consumption despite high rainfall in Malaysia. Many water sensitive countries ventured into greywater recycling as a measure to curb water scarcity (Pham & Ngo et al., 2011). For instance, United States of America (USA), Australia and Japan have long practiced greywater recycling to relief water scarcity in their countries (Christova-Boal, 1995; Dixon & Butler et al., 1999; Ryan & Spash et al., 2009).

1.1 Greywater

Greywater is a fraction of domestic wastewater, which originates from laundry, kitchen, bathroom, sink, and washbasin (Pidou & Memon et al., 2007). Unlike blackwater (toilet wastewater), greywater contains lower organic matters and pathogens. This is due to the fact that greywater does not contain heavy excrement and urines that are present in blackwater (Thakur & Chauhan, 2013). Figure 1.1 shows the average distribution of household water end-uses for 1792 families in Malaysia. Malaysia was documented to consume freshwater of approximately 226 L/person/day (FOMCA, 2010). This water consumption is much higher as compared to its neighbouring countries such as Thailand (90 L/person/day) and Singapore (155 L/person/day) (Choong, 2011; Ho, 1996). Based on Figure 1.1, 67 % of potable water in Malaysia is used for toilet flushing, showering and washing the laundry (FOMCA, 2010; Ho, 1996). The remaining activities that use potable water are gardening, car washing, outdoor activities, bath and household cleaning, while 15 % of water is lost due to pipe leakage, which is normally undetected after long periods of time (FOMCA, 2010; Ho, 1996). According to the water usage percentage in Malaysia, 43 % ended up as greywater, equivalent to the greywater generation of 97.18 L/person/day. In comparison, UK was reported to generate a slightly lower volume of 88.37 L/person/day of greywater (Liu & Butler et al., 2010).

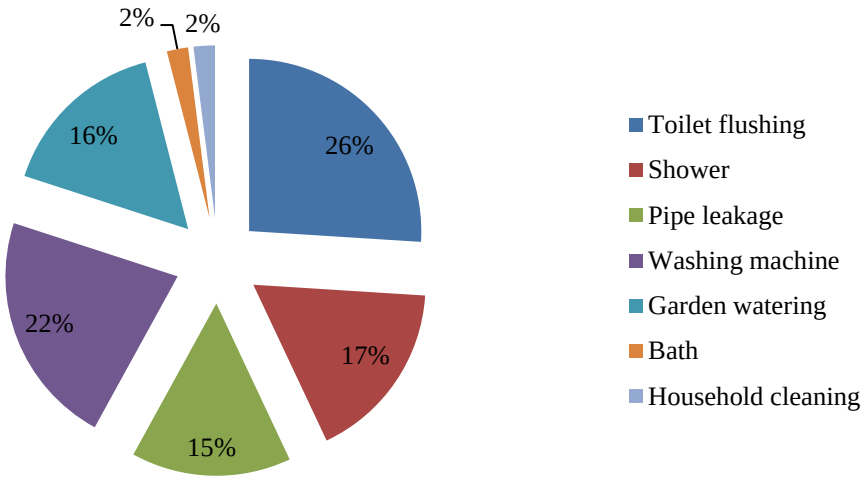

Figure 1.1 Average water usage distribution (%) of 1792 families in Malaysia (FOMCA, 2010)

Non-potable household activities, such as toilet flushing and garden irrigation usually requires huge amount of freshwater. Studies have showed that recycling greywater for garden irrigation and toilet flushing could save 30-50 % of potable water (Al-Jayyousi, 2003; Eriksson & Auffarth et al., 2002; Gross & Shmueli et al., 2007; Prathapar & Jamrah et al., 2005). Thus, there is an opportunity for Malaysia to implement greywater treatment and implement for non-potable end-uses as vast amount of freshwater can be conserved for consumption to overcome water scarcity issues in many areas worldwide (Al-Jayyousi, 2003; Boyjoo & Pareek et al., 2013a; Chen & Ngo et al., 2012).

Despite low organic pollutants and pathogens contaminations in greywater, it still contains microorganisms such as *E. coli* and *Enterococci* due to the presence of trace amount of urine and feces from shower (Donner & Eriksson et al., 2010). Total coliforms and feacal coliforms are also key contributors to biological pollutants in the greywater (Widiastuti & Wu et al., 2008). These

pathogens in the greywater risk human health when the reclaimed water comes into contact with human via activities such as toilet flushing and irrigation (Chaillou & Gérente et al., 2011). Hence, greywater needs to be treated appropriately to ensure that it is safe for reuse. In general, pollutants of sizes range between 0.001 μm to 100 μm in wastewater are the major constituents that need to be removed in the treatment process (Chen & Mou et al., 2008).

1.2 Greywater treatment technology

Treatment of greywater encompasses of several processes, namely physical, chemical, biological and extensive treatment. In greywater treatment process, coarse particles such as, sand, stones, debris, hair, leaves, dust and etc. will first be removed. The pre-treated greywater will then be transferred to the next treatment unit to remove suspended solids, organic matters, and the treatment ends with disinfection for bacteria eradication. Table 1.1 summarizes the type of treatment technologies that is currently adopted for greywater treatment.

Table 1.1. Greywater treatment technologies (Birks & Colbourne et al., 2004; Gilboa & Friedler, 2008; Nolde, 2005; Pidou & Memon et al., 2007; Tchobanoglous & Burton, 1991).

Category	Type of treatment
Biological treatment	Biological Aerator Floatation (BAF)
	Rotary Biological Contactor (RBC)
	Membrane bioreactor (MBR)
Physical treatment	Coarse filter
	Sand filter
	Membrane
Chemical treatment	Electrocoagulation
	Photocatalysis
	Coagulation
	Disinfection
Wetland/ Ponding	Reed bed
	Ponds

MBR is considered as one of the most commonly used biological treatment technologies for greywater. This is due to the fact that MBR is capable of removing organic matters and at the same time eradicating pathogenic bacteria from greywater (Li & Wichmann et al., 2009). MBR was found to be able to remove at least 86% of COD in greywater (Liu & Huang et al., 2005). On the other hand, coagulation process is regarded as one of the common chemical treatment technologies. Previous study showed that faecal coliform concentration in treated greywater was below detection limit and 64% of COD was removed using aluminum salt as the coagulant (Pidou & Avery et al., 2008). However, the treated greywater did not meet the reuse standard in terms of turbidity. On the other hand, greywater treatment using membrane technology usually produces treated greywater that is free of suspended solids and turbidity. It was found that direct filtration using only ultrafiltration (UF) membrane could remove up to 83% of TOC, 100% of suspended solids, turbidity and *E. coli* (Li & Behrendt et al., 2008).

Unlike countries that recycle greywater, greywater is treated together with blackwater in a centralized treatment facility in Malaysia. Wastewater is first collected in a septic tank and transferred to the centralized treatment facility before discharging to the surrounding. Aerobic treatment processes such as, extended pond, tickling filter activated sludge, aerated lagoons, RBC, submerged biological contactor and etc. are mainly adopted for wastewater treatment in Malaysia (IWK, 2016). This is mainly due to the fact that these systems is suitable for medium to high strength wastewater, and it is managed to remove huge portion of organic matters present in the wastewater (Li & Wichmann et al., 2009).

1.3 Problem statement and proposed solution

In order for effective greywater recycling and reuse to happen in Malaysia, greywater should be treated separately in a decentralized system. This is due to the fact that transferring the wastewater to a centralized treatment system is associated to high energy consumption and piping cost (Massoud & Tarhini et al., 2009). Furthermore, treatment of greywater in a decentralized system can also reduce the burden of existing sewage treatment plants due to increasing urban population in major cities in Malaysia.

Amongst the treatment technologies available, membrane treatment system that can achieve high treatment efficiency while having low space requirements (Chen & Mou et al., 2008) has the potential to be developed for decentralized greywater treatment system. This is due to the fact that membrane technology is the most effective, simplified and direct technology that can be employed for separating pollutants and water molecules of different in particle sizes with the use of physical barrier (Hourlier & Masse et al., 2010). In fact, membrane can be used effectively for the treatment of low strength wastewater (eg. greywater) but not for the treatment of high strength wastewater due to the formation of filtered cake, which reduces the filtration efficiency.

Membranes are conventionally produced from synthetic polymers, such as cellulose acetate, cellulose nitrates, polyamide, polysulphone, poly (ether sulphone), polycarbonate, poly (ether imide), poly (vinylidene fluoride), polytetrafluoroethylene, polypropylene and polyacrylonitrile (Chen & Mou et al., 2008; Geise & Lee et al., 2010; Wang, 2011). The use of synthetic polymers membrane is more common as these polymers have satisfactory mechanical strength, thermal and chemically stable over a wide range of pH (Ren & Wang, 2008). However, synthetic polymers are

derived from fossil resources. This draws concern on the impacts of these materials on the environment. Besides that, regeneration or replacement of new membrane is necessary when the membrane is worn-off to retain the process efficiency. As most of these synthetic polymers are non-biodegradable, the disposal of membranes will lead to the massive production of secondary waste with wide scale implementation of membrane filtration technology (Gross & Kalra, 2002; Lu & Xiao et al., 2009). Therefore, biodegradable and renewable polymers could be an alternative to overcome the constraints of synthetic polymeric membranes to encourage the adoption of membrane filtration system for greywater recycling. Since the use of biopolymeric membrane for greywater treatment is scarce, especially a biopolymeric membrane with filtration and disinfection functions, this study proposes the development of a dual-functional biopolymeric membrane consisting of biopolymers and bacteria biocide.

Owing to the dissolution of chitosan (D-glucosamine and N-acetyl-D-glucosamine) in mild acidic solvent, chitosan can be structured into various shapes (eg. fiber, bead, film, membrane) depending on its respective applications (Ageev & Matushkina et al., 2007; de Alvarenga, 2011b). Derived from de-acetylation of biopolymer chitin, chitosan was found to exhibit anti-microbial property (Mello & Bedendo et al., 2006; Regiel & Irusta et al., 2012). In the medical application, chitosan is utilized as a contact-killing film to avoid the growth of the bacteria (Cui & Szarpak et al., 2010). The proposed mechanism of the antimicrobial effect indicated that the anti-microbial surface provides resistance to the approaching bacteria or disturbing the bacteria's metabolism, eventually lead to cell fatality (Hasan & Crawford et al., 2013; Wang & Liu et al., 2012). In addition to that, chitosan membrane was utilized in pervaporation technology due to its chemical, mechanical stability and hydrophilicity (Huang & Pal et al., 2000). Therefore, it is proposed to

utilize chitosan as a backbone to the greywater filtration membrane in this study. However, owing to the pK_a of chitosan ≈ 6.3, the structure of chitosan membrane could become unstable and soluble when the pH of the greywater is lower than pH 6.0 (Pillai & Paul et al., 2009).

Thus, alginate/ alginic acid (β-D-mannuronic acids and α-L-guluronic acids) was proposed to be incorporated to the membrane to improve the stability of the membrane. Alginate is mainly extracted from brown algae (Bayer & Herrero et al., 2011). Due to the naturally occurring poly-anionic property of alginate, it can couple with poly-cationic chitosan to form insoluble polyelectrolyte complex (PEC) (Moon & Pal et al., 1999; Sharma & Sanpui et al., 2012b). Study showed that membrane stability towards changes in pH was improved through the formation of PEC between chitosan and alginate (Khor & Lim, 2003). Furthermore, the overall water flux of the membrane could be enhanced with the formation of PEC between chitosan and alginate attributed to the superior water selectivity of alginate (Huang & Pal et al., 2000). Due to the fact that formation of PEC involves interaction between amide groups in chitosan and carboxyl anions in alginate, it could hinder the anti-microbial property of chitosan and alginate caused by reduction of functional groups that are responsible for the anti-microbial effect.

As a result, silver nanoparticle (AgNP) could be incorporated during the fabrication of membrane to enhance the anti-microbial property of the membrane. Similar to the biopolymers aforementioned, it was found that heavy metal ion can be used to attack microorganisms to cause failure in the cell nutrient uptake (Lin & Vidic et al., 1996). This would upset the cell and eventually create a pathway for the entrance of heavy metal ions into the cell of the microorganism. Other than that, the heavy metal ions cause stronger disturbance to the cells through binding to the DNA and RNA of the cell which ultimately immobilizes the bacteria cells (Lin & Vidic et al.,

1996). The silver ions could also attack the enzymes of the bacteria, where the sulfhydryl group in the cell will bond with the silver ions to form silver sulfides or sulfhydryl-binding property which disrupt and disable protein and enzymes activity (Semikina Anna & Skulacher Vladimr, 1990; Shrestha & Joshi et al., 2009).

The combination of biopolymers and AgNP as alternative materials to fabricate the membrane could compliment the greywater treatment technology by having biodegradable and renewable membrane. However, as biopolymers are rarely used in wastewater filtration due to its originally dense structure and mechanical weakness (Ghaee & Shariaty-Niassar et al., 2013), the performance of biopolymers in greywater filtration was not thoroughly investigated. The mechanisms of biopolymeric membrane on pollutants removal (eg. size exclusion and disinfection) of greywater were also yet to be evaluated. Understanding of the pollutant removal mechanism is essential to devise proper operating procedures for greywater treatment using the biopolymeric membrane.

1.4 Research objectives

The main objective of this research is to develop a decentralized greywater treatment system using a novel dual layer biopolymeric membrane. The detailed objectives of this research are listed as follow:

- To develop a dual layer biopolymeric membrane consisting of chitosan, alginate and AgNP for decentralized greywater treatment

- To modify dual layer biopolymeric membrane to achieve greywater reuse standard of turbidity < 5 NTU, BOD_5 < 20 ppm and non-detectable level of *E. coli* and coliform bacteria and to study the characteristics of modified membrane structure before and after treatment.

- To evaluate the anti-microbial effect and rejection efficiency of the dual layer biopolymeric membrane on greywater filtration.

- To design an integrated lab-scale decentralized greywater treatment system and evaluate the treatment efficiency and flux decline mechanism of the dual layer biopolymeric membrane, on greywater treatment.

- To perform life cycle assessment on the dual layer biopolymeric membrane and to compare with conventional synthetic polymer membrane.

1.5 Scope of research

In this research, a novel biopolymeric greywater treatment membrane was carefully designed using chitosan, alginate and AgNP. This membrane provides an alternative to the current use of synthetic polymer for greywater treatment. The utilization of this biopolymeric based membrane can contribute to lowering environmental impacts by conserving freshwater sources and eliminate the use of synthetic polymers during greywater treatment.

The different phases of this research are focused on the development of dual layer biopolymeric membrane to investigate on filtration efficiency, water flux, and disinfection efficiency to meet the greywater reuse standards established in Canada and Australia (Chaillou &

Gérente et al., 2011; Couto & Calijuri et al., 2015). Due to the fact that coupling biopolymers with synthetic polymer could lead to changes in properties and biodegradability of biopolymers (Moore, 2008), the membrane was first designed using only chitosan as the core structure. Further development includes the incorporation of thin layer of alginate to form PEC structure. The formation of PEC could also lead to the reduction in membrane MWCO that enhanced the filtration efficiency. Lastly, AgNP was integrated to the membrane structure to further enhance its disinfection efficiency to ensure complete eradication of harmful bacteria from the greywater.

The membranes developed at each phases were characterized based on changes to membrane surface water contact angle, swelling ratio, molecular structure and physical structure. In addition, changes in other properties such as water flux based on various operating pressure and MWCO of the membrane were also carefully monitored at each phases of the research.

Subsequently, treatment efficiency of the dual layer biopolymeric membrane on bathroom greywater was studied. The bathroom greywater and treated greywater were analysed to identify effect of the changes in the membrane structure on greywater treatment efficiency. The treated greywater was treated to meet the greywater reuse standard of turbidity < 5 NTU, BOD_5 < 20 ppm and non-detectable pathogenic bacteria.

Last but not least, a greywater treatment system using the biopolymeric based membrane was designed and fabricated to evaluate on the greywater treatment efficiency of the membrane on a larger scale. In addition, the disinfection and flux decline mechanism of this membrane was also investigated using the fabricated greywater treatment system. Life cycle assessment (LCA) was

also conducted to evaluate the possible environmental impacts associated with using this membrane as compared to the synthetic polymer membrane.

1.6 Organization of thesis

This thesis consists of five main chapters. Chapter 1 is an introduction to the topic of interest, highlighting the environmental issues that the world is facing, especially freshwater scarcity and water shortage. As a result, it is crucial to promote water recycling to relief the water stress level across the globe. Reuse of greywater from households in non-portable purposes such as toilet flushing and garden irrigation could help to conserve the freshwater uptake. This chapter also draws attention on the issues that need to be addressed to promote effective greywater recycling, followed by the research objectives and scope of this project.

Chapter 2 consists of a critical review on several aspects that are crucial to the formation of research problems and objectives. The topic covers in this chapter includes the characteristics of greywater and its treatment technologies. Besides that, the pros and cons of centralized and decentralized wastewater recycling systems are evaluated. Subsequently, the chapter also emphasizes on the mechanism of various membrane technologies in removing pollutants and its fouling mechanisms. The conventional materials that are used to fabricate membrane are critically reviewed. On top of that, the characteristics and existing applications of biopolymers in wastewater treatment, such as chitosan and alginate are discussed. The feasibility of biopolymeric materials to be made as greywater recycling membrane is also covered in this chapter. Last but not least, the chapter discussed on the property and role of AgNP in greywater treatment and the benefits of AgNP in greywater treatment.

Chapter 3 lists the materials that were utilized throughout the duration of this research project. In addition, the research flow and descriptions of different research phases are included in this chapter. Moreover, chapter 3 also covers the detailed methodology on the experimental works in each phase. It includes membrane fabrication, characterization, greywater filtration, analytical method for greywater quality analysis, flux decline, LCA and etc.

Chapter 4 mainly consists of 4 sub sections, namely phase I to phase IV, presenting the results and discussing all the findings in this research. In phase I, a single layer chitosan membrane was fabricated with chitosan concentration varied from 1 wt% to 2 wt%, and loading of porogen poly (ethylene) glycol (M_w = 6000). The weight ratio of the chitosan: PEG was varied from 4: 0, 4: 1, 2: 1, 4:3 and 1: 1 for each of the concentration of chitosan. In this section, it involves the study of changes in membrane structure, membrane molecular structure, swelling ratio, swelling equilibrium, de-ionized (DI) water flux and mechanical testing. Thereafter, the membranes were installed in dead-end stirred cell unit for the evaluation of its efficiency in greywater treatment.

In phase II, alginate was introduced to the single layer chitosan membrane. The incorporation of alginate is on the top layer of the chitosan to form polyelectrolyte complex bilayer membrane (PCBM) to reduce molecular weight cut-off (MWCO) and improve the filtration flux. In this chapter, there are two type of PCBM fabricated, namely dense PCBM and porous PCBM. In details, the dense PCBM was fabricated with alginate as the second layer, whilst porous alginate was fabricated using alginate and PEG as the second layer. The 6 sets of PCBMs were characterized in terms of membrane structure, molecular structure, swelling ratio, porosity, ultrapure (UP) water flux and MWCO. Porous PCBM showed higher UP water flux and greywater treatment performance as compared to other PCBM and single layer chitosan membrane.

Due to the presence of trace amount of pathogens found in the treated water, AgNP was loaded in the porous alginate layer in PCBM to investigate on its effect on disinfection. In phase III, the concentration of AgNP was carefully controlled at 0.5ppm, 1ppm to 1.5ppm. Thereafter, phase IV covers the scale-up membrane with the selected conditions from phase III to be utilized in the lab scale decentralized treatment system. The decentralized greywater filtration system was designed to have 20 L greywater tank and treated greywater tank, and a 12 cm diameter dead–end membrane filtration unit. The membrane was installed in the dead–end membrane filtration unit to treat bathroom greywater and was closely monitored throughout the treatment process. The treatment process was monitored to investigate on the possibility if long term running the membrane and its fouling mechanisms. In this chapter, the flux obtained from filtering the greywater will be analysed using different flux decline model to identify the possible fouling of using PCBM.

In addition, the used membrane from phase IV was removed and analysed to investigate on bacteria deactivation mode. The purpose of this study is to study on the mechanism of PCBM in eradicating bacteria whether it is on size exclusion or contact-killing mechanism. Then, LCA was conducted on PCBM, and it was compared to the conventional nylon 66 membrane. The completion of this stage could provide insights on the applications of PCBM and contribute to new alternative materials for greywater recycling

Last but not least, chapter 5 concludes the main findings of this research project and chapter 6 emphasizes on the possible future developments of this project.

CHAPTER 2

2 Literature review

2.1 Chapter overview

This chapter comprises of critical reviews on topics related to the scope of this research project. Firstly, the characteristics of greywater and treated greywater standards established in various countries were reviewed. Following that, the differences between centralized treatment system and decentralized treatment system were identified and evaluated. Recent advancements of greywater treatment technologies were reviewed to provide an in depth understanding on the principles of various treatment technologies. Based on the criteria of different greywater treatment technology, membrane technology was selected as the appropriate treatment for decentralized greywater treatment system. Therefore, the review also emphasized on the details of membrane technology. Different flux decline models of membranes were also critically assessed for thorough understanding on the operation of membrane filtration systems. Different membrane materials were reviewed with focus placed on the use of biopolymers due to the shortcoming of non-biodegradable materials. Thereafter, the chapter emphasized on the additives to fabricate membranes fit for greywater treatment such as formation of PEC and loading of AgNP.

2.2 Greywater

Greywater was found to be a suitable alternative water source to address the issues of scarcity and increasing demand of freshwater. The advantages of having constant volume generated and containing light pollutants made greywater an appropriate source to be reused in a household for non-potable activities. The characterization of greywater and understanding of its characteristics

are crucial to identify harmful compounds that have to be removed prior reuse (Boyjoo & Pareek et al., 2013b; Eriksson & Auffarth et al., 2002). Understanding greywater characteristics also enables a proper treatment system to be devised to produce treated effluent that is fit for use.

2.2.1 Greywater characteristics

Typically, the pollutants of greywater can be classified under categories of physical, chemical and biological parameters (Chaillou & Gérente et al., 2011; Eriksson & Auffarth et al., 2002). Examples of physical parameters are temperature, color, suspended solids and turbidity of the greywater, while chemical parameters include COD, BOD, nutrients (eg. total nitrogen and total phosphorus) and pH of the greywater. As summarized in Table 2.1, it was found that the combined source of greywater has a moderate to alkaline pH range of 6.35 to 8.1, giving a wider range of treatment options. Due to the fact that greywater is generated from human daily activities such as shower, hand wash and cooking, greywater should contain significant amount of solid particles, organic matters and microorganisms. It could be observed from Table 2.1 that combined greywater contains 12 mg L^{-1} - 168 mg L^{-1} of suspended solids, 20.6 – 100.6 NTU of turbidity, and 56 – 1056 mg L^{-1} of BOD_5. Hence, it is essential to treat the greywater to maintain the esthetic and hygiene condition of the treated greywater.

Table 2.1. General characteristics of mixed greywater (Boyjoo & Pareek et al., 2013b; Jefferson & Palmer et al., 2004)

Parameter	Unit	Greywater
pH	n.a	6.35 – 8.1
BOD_5	mg L^{-1}	56 – 1056
COD	mg L^{-1}	245 – 1004
Turbidity	NTU	20.6 – 100.6
Total suspended solid	mg L^{-1}	12 – 168
Total phosphorus	mg L^{-1}	5.2 – 19.5
Total nitrogen	mg L^{-1}	9.7 – 57.7

Parameter	Unit	Greywater
E. coli	CFU 100 mL^{-1}	$7.5 \times 10^3 – 2.6 \times 10^5$
Total coliforms	CFU 100 mL^{-1}	$1.4 \times 10^4 – 1.0 \times 10^7$

Apart from that, biological parameters were characterized to detect and enumerate pathogens. Pathogenic bacteria such as *E. coli* and *Enterococci* could be commonly found in the greywater due to the presence of trace amount of urine and faeces (Donner & Eriksson et al., 2010). Others such as total coliforms and faecal coliforms, are also key contributors to biological pollutants in the greywater (Widiastuti & Wu et al., 2008). These pathogens in the greywater risk human health when the treated greywater comes into contact with human via activities such as toilet flushing and irrigation (Chaillou & Gérente et al., 2011).

Pathogens were usually removed using conventional chemical disinfectant such as chlorine, ozone, chlorine dioxide, and chloramines to assure the safety of greywater reuse (Richardson & Postigo, 2012). However, the use of chemical disinfectants could lead to the formation of disinfectant by-products with the residual organic contents in greywater. The disinfection by-products were found to be harmful to human respiratory system (Richardson & Postigo, 2012) and thus, this issue urges the need to use a relatively inert disinfectant to avoid impact to the human body.

As discussed earlier, suspended solids, dissolved solids, organic matters and pathogens are the main components that need to be removed from greywater prior reuse. Typically, pollutants with the size range between 0.001 μm to 100 μm in wastewater are major compounds that need to be removed in the treatment process (Chen & Mou et al., 2008). Thus, information on pollutant size distribution is crucial for the selection and design of an appropriate treatment system (Levine & Tchobanoglous et al., 1991). Table 2.2 gives an overview on the typical size distribution of the

pollutants that could be found in greywater. In addition, previous study by Hocaoglu and Orhon (2013) indicated that distribution of pollutants in greywater are 7% < 2 nm, 17% 8 – 14 nm, 31% 4 – 220 nm and 37% > 0.45 nm. Based on information from the literature, it was found that majority of the pollutants in greywater fall in the nano-size to micro-size range, which is difficult to be removed using simple coarse filtration technique.

Table 2.2. Typical particle size distribution of pollutants in greywater

Pollutants	Sizes	References
Suspended solids	1 to 100 μm	Levine, Tchobanoglous, & Asano, 1991)
Dissolved solids	< 0.001 μm	Levine, Tchobanoglous, & Asano, 1991)
Organic contents (BOD, COD, TOC)	< 0.001 μm	Levine, Tchobanoglous, & Asano, 1991)
Filamentous bacteria	> 100 μm	(Bitton, 2005)
Cyanobacteria	5 to 50 μm	(Bitton, 2005)
Bdellovibrio bacteriovorus/ Mycoplasma	approx.0.3 μm	(Bitton, 2005)
E. coli	1 – 2 μm	(Bitton, 2005)
Viruses	25 – 350 nm	(Bitton, 2005)

2.3 Treated greywater standards

Having a treated greywater standard is crucial to control the quality of treated greywater upon reuse. However, there is no international standard for the quality of greywater for reuse purposes (Alkhatib & Roesner et al., 2006; Boyjoo & Pareek et al., 2013b). Different countries have established their own treated greywater standard according to their respective applications. Countries such as Australia, the United States (USA), the United Kingdom (UK), and Israel have developed individual guidelines on treated greywater quality (Boyjoo & Pareek et al., 2013b). In addition, the United States Environmental Protection Agency (US EPA) also released a guideline in 2004 to encourage states to construct their own standard of treated greywater (Haering &

Evanylo et al., 2009). The standards set by these countries were highlighted and these standards could be taken as references for authorities to set up national standards in countries that intend to perform greywater recycling. It will also be used to form the treatment benchmark for this project.

Table 2.3 summarizes the treated greywater standards released by a few countries. Due to the fact that greywater recycling is not common in Malaysia, water quality standards for treated greywater in Malaysia are not available. Based on the standards listed in Table 2.3, it is mandatory for pH of the treated water to be controlled at the pH of 5 - 9.5, as any pH beyond this range will render the treated water unsuitable for usage. USA and Israel have a more stringent discharge requirement for (BOD_5) while Australia, Italy, UK and Canada allowed discharge of treated greywater with BOD_5 of 20 mg L^{-1}. In addition to BOD_5 discharge requirements, Israel and Italy also made it mandatory for COD of treated greywater to achieve a standard of 100 mg L^{-1} and below. Italy has included the requirements for total nitrogen (<15 mg L^{-1}) and total phosphorus (< 2 mg L^{-1}) of the treated greywater to minimize the impacts of these organic pollutants to the environment. Monitoring of turbidity and TSS were also found to be crucial to maintain the aesthetic condition of treated greywater. Most countries imposed strict standards for turbidity and TSS. In most cases, treated greywater turbidity and TSS should not exceed the maximum limit of 10 NTU and 30 mg L^{-1} respectively.

Most guidelines required the level of pathogenic microorganisms in the treated greywater to be as low as possible to assure human safety. Based on Table 2.3, UK and Canada had more relaxed standards compared to other countries such as Australia and US. In the UK, 1000 CFU 100 mL^{-1} of faecal coliform is allowed in the treated greywater, and 200 CFU 100 mL^{-1} of faecal coliform is allowed in the treated greywater in Canada. In contrast, the US and New South Wales

(Australia) are more stringent in the control of faecal coliforms, in which the US does not permit the presence of faecal coliforms in the treated greywater and New South Wales only allows less than 1 CFU 100 mL^{-1} of faecal coliforms in the treated greywater. This is due to the fact that treated greywater in the USA and Australia are used for various applications that involved human contact, such as irrigation, laundry, fire protection, commercial air conditioning, and car washing. On the other hand, Italy utilized another bacteria indicator, *Salmonella,* into monitoring the treated greywater quality. This is due to the fact that *Salmonella*, which is responsible for causing typhoid fever and salmonellosis, poses a risk to human health, and thus the presence of *Salmonella* in treated greywater is not acceptable. In view of the risks that can be caused by *Salmonella*, other countries should consider including *Salmonella* as part of the bacteria indicators or at least perform *Salmonella* check monthly on the treated greywater to avoid outbreak of typhoid fever and diseases caused by *Salmonella sp.*

The final end-use of treated greywater will be the main criteria to determine the water quality standard for treated greywater discharge in Malaysia. Treated greywater does not need to achieve drinking water quality standards if it is not intended for human consumption. Hence, the treated greywater could be treated to a lenient acceptance level of BOD_5 at 20 mg L^{-1}, pH of 6 – 9, and turbidity of 5 NTU (assuring the aesthetics of the treated water). Nevertheless, due to the potential of bacterial and viral re-growth which would eventually lead to risks of human health, the treated greywater should contain non-detectable to a maximum concentration of < 10 CFU 100 mL^{-1} of *E. coli.*

Table 2.3. Treated greywater (for non-potable applications) standard in various countries

	Unit	Australia	Israel	USA	Italy	New South Wales	UK	Canada
References		Chaillou & Gérente et al. (2011) Australian Capital Territory (2004)	Chaillou & Gérente et al. (2011) Ramona & Green et al. (2004)	Couto & Calijuri et al. (2014), Chaillou & Gérente et al. (2011), US EPA (2004)	Chaillou & Gérente et al. (2011)	Couto & Calijuri et al. (2014)	Couto & Calijuri et al. (2014) Environment Agency (2011)	Couto & Calijuri et al. (2014) MHC (2010)
pH	-	-	-	6 to 9	6 to 9.5	-	5 to 9.5	-
TSS	mg L^{-1}	< 30	< 10	-	< 10	< 20	-	<20
Turbidity	NTU	-		< 2	-	-	< 10	< 5
COD	mg L^{-1}	-	< 100	-	< 100	-	-	
BOD_5	mg L^{-1}	< 20	< 10	< 10	< 20	< 20	-	<20
Total N	mg L^{-1}	-	-	-	< 15	-	-	
Total P	mg L^{-1}	-	-	-	< 2	-	-	
Cl_2 residual	mg L^{-1}	-	-	> 1	-	2	< 2	> 0.5
E. coli	CFU $100mL^{-1}$	-	-	-	< 10	-	-	-
Thermotolerant coliforms	CFU $100mL^{-1}$	< 10	-	-	-	-	-	-
Faecal coliforms	CFU $100mL^{-1}$	-	-	N.D	-	< 1	1000	< 200
Salmonella	CFU $100mL^{-1}$	-	-	-	N.D	-	-	-
Type of reuse	-	Surface irrigation, toilet flushing, laundry use, car washing	-	Landscape irrigation, toilet flushing, fire protection, commercial air conditioning	-	Toilet flushing	Toilet flushing	Toilet flushing

2.4 Centralized and decentralized greywater treatment

In general, there are two different treatment facilities available for greywater treatment namely, centralized and decentralized treatment facilities, which work on completely different water distribution systems. It is crucial to identify the differences of the two different treatment structures to assess the suitability of these frameworks on greywater recycling.

A decentralized or onsite wastewater treatment system uses natural or mechanical parts to collect, treat, discharge or reclaim water without passing through the centralized treatment facilities (Casey & Moore et al., 2000). Recycle greywater in a decentralized system avoids the needs of long piping system and energy for transferring water between the treatment facilities and houses. Therefore, the implementation of onsite treatment or decentralized treatment can be a solution to the high cost of reuse systems (Naylor & Moglia et al., 2012). Slightly different from onsite treatment facilities, the cluster treatment facility provides treatment for two or more dwellings but less than the entire community (Casey & Moore et al., 2000; Massoud & Tarhini et al., 2009). Decentralized wastewater treatment therefore utilizes and combines the two concepts to perform treatment on higher amount of wastewater.

Figure 2.1 illustrates the difference between centralized and decentralized systems. This clearly shows that long pipelines are required to connect each dwelling in different households to transfer the wastewater to a centralized treatment system, while a relatively short pipeline is required to manage treatment decentralized treatment system. Therefore, due to the simplicity and cost effectiveness of a decentralized greywater treatment system, such system is attractive for remote areas that do not have access to piping leading to centralized treatment facilities, such as

rural villages (Geisinger & Chartier, 2005; Hophmayer-Tokich, 2006). This is because the long piping system used for transferring wastewater to a centralized system can be costly, especially for remote areas (Otis & Wright et al., 1996). For instance, a study conducted in China revealed that capital cost of USD 0.12 Million is required to purchase a decentralized wastewater treatment system and install under a basement parking (Wang & Chen et al., 2008). However, the same funding is only sufficient for the construction of 3.4 km out of 8 km pipeline of a centralize wastewater treatment system (Wang & Chen et al., 2008). In addition to that, the operating and maintenance of this decentralized treatment system is approximately USD 0.12 per m^3 of water, which is USD 0.05 per m^3 lower as compared to the current water tariff in China (Wang & Chen et al., 2008).

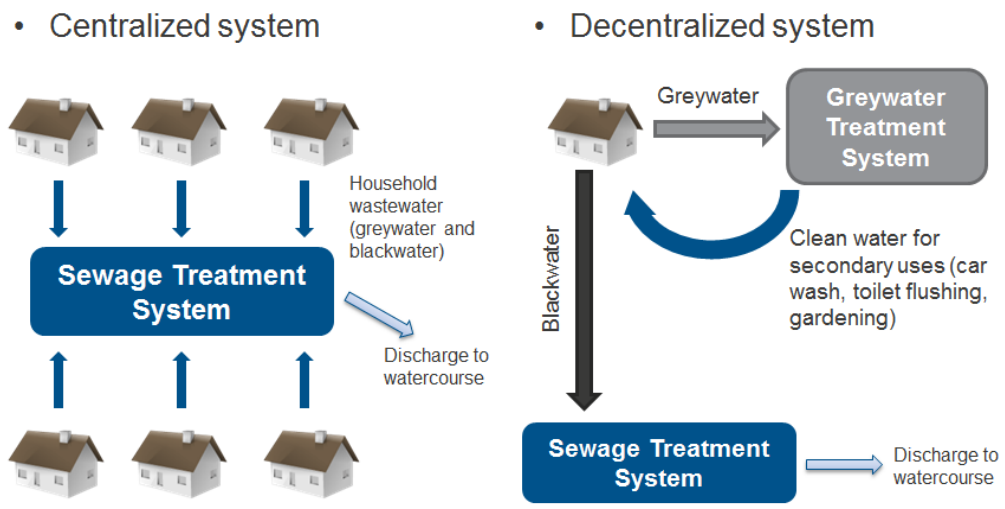

Figure 2.1 Conceptual illustration of centralized and decentralized water treatment system

Moreover, other than providing the community with the benefits in terms of ease of management and remote quality control of the decentralized treatment system, a decentralized greywater system allows users to monitor the system's performance and maintain it when

necessary (Al-Jayyousi, 2003; Norton, 2009). Furthermore, other than remote areas, condominiums, apartments, or office buildings with lower population could also be one of the targets to adopt the decentralized treatment system. For instance, a new multi-storey building in Metropolitan area of Barcelona has implemented the decentralized greywater recycling system to reduce the problem of water scarcity (Domènech & Saurí, 2010).

The centralized treatment system, which is usually out of sight to the public, indirectly caused the lack of understanding, public awareness and involvement in the wastewater treatment process (Massoud & Tarhini et al., 2009). In fact, the centralized treatment system requires numerous pumps and installation of a piping system, which increases energy consumption and system costs (Massoud & Tarhini et al., 2009). As reported by Geisinger and Chartier (2005), 60 % to 70 % of the total project cost of centralized wastewater treatment is contributed by the collection system. Hence, decentralized system was suggested for greywater recycling as the alternative to centralized treatment to reduce the cost of collecting system by increasing the flexibility of pipeline arrangement and collection system (Geisinger & Chartier, 2005).

2.5 Greywater treatment technology

Depending on the applications of treated greywater, the treatment process could be as simple as a single filtration unit or it could be a complex integrated treatment system. A flow diagram of a typical greywater treatment system is presented in Figure 2.2. In general, treatment of greywater usually involves solids removal (including hair, leaves, sand, dust and etc), organic matters (chemicals in detergents, daily appliances and etc), and pathogenic bacteria removal. As such, the treatment of greywater can be categorized, but not limited to four major categories,

namely, biological treatment, chemical treatment, physical treatment and wetland/ ponding system. In this section, various treatment technologies available for greywater will be discussed.

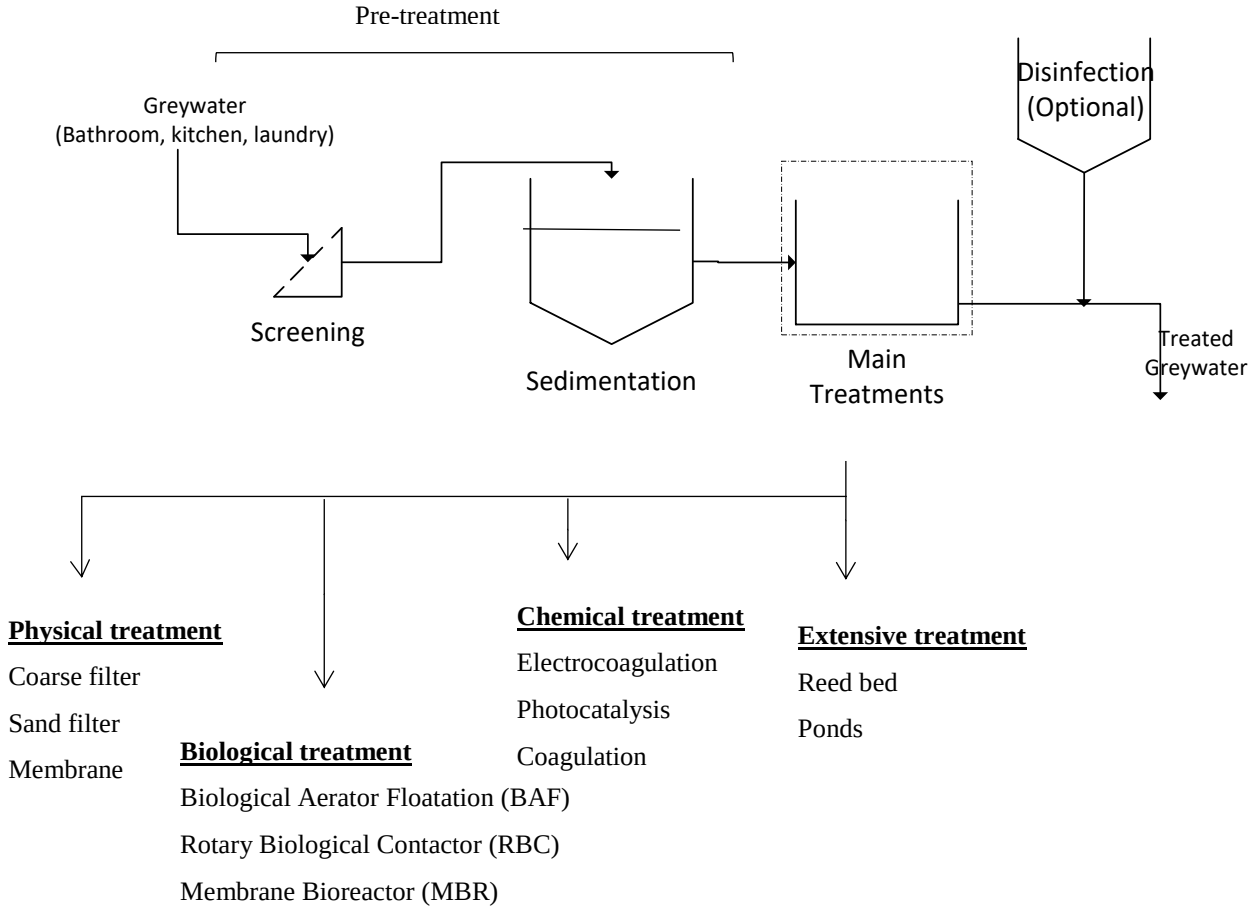

Figure 2.2. Flow diagram of common greywater treatment system

2.5.1 Physical treatment

Physical treatment is usually regarded as the pretreatment process in a wastewater treatment system. A physical treatment unit separates pollutants from greywater based on particle size exclusion mechanism. Some examples of physical treatment unit are screener, coarse filters and membrane filtration.

In a greywater treatment system, screener is normally used to separate big solid particles that could possibly be present in the greywater such as hair, rocks, leaves, trashes, fragment of clothes and etc. to prevent them from entering the main treatment unit. The screener is typically made out of mesh wires or bars to allow greywater to flow through and solids particles to be trapped and removed periodically. On the other hand, coarse filter (eg. sand filter) consists of layers of sand or rocks of different sizes to trap solid particles of variable sizes. In some cases, the greywater is simply filtered through coarse filter and reused for outdoor irrigation. Despite the simplicity of these units, the screener and sand filter is not sufficient to remove organic matters and pathogens which are generally very small in size. As a result, the screened greywater is transferred to the main treatment unit for further treatment.

Apart from screener and coarse filter, membrane filtration is a more enhanced physical treatment technology. Membrane is commonly used as tertiary treatment process in a wastewater treatment plant due to its decent ability in removing organic, inorganic and microorganisms (Jacob & Guigui et al., 2010) . Depending on the size of the targeted pollutants, membrane filtration can be operated under a wide range of conditions, such as microfiltration (MF), ultrafiltration (UF), nanofitration (NF), reverse osmosis (RO) and forward osmosis (FO) to remove targeted pollutants. In fact, membrane technology could be effectively adopted in a decentralized greywater recycling system attributed to the characteristics of the system of having low space requirement for the installation (Fakhru'l-Razi & Pendashteh et al., 2009). In addition to that, the absence of toxic chemicals in the treatment system is one of the advantages of utilizing membrane technology in a decentralized treatment system (Fakhru'l-Razi & Pendashteh et al., 2009). Other factors such as the ease for controlling and monitoring the treatment process are also important features of

membrane technology that allowed it to be implemented in a decentralized treatment system. Detailed description of membrane technology will be further elaborated in Section 2.6.

2.5.2 Biological treatment

Biological treatment utilizes microorganisms to transform the pollutants present in the greywater into simpler end products. The mechanisms involved in biological treatment include the oxidization of organic/ biodegradable pollutants by the microorganisms, detention of suspended solids onto the bio floc or biofilm, removal of nitrogen and phosphorus (Tchobanoglous & L. Burton et al., 2004). The equation for the conversion of pollutants is established as shown below:

$$Organic\ matters + oxygen + phosphate + ammonia \xrightarrow{microorganism} Biomass + carbon\ dioxide + water \quad \text{(Eq. 2.1)}$$

As shown in Eq. 2.1, organic matters are oxidized in the presence of microorganisms and converted into products such as CO_2 and H_2O. At the same time, biomass is also generated as a product of the treatment process (Nolde, 2005; Pidou & Memon et al., 2007). Attributed to the nature of different microorganisms, biological treatment can be performed under aerobic (presence of oxygen) and anaerobic (absence of oxygen) conditions. Some systems combine both aerobic and anaerobic treatment to achieve better treatment efficiency (Abu Ghunmi & Zeeman et al., 2010) .

For greywater treatment, aerobic treatment is most commonly adopted due to the good removal efficiency of organic pollutants in the greywater. Under aerobic treatment, there are two types of system: attached and suspended growth (Tchobanoglous & L. Burton et al., 2004). Rotary Biological Contactor (RBC) and biological aerated filter (BAF) are the most frequently used

attached growth aerobic treatment system for greywater treatment (Birks & Colbourne et al., 2004; Gilboa & Friedler, 2008; Nolde, 2005). In the RBC system, microorganisms are deposited onto an inert media (such as layers of plastic disc) that is partially submerged into the greywater. With the greywater passing through the contactors, the biodegradable pollutants will be degraded by the microorganism attached on the inert media. On the other hand, bacteria sludge is packed within a media support and submerged in greywater in a BAF system. Air or oxygen is supplied via a diffuser in the tank in a down-flow or up-flow manner in the system. The air supplied to the system allows the bacterial sludge to oxidize the pollutants.

In 2005, Nolde (2005) reported a few RBC greywater treatment system that have been operating for the past 10 years in Germany. These RBC units have functioned over the years to recycle water for small-scale treatment (65 - 70 person) as well as a large-scale treatment system, which caters for a 400 beds hotel (corresponding to 20 m^3/ day). Besides, another greywater system, which consists of sedimentation, RBC and UV disinfection unit was found to be able to reduce BOD_7 from 50 ppm – 250 ppm in the influent, to as low as 5 ppm in the treated greywater effluent (Li & Wichmann et al., 2009). Another study conducted by Friedler & Kovalio et al. (2005) showed that 71% of COD and 88.8% of BOD was removed by the RBC and sedimentation process. However, only 94% of turbidity and 63% of TSS was removed by the system, in which another filtration unit was required to further remove the remaining turbidity and TSS of greywater (Friedler & Kovalio et al., 2005). As such, a sand filtration unit was added as a polishing step to reduce the turbidity from 1.9 NTU to 0.61 NTU, TSS from 16 ppm to 7.9 ppm, COD from 46 ppm to 40 ppm and BOD from 6.6 ppm to 2.3 ppm (Friedler & Kovalio et al., 2005). Despite the reduction in these pollutants, feacal coliform concentration was found to increase after the sand

filtration unit (from 9.7×10^3 cfu 100 mL^{-1} to 5.6×10^4 CFU 100 mL^{-1}), indicating that a disinfection unit is essential to assure the treated greywater from the system is safe for reuse.

In addition, BAF system was found to have good removal of nitrogen and COD (Pramanik & Fatihah et al., 2012). For instance, 99% of nitrogen, corresponding to 47.2 $gm^{-2}d^{-1}$ of nitrogen and 98% of COD, corresponding to 158.0 $gm^{-2}d^{-1}$ of COD were removed using a dual-stage packed bed system (Lee & Ong et al., 2004). Similarly, Ong & Hu et al. (2002) also reported a total removal of 97.5% - 100% nitrogen and 98.6% - 99.4% of COD in an anoxic-oxic packed bed system. However, Birks & Colbourne et al. (2004) utilized BAF system in treating greywater from an exhibition space (The Millennium Dome, London, UK) and found that BAF could not produce treated greywater that is free of pathogens. As such, the BAF system was suggested to be coupled with an extra disinfection process before reusing treated water.

On the other hand, activated sludge system is considered as a suspended growth system. In this system, the microorganisms that are responsible for the degradation of pollutants are suspended in the liquid phase (Tchobanoglous & L. Burton et al., 2004). Agitation or aeration is normally present to supply oxygen to the bacteria sludge in the wastewater. After the treatment process, the mixture of water and biomass will be transferred to a clarifier to have the biomass settled as the activated sludge, and sludge will be recycled back to the aeration tank. In most of the suspended system, removal of biomass is a daily/ periodically routine, as excess biomass will transfer into the treated water (Tchobanoglous & L. Burton et al., 2004). Membrane bioreactor (MBR) is an example of suspended growth system that was integrated with membrane technology. In the MBR system, greywater first undergoes biological treatment in the suspended growth system to remove biodegradable pollutants. Subsequently, the partially treated greywater will be

channelled to the membrane unit to remove bacteria and solids that were not removed from the previous process. MF and UF membrane are the most commonly used membrane in a MBR. It was reported that MBR is capable of removing 97 % to 99 % TOC (Nguyen & Hai et al., 2012) and 92.2 % - 95 % COD (Atasoy & Murat et al., 2007; Paris & Schlapp, 2010) in greywater. Due to the presence of membrane, the effluent from MBR unit is free of suspended solid, turbidity (Atasoy & Murat et al., 2007; Nguyen & Hai et al., 2012; Paris & Schlapp, 2010).

However, despite the high removal of organic matters in biological system, a disinfection step was needed to eliminate all the bacteria remaining in the treated greywater effluent. In addition, the sludge removal step is essential in biological treatment system, as the accumulation of sludge and microorganisms in the treatment system could result in clogging of the water distribution system (Abu Ghunmi & Zeeman et al., 2010). Thus, these additional treatment processes would require higher amount of energy and resources to ensure the efficient operation of greywater recycling system. Furthermore, there are also problems associated with biological treatment system such as odour, mosquito breeding, soil and water pollutions (Abu Ghunmi & Zeeman et al., 2010). Thus, to avoid the issues such as odour, and mosquito breeding, extra treatment processes would be required if biological treatment systems were implemented for greywater treatment.

2.5.3 Chemical treatment

There are very limited applications of chemical treatment in greywater treatment system due to the complex operation and addition of chemical to the treatment system. The most common greywater chemical treatment technology employed was chemical coagulation (Pidou & Memon

et al., 2007). Chemical coagulant, such as alum ($Al_2(SO_4)_3 \cdot 18H_2O$ or $Al_2(SO_4)_3 \cdot 14H_2O$), is dosed to destabilize the pollutants in the greywater (Li & Wichmann et al., 2009; Pidou & Memon et al., 2007). During the process, the insoluble aluminium hydroxide ($Al(OH)_3$) is formed and settled. The aggregation of these compounds can then be removed via separation or filtration techniques. Other than alum, other chemical coagulants available are calcium hydroxide (lime), aluminium chloride, ferric chloride, ferric sulphate, ferrous sulphate and sodium aluminate. Study showed that treating greywater using alum could remove 68% of BOD while 99% of BOD can be removed using ferric coagulants (Pidou & Avery et al., 2008). Similar study also showed that coagulation using alum removes 74% of COD from greywater. However, the treated greywater failed to meet the reuse standard of turbidity < 5 NTU (Li & Wichmann et al., 2009). In addition to that, minimum dosage of coagulant could vary due on the change in pH of the greywater, and surface property of the pollutants. Pidou & Avery et al. (2008) also pointed out that a chemical treatment system is only suitable for single household with low strength greywater that has less fluctuations in the characteristic of the greywater. Therefore, operation of decentralized greywater treatment system, which utilizes chemical treatment, can prove to be challenging when dealing with greywater with consistently varying characteristics and sometimes with relatively higher organic load at certain periods of time.

2.5.4 Wetland/ ponding system

Alternatively, greywater could also be treated in wetland/ ponding system. In brief, the settable pollutants in greywater are first allowed to settle in a sedimentation process. Then, the pretreated greywater is transferred to the constructed wetlands, which usually consists of reed beds

and pond for further treatment. This technology utilizes plants as the treatment media and thus, it is considered to be a more environmental friendly and a low-cost treatment technology. The type of plants found in the reed beds are *Phragmites australis, Coix lacryma-jobi, Iris pseudocorus, Veronica beccabunga, Glyceria variegates, Juncus effuses, Iris versicolor, Caltha palustris, Lobelia cardinalis, Mentha aquatic, alisma, iris, typha, metha, canna, thalia, lysimachia, lytrum, ponyederia and preselia.* (Pidou & Memon et al., 2007).

Wetland/ ponding system was reported to have good removal efficiency for organic pollutants, such as BOD. However, this technology does not have the ability to eliminate pathogenic bacteria to a satisfactory level (eg. *E.coli* and coliforms bacteria). This indicates that a disinfection unit is essential to ensure that the treated water is safe for reuse. In addition, the wetland/ ponding system does not produce treated water that is free of suspended solids and turbidity. Hence, an extra filtering media (eg. sand filter) is also required to capture any solids that travel out of the system with the treated water. Other than that, the constructed wetlands usually occupy big area resulting in higher treatment area as compared to other treatment technologies. As a result, the extensive treatment is not suitable to be installed in the area with high building density such as urban area. Studies showed that treatment area of 5.7 m^2 to 10 m^2 per person is required for wetland/ ponding system, whilst only 0.2 m^2 is needed for RBC greywater treatment system (Pidou & Memon et al., 2007). Last but not least, the long hydraulic retention time (HRT) is another drawback of the extensive treatment system. As reported by Pidou & Memon et al. (2007), the extensive treatment system required an average of 4.5 days to achieve similar treatment performance compared to 19 hours with biological treatment. As such, a more rapid treatment system that requires shorter HRT is favourable to ensure fast and consistent availability of treated water.

2.5.5 Comparison of various greywater treatment technologies

Based on the greywater treatment technologies reviewed in previous sections, there are various pros and cons associated with different greywater treatment technologies. Table 2.4 summarized the advantages and disadvantages of various greywater treatment technologies. It was found that advanced physical treatment (eg. membrane technology) is the most suitable treatment technique to be implemented in a decentralized greywater recycling system. This is due to the capability of membrane to eliminate high concentrations of TSS, turbidity, bacteria and satisfactory level of organic matters. At the same time, treatment efficiency of membrane system is not source dependent and has low space requirement, making it an appropriate option for decentralized greywater recycling system. More details on membrane technology will be further discussed in the next section.

Table 2.4. Advantages and disadvantages of various treatment technologies

Greywater treatment	Advantages	Disadvantages
Biological treatment	High organic matters removal	Low turbidity removal
	High nitrogen removal	Low suspended solid removal
	Low space requirement	Mosquito breeding
		Malodour
		Soil and water pollutions
		Clogging of distribution system
Chemical treatment	High organic matters removal	Low turbidity removal
	High bacteria eradication	Low suspended solid removal
		Addition of chemicals
		Source dependent
Physical treatment	Inert treatment technique	Moderate organic removal
	High bacteria eradication	
	High removal of TSS	
	High removal of turbidity	
	Low space requirement	
Wetland/ ponding	High removal of organic matters (eg. BOD)	Low bacteria eradication
	Low treatment cost	Huge land requirement
		Low removal of turbidity
		Low removal of TSS
		Long retention time

2.6 Membrane technology

Membrane technology is regarded as the most effective, simplified and direct technology of separating pollutants and water molecules based on difference in particle sizes using a physical barrier (Hourlier & Masse et al., 2010). To date, membrane technology has been widely applied in petrochemical industry, gaseous industries, desalination and water treatment system (Shirazi & Kargari et al., 2013). Membrane technology has gained impetus in various industries as an effective separation method and it was reported to be one billion-dollar industry worldwide over the past 52 years (Khulbe & Matsuura, 2000).

Wang (2011) identified four main categories of membranes according to their respective driving forces - pressure driven, concentration gradient, temperature gradient and electrical potential. Dialysis membrane falls under the concentration driven category. In this system, water molecules diffuse through the membrane under a concentration gradient. Distillation membrane, on the other hand, functions based on the temperature difference in the system. Electro-dialysis membrane is a special kind of membrane, where the membrane works under electrical potential difference. On the other hand, MF, UF, NF and RO were categorized as pressure driven membranes (Fane & Wang et al., 2008). These membranes work under pressurized condition to force the water molecules through the barrier while filtrate is left behind.

Pressure driven membranes are most commonly used in wastewater treatment. Table 2.5 lists the different operating conditions of pressure driven membranes system and the particles rejected from different membranes. NF and RO are typically used for drinking water treatment, seawater desalination and blackwater treatment (Fane & Wang et al., 2008; Kajitvichyanukul & Hung et al., 2008). This is due to the fact that RO membrane can be used to reject very tiny

monovalent ions such as K^+, Na^+, while UF focuses on the removal of divalent ions such as Ca^{2+} and Mg^{2+} (Ren & Wang, 2008).

Table 2.5. An overview of the membrane technology conditions in wastewater treatment. (Fane & Wang et al., 2008)

Pressure driven membrane	Membrane average pore size (μm)	Operating condition	Solutes rejection
MF	0.1 to 10	0.05 to 5 bars	Suspended solids, bacteria, giardia, cryptosporidium
UF	0.01 to 1	< 10 bars	Suspended solids, oil and grease, proteins, macromolecules
NF	0.001 to 0.1	< 40 bars	Multivalent salts, sugars
RO	0.0001 to 0.001	> 50 to 100 bars	Monovalent salts, BOD, COD, trace oil and grease

On the other hand, MF (or UF) is used as a pretreatment process to eliminate larger pollutants (eg. bacteria and suspended solid) before the partially treated water undergoes further purification using a RO (or NF) membrane. The incorporation of pretreatment unit in the system helps to reduce the fouling rate of the RO (or NF) membrane and hence, optimizes the overall treatment efficiency. MF membrane alone was also used as a sterile membrane in the wine and beverage industry (Fane & Wang et al., 2008). MF membrane was also reported to have the ability to successfully disinfect lake water, surface water and reservoir water without the use of chemical disinfectants (Fane & Wang et al., 2008).

MF membranes have average pore sizes of 0.1 μm to 10 μm, while UF is able to remove pollutants in the range of 0.01 to 1 μm. Typically, most of the suspended solids and bacteria could be removed using a 0.2 μm MF membrane (Chen & Mou et al., 2008; Geise & Lee et al., 2010). In additon, the low operating pressure (< 2 bar) of MF membrane makes it an advantage as the treatment energy requirement can be minimized as compared to other pressure driven membranes

(Chen, Mou, Wang, Matsuura, & Wei, 2008). The ability of MF and UF to eliminate pollutants while maintaining low energy requirement makes it an appropriate process for decentralized greywater treatment system.

Other than the categories mentioned above, membrane can also be classified as dead-end, crossflow, submerged flow or hybrid flow depending on the flow direction of the solution relative to the membrane (Kishino & Ishida et al., 1996; Ní Mhurchú, 2008; Nitiyanontakit & Varanusupakul et al., 2013; Rosenberger & Krüger et al., 2002). Up to date, UF, NF and RO membrane with different flow configurations are those that have been widely applied in greywater recycling (Li & Wichmann et al., 2009; Pidou & Memon et al., 2007). Instead of the using the dead-end flat-sheet membrane module, cross-flow or hybrid flow tubular (eg. hollow fiber and capillary) and spiral wound membrane module are more commonly used in greywater treatment system due to its small space requirement (Merz & Scheumann et al., 2007; van Voorthuizen & Zwijnenburg et al., 2005). Amongst the two modules, tubular membrane module is favourable as the structure of these membrane results in lower degree of fouling (van Voorthuizen & Zwijnenburg et al., 2005).

In general, most membrane treatment system can produce treated water with very low turbidity (eg.<1 NTU), high aesthetic quality and free of suspended solids. In terms of organic matters, it was reported in the literature that as much as 93% of COD was removed by using a 0.2 kDa NF membrane (Pidou & Memon et al., 2007). Besides, direct greywater filtration using UF membrane also showed good removal of total organic carbon (TOC), with the average removal of 83.4% (Li & Behrendt et al., 2008). On the other hand, 56% of BOD can be removed using UF membrane, whilst 98% BOD is removed using RO membrane (Pidou & Memon et al., 2007). As

such, it could be deduced that membrane with smaller pore size will have better organic matters removal as compared to others. This suggested that selection of appropriate membrane pore size is crucial in membrane technology to achieve the desired treatment efficiency. As such, UF membrane was identified to be the most suitable membrane for greywater treatment, as the moderate pore size (0.01 μm to 1 μm) of UF membrane could effectively remove bacteria and organic matters, while the treatment process requires lower energy as compared to other membranes (eg. NF and RO).

2.7 Flux decline models

Despite the effectiveness of membrane technology in wastewater treatment system, the flux of membrane tends to be reduced after a period of operation due to the clogging of various pollutants in the greywater. It is vital to conduct analysis on membrane fouling in order to fully comprehend the filtration mechanisms of a specific membrane in use. Proper operating conditions and protocols to prolong membrane lifespan then can be devised based on the results from membrane fouling study.

The foulant of membrane can be categorized into organics, inorganics, colloids, and particulates (Field, 2010). Besides the type of foulants, other factors that affect membrane flux include, membrane type, membrane surface properties, membrane pore-size and distribution, concentration of the greywater and hydrodynamics of membrane element (Field, 2010). As membrane pores represent the active area of a membrane, the flux decline of membrane was closely related to the clogging of membrane pores. Essentially, there are four flux decline models that can be used to describe the fouling of membranes namely, standard pore blocking,

intermediate pore blocking, complete pore blocking and cake formation (Field, 2010). In a dead-end filtration setup, the flux decline could be represented with Hermia's equation, where the original equation is presented in Eq. 2.2:

$$\frac{d^2t}{dV^2} = k\left(\frac{dt}{dV}\right)^2 \qquad \text{(Eq. 2.2)}$$

where t is time, k is the mass transfer coefficient and V is the volume of filtrate collected.

However, when analysis is focused mainly on the flux and flux decline, Hermia's equation can be simplified and presented in Eq. 2.3 as shown below:

$$\frac{d\,J}{dt} = -kJ^{3-n} \qquad \text{(Eq. 2.3)}$$

where t is time, k is the mass transfer coefficient, J is flux of the membrane and *n* is an index of ≤ 2

2.7.1 Standard pore blocking (n = 1.5)

Standard pore blocking is the result of particles reaching the surface of the membrane that caused complete or partial clogging of the pores and attachment of particles on the inactive area of the membrane (as shown in Figure 2.3). As such, the blocking mechanism caused the reduction of the membrane pores area, resulting in flux decline. This flux decline model can be modelled using the equation below:

$$J = \frac{J_o}{(1+k_s\cdot(A\cdot J_o)\cdot t)} \qquad \text{(Eq. 2.4)}$$

where t is time,
k is the mass transfer coefficient
J is flux of the membrane

J_o is the initial flux

A is the area of the membrane

Figure 2.3. Illustration for the mechanism of standard pore blocking

2.7.2 Intermediate pore blocking (n = 1)

On the other hand, the intermediate pore blocking model described the flux decline due to the pore size reduction resulting from clogging/ blocking of foulant. As shown in Figure 2.4, the particles that are smaller than the pore size of the membrane in contact with the particles, resulting in the particles entering the pores and deposit on the pore walls. As a result, the flow of solution into the pores will be retarded. Intermediate pore blocking is described by the equation as below:

$$J = \frac{J_o}{\left(1+\frac{1}{2}\cdot k_i\cdot(A\cdot J_o)^{0.5}\cdot t\right)^2} \qquad \text{(Eq. 2.5)}$$

Where t is time,

k is the mass transfer coefficient

J is flux of the membrane

J_o is the initial flux

A is the area of the membrane

Figure 2.4. Illustration for the mechanism of intermediate pore blocking

2.7.3 Complete pore blocking (n= 2)

Different from the standard pore blocking, instead of partially blocking the pore of the membrane, complete pore blocking describes the particles that are way bigger than the pore size of the membrane that blocks the pore of the membrane (as shown in Figure 2.5). The mechanism reduces the active area of the membrane and hence retards the flux of the membrane. The equation that governs the flux decline caused by complete pore blocking is as shown in Eq. 2.6:

$$J = J_o \cdot k_b\, A \cdot t \qquad \text{(Eq. 2.6)}$$

Where t is time,
k is the mass transfer coefficient
J is flux of the membrane
J_o is the initial flux
A is the area of the membrane

Figure 2.5. Illustration for the mechanism of complete pore blocking

2.7.4 Cake formation (n = 0)

As shown in Figure 2.6, cake formation describes the accumulation of particles on the surface of the membrane, whereby the particles do not enter or clog the pore of the membrane. In the case of cake formation, the flux decline of the membrane is the resultant effect of the resistance of the cake layer and combinations of other fouling mechanisms. Cake formation is governed by Eq. 2.7. as follow:

$$J = \frac{J_o}{(1+2 \cdot k_c \cdot (A \cdot J_o)^2 \cdot t)^{\frac{1}{2}}} \qquad \text{(Eq. 2.7)}$$

Where t is time,
k is the mass transfer coefficient
J is flux of the membrane
J_o is the initial flux
A is the area of the membrane

Figure 2.6. Illustration for the mechanism of cake formation

Amongst the membrane fouling models, intermediate pore blocking is considered as irreversible fouling and it is the most severe membrane fouling (Field, 2010; Skouteris & Hermosilla et al., 2012). It was found that in irreversible fouling, the foulant that deposited inside

the pores can neither be removed by changing the flow configuration to cross-flow nor membrane cleaning (Field, 2010). On the other hand, the fouling due to accumulation of pollutants externally is regarded as the reversible fouling (Skouteris & Hermosilla et al., 2012). In reversible fouling, the foulant tend to accummulate on the surface of the membrane, and it could be removed by physical cleaning (Mutamim & Noor et al., 2013). Cake formation is the example of reversible fouling. As such, it could be deduced that selection of pore size is crucial to avoid the occurance of irreversible fouling in membrane (Field, 2010). Due to the fact that most of the pollutants in greywater are in the size of 4.5×10^{-4} μm to 100 μm, UF membrane with moderate pore size could be suitable for greywater treatment to minimize irreversible fouling.

2.8 Membrane materials

There are two major classes of membrane, which includes inorganic and synthetic polymeric membranes (Fakhru'l-Razi & Pendashteh et al., 2009). Inorganic membranes are manufactured using ceramic, bentonite clay, zeolite, while synthetic polymeric membranes are usually derived from synthetic polymers, such as nylon, polyethylene (PE), polypropylene (PP), polyvinylidene fluoride (PVDF), polystyrene (PS), polyeyther-sulphone (PES) and etc (Gander & Jefferson et al., 2000; Li & Sanderson et al., 2002; Shirazi & Kargari et al., 2013). In comparison to inorganic membranes, the use of synthetic membrane is more common as synthetic polymers have satisfactory mechanical strength and lower in cost (Gander & Jefferson et al., 2000). In addition, synthetic membrane are thermal and chemically stable over a wide range of pH, while having high flexibility to be processed into various geometries, such as flat sheet or hollow fibers structure (Ren & Wang, 2008).

In general, synthetic polymers can be divided into few categories, namely thermoplastics, fibers and elastomers. Low density polyethylene (LDPE), high density polyethylene (HDPE), PP, polyvinyl chloride (PVC) and PS are the most common examples of thermoplastics (Moore, 2008). These polymers are normally rigid in room temperature, but become soft when the temperature increases. Thus, the shape of the polymer can be varied to suit respective applications. These materials have been widely used in household appliances, due to its high mechanical properties, ease in shaping, light, inert to chemicals, corrosion resistance and good insulation for electric and heat (Heckele & Schomburg, 2004). Nylon is the most common example for fiber synthetic polymers (Friedrich & Zalar et al., 2007; Guebitz & Cavaco-Paulo, 2008). Owing to the durability of nylon, it has been widely used to make rope, fishing lines, and clothing (Pandey & Raghunatha Reddy et al., 2005). On the other hand, elastomers are polymers that can return to its original shape after stretching or compression (Lendlein & Kelch, 2002; Mehrabzadeh & Rezaie, 2002). Typical examples for elastomer are polyurethane and polybutadiene rubber, which are commonly used in the fabrication of wheel and tire (Mehrabzadeh & Rezaie, 2002).

Statistical data indicated that 250×10^9 pounds of synthetic polymers were sold per annum, which was 1000 times higher as compared to biodegradable polymers (Moore, 2008). As the raw material synthetic polymers are derived from non-renewable fossil resources, it draws concern on the impacts of these materials on the environment (Moore, 2008; Siracusa & Rocculi et al., 2008). Due to the fact that synthetic polymers are non-biodegradable, it leads to the production of secondary waste with wide scale implementation of membrane technology (Gross & Kalra, 2002; Lu & Xiao et al., 2009; Siracusa & Rocculi et al., 2008). Thus, biodegradable and

renewables materials, such as biopolymers are considered as an alternative to overcome the constraints of using synthetic polymers.

The following sections provide reviews on synthetic membranes and possible alternative materials to fabricate membrane specifically for greywater treatment.

2.8.1 Synthetic polymers for wastewater treatment

Attributed to the stability over wide range of pH and flexibility of PS, PS was electrospun into nanofibrous membrane (Shirazi & Kargari et al., 2013). The PS membrane was used to treat washwater from biodiesel production in Malaysia. Study showed that thermal treatment on this electrospun membrane reduced the mean pore size from 0.91 μm to 0.79 μm. The treatment of biodiesel washwater using the PS membrane showed that the membrane was able to remove 58% COD, 26% BOD, 92% TS and 58% TSS, while 75% COD, 55% BOD, 30% TSS, 96% TDS, and 92% TS can be removed using the thermal treated PS membrane. It was found that the pollutants in washwater could be completely removed by controlling the pore size of the membrane. However, this membrane was found to have a reduced TSS removal efficiency after heat treatment. The reduction in TSS removal efficiency was mainly attributed to the smoother membrane structure after heat treatment (Shirazi & Kargari et al., 2013). Hence, it resulted in the reduction in the adsorption of TSS onto the membrane.

On the other hand, nylon membrane was also utilized for the treatment of paper mill effluent. The study uses a 0.2 μm nylon membrane to evaluate the fouling of the membrane during the treatment of paper mill effluent. A cross flow filtration setup was used to evaluate the fouling with a feed flowrate of 0.125 ms^{-1} and operating pressure of 0.5 bar (Li & Sanderson et al., 2002).

The turbidity of the paper mill effluent was reduced from 64 NTU to 1 NTU after filtration using the nylon membrane. Due to the tendency of fouling in nylon membrane, an ultrasonic unit was also incorporated to the system to clean the membrane. It was found that coupling ultrasonic unit for cleaning and forward flushing can improve the flux by 97.8%. Despite, the effectiveness of ultrasonic cleaning, the ultrasonic unit required high operating energy, making it one the drawbacks of using nylon membranes for wastewater treatment.

On the other hand, PVDF is one of the most commonly used membranes due to its mechanical properties and good separation efficiency (Méricq & Mendret et al., 2015; Zhang & Zhang et al., 2013). Masuelli & Marchese et al. (2009) evaluated the treatment efficiency of PVDF membrane in treating emulsified oily wastewater and reported that 95.46% oil content was removed, while 96.63% to 96.71% of treated effluent contain < 100 ppm COD. However, the use of PVDF alone is limited by its hydrophobicity, which can result in high fouling rate during operation (Méricq & Mendret et al., 2015). As such, PVDF is usually coupled with other copolymers such as PVP, PVC, TiO_2, and SPC during the fabrication to improve the hydrophilicity and treatment efficiency (Masuelli & Marchese et al., 2009; Méricq & Mendret et al., 2015; Zhang & Zhang et al., 2013).

Polyurethane on the other hand is an elastomer which has unique property of both soft and hard domain in its molecular structure. The soft segments consists of the high molecular weight of polyether or polyester macrogel while the hard segments consists of diol or diamine (Chen & Tien et al., 2000). Conventionally, polyurethane is produced by mixing of inorganic fractions with alcohol and followed by the reaction with diiocyanate (Wang & Pinnavaia, 1998). Kim & Sea et al. (2006) fabricated a gas separation membrane by blending polyurethane with polyetherimide

and poly (amide-imide). The blended membrane was reported to have successfully increased the selectivity of separation towards carbon dioxide and nitrogen.

In fact, there are only few studies found on the utilization of polyurethane in wastewater treatment. The polyurethane foam was previously used as a heavy metals sorbent in a packed column (Anthemidis & Zachariadis et al., 2002). The successful use of polyurethane foam to recover trace heavy metals (copper, lead, chromium) of up to 98% showed that polyurethane can be potentially used for heavy metals adsorption. Recently, polyurethane foam has also been studied as suspension fillers in wastewater treatment and soil conditioner in the subsurface of wastewater infiltration system (Yuan & Nie et al., 2013). The incorporation of polyurethane foam was reported to optimize the system with reduction of 82% of COD, 62% of total nitrogen, and 99% of total phosphorus. Despite achieving the high reduction efficiency of organic pollutants, polyurethane foam was found to promote bacteria adhesion, which eventually led to the growth of bacteria on its surface (Yuan & Nie et al., 2013). This is an undesirable situation for a membrane as the bacteria adhesion on a membrane can cause the accumulation of bacteria on the membrane surface to form bio-fouling.

2.8.2 Biopolymers for wastewater treatment

Another category of polymer corresponding to the naturally occurring polymer is biopolymers (Sionkowska, 2011). The use of biopolymers is gaining attention over the years due to its renewability and biodegradability (Siracusa & Rocculi et al., 2008). The constituents after decomposition of biopolymers are water, carbon dioxide and inorganic matters that are non-toxic to the environment (Siracusa & Rocculi et al., 2008). Collagen, pectin, cellulose, starch, protein, alginate and chitin/chitosan are the most famous examples of biopolymers that were used for

various applications. Table 2.6 lists the advantages and disadvantages of biopolymers in greywater treatment and the current applications of these polymers in the industry.

Table 2.6. Comparison of between different biopolymers

Biopolymers			
Type	Characteristics	Current Applications	References
Cellulose	Advantages: Most abundant renewable polysaccharide, biodegradable, satisfactory mechanical strength, thermal resistance, hydrophilic Disadvantages: Thermally and chemically unstable beyond pH 4 to 6.5, negative anti-microbial effect	Fiber, paper, membrane, activated adsorbents, and paints industries	(Roy & Semsarilar et al., 2009; Svensson & Nicklasson et al., 2005)
Starch	Advantages: Low cost, biodegradable, renewable, hydrophilic, biocompatibility Disadvantages: Easily dissolved in water, negative anti-microbial effect	Packaging, drugs delivery, edible film, anaerobic and aerobic treatment	(Lu & Xiao et al., 2009; Parvin & Rahman et al., 2010)
Protein	Advantages: Biodegradable, renewable, hydrophilic, biocompatibility Disadvantages: Negative anti-microbial effect	Food, pharmaceutical, Photographic, coagulants	(Vasilenko & Guzenko et al., 2010)
Anti-microbial biopolymers			
Type	Characteristics	Applications	References
Alginate	Advantages: Renewable polysaccharide, heavy metal adsorption, biodegradable, biocompatible, anti-microbial effect Disadvantages: Low mechanical strength, easily dissolved in water	Tissue engineering, small chemical drugs delivery, wound dressing, wastewater nutrients removal, heavy metals removal, edible films	(de-Bashan & Moreno et al., 2002; Fazilah & Maizura et al., 2011; Lee & Mooney, 2012)
Chitin/Chitosan	Advantages: Second most abundant renewable polysaccharide, heavy metal adsorption, biodegradable, biocompatible, anti-microbial effect Disadvantages: Low mechanical strength, dissolved in water with pH lower than 6.5	Tissue engineering, small chemical drugs delivery, wound dressing, adsorbents, dyes adsorption in wastewater treatment	(Berger & Reist et al., 2004; Chen & Hwang et al., 2007; Crini, 2005; Gu & Xue et al., 2001; Yu & Wu et al., 2013)

i. Cellulose

Cellulose is the most abundant natural polysaccharide compared to the rest listed in Table 2.6. The extraction of cellulose are mostly from plants cell wall, and a small fraction are extracted from bacteria (Svensson & Nicklasson et al., 2005). The strong intermolecular hydrogen bonding in between linear glucose polymer chains (as shown in Figure 2.7) has led to the high mechanical strength and thermal resistance of cellulose. The strong properties of cellulose allows it to be widely used for the production of fiber, paper, membrane, polymer, and also application in the paint industry (Swatloski & Spear et al., 2002).

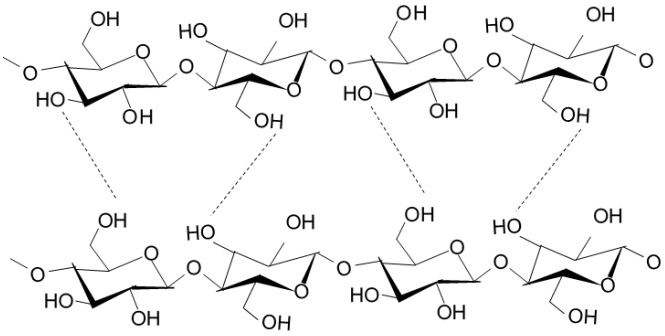

Figure 2.7. Molecular structure of cellulose

In terms of wastewater treatment, cellulose can be used for the adsorption of phenols, dyes and metal ions (Phan & Rio et al., 2006). The use of cellulose in the form of activated fibers that has high specific area, porous structure and acidic surface makes it an effective material for adsorption of pollutants (Phan & Rio et al., 2006). Moreover, cellulose has also been incorporated into polysulfone membrane in the form of Microcrystallized Cellulose (MCC) or Nanocrystallized Cellulose (NCC) with the purpose of enhancing the mechanical strength and adsorption capacity of membrane for paper mill wastewater treatment (Zhou & Zhao et al., 2012). The optimal

filtration pressure of the polysulfone/ NCC membrane was found to be 0.1 MPa, reducing 89.1% of lignin content, 92.8% of suspended solids and 65.9% of COD.

On the other hand, the used of cellulose acetate, cellulose diacetate and cellulose triacetate in the fabrication of pressure driven membranes were also reported (Ren & Wang, 2008). Despite the high hydrophilicity of these fabricated membrane, these membrane were found to be unstable outside the pH range of 4.0 to 6.5 (Ren & Wang, 2008). Moreover, the lack of anti-microbial property of these membranes caused it to be unable to disinfect and promotes biofilm formation on the membrane. Therefore, it can be difficult to utilize membranes derived from cellulose for greywater treatment as the pH of greywater could fall in the acidic region depending on the activities conducted in the household.

ii. Starch

Similar to cellulose, starch is also derived from plants, such as rice, cereal grain, and corn seeds. Starch is one of the abundant edible polysaccharides. Owing to the difference in polymer units' arrangement of α-1, 4–glycosidic linkages and α-1, 6–glycosidic linkages, starch is present with different ratio of amylose or amylopectin based on the source of extraction (Almeida & Alves et al., 2010; Dhepe & Fukuoka, 2008). Amylose contributed to the linear arrangement of polymer units while the branches polymer units are named as amylopectin (as shown in Figure 2.8). Upon contact with water, the formation of hydrogen bonding between water and hydroxyl groups in starch contributes to the superior hydrophilic characteristic of starch. In addition to low cost, biodegradability and renewability of starch, this material is used in many development of sustainable materials and medical usage (Lu & Xiao et al., 2009).

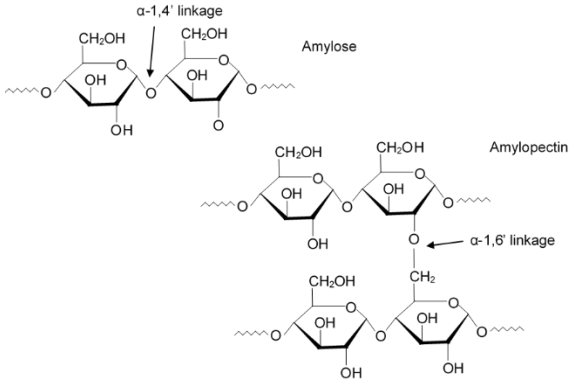

Figure 2.8. Molecular structure of starch

The hydrophilic property and biocompatibility of starch allows it to be widely used as drug delivery agents in the form of hydrogels or microbeads (Balmayor & Tuzlakoglu et al., 2008). The fabrication of crosslinked starch/ PVA hydrogels for medical use by Lu & Xiao et al. (2009) offered effective water uptake rate with an equilibrium water uptake in 12 minutes. Likewise, starch grafted PVA and starch grafted polyethylene packaging materials were successfully prepared and found to be potential substitutes of current non-biodegradable packaging due to its biodegradability and comparable mechanical property (Kaur & Gautam, 2010; Parvin & Rahman et al., 2010).

Besides, starch could also be used in wastewater treatment as coagulants. Shahriari and NabiBidhendi (2012) used starch as a coagulant for the removal of ferric chloride in wastewater. The removal efficiency of ferric chloride was determined to be 92.4% in this particular system. On the other hand, additive of starch and azo dye in the anaerobic-aerobic treatment tank of a textile wastewater treatment was reported to achieve BOD removal of 99%, COD removal of 88% and 77% reduction of dyes (O'Neill & Hawkes et al., 2000). However, due to the high sensitivity of biological treatment technology, the ratio of starch and azo dye additive needs to be closely

monitored in the system. Hence, such system is not suitable to be used as a decentralized treatment system due to the difficulty in managing and controlling the system.

iii. Protein

Unlike cellulose and starch, protein can be extracted from both plants and animals (Boland, 1989; Laing & Christeller, 2004). Plant derived protein are mostly produced from the extraction of soy, corn and wheat gluten while casein is the main protein source extracted from mammal's milk (Millward, 1999). The molecular structure of protein is bonded by polypeptide chains between carboxyl and amino groups of adjacent amino acids (JM & JL et al., 2002). The combinations of different amino acids contribute to complex macromolecular structures of protein. Out of the wide range of proteins available, collagen and gelatin are most commercially used in the industry.

Collagen is the most abundant source of protein that originates from animal. The triple helical chain complex of collagen can provide mechanical support to tissues and help in cell proliferation (Ha & Quan, 2013). Therefore, collagen is widely used in biomedical applications as wound dressing, for delivery of drugs and in tissue regeneration (Ha & Quan, 2013). The partial hydrolyzed form of collagen will be converted into gelatin, as shown in Figure 2.9 (Ames, 1952). Gelatin is relatively easier to be crosslinked and dissolved in most organic solvents (Antoniewski & Barringer et al., 2007). The current used of gelatin mainly on the food production, pharmaceutical and photographic field.

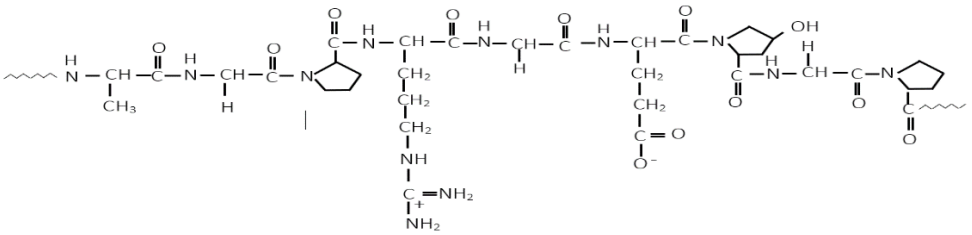

Figure 2.9. Molecular structure of gelatin

A recent research utilized plant extracted protein from *Brassica* species as a natural coagulant. It was found that the use of this protein can potentially substitute the use of conventional coagulant, alum in wastewater treatment (Bodlund, 2013). The proposed coagulation mechanism is based on the electrostatic interaction between the positive charges proteins and negative charges of the pollutants such as suspended solids and bacteria. The used of this natural coagulant was reported with the successive of turbidity removal up to 95% and 81% faecal coliforms reduction (Bodlund, 2013).

2.8.3 Anti-microbial biopolymers for wastewater treatment

The polymers mentioned above lacked of one common property of not being able to treat bacteria in greywater. The use of anti-microbial biopolymers is a promising approach as a low cost disinfection application (Li & Mahendra et al., 2008; Regiel & Irusta et al., 2013). There were several mechanisms being reported on the anti-microbial effect of these peptides, including the formation of nano-sized channel on the membrane of the bacteria to result in the osmotic collapse of the bacteria. Similarly, Qi & Xu et al. (2004) also reported that the mechanisms of anti-microbial effect of peptides involves the attraction of opposite charges of anti-microbial polysaccharides and

bacteria. The bacteria cell will then rupture and losses its intracellular components due to the increase in permeability of the bacteria cell upon binding of anti-microbial polysaccharides to the membrane of the bacteria.

The anti-microbial property of polysaccharides was also explored and utilized as a material to prevent biofilm formation in biomedical applications (Regiel & Irusta et al., 2013). Therefore, anti-microbial polysaccharides, such as alginate and chitosan, have high potential to be utilized for membrane fabrication as these materials do not only function as a disinfectant, at the same time, the membrane will have an additional capability of lowering the bio-fouling due to its anti-adhesion effect (Regiel & Irusta et al., 2013) .

i. Alginate

Alginate, or alginic acid, is a linear polysaccharide extracted mainly from brown algae (Bayer & Herrero et al., 2011). As shown in Figure 2.10, the molecular structure of this anionic polysaccharide consists of different fractions of β-D-mannuronic acids and α-L-guluronic acids. Alginate from different algae source would contribute to the different ratio of β-D-mannuronic acids and α-L-guluronic acids (Donati & Vetere et al., 2003; Fenoradosoa & Ali et al., 2010). The formation of alginate network contributed to the interactions of guluronic residues to form the egg-box structure (Bayer & Herrero et al., 2011). Hence, the ratio of β-D-mannuronic acids and α-L-guluronic acids is an important factor that will affect the mechanical property of alginate derivatives.

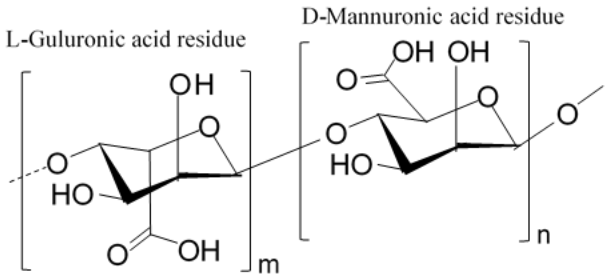

Figure 2.10. Molecular structure of alginate

The properties of alginate having anti-microbial properties, biodegradability, biocompatibility, and the ability to easily dissolve in water, created a wide range of potential usage for alginate. Typically, alginate is fabricated into matrix box, large beads and microbeads structures depending on their applications. The hydroxyl and carboxyl group in the polymer chains contribute to the anionic charges of alginate. Thus, it is commonly used for adsorption of heavy metal ions from wastewater (Mehta & Gaur, 2005).

In wastewater treatment, alginate was found to be a good substitute for carbon nanotubes as an adsorbent. Alginate was reported to have an adsorption capacity of 122.1mg silver (I) ions per gram of alginate, 254.4 mg lead (II) ions per gram of alginate, and 64.9 mg cadmium (II) ions per gram of alginate (Qin et al., 2007). Besides, alginate was also used as a coagulant to reduce turbidity in drinking water (Devrimci, Yuksel, & Sanin, 2012). Devrimci et al. (2012) found that the turbidity of water could be reduced to 1 NTU from the original turbidity of 150 NTU with the use of alginate. In fact, the use of low toxicity alginate is more appropriate for drinking water treatment, as compared to synthetic coagulants. Moreover, dosages of alginate were also used to improve the flocculation in humic acid water treatment (Wang et al., 2013). The use of alginate as flocculants was reported to have successfully improved the treatment efficiency by producing

compact and larger flocs which eases the recovery process. With the improvement of the flocculation process in this system, it was found that the fouling in ultrafiltration membrane can be significantly reduced and hence, achieving better treatment efficiency.

ii. Chitin/chitosan

Chitin is extracted from the exoskeleton of shrimp and crabs. As shown in Figure 2.11, the polycationic chitosan is derived from chitin via deacetylation in the presence of sodium hydroxide (Piccinno & Hischier et al., 2015). Chitosan has a molecular structure consisting of D-glucosamine and N-acetyl-D-glucosamine (Seyfarth & Schliemann et al., 2008). It is the second most abundant polysaccharide after cellulose (Lim & Hudson, 2004). The biodegradability, anti-microbial properties, high biocompatibility and low toxicity of chitosan promoted extensive researches on the application of chitosan (Mello & Bedendo et al., 2006).

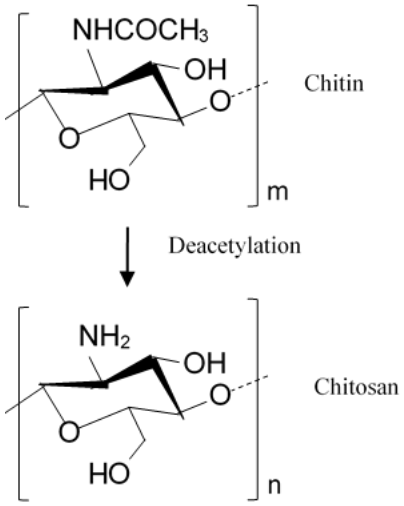

Figure 2.11. Deacetylation of chitin to chitosan

In particular, the anti-microbial property of this polymer has successfully attracted many studies on biomedical application (Burke & Yilmaz et al., 2000; Chang & Lee et al., 2012). In the medical application, chitosan is utilized as a contact-killing film to avoid the growth of bacteria (Cui & Szarpak et al., 2010). The proposed mechanism of the antimicrobial effect indicated that the anti-microbial surface provides resistance to the approaching bacteria or disturbing the bacteria's metabolism, eventually lead to cell fatality (Hasan & Crawford et al., 2013; Wang & Liu et al., 2012). The studies done on the anti-microbial effect of chitosan suggested that the anti-microbial effect varied with the molecular weight of chitosan and the concentration of the polymer (Freitas & Spin-Neto et al., 2011; Liu & Chen et al., 2006). As such, the cationic chitosan could inhibit the growth of microorganisms with opposite charge (for instance, *E. coli*- gram negative bacteria*)* (Jeon & Kim, 2000).

Besides the anti-microbial property of the polymer, the molecular structure of chitosan which consists of hydroxyl and amino groups offer coordination sites for formation of heavy metal complexes (Yu & Wu et al., 2013). As compared to hydroxyl group, amino groups in chitosan contribute to a stronger chelating and ion exchange site of cationic metal ions, such as Ag^{+} (Guibal, 2004). The ability of chelating heavy metals on chitosan opens up the potential of incorporating heavy metals bacteria biocides to improve the bacteria eradication efficiency of chitosan alone.

Chitosan is more commonly used in the form of hydrogel or other structures than its powder form. Similar to alginate, upon successful dissolving of chitosan, it can be molded into various shapes to suit respective applications. However, chitosan is not soluble in water (pH of higher than 6.5) but easily dissolved in diluted acid solvents owing to the protonation of amino group (pK_a of

6.2 to 7) (Ageev & Matushkina et al., 2007). The most common acid organic solvents used are acetic acids and formic acids (Chen & Hwang et al., 2007).

Chitosan has been shaped into various structure, such as beads, films, and fibers to suit various applications (de Alvarenga, 2011a). Up to date, many studies were done on the utilization of chitosan as coagulants and microbeads for heavy metal (iron, lead and copper) and dyes adsorption in the wastewater (Ngah & Fatinathan, 2010; Ngah & Ab Ghani et al., 2005). Meyssami and Kasaeian (2005) reported 90% removal of turbidity with the use of chitosan as a co-coagulant in olive oil wastewater treatment. Another chitosan derived material would be thin film consisting chitosan nanofibers targeting for bio-medical application. Homayoni & Ravandi et al. (2009) had successfully electrospun pure chitosan nanofibers using 80% acetic acid concentration. Moreover, chitosan film could also be used as scaffolds and wound dressing membrane in medical applications (Azad & Sermsintham et al., 2004; Madihally & Matthew, 1999).

In fact, chitosan membrane is seldom used in direct filtration due to its weaknesses in mechanical strength and chemical stability (Oh & Poh et al., 2016; Zeng & Fang, 2004). Several approaches had been done to overcome these limitations such as the use of crosslinking reagents (eg. glutaraldehyde (GA), sodium tripolyphosphate (TPP), formaldehyde (FA)) and supportive materials (Young Moon & Pal et al., 1999; Yu & Wu et al., 2013). The GA cross-linked chitosan membrane fabricated by Zeng and Fang (2004) had a significant 55% increase of tensile strength as compared to the non-crosslinked film. Similarly, a porous chitosan/ Ag membrane fabricated with GA as the crosslinking reagent showed satisfactory tensile strength (Vimala & Mohan et al., 2010). Although GA cross-linked chitosan showed an improvement in tensile stress, the membrane lost its elasticity and became brittle (Schiffman & Schauer, 2007). Therefore, it drew researchers'

attention to seek for alternative crosslinkers to cater for water filtration application. Crosslinking chitosan with TPP was suggested to give more flexibility and chemical stability (Liu & Bai et al.). The TPP cross-linked membrane was successfully used to remove humic acids from wastewater. In fact, the success in strengthened and cross-linked chitosan membranes offer the potential of chitosan to be used as a greywater filtration membrane.

Other than chemically crosslinking chitosan to improve its stability, another approach would be the formation of PEC of chitosan with another copolymers, such as alginate (Oh & Poh et al., 2016). The following section gives an overview of PEC of chitosan with copolymers.

2.9 Polyelectrolyte complex (PEC)

PEC is formed when two oppositely charged polymers are combined (Verma & Verma, 2013). The formation of PEC is mainly attributed the electrostatic interactions between these charged polymers (Verma & Verma, 2013). Due to the fact the formation of PEC do not required organic solvents and chemical cross-linker, it reduce the toxicity of end products (Verma & Verma, 2013). As a result, PEC is gaining attention especially in medical applications, drug release, membrane, environmental sensors, antistatic coating, chemical detectors and etc. (Lee & Lee et al., 2003; Sæther & Holme et al., 2008).

Other than formation of PEC between natural polymers, PEC can also be formed between natural and synthetic polymers, for instance PEC between synthetic polymers, protein PEC, surfactant PEC and charged drugs PEC (Verma & Verma, 2013). Birch and Schiffman (2014) fabricated nanoparticles using chitosan as the base material. Instead of cross-linking the chitosan with ionic salt, polyanionic pectin was used as the counter charged polymer for the fabrication of

PEC nanoparticles. The PEC formed by using the two polymers was found to retain its stability for the course of 14 days. It shows that the PEC of the two functionalized polymers is a potential material to be utilized as antimicrobial wound dressing (Birch & Schiffman, 2014). Similarly, Lee & Lee et al. (2003) used chitosan to form PEC with hyaluronic acid. The sponge PEC wound dressing was found to be lower in crystallinity, which makes the wound dressing softer and less brittle. It could be deduced that the formation of PEC between polymers could improve the stability and mechanical properties of the original material to suit its applications.

The formation of PEC between polycationic chitosan and polyanionic alginate is also one of the renowned PECs. The PEC formed using the two naturally occurring polyanionic polymers was found to exhibit immune stimulating property making it an attractive material to be utilized for medical applications (Sæther & Holme et al., 2008). Sæther & Holme et al. (2008) represented the PEC between chitosan and alginate as a core-shell model. According to the net charge ratio (K) of <1, ≈ 1 and >1, the size of the PEC particles varied from one to the other. With the K value ≈ 1, PEC particles formed between chitosan and alginate was found to be largest due to the agglomeration of polymers, while $K > 1$ and < 1 produced PEC particles that were smallest with stabilizing shell structure formed around the particles (Sæther & Holme et al., 2008). As such, it could be deduced that PEC particle size could be varied to suit respective application by carefully controlling the net charges between the two polymers. For example, excess chitosan or alginate should be used when fabricating smaller PEC particles for applications that require high surface area.

However, as mentioned previously, the antimicrobial effect of chitosan is mainly attributed to its naturally occurring polycationic charges. Due to the fact that formation of PEC is based on the electrostatic interactions between polymers, the antimicrobial effect of polymers could be hindered. Thus, biocides such as silver nanoparticles (AgNP) can be introduced to enhance the antimicrobial property of the PEC network.

2.10 Silver nanoparticles (AgNP)

Nanoparticle is defined as a particle that has at least one dimension that is less than 100nm (Ahamed & AlSalhi et al., 2010). The antimicrobial property of silver has been widely recognized in literatures over the centuries (Burridge & Johnston et al., 2011). Studies showed that antimicrobial effect of silver is effective towards 16 species of bacteria including, but not limited to, *E. coli* and *Staphylococcus aureus* (Kim & Kuk et al., 2007; Prabhu & Poulose, 2012). In fact, the nano structure of silver is more auspicious, due to the fact that the effective surface area of silver in contact with the bacteria increases as the particle size reduces (Burridge & Johnston et al., 2011; Prabhu & Poulose, 2012).

AgNP is one of the nanoparticles that has the most commercial value due its potential applications (Ahamed & AlSalhi et al., 2010). In recent years, AgNP has been immobilized on various materials to introduce the antimicrobial function in end products. For instance, AgNP is widely used in medical applications, wound dressing, clothing, disinfecting and water treatment (Ahamed & AlSalhi et al., 2010; Burridge & Johnston et al., 2011; Kim & Kuk et al., 2007). Other than that, previous studies showed that, AgNP exhibit excellent anti-microbial effect when it is coupling with alginate and chitosan polymers (Lin & Huang et al., 2013; Wei & Sun et al., 2009).

2.10.1 Antimicrobial effect of AgNP

Despite AgNP is widely used due to its antimicrobial properties, the mechanisms of AgNP eradicating bacteria is debatable. AgNP can attach to the cell wall of the bacteria when the bacteria and AgNP is in contact. This could be attributed to the electrostatic interaction between the positively charged nanoparticles and negatively charged bacteria cell membrane (Kim & Kuk et al., 2007). The accumulation of AgNP and pits formation on the cell membrane alters the permeability of the bacteria, and eventually leads to the death of bacteria cell (Kim & Kuk et al., 2007; Prabhu & Poulose, 2012).

Studies also suggested that the antimicrobial effect of AgNP is contributed by the release of silver ions from the AgNP. The inactivation of bacteria occurred mainly due to the interactions between silver ions and the thiol groups (-SH) (Burridge & Johnston et al., 2011). As the interaction occurred, the silver ions can deactivate the functionality of the cell by hindering the transport of essentials cations and electron, which results in the fatality of the bacteria cell (Burridge & Johnston et al., 2011; Prabhu & Poulose, 2012). In addition to that, as the silver ions enter the bacteria cell, it attacks the oxidative phosphorylation and respiratory enzyme in the bacteria cell (Burridge & Johnston et al., 2011). As the phosphotyrosine profile of the bacteria is altered, it stops the bacteria from growing due to the signal transduction inhibition (Prabhu & Poulose, 2012). On top of that, the inhabitation of respiratory enzyme caused the formation of reactive oxygen species which is lethal to the bacteria cell (Prabhu & Poulose, 2012). In addition, AgNP was found to be able to release radicals (Kim & Kuk et al., 2007). These radicals were reported to be harmful to bacteria cell and it formed porous structure in the cell membrane that leads to the death of the bacteria cell.

Other than the effect on the cell membrane and changes on the bacteria cell permeability, studies also showed that the antimicrobial effect of AgNP is mainly due to the interaction between silver and the DNA of the bacteria cell. Due to the fact that silver is considered as a soft acid, it has a tendency to react with soft bases such as phosphorus and sulphur in the DNA of bacteria (Rai & Yadav et al., 2009). As the reaction occurs between phosphorus and sulphur bases in the DNA, it results in bacteria termination by destroying the replication function of the bacteria (Jose Ruben & Jose Luis et al., 2005). As a result, AgNP is selected for incorporation in the biopolymeric membrane network to enhance the antimicrobial effect of the original membrane to ensure the treated greywater is free of pathogenic bacteria such as *E. coli* and coliforms bacteria.

CHAPTER 3

3 Materials and methods

3.1 Chapter overview

The chemicals and consumables used in this research are listed in this chapter. Research flowchart is also included to depict the sequence of research work involved in this project. In addition, experimental and analytical procedures involved in this project will be elaborated in this chapter.

3.2 Chemicals and reagents

Table 3.1 lists all the chemicals and reagents used in this research. The chemicals were purchased from suppliers and used without further purification.

Table 3.1 List of chemicals and reagents

Chemicals	Brand	Properties	Purpose of use
Chitosan	Sigma Aldrich	M_w > 310 kDa	Membrane fabrication
Sodium alginate	FMC biopolymer		
Silver nanoparticle	Sigma Aldrich	TEM size: 60 nm, 0.02 mg/mL in sodium citrate buffer	
Poly (ethylene) glycol (Multiple molecular weight)	Sigma Aldrich	M_w = 200, 400, 600, 1000, 2000, 3000, 6000, 10000 Da	Molecular weight cut-off study
Poly (ethylene) oxide	Sigma Aldrich	M_w =100000 Da, 350000 Da	
Silver test kit	HACH	-	Treatment analysis
Acetic acid	Friendemann Schmidt	98%- AR Grade	Solvent for CS

Chemicals	Brand	Properties	Purpose of use
Sodium hydroxide	SYSTERM	Pellets	De-protonation of CS
Chemical oxygen demand (COD) digestion vials (LR) and (HR)	HACH	3 – 150 mg/ L 20 - 1500 mg/ L	Treatment analysis
5-Days biological oxygen demand (BOD_5) nutrient pillow, 300 mL **Nitrification inhibitor** **Formula 2533™, TCMP**	HACH, USA	-	Treatment analysis
Distilled water	-	-	
Ultrapure water	-	-	
OXOID Brilliance *E. coli* selective agar	OXOID CM 1046B	Powder	Treatment analysis
Sodium chloride	Sigma Aldrich	ACS reagent	Preparation of 2X SSC saline solution for bacteria suspension
Sodium citrate	Sigma Aldrich	Powder	
Propedium iodide	Acros brand	95 %	Bacteria inactivation
Ethanol (70%)	-	-	Disinfection

3.3 Experimental flowchart

Figure 3.1 gives the flow of this research project, which the studies in this research project can be divided into four major phases.

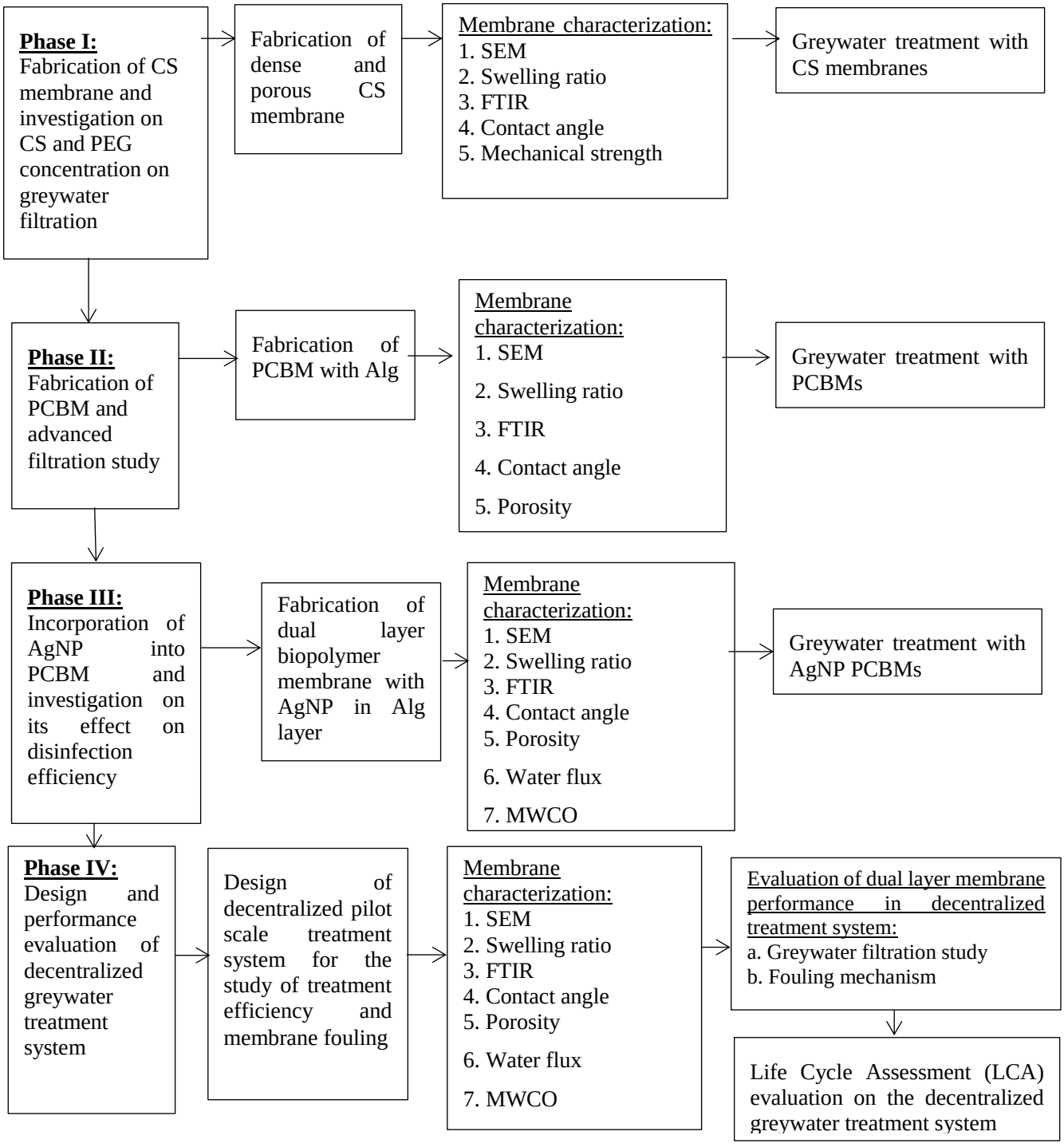

Figure 3.1. Research flowchart

3.4 Biopolymeric membrane fabrication

3.4.1 Phase I: Fabrication of CS membrane to investigate the variation of CS and PEG concentration on greywater filtration

During the preliminary development of single layer CS membrane, concentration of CS was varied from 0.5 wt% to more than 2 wt%. It was found that membrane fabricated using 0.5 wt% chitosan concentration was too fragile to be handled. On the other hand, when the CS concentration was varied to higher than 2 wt%, the solution became too viscous to be stirred, and it increased the energy required to obtain a homogenous chitosan solution for casting. As a result, the concentration of CS for the fabrication of membrane in phase I was fixed between 1 wt% to 2 wt%.

Phase I mainly focuses on the effects of various PEG concentration on the properties of CS membrane and its greywater treatment efficiency. During the preparation of the porous CS membrane solution, 1 g of PEG M_w 6000 (P-6000) was dissolved in 100 mL of 2 vol% acetic acid (Ac). The solution was allowed to stir for 15 mins. Thereafter, 1 g of CS powder was added into the solution and stirred for 4 hours, until a homogenous light yellow colour mixture was obtained. PEG concentration was varied from CS: PEG weight ratio of 1: 1, 4: 3, 2: 1 to 4: 0. The solution was then degassed for 24 hours before 20 mL of the CS-PEG solution was casted on a petri dish using syringe and dried in the convection oven (Brand: Memmert, Model: UF 55) at 60 °C for 24 hours. Similar dissolution and casting procedures were repeated to prepare 2 wt% CS membranes by dissolving 2 g of CS powder in 100 mL Ac solution.

Upon drying, membrane was removed from the oven and deprotonated with 15 mL of 2wt% NaOH solution for 15 mins. After that, the membrane was washed multiple times with clean

DI water to remove excess NaOH. The membrane was then immersed 24 hours in clean DI water and 2 hours of 80 °C hot water bath to wash off P-6000 and generate porous structure. The conditions of membranes fabricated in Phase I is tabulated in Table 3.2.

Table 3.2 Single layer CS membrane fabrication in phase I

CS concentration (wt%)	CS : PEG (wt% : wt%)
1	4 : 0
	2 : 1
	4 : 3
	1 : 1
2	4 : 0
	2 : 1
	4 : 3
	1 : 1

3.4.2 Phase II - (1) and (2): Fabrication of PCBM and advanced filtration study

In phase II, Alg was incorporated to form PCBM with CS. Phase II emphasizes on the changes on the membrane from a single layer to a dual layer structure. The membranes fabricated in phase II are named dense PCBM [Phase II (1)] and porous PCBM [Phase II (2)]. Due to the fact that, CS layer is to be maintained as the dominant structure of the membrane, the concentration of Alg was not varied beyond 2 wt%. During the fabrication of dense PCBM, 1 wt% of P-6000 was first dissolved in 2 vol% Ac. This was followed by the addition of 1 wt% CS into the earlier solvent mixture and continuously stirred for 4 hours until a homogenous light yellow solution was obtained. The weight ratio of CS: PEG was maintained at 1: 1, which produces highest water flux amongst other CS: PEG ratio (Oh, Poh & Chong, Unpublished work). On the other hand, 0.5 wt% of Alg was dissolved in ultrapure (UP) water. Polymer solutions with 1 wt% and 2 wt% Alg were also prepared. All the homogeneous-stirred solutions were allowed to degas for 24 hr to obtain bubble-free solution prior to the membrane casting process.

During the membrane casting process, 5 mL of 0.5 wt% Alg solution was casted on a standard petri dish. Upon successive formation of the Alg membrane layer, 20 mL of CS/ PEG solution was casted on top of the first Alg layer to form PCBM. PCBMs were also fabricated with 1 wt% and 2 wt% Alg as the first PBCM layer. The casted solution in the standard petri dish was placed on a flat surface for approximately 10 mins before drying in a convective oven operated at 60 °C for 24 hours.

After the convective drying process, the PCBMs were removed from the oven and treated with 2 wt% of sodium hydroxide (NaOH) solution for 15 mins. All PCBMs were washed multiple times with UP water to remove excess NaOH and solvents. The membranes were then removed from the petri dishes and immersed in UP water for 24 hours, followed by 2 hours immersion in a hot water bath at 80 °C, in order to wash away the PEG in the membrane skeletal network and to generate porous structure. Similar procedure was adopted for the fabrication of porous PCBM, but with the addition of PEG in the Alg solution according to its various fabrication conditions.

Figure 3.2 shows the flow diagram of the fabrication steps while Table 3.3 lists the PCBM fabrication conditions and abbreviations used throughout this study.

Table 3.3. PCBM fabrication conditions

	Alg: PEG (wt% : wt%)	CS : PEG (wt% : wt%)	Membrane name[i]
Phase II (1): Dense PCBM	0.5: 0	1 : 1	0.5A1CP
	1: 0	1 : 1	1A1CP
	2: 0	1 : 1	2A1CP
Phase II (2): Porous PCBM	0.5: 0.5	1 : 1	0.5AP1CP
	1: 1	1 : 1	1AP1CP
	2: 2	1 : 1	2AP1CP

[i] C- Chitosan, A – Alginate, P – Poly(ethylene) glycol

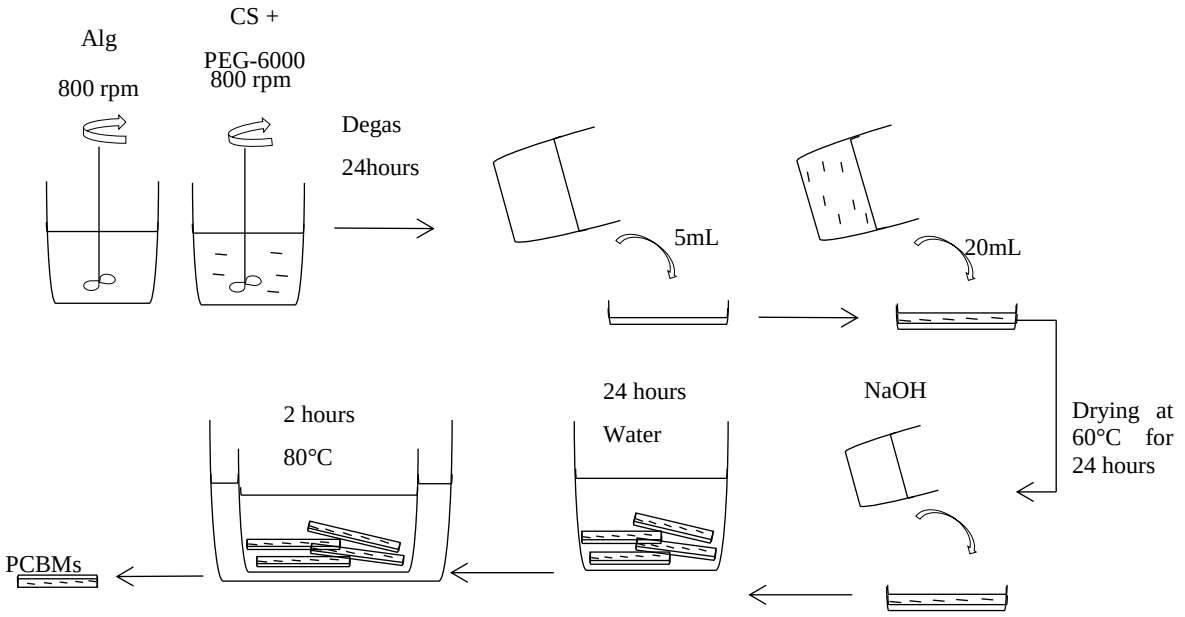

Figure 3.2. Flow diagram of PCBMs fabrication

3.4.3 Phase III: Incorporation of AgNP into porous PCBM and investigation on its effect on disinfection

The fabrication process of membrane in Phase III is similar to Phase II. The membrane selected from Phase II (eg. 2AP1CP) was modified in Phase III by incorporating various concentrations of AgNP in the Alg layer, while the preparation of 1 wt% CS-PEG solution remains the same.

The Alg side of the PCBM was selected as the active side of the membrane due to the hydrophilicity of Alg. As such, AgNP was loaded to the Alg layer of the PCBM. During the preparation of Alg solution with AgNP, 2 g of PEG was first dissolved in clean UP water. Upon dissolution, 2 g of Alg was added and stirred continuously at 800 rpm to obtain a clear yellow solution. After degassing for 24 hours, 7.5 mL of 0.02 mg/ mL AgNP suspension was added drop

wise into the Alg mixture. The solution was allowed to stir for another 15 mins at 800 rpm to disperse AgNP in the Alg mixture. The resulting solution contains 1.5 ppm AgNP in a 2 wt% Alg-PEG solution. The concentration of the AgNP was varied from 0.5 ppm to 1.5 ppm in phase III.

The casting and de-protonation procedures of the membrane are the same, as mentioned in Section 3.4. The conditions of the AgNP PCBM are given in Table 3.4.

Table 3.4 AgNP PCBM fabrication conditions in Phase III

	AgNP concentration (ppm) in 2AP1CP	**Membrane name [ii]**
	0	0 PCBM
AgNP	0.5	0.5 PCBM
PCBM	1.0	1.0 PCBM
	1.5	1.5 PCBM

[ii]PCBM – Polyelectrolyte Complex Bilayer Membrane

3.5 Membrane characterization

The membranes prepared in this project were subjected to characterization before they are used for greywater filtration. The membranes were characterized in terms of its physical and molecular structure, swelling ratio, water flux at fixed pressure, molecular weight cut-off (MWCO) and mechanical property. The following sections describe the procedures to conduct membrane characterization.

i. Scanning Electron Microscope (SEM)

The structure of the membrane samples was analysed using SEM (Brand: Hitachi, Model: S-3400-N). The surface morphology and cross sectional structure of samples was scanned without coating.

ii. Fourier Transform Infrared Spectroscopy (FTIR)

Meanwhile, changes in molecular structure of the membranes during the fabrication process were investigated using FTIR (Brand: Thermo Scientific, Model: Nicolet iS10). The transmittance wavelength for this study was in the range of 525 cm^{-1} to 4000 cm^{-1}. Each spectrum was obtained by overlapping 16 scans.

iii. Contact angle study

Goniometer (Brand: Ramé-hart instrument co.) was used to study the hydrophilicity of the membranes. The study was conducted by dropping 0.2 μL of clean UP water on the surface of the membrane. Due to the changes of the water contact angle when water was dropped on the membrane, the water droplet was allowed to stabilize for 6 minutes before the final contact angle was captured. The study was repeated 3 times to obtain an average surface contact angle for every membrane tested.

iv. Swelling ratio

The swelling ratio was measured to investigate the water uptake ability as well as the swelling ability of membranes. In this study, the membranes were cut into 1 cm width × 1 cm length segments and immersed into UP water at room temperature. Thereafter, the membranes were removed from the UP water bath and wiped with filter paper to remove excess water on the membrane surface. Subsequently, the membranes were weighed at different time intervals of 5, 10, 15, 20, 25, 30, 60, 90 and 120 mins. The study was repeated twice for each membrane and the swelling ratio was calculated using Eq. 3.1 as shown below:

$$\textbf{Swelling ratio (\%)} = \frac{W_{wet} - W_{dry}}{W_{dry}} \times 100 \quad \text{(Eq. 3.1)}$$

where, W_{wet} is the weight of wet membrane

W_{dry} is the weight of dry membrane

v. Equilibrium Moisture Content (EMC)

The EMC of membrane was recorded to identify the amount of water can be stored in a membrane at equilibrium state. For the study of EMC, the membrane was cut and immersed into DI water for 24 hr. Excess water on the surface of the specimen was removed using clean filter paper, and weighed to the accuracy of four decimal places to obtain the wet weight (W_{wet}). Then, the specimen was oven dried at 60 °C for 4 hours weighed to get the dried weight (W_{dry}). EMC was then calculated using Eq. 3.2.

$$\textbf{EMC (\%)} = \frac{(W_{wet} - W_{dry})}{W_{wet}} \times 100 \quad \text{(Eq. 3.2)}$$

where, W_{wet} is the weight of the wet membrane

W_{dry} is the weight of the dry membrane.

vi. Tensile strength

Texture analyser (Brand: TA.XT Plus) was used to evaluate the mechanical property of membranes. The membranes were cut into 25 mm × 75 mm films and crosshead speed of 30 mm/min was used to pull the films to their breaking point. The test was repeated five times to obtain average stress and strain of the material. Tensile strength of the membrane was calculated with Eq. 3.3 as below:

Tensile strength (MPa) = $\frac{F_l}{A}$ (Eq. 3.3)

where, F_l is the maximum force required to break the membrane sample

A is the cross sectional area of the membrane

vii. Water flux

Membrane water flux was investigated in a dead-end stirred cell filtration unit (Brand: Sterlitech, Model: HP 4750) at various operating pressures [eg. 1, 2, 3, 3.2, 4 bar (g)]. A clean membrane was inserted into the dead-end stirred cell on a metallic support, where the cell was loaded with 250 mL of clean UP water. The weight of permeate collected with respect to various operating pressures was recorded using a weighing balance, which is connected to a computer to collect data over the duration of the experiment. The duration of water flux study was fixed at 30 minutes and a stirring speed of 300 rpm. The set-up of the dead-end stirred cell filtration unit is shown in Figure 3.3.

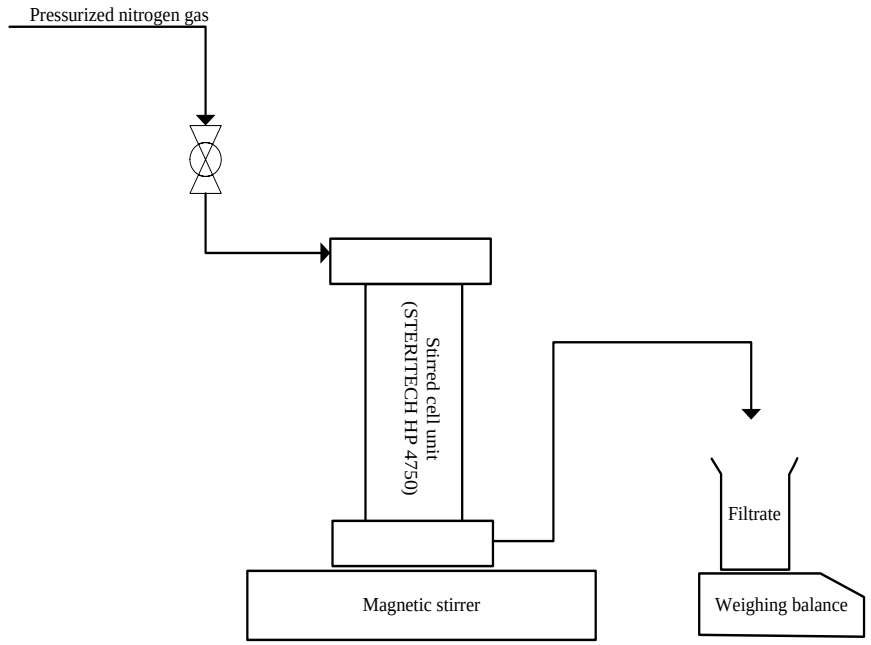

Figure 3.3. Dead-end stirred cell filtration unit (Brand: Sterlitech, Model: HP 4750)

Subsequently, the water flux was calculated based on Eq. 3.4. Average water flux for each membrane sample was obtained from 5 repetitions this study.

$$\textbf{Flux, J } \left(\mathbf{L/_{m^2 hr}}\right) = \mathbf{V_{permeate}} \,/\, (\boldsymbol{A_e} \times \mathbf{t}) \quad \text{or} \quad \mathbf{M_{permeate}} \,/\, (\boldsymbol{A_e} \times \mathbf{t}) \qquad \text{(Eq. 3.4)}$$

where, $V_{permeate}$ is the volume of permeate collected in liter/ $M_{permeate}$ is the mass of permeate collected in grams

A_e is the effective area of the membrane in m^2

t is the duration of the filtration in hr

viii. Molecular weight cut-off (MWCO)

MWCO of a membrane is defined as the lowest molecular weight solute (in Da), in which 90 to 95% of the solute is rejected by the membrane (Schock, Miquel & Birkenberger, 1989). In essence, 0.1 g of PEG M_w = 2000 Da (P-2000), PEG M_w = 3000 Da (P-3000), PEG M_w = 4000 Da (P-4000), PEG M_w = 6000 Da (P-6000), PEG M_w = 10,000 Da (P-10,000), PEG M_w = 100,000 Da (P-100,000), PEG M_w = 350,000 Da (P-350,000) were dissolved in UP water separately. Then, 250 mL of PEG solution was filled into the dead end stirred cell unit loaded with fresh membrane. Permeate was then collected under the operating pressure of 3 bar (g) and stirring speed of 300 rpm to avoid concentration polarization and accumulation of solutes on the surface of membranes, which might lead to the blockage of pores. A new membrane was used for every molecular weight tested.

Both the feed and permeate were analysed with a TOC analyser (Brand: O.I. Analytical Aurora, Model: 1030) to determine the TOC concentration before and after solute rejection. The concentration of PEG was quantified in terms of TOC and TOC rejection was calculated using Eq. 3.5 as shown below:

$$\textbf{Rejection (\%)} = \frac{C_i - C_f}{C_i} \times 100 \qquad \text{(Eq. 3.5)}$$

where, C_i is the initial TOC concentration of feed solution in mg L^{-1}

C_f is the final TOC concentration of permeate in mg L^{-1}

ix. Thermogravimetric Analyser (TGA)

TGA was used to identify the presence of AgNP in membrane. The membrane samples were first pre dried in an oven at 60°C for 24 hours. Then, the dried films were cut into small pieces and placed into the combustion chamber. The range of temperature studied was from 25°C to 800°C with the presence of nitrogen gas.

x. Flux decline

Deposition of pollutants on the surface of the membrane can cause the membrane flux to decline from its initial state. In the dead-end filtration unit, UP water flux was first pressurized to 3 bar (g) and the water flux was recorded as the control over the duration of 30 mins. Then, UP water was replaced with greywater water and flux was obtained at the same operating pressure and duration. The normalized flux and flux decline percentage of the membrane were calculated using Eq. 3.6 and Eq. 3.7.

$$\textbf{Normalized flux} = J/J_o \quad \text{(Eq. 3.6)}$$

$$\textbf{Flux decline percentage} = (1 - J/J_o) \times 100\% \quad \text{(Eq. 3.7)}$$

Where J is the solution flux in L m^{-2} hr^{-1}

J_o is the initial flux in L m^{-2} hr^{-1}

xi. Bacteria inactivation

Propedium iodide (PI) fluorescent dye was used to investigate the viability of bacteria on the surface of the membrane. PI fluorescent dye will only penetrate into the dead bacteria cell and bind to its DNA/ RNA by intercalating the bases. The intensity of fluorescent dye is then enhanced

by 20 to 30 times to emit red fluorescent color. The excitation of PI dye is at the wavelength of 535 nm and emission wavelength of 617 nm.

In order to carry out the bacteria inactivation study, PI was first dissolved in UP water to make a concentration of 1 $mgmL^{-1}$. The solution was stored in a 4°C refrigerator in a dark condition. After greywater water filtration, the used membrane was carefully removed from the filtration unit and cut into a segment of 1.5 cm × 1.5 cm. Thereafter, it was immersed in 2X SSC buffer solution. The segment of the membrane was then removed from the buffer solution and 300 μL of PI solution was added onto the membrane and incubated for 5 mins before viewing under a fluorescent microscope (Brand: Olympus, Model: BX-51). TEXAS RED filter with 100x magnification was used for the purpose of this study.

3.6 Greywater sampling

Due to the low volume of generation and high level of oil and pollutants in kitchen greywater, kitchen greywater was not recommended for recycling (Boyjoo & Pareek et al., 2013b). In addition, laundry greywater is also excluded from recycling due to its high level in phosphate, heavy metals and low biodegradability (Boyjoo & Pareek et al., 2013b). Therefore, bathroom greywater was selected for studies in this project. Greywater is normally collected on the day of the experiment, which was provided by a single individual staying in Lagoon View Condominium, Sunway, Selangor Darul Ehsan, Malaysia (GPS coordinate: 3.067255, 101.605100). The bathroom greywater sample was characterized to obtain its characteristics before treatment upon receiving the samples in the lab. The greywater sample was stored in refrigerator at a temperature of 4°C when not in use. Table 3.5 lists the average characteristics of greywater used throughout this study.

Table 3.5. Bathroom greywater characteristics

	Unit	Average	Standard Deviation
pH	-	6.6	0.18
Turbidity	NTU	120.7	55.97
TSS	ppm	151.0	56.23
COD	ppm	398.2	131.57
BOD_5	ppm	179.0	71.66
E. coli	cfu $100mL^{-1}$	1.47×10^5	2.25×10^5
Other coliforms	cfu $100mL^{-1}$	1.99×10^6	3.34×10^6

3.7 Greywater treatment

3.7.1 Stirred cell filtration unit

Dead-end stirred cell filtration unit (Figure 3.3) was used to evaluate the greywater treatment performance in phases I, II and III. To study greywater treatment efficiency, 250 mL of UP water was fed into the dead-end stirred cell filtration unit for membrane compaction. After 30 minutes of membrane compaction using clean UP water, similar amount of greywater was replaced in the stirred cell unit and pressurized to desired pressures [eg. 1, 2, 3, 3.2, 4 bar (g)] using nitrogen gas. Treated greywater was collected in a clean Schott bottle for 30 mins. The characterization of treated greywater sample includes pH, TSS, turbidity, COD, BOD_5 and bacteria enumeration. Details of analytical methods conducted will be covered in Section 3.8.4. The treatment/ removal efficiency was calculated with Eq. 3.8.

$$\textbf{Treatment efficiency/ Removal percentage (\%)} = \frac{C_i - C_f}{C_i} \times 100 \qquad \text{(Eq. 3.8)}$$

where, C_i is the initial concentration in mg L^{-1}

C_f is the final concentration in mg L^{-1}

3.8 Phase IV: Design and performance evaluation of decentralized greywater treatment system

3.8.1 Membrane fabrication

The membrane identified to be optimum for greywater filtration from Phase III (1.5 PCBM) was casted at a larger scale in Phase IV to cater for the fabricated decentralized greywater treatment system. Preparation of solutions, drying, de-protonation, membrane dipping and annealing procedures are similar to Phase III. However, instead of casting the membrane on a standard petri dish, the membrane in Phase IV was casted in 15 cm diameter glass petri dish. The fabricated membrane was also characterized according to the procedures described in Section 3.5.

3.8.2 Decentralized greywater treatment system

In Phase IV, the treatment efficiency of membrane was evaluated in a decentralized greywater treatment system. The system consists of:

1. 1 × Screener
2. 1 × 20 L greywater storage tank
3. 1 × Electromagnetic metering pump
4. 1 × Membrane unit
5. 1 × 20 L treated greywater tank

Figure 3.4 illustrates the process flow diagram (PFD) of the decentralized greywater treatment unit. During the experiment, collected greywater will be transferred into the greywater

storage tank, which is installed with a mesh screener with an average mesh size of 80 μm. Thereafter, the greywater tank is pressurized with an electromagnetic metering pump (Brand: IWAKI, Model: EHN-C21VC3R) that could provide a maximum output pressure of 7 bar (g). In addition, the pump also features a pressure relief valve that act as the pressure controller to this system. As such, the greywater pressure in the membrane unit could be regulated between 1 bar (g) to 4 bar (g).

The pressurized greywater will be delivered to a cylindrical membrane unit with an inner diameter of 12 cm and height 12 cm. The unit also includes a 12 cm diameter porous metallic supporter and a base cover. The thickness of the vessel wall was designed to sustain the pressure up to 10 bar (g) of the unit. The porous metallic support was included to provide extra support to the membrane during operation.

Permeate from the greywater filtration system will be collected in the treated greywater tank. There are also sampling valves throughout the system, as shown in Figure 3.4.

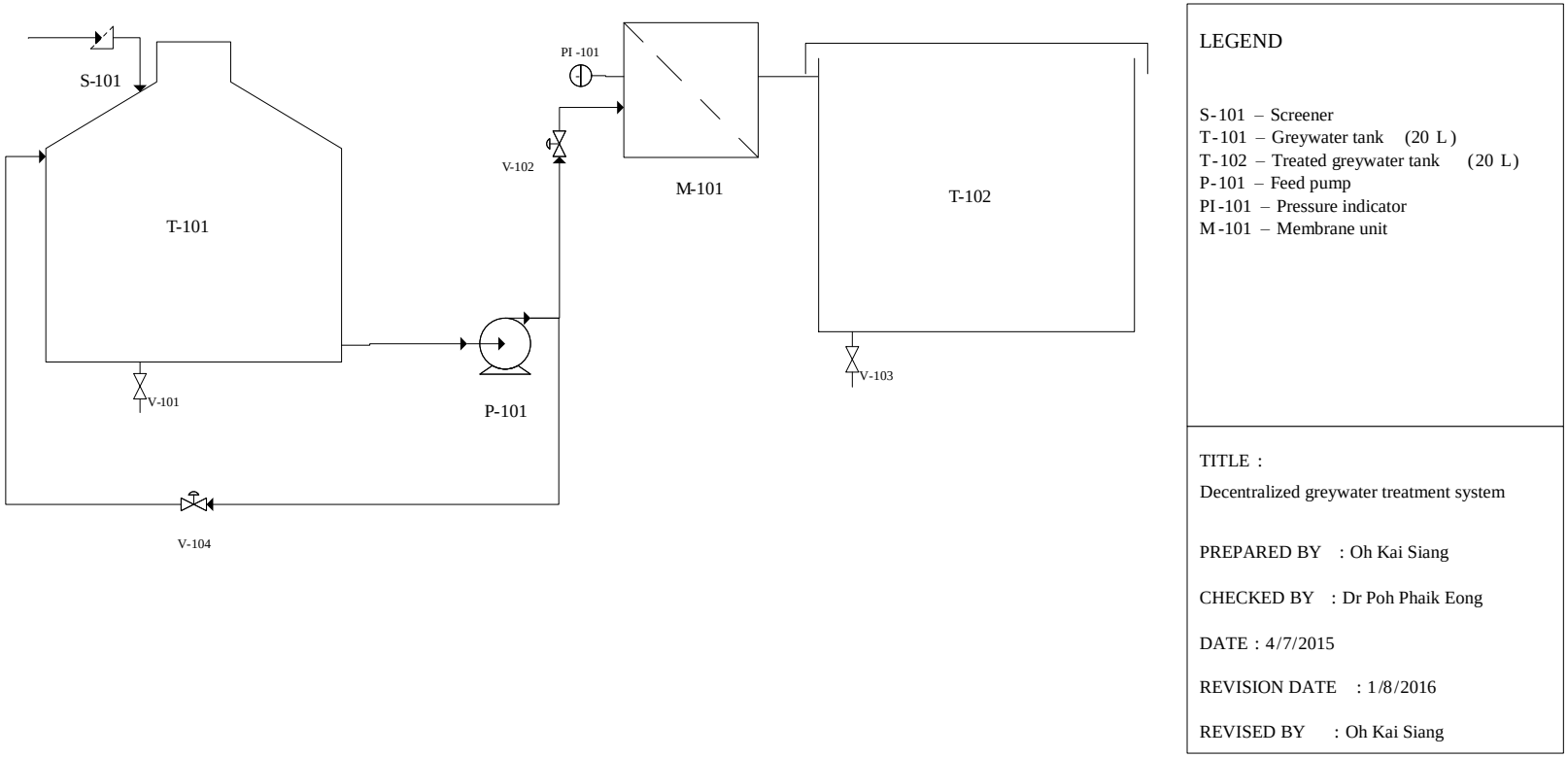

Figure 3.4 PFD of decentralized greywater treatment system

3.8.3 Greywater treatment efficiency in decentralized greywater treatment system

During operation of the decentralized greywater treatment system (Figure 3.5), greywater was pressurized and sent into the membrane unit at 3 bar (g) for a duration of 30 mins. The treated greywater was collected in a clean beaker and the quality of the treated greywater was analysed. To simulate an automatic operated greywater recycling system, the pump was stopped for 2 hours and greywater remaining in the membrane unit was left to be filtered with the remaining pressure in the membrane unit, with the permeate channelled to the treated greywater tank. Similarly, sample was collected from the treated greywater tank and analysed in terms of pH, TSS, turbidity, COD, BOD_5 and bacteria enumeration to evaluate the performance of the membrane in the decentralized greywater treatment system. The treatment/ removal efficiency was then calculated using Eq. 3.8 provided in Section 3.7.1. The detailed procedures for wastewater parameters analysed will be elaborated in the next section.

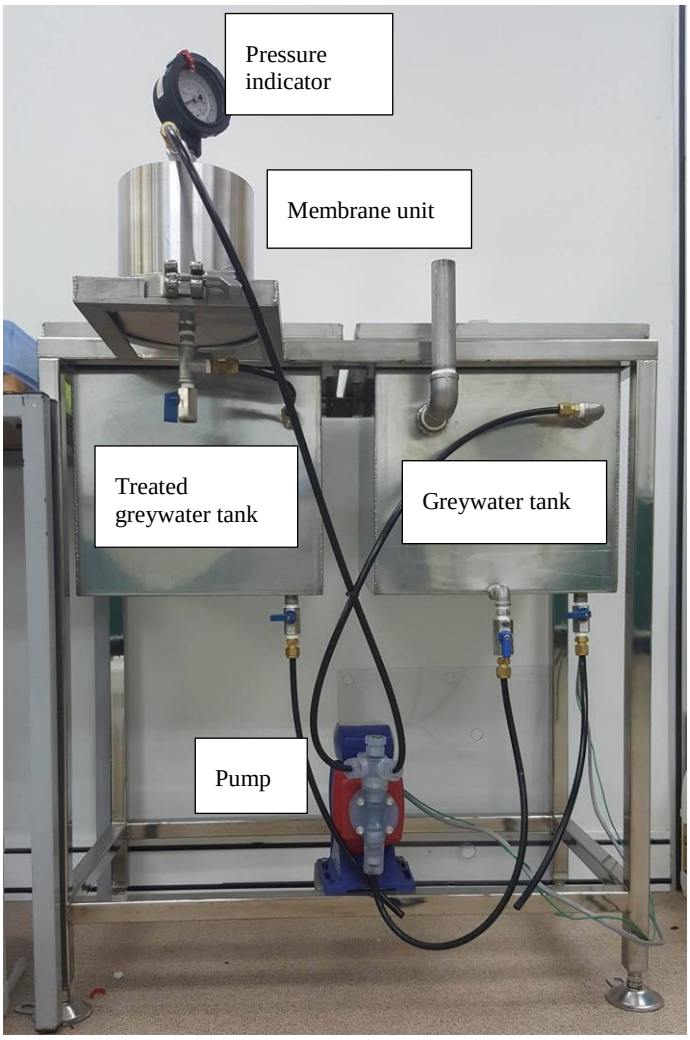

Figure 3.5. Set up of the decentralized greywater treatment system

3.8.4 Analytical methods for greywater treatment

i. Total suspended solids (TSS)

TSS value of the greywater was determined using HACH photometric method 8006, where 10 mL of the homogenous sample is filled into a square sample cell and swirled before inserted into the HACH spectrophotometer (Brand: HACH, Model: DR 2800). The TSS was measured at the absorbance wavelength of 810 nm.

ii. Turbidity

The turbidity of greywater samples was measured using turbidimeter (Brand: HACH, Model: 2100Q). The greywater sample was filled up to the line in the sample cell and swirled before getting the readings. The turbidity of the greywater samples were recorded in terms of NTU.

iii. pH

pH of greywater and treated effluent samples were recorded at ambient temperature using a pH meter (Brand: METTLER TOLEDO).

iv. Chemical oxygen demand (COD)

Colorimetric method (HACH Method 8000) was employed for this study. This technique complies with the APHA 5220 D Standard Methods. To analyse the COD of greywater samples, 2 mL of sample was pipetted into COD vials and transferred to COD digester (Brand: HACH, Model: DRB 200). The digestion was carried out at 150°C for 120 mins. Subsequently, the samples were allowed to cool to room temperature before taking the reading with a spectrophotometer (Brand: HACH, Model: DR 2800) at the wavelength of 620 nm.

v. 5- days oxygen demand (BOD_5)

BOD_5 readings for were obtained in accordance to HACH Method 8043. Dilution water was prepared by dissolving one nutrient buffer pillow in 300 mL of clean distilled water. Then, 0.16 g of nitrification inhibitor powder Formula 2533^{TM} was weighed into a clean Wheaton bottle (300 mL). Thereafter, a known volume of greywater sample was transferred into the Wheaton bottle and dilution water was filled into the Wheaton bottle to reach the lip of the bottle. The stopper was then placed to cover the bottle during the incubation.

The initial dissolved oxygen (DO) was measured using DO meter (Model: YSI 5000) and incubated in thermostatic cabinet (Brand: Lovibond, Model: ET618-4) for 5 days at 20°C. After the incubation period, the sample was removed from the incubator and measured using the DO meter to obtain a final DO measurement. The BOD_5 can be calculated using Eq. 3.9.

$$\mathbf{BOD_5} = \frac{DO_i - DO_f}{P} \quad \text{(Eq. 3.9)}$$

Where, DO_i is the initial DO in mg L^{-1}

DO_f is the final DO in mg L^{-1}

P is the fraction of sample x divided by total volume eg. ($\frac{x}{300}$)

vi. Bacteria (E. coli and other coliforms) and log removal value (LRV)

In order to identify bacteria and determine the disinfection efficiency of the membrane, selective agar (Brand: OXOID Brilliance *E. coli*, Model: CM 1046B) was used to enumerate the bacteria colonies in the greywater samples.

0.1 mL of the greywater sample was pipetted to the selective agar and spread evenly on the agar using spread plate technique. The sample was then incubated for 24 hours in the incubator (Brand: Redline, Model: RI-115) operating at 37°C. After incubation, the sample was carefully removed from the incubator and plate count technique was used to enumerate the number of colonies present on the selective agar. The number of colonies is recorded in terms of colonies forming unit per 100 mL (CFU 100 mL^{-1}). The LRV was then calculated with Eq. 3.10,

$$LRV = \log_{10} \frac{Ci}{Ce} \quad \text{(Eq. 3.10)}$$

Where C_i is the influent bacteria concentration and C_e is the effluent bacteria concentration

All the parameters in section 3.8.4 was repeated for 4 times. The values recorded are the arithmetic mean of each parameter.

3.8.5 Long-term flux decline study

To evaluate the life span of the fabricated membranes, flux of the membrane was recorded when in use for multiple cycles to evaluate the flux decline. In this particular study, the greywater flux was collected at two filtration conditions, which includes those permeate collected for 30 mins of 3 bar (g) filtration and 2 hours of filtration using the remaining pressure in the membrane unit without pressurizing the greywater. The normalized flux was then calculated using the same method described in section 3.5x.

3.8.6 Sustainability analysis

Cradle-to-grave life cycle assessment (LCA) was performed to identify the environmental impacts associated to the fabrication of AgNP PCBM. Due to the fact that comparison LCA is a

useful tool to identify suitable material production route from the environmental perspective (Piccinno & Hischier et al., 2015), a conventional nylon 66 membrane was included as a comparison to AgNP PCBM. GABI life cycle assessment software was used to conduct the analysis. In order to conduct LCA of the membranes effectively, a system boundary was first identified and the functional unit of the membranes was defined. Thereafter, the inputs and outputs of the processes such as the materials and resources required for the fabrication of membranes were identified. Last but not least, result analysis was conducted based on the data obtained and the environmental impacts were categorized into different impact categories and indicators groups.

i. System boundary

Due to the fact that both systems were assumed to have the same system configurations and treatment basis in this LCA study, only the materials required to fabricate the membranes, energy and resources involved in the extraction, fabrication and landfill of the membrane were included in the LCA. As shown in Figure 3.6, the transportation and reuse of greywater were excluded from the LCA study, as the two systems considered in this study was assumed to process the same amount of greywater and the treated greywater was going to be used for similar activities (eg. reuse in toilet flushing and outdoor irrigation.

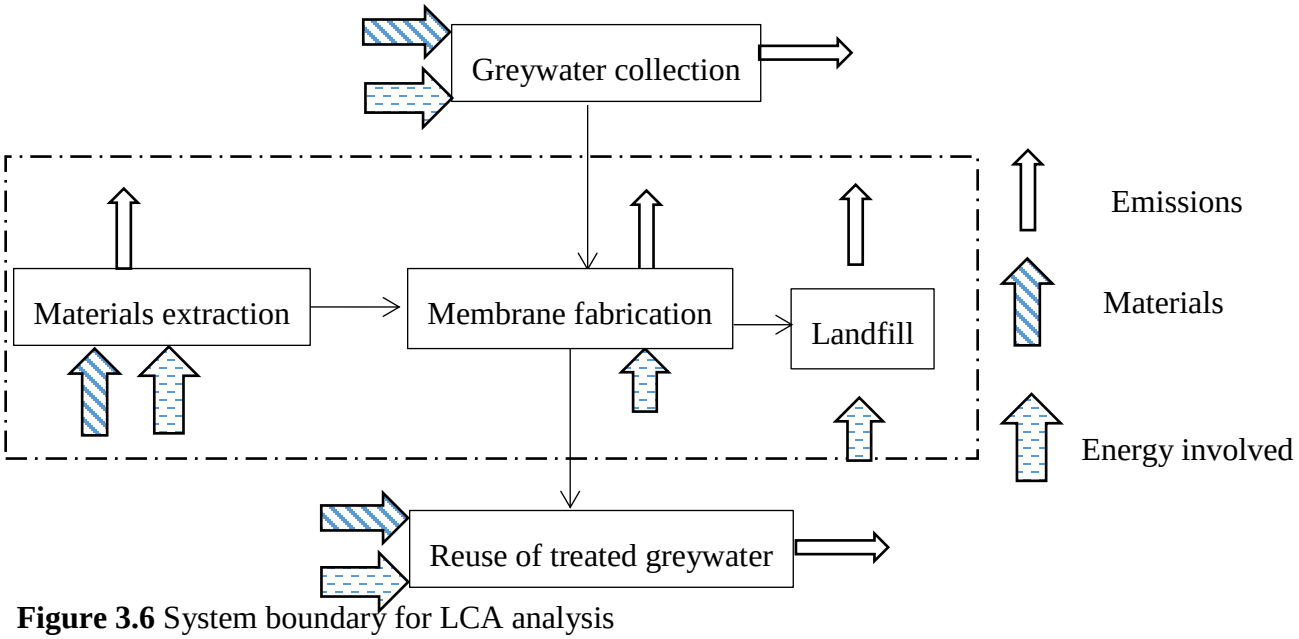

Figure 3.6 System boundary for LCA analysis

ii. Functional unit

Functional unit (FU) is defined as the unit of product generated in a certain process in its designed life span (Memon & Zheng et al., 2007). In the case of greywater treatment system, treated greywater is considered as the "product", while the "process" refers to the treatment facilities. In order to make an effective comparison, the same volume of treated greywater was retained in the analysis of both treatment systems. As such, the FU was defined based on processing of 17.9 L h^{-1} of water. Based on Poletto & Duarte et al. (2011), 1.12 m^2 of nylon 66 membrane was needed, while in this study, 1 m^2 of AgNP PCBM is required to process 17.9 L h^{-1} water. cation of respective membranes.

Table 3.6 provides the list of materials required for the fabrication of respective membranes.

Table 3.6. Materials required for the fabrication of membranes based on FU of 17.9 l h^{-1} water processed

Membrane	Polyamide (g)	HCl (g)	CS (g)	Alg (g)	Ac (g)	NaOH (g)	AgNP (g)	PEG (g)	Reference
Nylon 66	67.1	124.1	-	-	-	-	-	-	Poletto & Duarte et al. (2011)
AgNP PCBM	-	-	94.1	47.4	188.2	141.0	0.013	141.1	This study

iii. Inventory analysis

As mentioned in Section 3.8.6i, the LCA study involved 3 major stages including materials extraction, membrane fabrication and landfill of the membrane. The amount of materials required for membranes (eg. nylon 66 and AgNP PCBM) fabrication was tabulated in cation of respective membranes.

Table 3.6. In order to fabricate the nylon 66 membrane, 67.1g of polyamide per FU and 124.1g of HCl per FU is needed. Inputs and outputs data of the polyamide extraction from crude oil to natural gas was adopted from GREET model (Keoleian & Miller et al., 2012). In the GREET model, the data covers intermediate processes including production of hexamethylene diamine and adipic acids (Keoleian & Miller et al., 2012). Eventually, hexamethylene diamine and adipic acids will be reacted to produce nylon 66 (Keoleian & Miller et al., 2012). In the membrane fabrication process, polyamide will be dissolved in HCl, casted and immersed into the coagulation bath (water) to complete the membrane formation process. Then, the membrane will be washed to remove excess solvent and dried to form the nylon 66 membrane. In this study, 100% of the used membrane was assumed to be landfilled in the disposal stage.

On the other hand, in this study, 94.1g CS per FU, 47.4g Alg per FU and 0.013g AgNP per FU is needed for the fabrication of AgNP PCBM. Other materials, such as 141.1g of PEG, 188.2g of Ac and 141.0 of NaOH were needed for the fabrication of AgNP PCBM. As such, the inputs and outputs of the extraction of three main components of the membrane (CS, Alg and AgNP) from the raw materials were considered in the LCA. Therefore, the extraction of CS from crustacean shell waste that involved grinding, deproteinization, demineralization and deacetylation were taken into consideration (Piccinno & Hischier et al., 2015). In addition to that, extraction of Alg was also considered in the system boundary. Brown seaweed is harvested and involved ion exchange in hot alkaline solution to produce sodium Alg solution (Piccinno & Hischier et al., 2015). The Alg solution subsequently undergoes acid treatment, followed by drying and addition of Na_2CO_3 to produce sodium Alg (Piccinno & Hischier et al., 2015). On the other hand, the extraction of AgNP from chemical reduction of silver nitrate and trisodium citrate was included in the LCA (Pourzahedi & Eckelman, 2015). The process starts with the reaction of 0.74 kg citric acid and 0.46 kg of NaOH to obtain 1 kg of trisodium citrate (Pourzahedi & Eckelman, 2015). Meanwhile, 0.93 kg of glucose is required for the production of 1 kg citric acid, which involved in the production of trisodium citrate (Pourzahedi & Eckelman, 2015). Then, 1.57 kg of silver nitrate, 0.8 kg of trisodium citrate and 0.14 kg of water is reacted to form 1 kg of AgNP and 0.6 kg of citric acid, 0.8 kg of sodium nitrate, 0.006 kg of hydrogen gas, 0.12 kg of oxygen gas are produced as the by-products (Pourzahedi & Eckelman, 2015).

Last but not least, in order to evaluate the environmental impacts based on local perspective, Malaysian Electricity Mix was adopted for all the electricity required in the process.

iv. Results analysis

In order to assess the environmental impacts of the greywater treatment, the analysis was conducted based on categories such as Global warming potential [kg – CO_2 eq.], Ozone depletion [kg – CFC 11 eq.], Human Toxicity [CTUh], Particulate matters [kg – PM2.5 eq], Ionizing radiation [kBq U235 eq.], Photochemical ozone formation [kg - NMVOC], Acidification [Mole of H^+ eq], Eutrophication (Aquatic, marine) [kg – P eq], Ecotoxicity [CTUe], Resource depletion (water) [m^3 eq] and Resource depletion (Mineral, fossils, renewables) [kg – Sb eq.].

3.8.7 Cost analysis

In addition, the cost of the greywater recycling system was evaluated to find out the payback period of implementing the greywater recycling system in a 5-members' family. In order to evaluate the water and electricity utility, local water tariff and domestic electricity tariff was adopted with the corresponding tariff listed in Table 3.7. Thereafter, the Net Profit Value (NPV) is calculated based on the cost of various components such as the capital cost of the system and operating cost tabulated in Table 4.13, Section 4.5.7.

Table 3.7. Water and electricity tariff (Syarikat Bekalan Air Selangor Sdn. Bhd., 2017; Tenaga Nasional Berhad, 2017)

Components	Tariff rate in MYR	Tariff rate in USD
Water (0 – 20 m^3)	Code 10: MYR 0.57/ m^3	Code 10: USD 0.13/ m^3
Water (21 – 35 m^3)	Code 10: MYR 1.03/ m^3	Code 10: USD 0.23/ m^3
Electricity (First 200kWh)	Domestic: MYR 0.218/ kWh	Domestic: USD 0.049/ kWh

Based on information abovementioned, the Net Profit Value (NPV) was then calculated based on Eq. 3.10:

$$\text{NPV} = \text{- Capital cost} + \sum \frac{Water\ utility\ saved}{(1+discounted\ rate)^{period\ of\ time}} \quad \text{(Eq. 3.10)}$$

Eventually, the payback period was estimated as the time required for the NPV to break zero.

Chapter 4

4 Results and discussion

4.1 Phase I: Fabrication of CS membrane and investigation on CS and PEG concentration on greywater filtration

4.1.1 Phase overview

In phase I, a single layer CS membrane was developed for the application in greywater filtration. In this phase, the membrane was designed using CS as the main structure due to its distinct characteristics, as mentioned in Chapter 2. In order to introduce porous structure in the CS membrane, porogen PEG (P-6000) was used to modify the structure of the membrane. The concentration of P-6000 was carefully varied throughout the study to investigate the effect of PEG on membrane characteristics and greywater treatment efficiency.

4.1.2 Membrane characterizations

i. Molecular structure

P-6000 was added in the CS solution and extracted after the deprotonation process in water bath to generate porous structure in the membrane. As a result, the study on the changes of the membrane molecular structure is crucial to identify the formation of porous structure. Figure 4.1 shows the FTIR spectra of pure CS membrane and CS/ PEG membranes fabricated before and after extraction of P-6000. In Figure 4.1 (a), the broaden peak at 3285.01cm^{-1} indicates the presence of -OH and -NH stretching (i.e. 3000 – 3500 cm^{-1}). On the other hand, the absorption peaks at

1651.58 cm^{-1} and 1557.47 cm^{-1} correspond to the amide I (1600 – 1670 cm^{-1}) and amide II (1550 – 1640 cm^{-1}) of CS respectively. In addition, 1150.20 cm^{-1} and 1026.43cm^{-1} are the absorption bands for the amino group and -CO (1000 – 1300 cm^{-1}) in CS respectively.

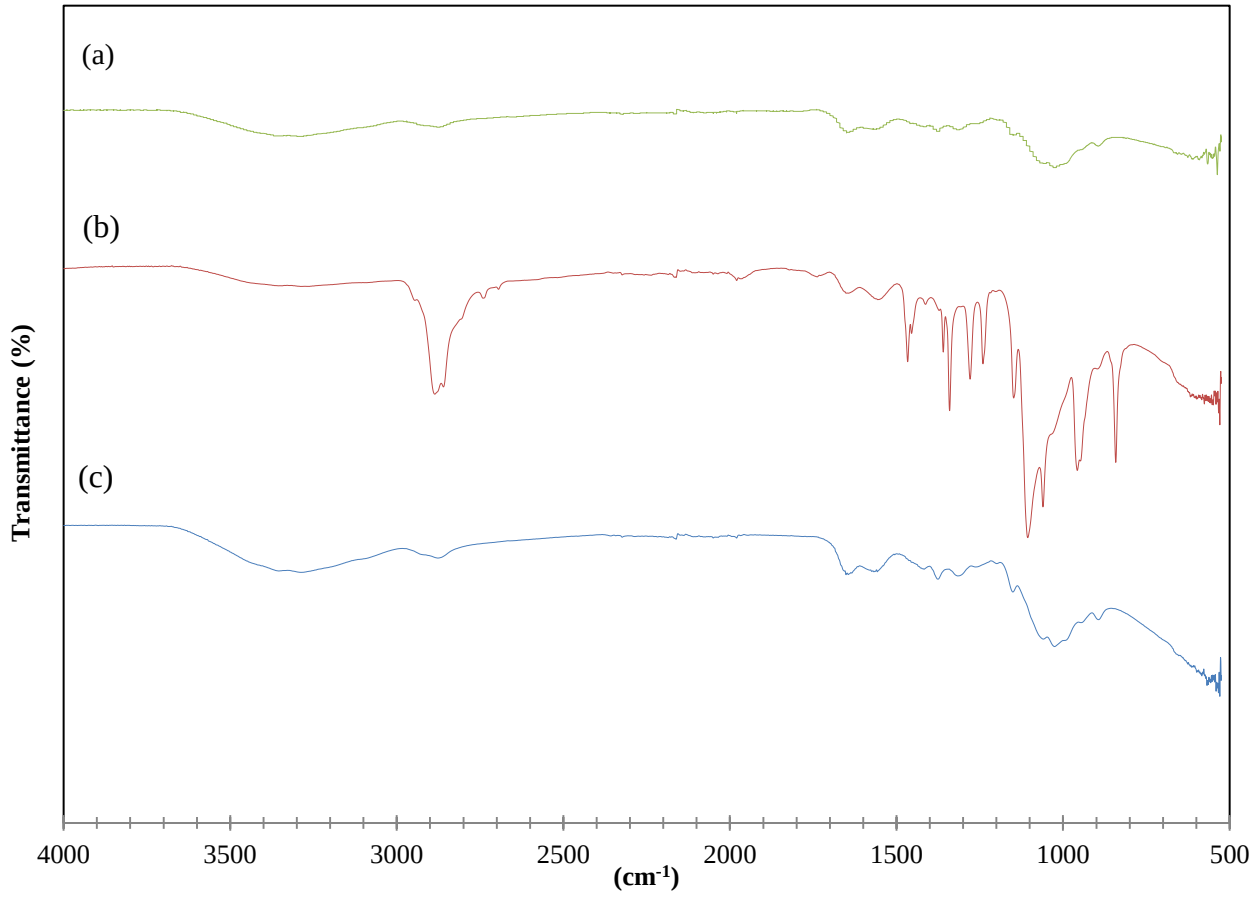

Figure 4.1. (a) FTIR spectrum of pure CS membrane; (b) FTIR spectrum of CS/ PEG membrane before washing of PEG; (c) FTIR spectrum of CS/ PEG membrane after washing of PEG

From Figure 4.1 (b), a few additional peaks were observed from the spectrum: 841.84 cm^{-1}, 957.33 cm^{-1}, 1240.49 cm^{-1}, 1279.08 cm^{-1}, and 1466.44cm^{-1} after the addition of P-6000. This result coincides with those reported by Zeng and Fang (2004), indicating that P-6000 has been successfully blended into the highly dense pure CS membrane. In addition to that, the reduction in

the intensity of absorbance peak near 3000 cm^{-1} - 3500 cm^{-1} showed that the P-6000 was introduced into CS mainly via the formation of hydrogen bonding between the hydroxyl groups in CS and P-6000.

After deprotonation and extraction of P-6000 from the CS membrane in water, the FTIR spectrum in Figure 4.1 (c) showed that the peaks corresponding to P-6000 were not detected. This indicates that the P-6000 was completely extracted from the membrane structure. Moreover, the increase in the broaden peak at 3288.42 cm^{-1} showed that the hydroxyl groups of CS that were previously bounded with PEG were free.

ii. Surface wettability

Surface water contact angle of the membranes was measured to identify the change in membrane hydrophilicity due to the modification with P-6000. The surface water contact angle was measured 30 seconds after 0.2 µL of water droplet was placed on the membrane surface. Figure 4.2 shows the surface water contact angle of membranes fabricated with different CS: PEG weight ratios. It was observed that there is no specific trend on the surface water contact angle with the increase in PEG ratio. However, the surface water contact angle increased by approximately 20% when P-6000 was added into the pure CS membrane. The increase in surface water contact angle could be attributed to the formation of porous structure in the membrane network. It was found that the water contact angle of a porous material is generally higher than the same material with a dense structure (Yuan & Lee, 2013). This is mainly due to the presence of air gap under the water droplet that leads to the hydrophobic effect (Lafuma & Quéré, 2003).

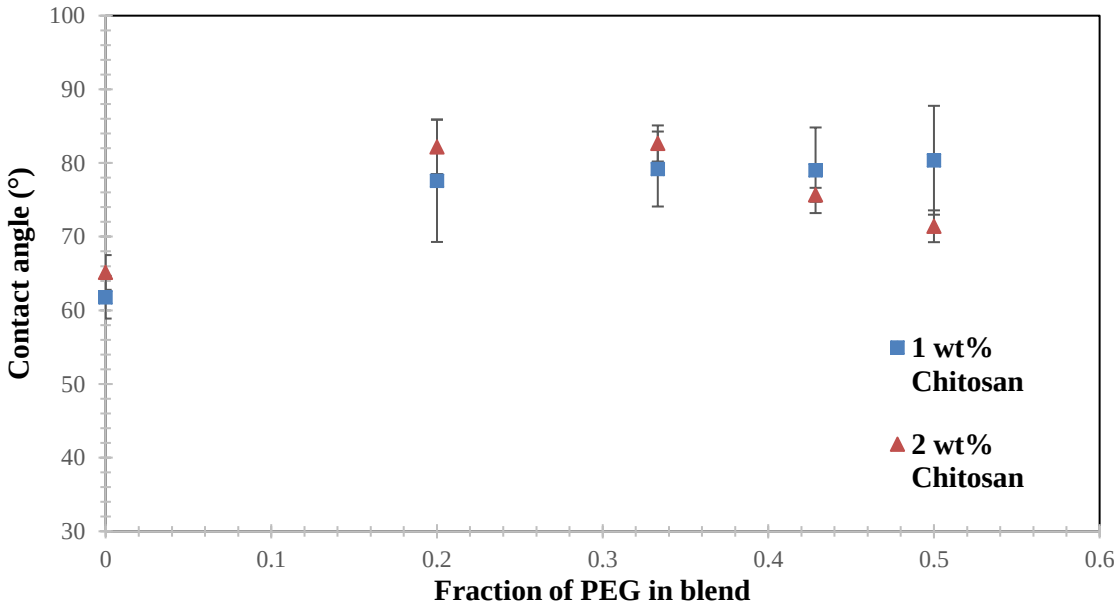

Figure 4.2. Surface contact angle (°) of the membrane

On the other hand, Zhang & Li et al. (2002) reported that -OH group in PEG polymer chains play an important role on the improvement in hydrophilicity of CS/ PEG membrane. However, since P-6000 was washed away to generate porous structure on the CS membrane, the surface hydrophilicity of the CS/ PEG membrane was not significantly improved with the modification due to the absence of -OH group of PEG polymer chains. Nevertheless, all the fabricated CS/ PEG membranes had a water contact angle of less than 90°, indicating that the membranes are hydrophilic.

iii. Porosity

The porosity (%) of the CS/ PEG membranes was studied to identify the volume of pores being introduced into the membranes under different PEG loadings. Overall, it could be observed in Figure 4.3 that the CS/ PEG membranes (except CS: PEG weight ratio 4: 1) have higher porosity

as compared to the pure CS membrane. Also, it was observed that high PEG weight ratio (CS: PEG of 1: 5) would deteriorate the CS polymer network and caused membrane to disintegrate during the drying process. Therefore, the optimum CS: PEG weight ratio in this study was fixed at 1:1. Pure CS membranes of 1 wt% and 2 wt% were fabricated with the porosity of 20.36 ± 0.30 % and 23.60 ± 0.40 %, respectively. Overall, the porosity of 2 wt% CS/ PEG membranes is slightly higher than 1 wt% CS/ PEG membranes. This is mainly due to the increase in amount of polymers at higher polymer concentration that eventually led to the slight increase in the volume of voids in the membrane network.

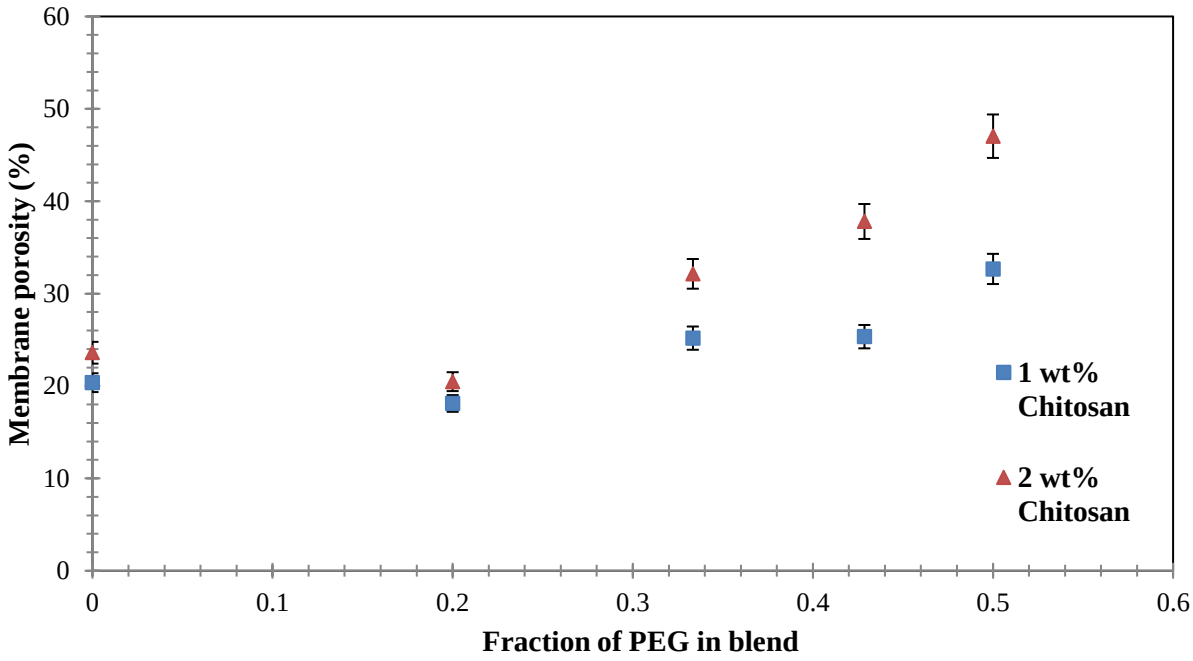

Figure 4.3. Membrane porosity (%)

On the other hand, due to the low concentration of PEG, it was found that CS: PEG weight ratio of 4: 1 was insufficient to form porous structure in CS membrane. The porosity of membrane fabricated with CS: PEG weight ratio of 4: 1 was found to be lower as compared to those having

higher PEG loadings. When the PEG ratio was increased to 2: 1, 4: 3 and 1: 1, the porosity showed an increasing upward trend. Overall, the porosity of the CS/ PEG membrane increased by 14.56 % for 1 wt% membrane when the PEG loading was increased from 4: 1 to 1: 1. As for 2 wt% membrane, the porosity of the CS/ PEG membrane was improved by 26.57 % when the PEG loading was increased from 4: 1 to 1: 1. It could be deduced that the excess interaction of hydroxyl groups in PEG polymers due to higher concentration of PEG hindered the hydrogen bonding interaction between CS and PEG. Thus, this has led to a higher porosity polymer network after washing off PEG from the CS membrane. This also indicates that CS membrane with higher porosity could be fabricated with higher concentration of PEG。

iv. Swelling ratio and EMC

The swelling ratio of the CS/ PEG membranes was studied to determine the variation in water uptake percentage of the membrane due to changes in membrane structure. On the other hand, the swelling ratio can also be used to identify the duration required for membrane to be fully wet prior to its usage. The swelling curves for 1 wt% and 2 wt% membranes were plotted in Figure 4.4 (a - b), respectively.

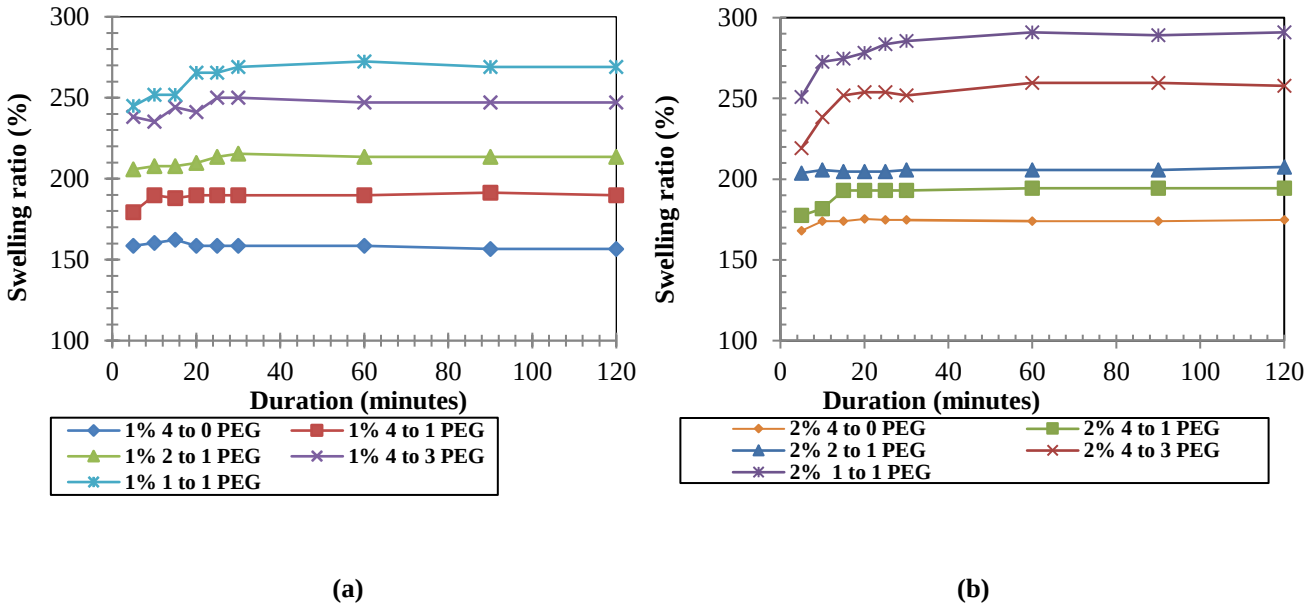

(a) **(b)**

Figure 4.4. Water uptake/ swelling ratio (%) of (a) 1 wt% CS membranes; (b) 2 wt% CS membranes

As shown in the swelling curves, it can be observed that most of the CS/ PEG membranes reached the swelling equilibrium after 30 minutes of immersion in DI water. For the first 30 minutes of immersion in DI water, both the 1 wt% and 2 wt% pure CS membranes were found to achieve swelling ratio of 158.49% and 174.67%, respectively. Higher swelling ratio was recorded for higher weight percentage of pure CS membrane owing to the presence of higher volume of CS polymers in the membrane, resulting in a higher degree of water uptake. The increase in swelling ratio could be attributed to the higher degree of interaction between the hydroxyl functional groups of CS and water molecules.

Generally, the CS/ PEG membrane showed higher swelling ratio as compared to the pure CS membrane. By comparing the swelling ratio at 30 minutes immersion in DI water, the swelling ratio of 1 wt% of 4: 1, 2: 1, 4: 3 and 1: 1 CS/ PEG membranes was found to be 189.66%, 215.38%, 250.00% and 268.92% respectively. Meanwhile, the swelling ratio of CS/ PEG membrane of 2

wt% with ratio 4: 1, 2: 1, 4: 3 and 1: 1 was recorded to be 192.96%, 205.66%, 251.92% and 285.45% respectively.

Table 4.1 EMC of membranes

Fraction of PEG blend	1 wt% CS	2 wt% CS
0	67.32 ± 0.28	69.16 ± 0.21
0.2	71.23 ± 0.62	71.60 ± 0.57
0.33	71.45 ± 0.69	71.80 ± 0.93
0.43	73.86 ± 0.13	75.28 ± 0.27
0.50	75.82 ± 0.22	75.65 ± 0.49

EMC was used to identify the amount of moisture that a membrane can store at its equilibrium state. As shown in Table 4.1, results showed that the EMC of the membranes increased with the weight ratio of PEG and it was in good agreement with the swelling ratio and porosity of CS/ PEG membranes where the EMC increases with porosity. The increase in CS concentration from 1 wt% to 2 wt% at a fixed CS: PEG weight ratio resulted in higher volume of porous structure in the membrane (as shown in Figure 4.3). As a result, the 2 wt% membrane that had higher volume of porous structure was found to have higher EMC as compared to 1 wt% membranes.

v. DI water flux

In addition, the increase in swelling ratio, EMC and porosity implies that the membrane can take up higher volume of DI water to result in higher DI water flux. As shown in Figure 4.5, 1 wt% and 2 wt% CS: PEG 4: 0 and 4: 1 membranes with very low porosity were not able to generate any water flux up to 30 mins under the filtration pressure of 3.2 bar (g). Hence, the DI water fluxes of 1 wt%, 2 wt% CS: PEG 4: 0 and 4: 1 were recorded as 0 L $m^{-2}hr^{-1}$.

In contrast, the 1 wt% CS: PEG 1: 1 membrane resulted in the highest DI water flux of 24.42 L $m^{-2}hr^{-1}$ (Figure 4.5). However, Zeng & Fang et al. (2004) indicated that the permeation flux obtained with the membrane at similar pressure range was 253.39 L $m^{-2}hr^{-1}$. It could be deduced that due to the differences in membrane casting method (eg. volume of membrane casted, PEG extraction period), type of water used for the study and the grade of CS would eventually lead to the variation in the water permeation flux. For instance, Zeng & Fang et al. (2004) used double distilled deionized water; while normal deionized water was used in the current study. Hence, this might lead to higher water flux observed by Zeng & Fang et al. (2004) as the water used is purer. Furthermore, degree of deacetylation of CS used in Zeng & Fang et al. (2004) was 91%, while the degree of deacetylation of CS used in the current study was 75%. This is one of the contributing factors to lesser bonding between CS and PEG. Hence, it resulted in lower membrane porosity after the washing of membrane and lower water flux observed in our study. Other than that, the casting volume of the CS solution was not mentioned in the study of Zeng & Fang et al. (2004). The amount of casting solution affects the membrane thickness, which in turn could result in different water flux obtained from a membrane with similar materials.

On the other hand, when the 1 wt% CS: PEG weight ratio was reduced to 4: 3 and 2: 1, it was found that the DI water flux reduced significantly to 15.31 L $m^{-2}hr^{-1}$ and 5.17 L $m^{-2}hr^{-1}$, respectively. In particular, the DI water flux of 1 wt% 2: 1 CS/ PEG membrane is 78.84% lower than the 1 wt% 1: 1 CS/ PEG membrane. This showed that higher amount of water molecules penetrate through the membrane with higher porosity due to less resistance at similar applied pressure. The result is coincides with the finding of Zeng & Fang et al. (2004), whereby the increase in porosity of the membrane leads to the increase in water permeation flux and

Mohammad & Megat Johari et al. (2009) suggested that an increase in the weight ratio of PEG would improve the permeate water flux.

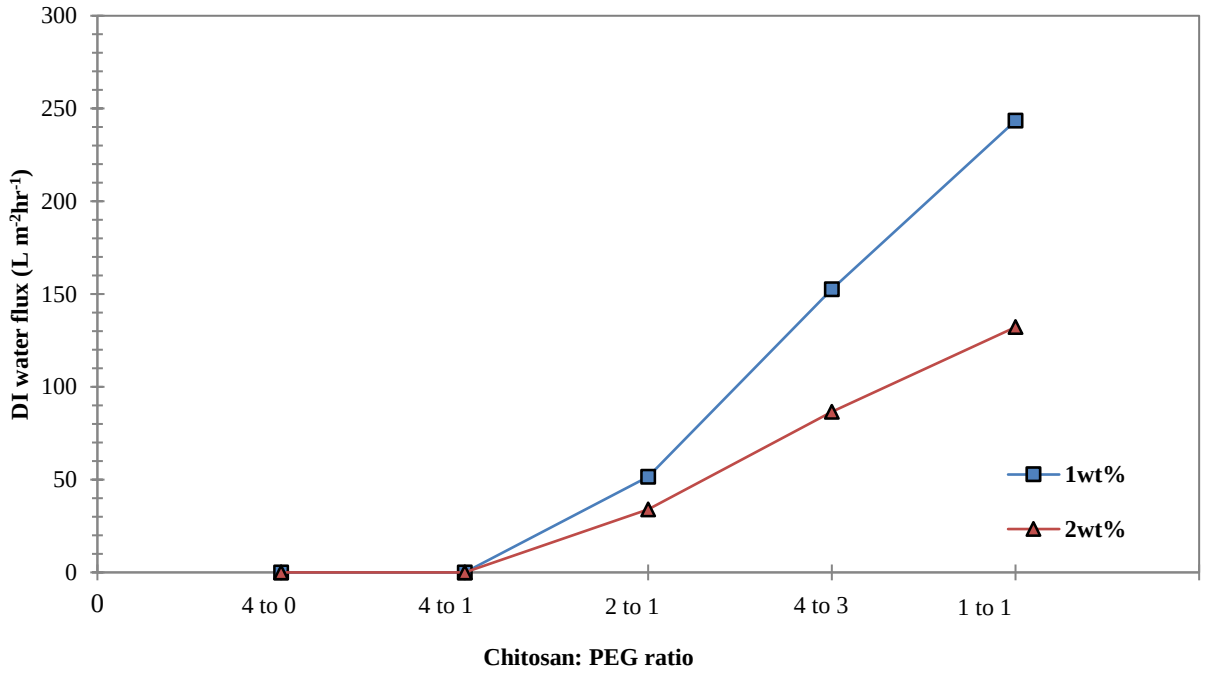

Figure 4.5. DI water flux (L $m^{-2}hr^{-1}$) of membranes

Similarly, the DI water flux of membrane fabricated at higher CS concentration of 2 wt% was found to increase with the PEG weight ratio. However, the DI water flux was lower than those of 1 wt% CS membranes. This can be explained by the increased amount of polymer, which leads to the formation of a denser CS network and increased thickness. This has resulted in higher resistance for water molecules to pass through the membrane. Therefore, the use of lower CS concentration and higher PEG ratio are more suited for applications when high water flux is required.

vi. Membrane structure

Based on the results from DI water flux, it could be deduced that water molecules could not permeate through the pure CS membrane due to its dense polymeric structure. Visual observation via scanning electron microscopy was conducted to analyse the change in membrane structure and confirm the findings from previous sections. Figure 4.6 (a) is a cross-sectional SEM image of the pure CS membrane that has a rather smooth surface without any pores. This supports the fact that the structure of the pure CS membrane is dense and compact. Hence, higher trans-membrane pressure or longer filtration duration was required for the permeation of water molecules through the pure CS membrane.

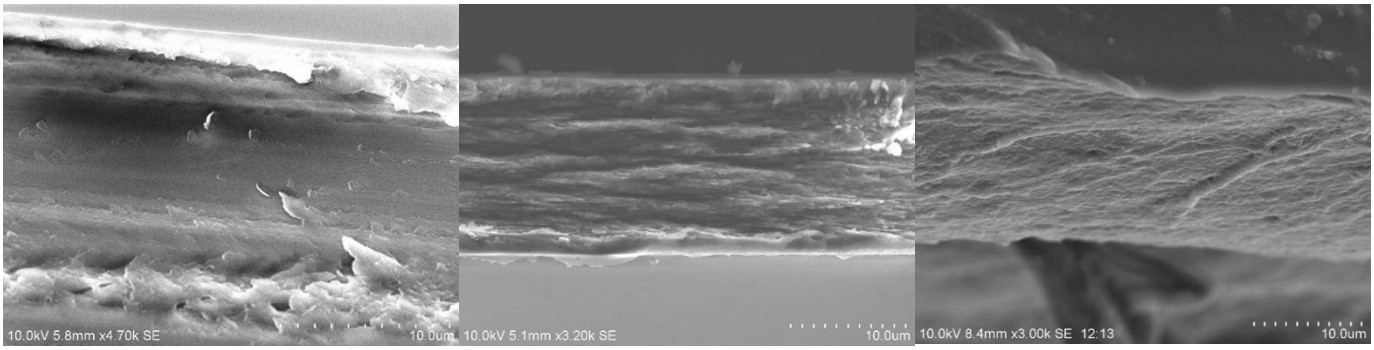

(a) **(b)** **(c)**

Figure 4.6. Cross-section images of (a) pure CS membrane; (b) 1 wt% CS: PEG 1: 1 membrane; (c) 2 wt% CS: PEG 1: 1 membrane

In comparison to the pure CS membrane, the fabricated CS/ PEG membrane showed significant improvement in terms of its porosity, swelling ratio, as well as DI water flux. This implies that the addition of PEG during the fabrication of CS membrane resulted in a change to the polymer matrix of CS membrane. The claims made in previous sections can be further

supported by Figure 4.6 (c), whereby porous structure was evidenced in the 1 wt % and 2 wt% CS/ PEG membranes. It can be observed that the CS/ PEG membrane exhibited high volume of voids, which contributed to the enhanced porosity, swelling ratio and permeate water flux.

vii. Bathroom greywater permeate flux and physicochemical treatment efficiency

From section 4.1.2 v, it was found that the pure CS membrane along with the CS/ PEG membrane of 4:1 ratio do not generate permeate up to 30 minutes at constant pressure filtration condition (i.e. 3.2 bar (g)). Thus, these membranes were excluded from the direct bathroom greywater filtration study. The selected membranes for this direct greywater filtration treatment were 1 wt% and 2 wt% CS/ PEG membranes with ratio of 2: 1, 4: 3 and 1: 1.

The direct bathroom greywater filtration treatment efficiencies using the CS/ PEG membranes were compared to a conventional nylon membrane. These results were presented in Table 4.2. Turbidity, total suspended solids, COD and BOD_5 removal using nylon membrane was found to be 94.16%, 100%, 43.29%, and 37.11%, respectively.

Table 4.2 Bathroom greywater treatment performance using CS membrane

Parameters	**Nylon membrane**	**1wt% 1:1**	**1wt% 4:3**	**1wt% 2:1**	**2wt% 1:1**	**2wt% 4:3**	**2wt% 2:1**
Turbidity (%)	94.16	94.73	98.31	95.91	96.26	96.39	95.85
Total suspended solids (%)	100.00	100.00	100.00	95.03	98.34	96.69	96.69
COD (%)	43.29	60.93	66.03	71.13	60.30	73.36	67.09
BOD_5 (%)	37.11	61.54	52.31	46.15	64.62	54.62	73.85
Pathogenic bacteria (%)	100.00	100.00	87.50	82.14	92.86	91.07	100.00

When compared to the conventional nylon membrane, the CS/ PEG membranes showed similar removal efficiencies in terms of physical pollutants such as turbidity and suspended solids. As shown in Table 4.2, 94.16% of turbidity was removed using nylon membrane, while CS/ PEG membrane was found to be able to remove 94.73% to 98.31% of turbidity under different membrane fabrication conditions. In addition, results in Table 4.2 indicated that 100% of total suspended solids were removed using the nylon membrane. It was found that the total suspended solid removals using CS/ PEG membrane ranged between 95.03% and 100.00%. In this particular study, the turbidity and total suspended solids concentration for the treated greywater effluent were found to be well below the minimum requirement for non-potable reuse, achieving turbidity values lower than 2 NTU and total suspended solids of 20 mg L^{-1}. The removal of turbidity and total suspended solids from greywater indicates that these membranes are able to function as a good physical barrier for substances of sizes ranging between 1 and 100 μm (Levine & Tchobanoglous et al., 1991).

Furthermore, CS/ PEG membrane was found to have better efficiency in removing organic matters with size lower than 0.001μm in comparison to the conventional nylon membrane based on results from the removal efficiency of COD and BOD_5. From Table 4.2, it could be observed that the COD removal of CS/ PEG membranes were relatively higher, with removal percentage ranging from 60.30% to 73.40%, while COD removal using conventional nylon membrane was found to be only 43.29%. Similarly, BOD_5 removal was found to be relatively lower using nylon membrane, only achieving 37.11%. On the other hand, BOD_5 removal using CS/ PEG membranes was measured to range from 46.15% to 61.54% using 1 wt% CS/ PEG membranes; and 54.76% to 73.85% using 2 wt% CS/ PEG membranes. The higher removal efficiency in terms of organic

matters can be attributed to the adsorption ability of CS as the membrane material (Crini & Badot, 2008). Despite higher removal percentage of organic matters with the use of CS/ PEG membranes, no specific trend could be observed for COD and BOD_5 removal with respect to the variation of PEG loadings. This could also be observed from the surface wettability of the membrane, which indicated that the surface structure of the different PEG ratio membranes is similar. Thus, this has led to similar removal efficiency of organic matters using CS/ PEG membranes.

Bathroom greywater permeate flux was also collected and analysed to investigate the greywater filtration performance of the fabricated CS/PEG membranes. It was observed that the overall bathroom greywater permeate flux increases with the weight ratio of CS: PEG from 2: 1 to 1: 1. As shown in Table 4.3, the highest bathroom greywater permeate flux of 15.88 L $m^{-2}hr^{-1}$ was obtained by using 1 wt% CS/ PEG membrane with a weight ratio of 1: 1. This was followed by the 1 wt% CS/ PEG membranes with weight ratio of 4: 3 and 2: 1 with bathroom greywater permeate fluxes of 13.18 L $m^{-2}hr^{-1}$ and 4.41 L $m^{-2}hr^{-1}$ respectively. On the other hand, the 2 wt% CS/ PEG membranes showed lower bathroom greywater permeate flux as compared to 1 wt% CS/ PEG membranes. A permeate flux of 15.05 L $m^{-2}hr^{-1}$ was achieved with 2 wt% CS/ PEG membrane with weight ratio of 1:1. Though the permeate flux was comparable to that obtained by the 1wt% CS/PEG membrane with weight ratio of 1:1, this result is not satisfactory as higher permeate flux is desirable to cater for treatment of high volumes of greywater. Similarly, 2 wt% CS/PEG membranes with weight ratio of 4: 3 and 2: 1 produced significantly lower permeate fluxes of 6.65 L $m^{-2}hr^{-1}$ and 3.17 L $m^{-2}hr^{-1}$ respectively compared to membranes with 1wt% of CS.

Table 4.3 Bathroom greywater permeates flux using CS/ PEG membranes

CS: PEG	**CS 1wt%**			**CS 2 wt%**		
	1: 1	4: 3	2: 1	1: 1	4: 3	2: 1
Bathroom greywater flux (L $m^{-2}hr^{-1}$)	15.88	13.18	4.41	15.05	6.65	3.17

In addition, it was observed that the bathroom greywater permeate fluxes were generally lower than measured DI permeate water fluxes. The differences in permeate fluxes between bathroom greywater and DI water was mainly attributed to the presence of pollutants in the bathroom greywater samples. Bathroom greywater was found to contain pollutants such as suspended solids, dissolved solids and organic matters, which could cause blockages to the membranes. It could also be deduced that bathroom greywater flux could vary due to the variation in the feeding conditions of bathroom greywater to the membrane. As such, the bathroom greywater flux would be higher when the bathroom greywater is relatively less polluted, and vice versa.

Based on the results obtained, it can be deduced that the variation in PEG weight ratio will significantly impact the water permeate flux and the efficiency of removing larger size particles due to variation in porosities, but not the smaller and fine organic pollutants. The moderate removal efficiency of small organic pollutants was due to the submicron pores sizes of the CS/ PEG membranes, which allowed the smaller size pollutants to penetrate through the membranes (Zeng & Fang, 2004).

viii. *Disinfection rate*

Besides the removal efficiency of physicochemical pollutants, the ability of the fabricated CS/ PEG membranes to remove bacteria from bathroom greywater source was also evaluated. In

this study, the microbial indicators used to evaluate the treatment efficiency of CS/ PEG membrane are *Staphylococcus aureus* and/or *Enterococcus faecalis* (shown in Appendix Figure A1 and A2) as *E. coli* and total coliform, which are the normal bacteria indicators were not present in all samples of greywater used in this stage of study. The nylon membrane was able to remove all the pathogenic bacteria in bathroom greywater. However, it was found that the removal efficiency of these microbial pathogens ranged between 82.14 % and 100 % using CS/ PEG membranes. This indicates that using CS/ PEG membrane alone is not sufficient to assure that the treated bathroom greywater effluent is fully disinfected and microbial-free.

No clear trend was observed for the microbial removal efficiency when different PEG weight ratio was used during the fabrication of CS/ PEG membranes. Table 4.2 shows that the highest microbial removal efficiency can be achieved using the 1 wt% CS/ PEG membrane with CS: PEG ratio of 1: 1, where a complete disinfection was achieved. However, the microbial removal efficiency declined to 87.15% and 82.14% when the CS/ PEG membranes of 4: 3 and 2: 1 weight ratio were used respectively. On the other hand the 2 wt% CS/ PEG membranes with weight ratio of 1: 1, 4: 3 and 2: 1 were able to disinfect up to 92.86%, 91.07% and 100%, respectively. Based on the results, it was found that the 2 wt% CS/ PEG membranes were in overall more superior than the 1 wt% membranes. This is due to the denser polymeric network formed in the 2 wt% CS membranes, which enable the formation of larger barrier boundary for the bacteria to penetrate through.

In general, though the microbial removal efficiency achievable from the CS/ PEG membranes achieved a minimum microbial removal efficiency of 82.14%, the microbiological quality of the treated bathroom greywater effluent did not meet the standard for non-potable reuse

(i.e. non-detectable bacteria). Furthermore, permeate flux will be compromised in order to achieve complete removal of microbes in greywater since better microbial removal efficiency can only be achieved using membranes with reduced porosity. This suggests that either further modification of the membrane is needed or the system has to be coupled with other water disinfection method such as chlorination, chloramination or UV.

In addition, the anti-microbial property of CS is mainly attributed to the protonated cationic functional groups that present in the CS molecule. The $-NH_3^+$ functional group also contributed to the binding of the oppositely-charged microorganisms such as *E. coli*, causing the disruption to cell metabolism that eventually leads to cell fatality (Hasan & Crawford et al., 2013; Jeon & Kim, 2000; Wang & Liu et al., 2012). Nevertheless, the CS molecule was deprotonated to avoid dissolution in water during membrane fabrication. Hence, the CS-based membrane material was expected to partially lose the anti-microbial ability. Besides, bacteria present in the bathroom greywater samples consisted of gram-positive bacteria such as *Staphylococcus aureus* or *Enterococcus faecalis* rather than the typical *E. coli* or total coliforms. Thus, it can be deduced that the microbial removal efficiency in this case was mainly attributed to the size exclusion mechanism, in which the CS/ PEG membranes acted as a physical barrier for the bacteria. Further modification on the CS/ PEG membrane, such as the loading of silver nanoparticles on to the membrane could be implemented to improve the microbial removal efficiency.

The current study shows that biodegradable CS/ PEG membrane can be utilized for direct bathroom greywater filtration as satisfactory treatment efficiency could be achieved using just a single-layered membrane. However, there is a need to increase the greywater permeate flux while maintaining or improve on the current membrane structure and treatment efficiencies achievable

by the CS/ PEG membrane in order to cater for treatment of highly contaminated greywater or higher volumes of greywater. The modification of the membrane will be discussed in the next section.

4.2 Phase II (1): Fabrication of dense PCBM and advanced filtration study

4.2.1 Phase overview

Results from Phase I indicated that 1 wt% CS: PEG 1: 1 membrane (1CP) was found to generate the highest water flux amongst other CS/ PEG membranes. As a result, it was selected to be further improved in this phase. Results also showed that greywater filtration using 1CP membrane could achieve high removal of turbidity and suspended solids. However, 1CP membrane was not effectively enough to eliminate biological contaminants, such as pathogenic bacteria and BOD_5 in the greywater. Therefore, polyanionic Alg is introduced to the structure of the membrane in this phase of study to enhance membrane stability and greywater treatment performance.

Thus, in phase II (1), Alg was incorporated with 1CP membrane to form dense PCBM. The structure of the membrane was designed to have the hydrophilic Alg as the active side of the membrane. The dense PCBM was then characterized and evaluated on its greywater treatment performance.

4.2.2 Membrane characteristics

i. Molecular structure

FTIR spectra of the dense PCBMs were analysed to identify the formation of PEC with the loading of Alg to 1CP membrane. Figure 4.7 and Figure 4.8 show the FTIR spectra for Alg, 1CP membrane and dense PCBMs. As shown in Figure 4.7 (a), the FTIR peaks at 1020.51 cm^{-1}, 1593.00 cm^{-1} and 1408.60 cm^{-1} indicate the present of carboxylic acids functional group, as well as

asymmetric and symmetric carboxylate anions of Alg (Sharma & Sanpui et al., 2012a). On the other hand, the 1CP membrane (Figure 4.7 (b)) showed broaden FTIR peak at 3285.01 cm^{-1} indicating the presence of O-H and N-H stretching (i.e., 3000 – 3500 cm^{-1}), while the FTIR absorption peaks at 1633.73 cm^{-1} and 1538.46 cm^{-1} correspond to amide I (1600 – 1670 cm^{-1}) and amide II (1550 – 1640 cm^{-1}) respectively. In addition, 1151.42 cm^{-1} and 1023.24 cm^{-1} are the absorption bands for the amino group and C-O (1000 – 1300 cm^{-1}) in CS.

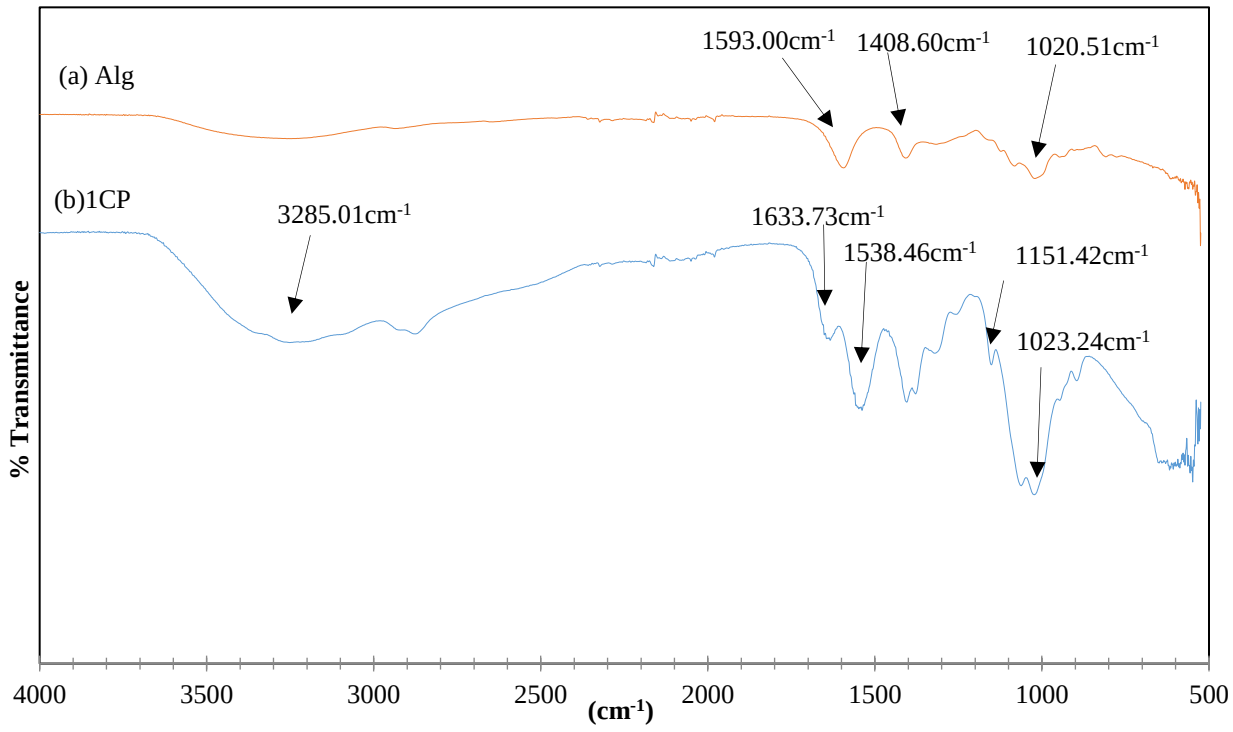

Figure 4.7. FTIR spectra of Alg and 1CP membranes

Due to the small amount of Alg added, the dense PCBM spectra shown in Figure 4.8 (a) to Figure 4.8 (c) have similar patterns as 1CP membrane since 1CP forms the main structure of the membrane. The FTIR peaks at 1538.46 cm^{-1} and 1633.73 cm^{-1} originally present in 1CP were shifted to 1557 cm^{-1} to 1651 cm^{-1} after the incorporation of Alg. Scheme 1 shows the interaction

between Alg and CS during the fabrication of dense PCBMs. The two broad peaks present for the three FTIR spectra in the range of 1557 cm^{-1} to 1651 cm^{-1} correspond to the overlapping of amide groups of CS and carboxyl anions in the Alg (as shown in Scheme 1) (Coates, 2000; Sharma & Sanpui et al., 2012a). Thus, the presence of these two peaks in the FTIR spectra confirmed the interaction between CS and Alg layer. When the concentration of Alg increases with fixed CS/ PEG concentration, it was noticed that the peak intensity at 1373 cm^{-1}(ie. N-O bonding) also increases. The increase in the intensity of this peak showed the formation of increased N-O bonding due to the interaction between the carboxylic groups in Alg with the amide group in CS. In addition, the rise in the intensity of peak 1026 cm^{-1} (i.e., carboxylic acids) and 3290.81 cm^{-1} (i.e., hydroxyl group) with the increase in Alg concentration also indicated the presence of Alg in the PCBMs.

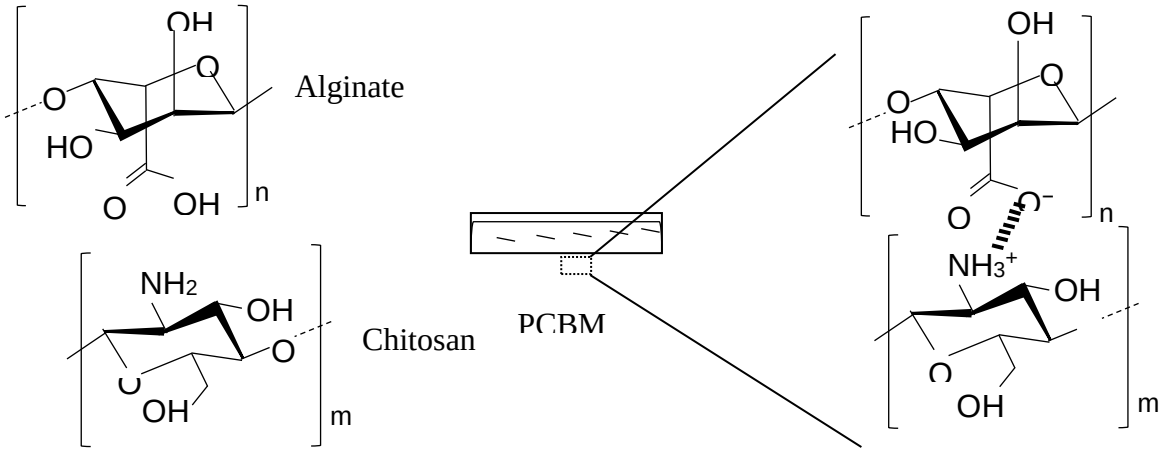

Scheme 1. Interaction between Alg, CS and formation of dense PCBM

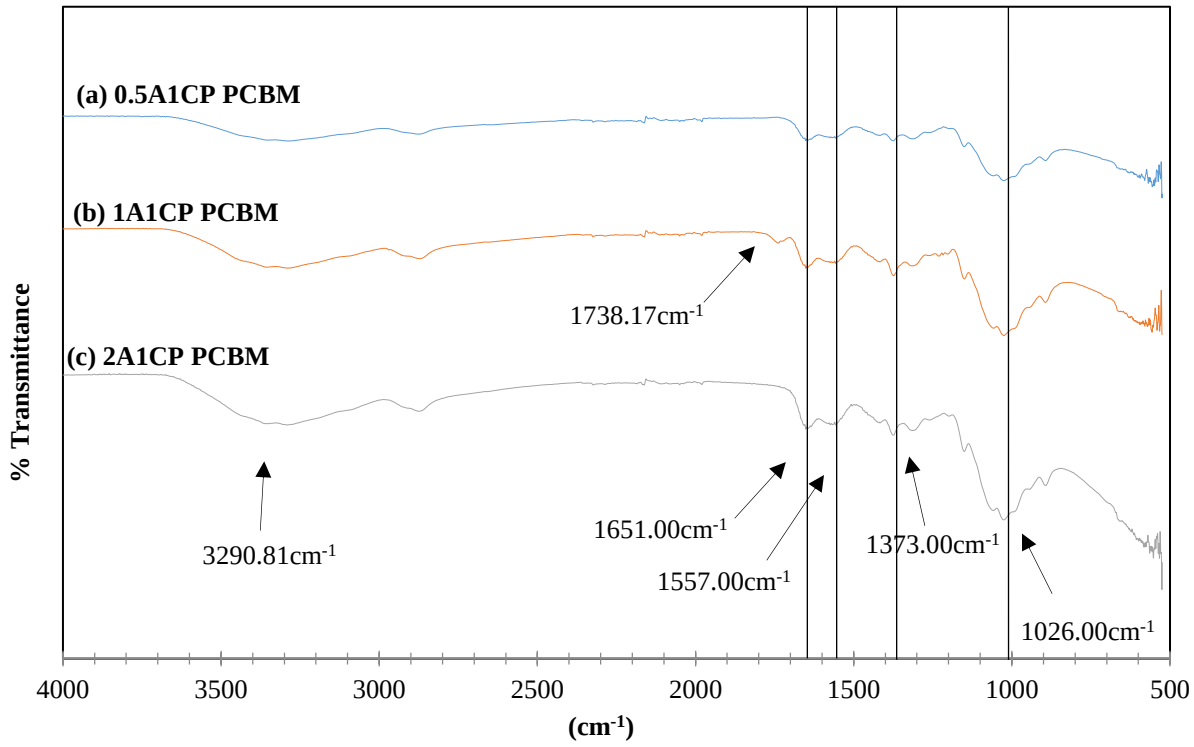

Figure 4.8. FTIR spectra of dense PCBMs

ii. Membrane structure

The cross-sectional structure of membranes was studied to identify the structural change in the membranes due to the incorporation of Alg to form PCBM. The cross-sectional structure of the 1CP membrane was shown in Figure 4.9 (a). On the other hand, Figure 4.9 (b) to Figure 4.9 (d) are the images of dense PCBM structures, where the top layer consists of porous CS while the bottom layer consists of Alg layer. The two distinct layers of membranes observed confirmed the formation of dense PCBM. From the images, it can be deduced that the formation of polyelectrolyte complex between Alg and CS occurs at the interface of the two layers. As discussed in Section 4.2.2i, the FTIR peaks shown in 1557 cm^{-1} to 1651 cm^{-1} after the incorporation of Alg verified the interaction between CS and Alg biopolymers. The formation of dense bottom Alg

layer was due to the absence of porogen and resulted in strong intermolecular interaction between Alg biopolymer itself. Besides that, it was found that the Alg layer becomes thicker as the concentration of pure Alg was increased from 0.5 wt% up to 2 wt%. The increasing thickness of Alg layer was due to the increase in concentration of Alg polymer in the casting solution.

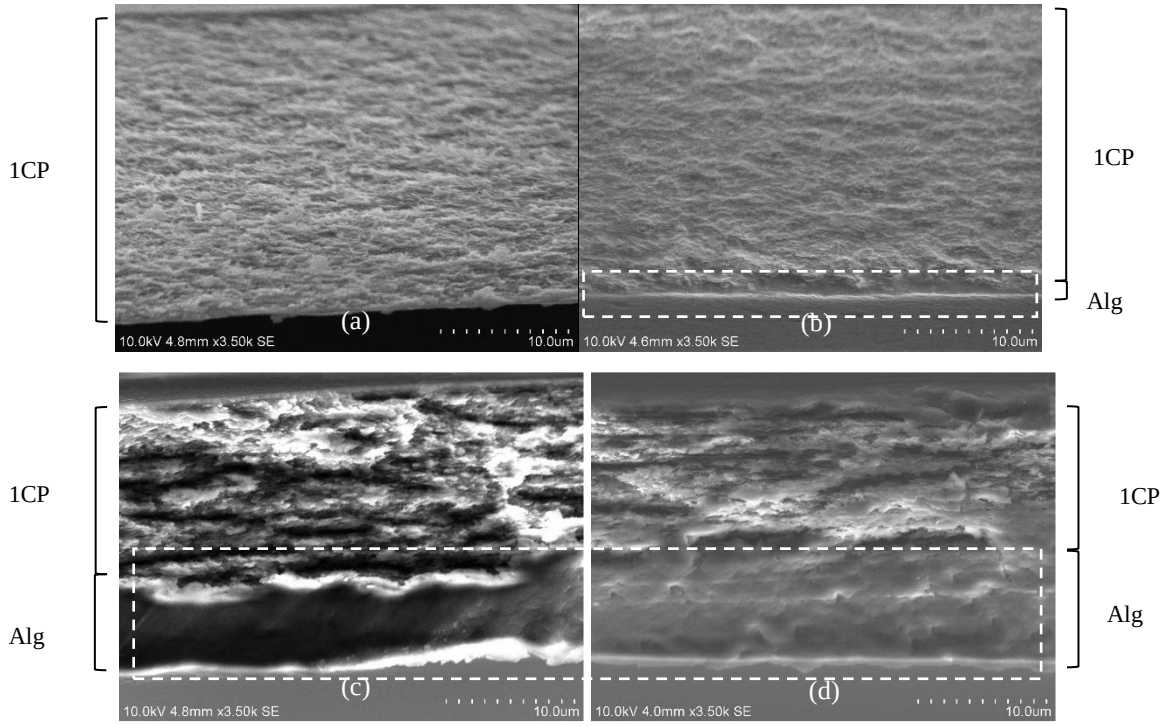

Figure 4.9. (a) Cross-section of 1CP membrane (b) Cross-section of 0.5A1CP membrane (c) Cross-section of 1A1CP membrane (d) Cross-section of 2A1CP membrane

In addition, the tensile strength of the 1CP membrane was found to be 41.55 ± 5.32 MPa with strain of 2.248 ± 0.65 %. The incorporation of increased alginate concentration in PCBM resulted in higher tensile strength and strain of the membrane. The tensile strength of the PCBMs was found to range from 50.37 ± 8.76 MPa to 63.24 ± 10.03 MPa with strain ranging from 3.43 ± 0.99 % to

4.16 ± 0.97 % with the increase in alginate concentration. This indicates that incorporation of alginate in 1CP membranes strengthens the structure.

iii. Swelling ratio

Besides understanding the water uptake ability of the membranes, swelling ratio is also an useful indicator to identify the degree of crosslinking of the membrane (Rhim, 2004). High degree of crosslinking leads to lower water penetration, which results in low swelling in the biopolymer network (Vimala & Mohan et al., 2010). The swelling curves of dense PCBMs were recorded in Figure 4.10. It can be observed that dense PCBMs have a lower swelling capability as compared to 1CP membrane. This is mainly attributed to the formation of PEC between the protonated amino groups and carboxylate groups of Alg (shown in Scheme 1) that caused the reduction in the functional groups responsible for water uptake (Kulig & Zimoch-Korzycka et al., 2016; Sharma & Sanpui et al., 2012a).

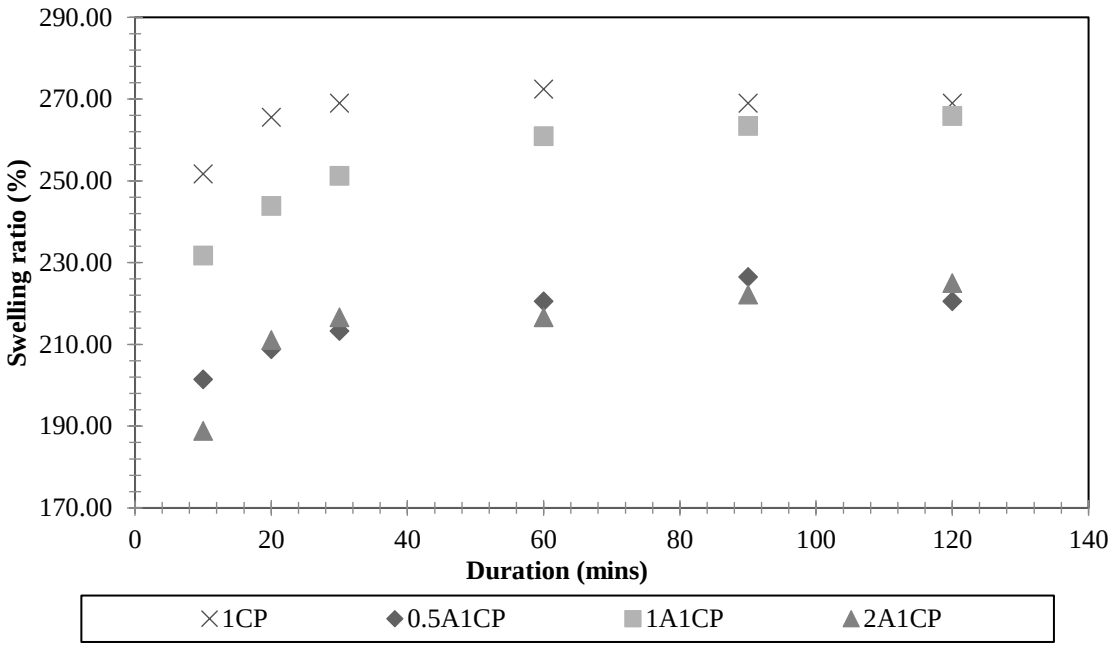

Figure 4.10. Swelling curves of 1CP and dense PCBMs

From the swelling curves, it was found that all the PCBMs reached the swelling equilibrium after 60 mins. At 60 mins, the swelling ratios of 1A1CP and 2A1CP PCBMs were 261.0 % and 216.7 %, respectively. Meanwhile, the swelling ratio of 0.5A1CP was 220.6 %. This indicates that the 1A1CP membrane has a lower ionic crosslinking degree and thus, having a higher degree of swelling as compared to the 2A1CP membrane. The presence of carboxylic functional group (C=O) in Alg observed from the FTIR spectrum peak of 1A1CP membrane at 1738.17 cm^{-1} (Figure 4.8) also suggests strong intermolecular interaction of Alg biopolymer at 1 wt% concentration, which also could be the cause of lower crosslinking degree in the 1A1CP PCBM. As for 0.5A1CP membrane, the low surface tension of Alg at 0.5 wt% Alg concentration, as compared to those at higher Alg concentrations (eg. 1 wt% and 2 wt%) (Lee & Chan et al., 2012) appears to be more dispersed and could easily interact with CS due to the weak intermolecular interaction of Alg.

Therefore, the high ionic crosslinking interaction between 0.5 wt% Alg and 1 wt% CS caused lower swelling ratio of 0.5A1CP than 1A1CP. Nevertheless, the swelling ratio of PCBMs is lower than 1CP membrane indicating the interaction of Alg and CS.

iv. Surface wettability

The membrane active surface (Alg surface) was selected to evaluate the surface wettability of dense PCBMs. Before formation of dense PCBM, the contact angle of 1CP membrane was measured at $88.10^0 \pm 1.02^0$. The contact angle of PBCM declined when 0.5 wt% of Alg was introduced, and then increased when the concentration of Alg was increased from 1 wt% to 2 wt%. The surface contact angle was found to be 67.51 ± 0.01^0 for 0.5 wt%, 79.66 ± 1.18^0 for 1 wt% and $87.49^0 \pm 0.45^0$ for 2 wt% Alg as shown in Table 4.4. The higher surface water contact angle measured on the 1CP membrane was mainly attributed to the porous structure in the membrane network. The presence of air gap under the water droplet has resulted in higher water contact angle (Yuan & Lee, 2013) as compared to other dense PCBMs. As the dense Alg layer was formed on top of the porous 1CP membrane, the hydrophilicity of Alg hindered the effect of air gap on the water droplets and thus, resulted in the decrease in water contact angle of dense PCBMs.

Table 4.4. Surface water contact angle (^{0}) of various fabricated PCBMs

Membrane	**Surface contact angle (°)**
1CP	88.10 ± 1.02
0.5A1CP	67.51 ± 0.01
1A1CP	79.66 ± 1.18
2A1CP	87.49 ± 0.45

Based on the trend observed from the contact angle study, the presence of Alg for complexation with CS is the main contributor that dictates changes of surface contact angle in the

dense PCBMs. Lee & Chan et al. (2012) also reported increase in surface tension of biopolymer solution with increasing Alg concentration from 0.5 wt% to 2 wt% (Lee & Chan et al., 2012). This indicates that at low Alg concentration, the weak surface tension (or surface energy) of Alg polymers results in a stronger intermolecular interaction between Alg and water molecules. Therefore, the Alg surface can be easily wetted at low Alg concentration. As the concentration of Alg increases, the surface tension (or surface energy) of Alg also increases, resulting in strong intermolecular interaction between Alg polymer chains. This has caused difficulty for water to wet the surface of the membrane, hence resulting in higher water contact angle when Alg concentration was increased to 2% in the PCBM.

Incorporation of Alg, especially with low concentration Alg has led to a better membrane surface wettability as compared to 1CP membrane. However, the surface wettability reduced when higher concentration of Alg was loaded and this would have resulted in the reduction of permeates water fluxes. Thus, the latter part of study investigated membrane water fluxes under various operating pressures.

v. UP Water flux

In order to investigate the effects of Alg-complexalated layer on permeate water flux, the UP water fluxes of PCBMs were obtained under various pressure conditions (Figure 4.11). Due to the fact that the dense PCBM is mainly targeted for application in decentralized greywater treatment, the treatment system should not be operated at very high operating pressure as a safety precaution and energy minimization effort. Therefore, the maximum operating pressure investigated in this study was set at 4 bar (g).

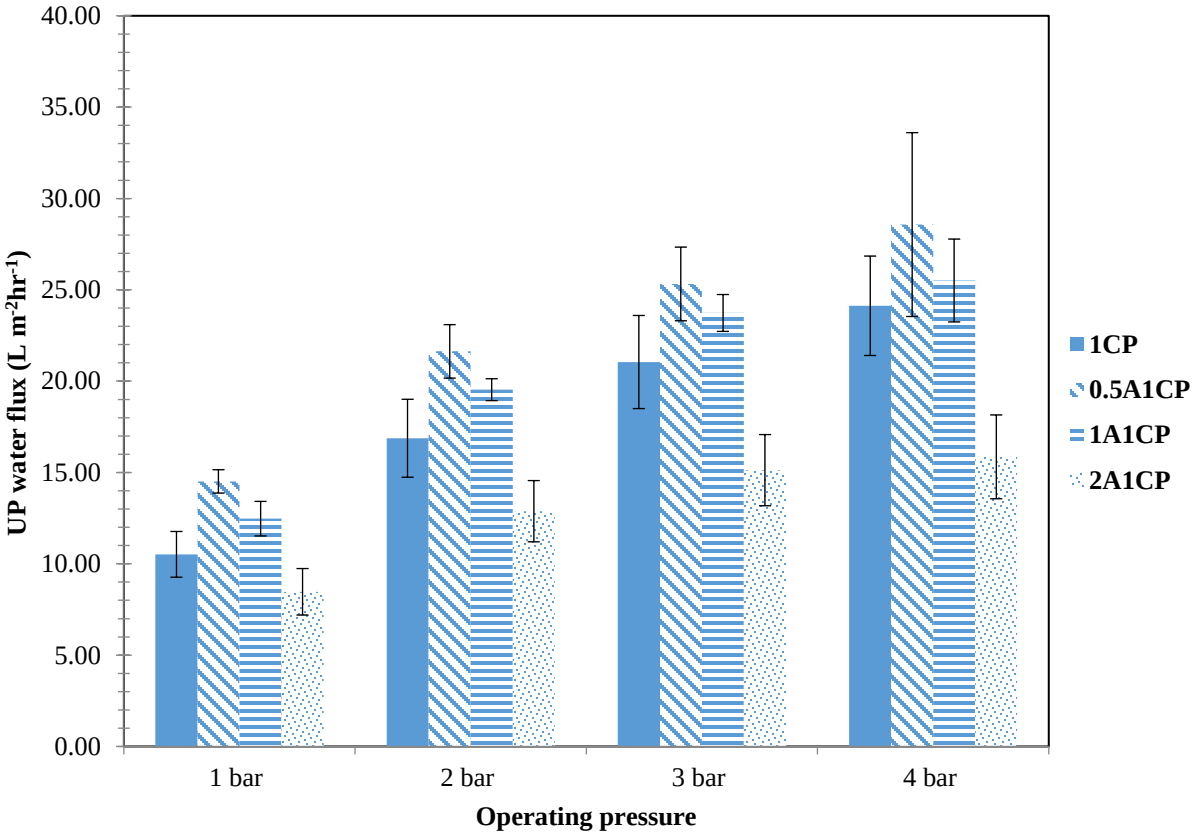

Figure 4.11. UP water flux of 1CP and dense PCBM membranes

Referring to Figure 4.11, the permeate water flux was found to be the lowest at an operating pressure of 1 bar (g) with an increasing trend against the operating pressure. The average UP water flux for 1CP membrane ranged from 10.52 L $m^{-2}hr^{-1}$ to 24.06 L $m^{-2}hr^{-1}$ when the operating pressure was varied from 1 to 4 bar (g). The 0.5A1CP PCBM showed the highest range of water flux readings with values between 14.51 L $m^{-2}hr^{-1}$ and 28.57 L $m^{-2}hr^{-1}$ under similar operating pressure conditions. However, the UP water flux produced by 1A1CP and 2A1CP PCBMs showed a declining trend as compared to the 0.5A1CP and 1CP membranes. The water fluxes produced by PCBMs were very much dependent on the concentration of Alg and surface wettability. Other than

that, based on the cross-section images of the membranes in Figure 4.9 (a) to (d), it can be observed that the increase in Alg concentration resulted in an increased thickness on the Alg layer, leading to a higher resistance of water molecules permeating through the membranes. In addition, as discussed in Section 4.2.2iv, the increase in Alg concentration was found to enhance the hydrophobicity of membrane, causing the PCBMs with higher Alg concentration to experience low permeation of UP water. Thus, the concentration of Alg in PCBMs should be minimized to avoid excessive flux reduction. Alternatively, porogens can also be introduced in Alg to enhance the porosity and thus improving the overall water flux.

*vi. **Molecular weight cut-off (MWCO)***

In this study, MWCO was used to determine the minimum size of solute that can be removed by the fabricated PCBMs. Prior to the complexation of Alg with CS to form PCBMs, the MWCO of pure CS 1CP membrane was found to be approximately 242 kDa (Figure 4.12 (a)). The complexation of Alg with CS to form PCBMs was expected to reduce the pore sizes or MWCO due to higher degree of crosslinking (Zeng & Fang, 2004). From Figure 4.12 (b) to (d), it was found that the MWCO of PCBMs down shifted from 242 kDa (1CP) to the range of 2.71 kDa to 3.08 kDa. The MWCO of PCBMs with increasing amount of Alg did not vary drastically. The MWCO of PBCMs fall in a narrow margin mainly due to the fact that the formation of PEC occurs at the interface of Alg and CS, but not throughout the entire biopolymer network. Thus, this has only resulted in a 12 % difference in the MWCO values of these membranes. Nevertheless, the incorporation of Alg layer on 1CP membrane has significantly reduced the MWCO. With the low MWCO in PCBMs, the membrane is expected to be able to remove higher amount of pollutants in

greywater than 1CP membrane. Subsequently, all the membranes were tested in greywater filtration to understand the effect of incorporation of Alg in the removal of pollutants.

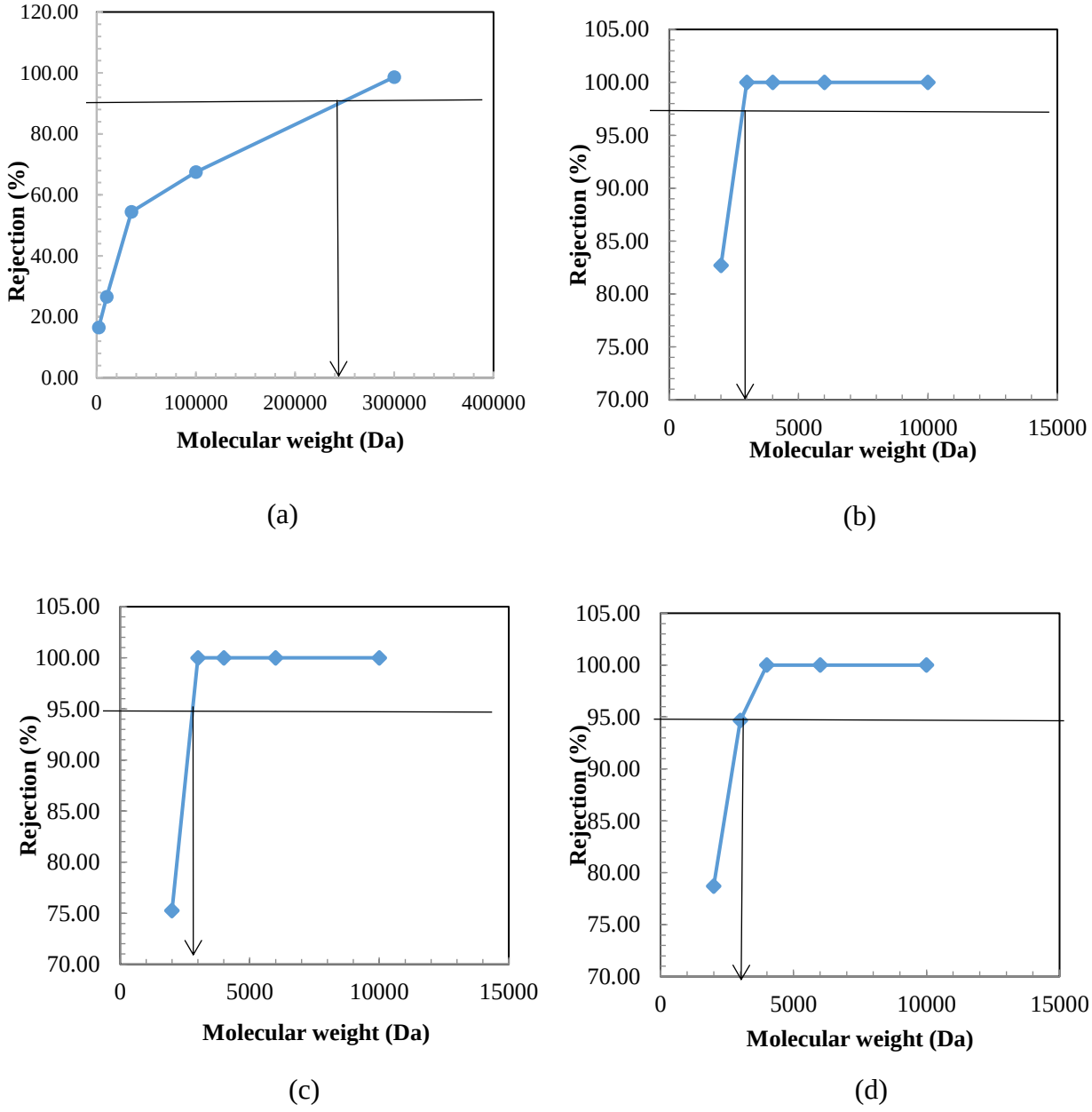

Figure 4.12. (a) MWCO of 1CP membrane (b) MWCO of 0.5A1CP PCBM (c) MWCO of 1A1CP PCBM (d) MWCO of 2A1CP PCBM**.**

4.2.3 Greywater treatment

Based on results obtained in Table 4.5, dense PCBMs showed superior ability in the removal of TSS and turbidity. In essence, 99.9% removal of turbidity and 100% removal of TSS can be achieved using PCBMs for greywater filtration. In addition, PCBMs showed higher turbidity removal efficiency of 5.2% higher than 1CP membrane, producing treated greywater effluents that meet the non-potable reuse standard in terms of turbidity and TSS levels (< 5 NTU for turbidity and < 30 mg L^{-1} for TSS).

Table 4.5. Greywater treatment efficiency using PCBMs

Parameters	Unit	1CP	0.5A1CP	1A1CP	2A1CP
pH	N/A*	6.65	6.84	6.94	6.99
Turbidity	%	94.7	99.9	99.9	99.9
TSS	%	100.0	100.0	100.0	100.0
COD	%	60.9	83.2	80.8	85.5
BOD_5	%	61.5	53.7	59.7	86.6
E. coli	%	N/A	100.0	100.0	99.9
Other coliforms	%	N/A	100.0	99.8	100.0
Pathogenic bacteria	%	100.0	99.7	81.6	99.0

*N/A = Not available

It was observed that the reduction of membrane MWCO also contributed to an improved removal of fine organic pollutants (i.e., COD) compared to 1CP membrane. As tabulated in Table 4.5, only 60.9% COD was removed using 1CP membrane, while COD removal with dense PCBMs was found to be ranging from 80.8% to 85.5%. This indicated that a 19.9% to 24.6% improvement in terms of COD removal could be achieved from greywater filtration using PCBMs. As reported by Hocaoglu & Atasoy et al. (2013), most of the COD size distribution is in the size range of > 1.2 µm and 14 nm to 220 nm, which is smaller than those that contributes to turbidity and TSS

contents. Thus, it could be deduced that the reduction in MWCO also contributed in the higher removal efficiency of finer-sized COD (eg. 14 nm to 220 nm).

Similarly, it was observed that the BOD_5 removal efficiency of PCBMs was enhanced when the concentration of Alg layer in the PCBMs increased. In addition, the increasing amount of anionic Alg biopolymer at higher Alg concentrations also resulted in higher repulsion of gram-negative microorganisms. Therefore, the improved bacteria removal also contributed to the higher BOD_5 removal efficiency when the concentration of Alg increased. The BOD_5 removal efficiencies of using PCBMs were found to be 53.7% to 86.6%. The relatively lower BOD_5 removal efficiencies of 0.5A1CP and 1A1CP membranes could be attributed to the thinner Alg layer that allowed higher amount of microorganism to penetrate through the membrane.

The ability of dense PCBMs in disinfecting the greywater was also investigated. Overall, the dense PCBMs showed 99.9% to 100% removal of *E. coli*, 99.8% to 100% removal of other coliforms and 81.6% to 99.7% removal of pathogenic bacteria. Despite the reduction in bacteria, the treated greywater effluents produced using dense PCBMs did not meet the reuse standard in terms of pathogenic bacteria. Bacteria were found to escape from the membrane filtration system even though there was a down shift in the MWCO of dense PCBMs. This implies that, the actual pore size of the membrane could be bigger than the actual MWCO obtained. In fact, Guo and Santschi (2007) found that a 0.02 µm (300 kDa) membrane could have an actual MWCO of 3 kDa. As such, some contaminants could escape from the membrane when its dimension is smaller than the membrane pores. In addition, the formation of PEC between CS and Alg biopolymers and also

the pH of raw greywater that ranged from 6.65 to 6.99 caused reduced antimicrobial property of CS due to lack of interactions between positive functional groups of CS with the bacteria.

Greywater flux of various membranes was recorded for duration of 30 mins (Figure 4.13). Higher greywater flux was recorded for 0.5A1CP and 1A1CP PCBM compared to 1CP, whilst 2A1CP had the lowest greywater flux. The study coincides with the finding of UP water flux from Section 4.2.2v, where 0.5A1CP PCBM has the highest water flux. Hence, 0.5A1CP PCBM was selected for further evaluation of greywater flux for 15 runs of 2 hours filtration per cycle. The fresh membrane was found to have highest greywater flux (31.99 L $m^{-2}hr^{-1}$), as the pores of the fresh membrane were not clogged up by the pollutants in the greywater. Greywater flux declined on the second and third cycle due to the accumulation of pollutants on the surface of the membrane. After the fourth cycle of greywater filtration, 0.5A1CP PCBM started to reach consistent greywater flux by producing an average of 13.26 L $m^{-2}hr^{-1}$ (318.26 L $m^{-2}day^{-1}$) of treated greywater. This indicated that approximately 37 hours was needed to process the greywater produced from a family with five members (In Malaysia, average of 97.18 L greywater generated per day per person) using a 1 m^2 0.5A1CP membrane. This showed that the dense PCBM is still not practical to be applied in greywater filtration due to low filtration flux and long operational hours required for greywater treatment.

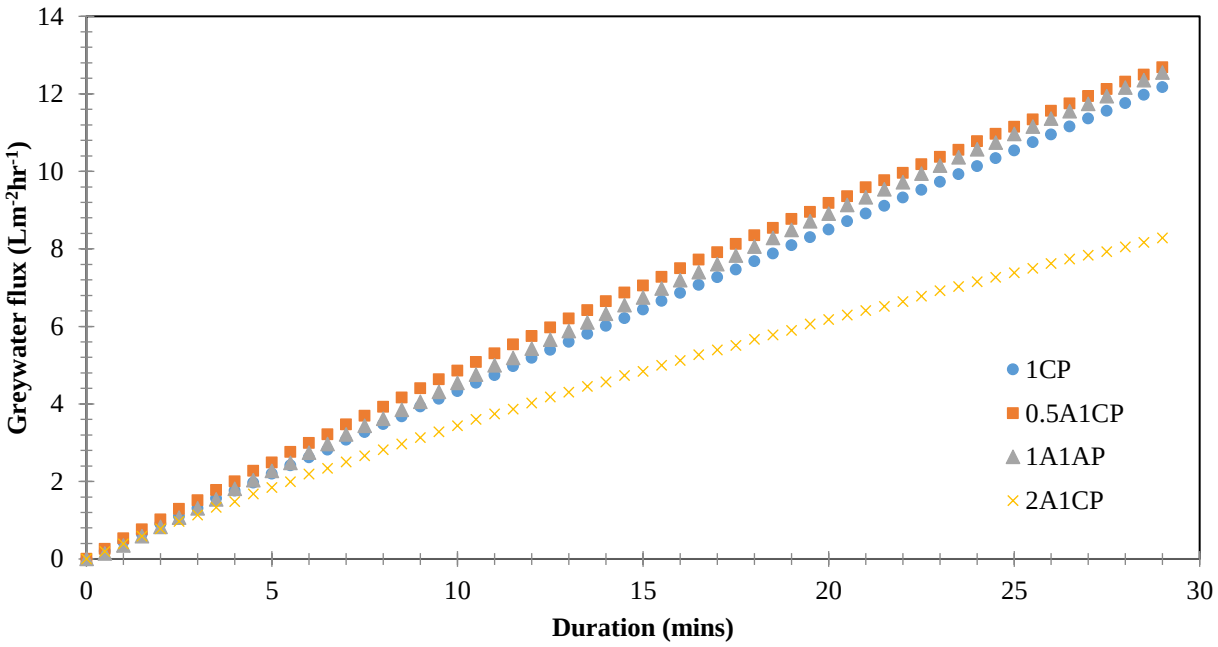

Figure 4.13. Greywater flux of various membranes

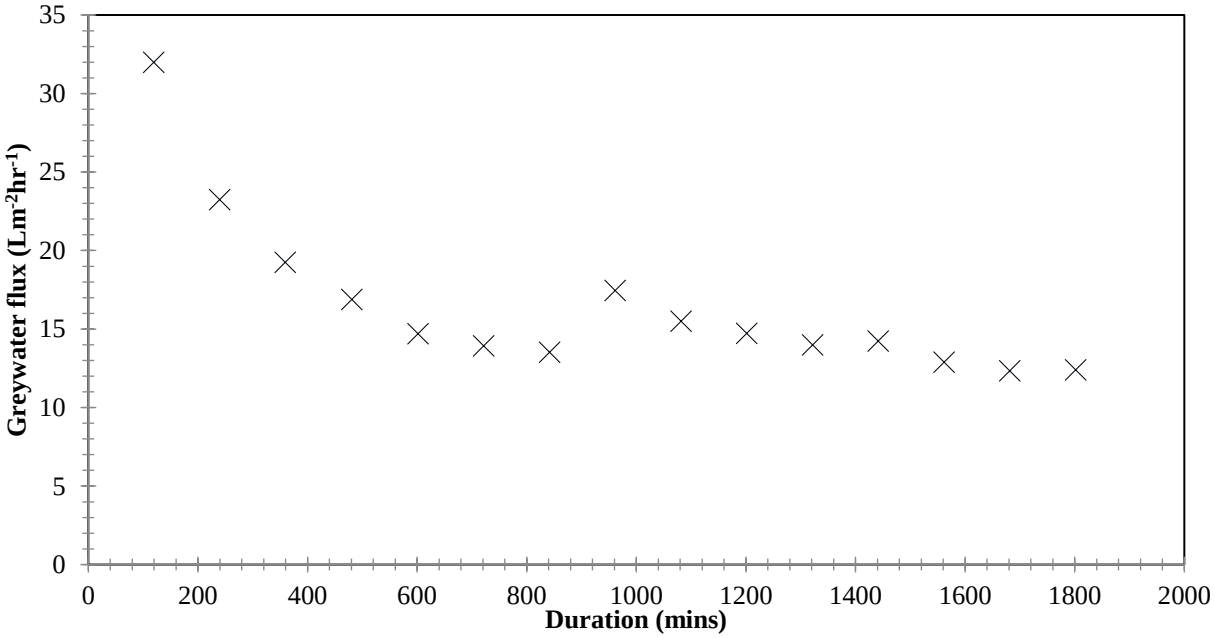

Figure 4.14. Greywater filtration flux of 15 cycles using 0.5A1CP PCBM (2 hours per cycle

4.3 Phase II (2): Fabrication of porous PCBM for greywater filtration

4.3.1 Membrane characteristics

i. Molecular structure and cross-sectional structure

Despite the ability of dense PCBM to produce consistent and high quality of treated greywater permeate, the dense PCMB has an issue of low water flux. For instance, the highest water flux achievable (31.99 L $m^{-2}hr^{-1}$) using fresh 0.5A1CP membrane was not sufficient and will be a potential problem when applied in the commercial scale due to the huge amount of greywater that has to be processed.

Therefore, Phase II (2) was conducted to introduce P-6000 into the Alg layer to obtain an entirely porous PCBM for greywater filtration. As a basis for comparison, dense 2A1CP PCBM was selected due to its high mechanical strength and decent greywater treatment efficiency. The FTIR tabulated in Figure 4.15 indicated that pores were successfully formed by blending and washing away P-6000 from the porous PCBMs. The FTIR peaks for porous PCBMs were similar to the dense PCBM (an example of FTIR results for 2A1CP was illustrated in Figure 4.15). Furthermore, SEM images in Figure 4.16 (b - d) showed the appearance of pores in the Alg layer in contrast to the dense PCBM (Figure 4.16 (a)).

However, it was observed that the broaden peaks at 3000 cm^{-1} to 3500 cm^{-1} (eg. 3291 cm^{-1}) for 1AP1CP is lower than other PCBMs. This is attributed to the partial miscibility of Alg and PEG when the casting mixture contains 1 wt% Alg and 1 wt% PEG (Siddaramaiah & Mruthyunjaya Swamy, 2007), which causes difficulty for PEG to be completely removed from the Alg layer of the porous PCBM. This is supported by the SEM image of Figure 4.16 (c), where there

is a distinct dense layer of Alg at the surface of the Alg layer. The dense Alg layer in 1AP1CP contributes to distinct differences in other membrane properties which will be discussed in subsequent sections.

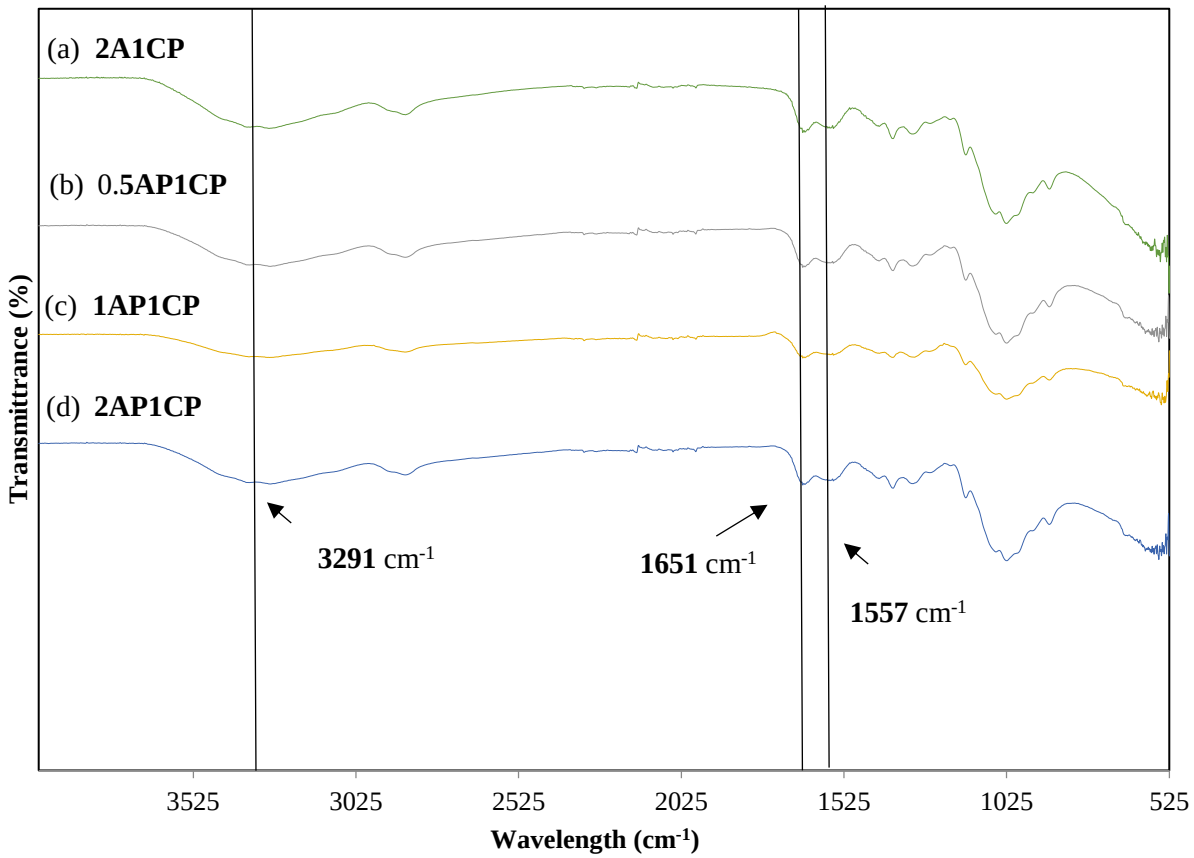

Figure 4.15. FTIR spectra for dense and porous PCBMs

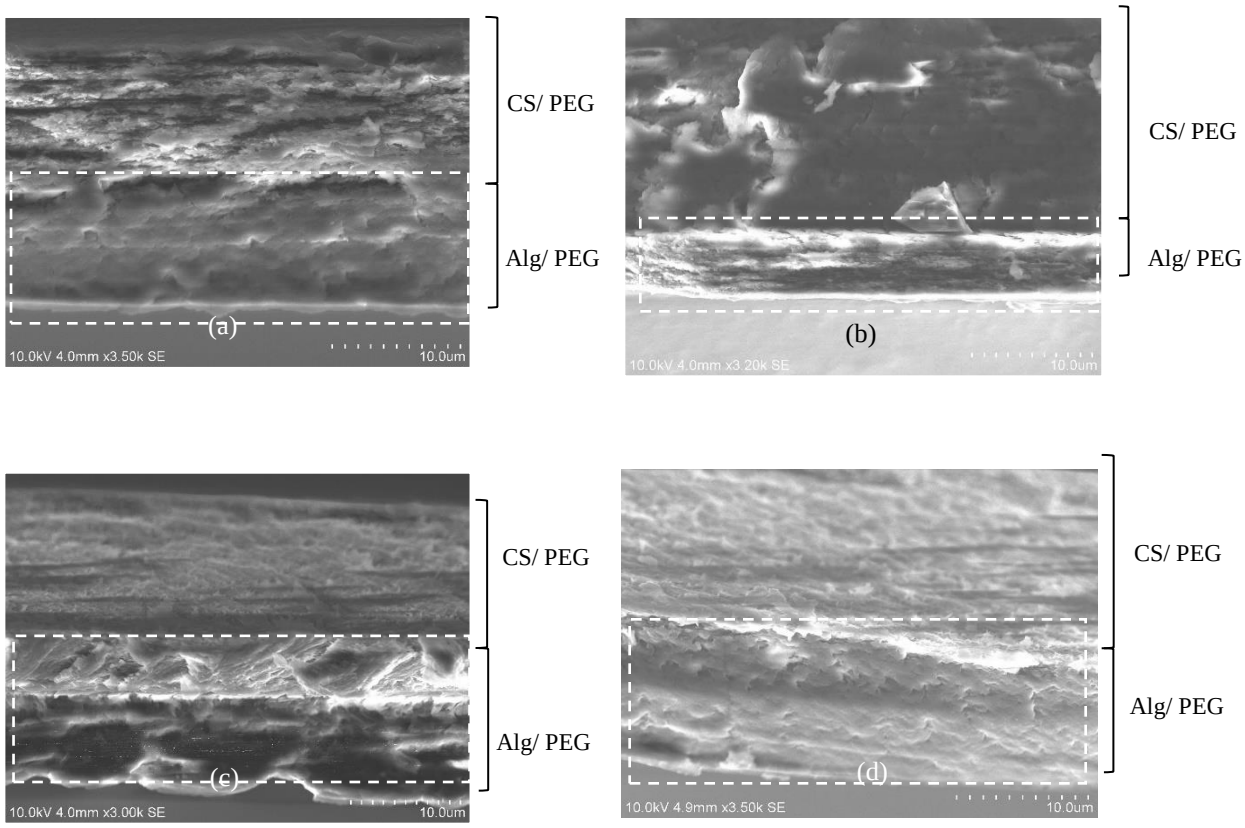

Figure 4.16. (a) Cross-section image of 2A1CP membrane (Oh & Poh et al., 2016) (b) Cross-section image of 0.5AP1CP PCBM (c) Cross-section image of 1AP1CP PCBM (d) Cross-section image of 2AP1CP PCBMs.

ii. Swelling ratio, MWCO and UP water flux

Swelling of the porous PCBMs were studied to investigate the effect of inducing pores to the Alg layer in the overall membrane structure. Figure 4.17 illustrates the swelling profiles of PCBMs. It was observed that these PCBMs reached equilibrium swelling at the duration of 60 mins. In general, the porous PCBMs had higher water uptake ability compared to dense PCBM (2A1CP), where the swelling ratio at 60 minutes ranged between 254.5% to 262.5%, as the Alg/ PEG concentration was varied from 0.5 wt% to 2 wt%. This implies that pores were successfully formed on the Alg layer as presence of porous structure allows more water uptake by the membrane, leading to higher swelling ratios as compared to dense PCBMs (Vimala & Mohan et al., 2010).

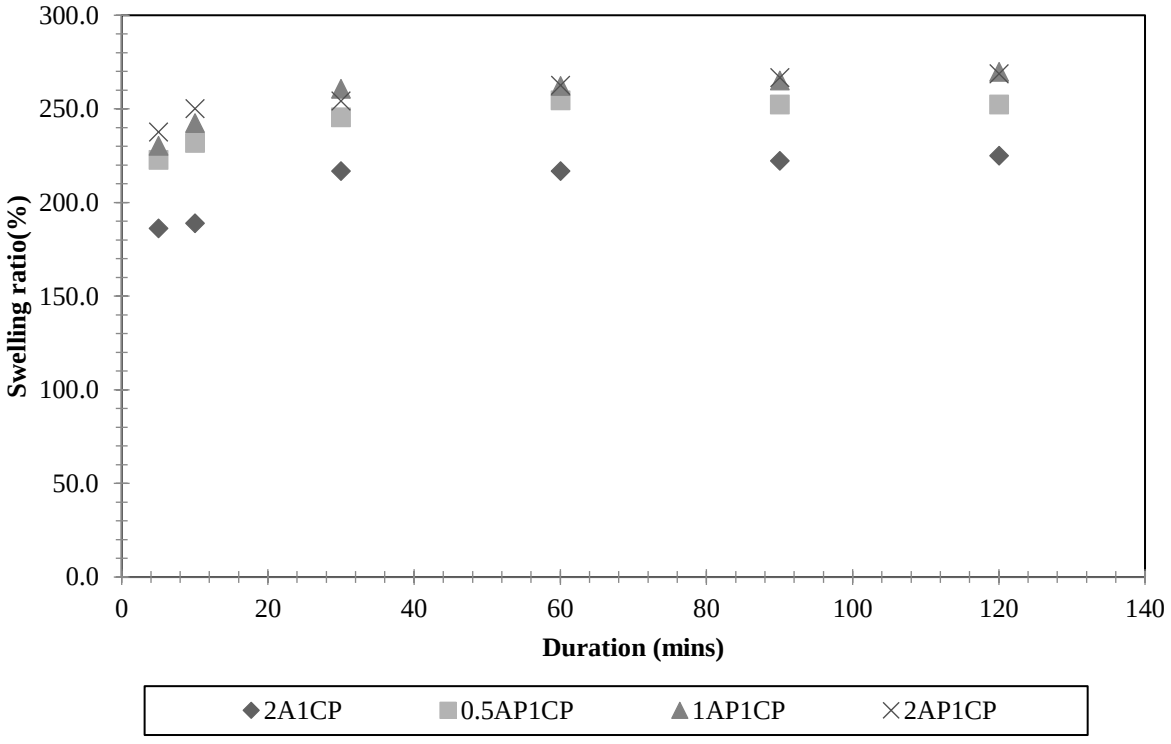

Figure 4.17. Swelling profiles of porous PCBMs

This result concurs with the MWCO study whereby the MWCO of the porous PCBMs are slightly larger than the 3.08 kDa of 2A1CP membrane. The presence of pores on the Alg layer caused a 7.4% to 19.0% increase to the MWCO of the PCBM. The additional pores present in the Alg layer has contributed to the additional water uptake onto the membrane. Hence, the increase in MWCO of the porous PCBMs implies that the water flux that can be obtained via filtration is expected to improve.

Despite the increase in MWCO of the porous PCBMs, the result in Table 4.6 reflected that the MWCO of 1AP1CP membrane was the least compared to the other porous membranes. This is in fact related to the earlier finding where two distinct layers were formed on the Alg layer of the 1AP1CP membrane due to partial miscibility of Alg and PEG at 1:1 weight ratio. The dense layer on the 1AP1CP layer caused the membrane to have relatively less pores as compared to the other porous PCBMs. The condition of 1AP1CP also affected the filtration performance of the membrane that will be elaborated below.

Table 4.6. Comparison of MWCO between dense and porous PCBM

Description	Membrane	MWCO	Percentage different of MWCO (%)
Dense PCBM	**2A1CP**	3080 Da	0
Porous PCBM	**0.5AP1CP**	3800 Da	19.0
	1AP1CP	3325 Da	7.4
	2AP1CP	3342 Da	7.8

Similar to previous phases, the UP water flux obtained from filtration using different PCBMs under various operating pressures was plotted on Figure 4.18. Results indicated that the water flux obtained via filtration of porous PCBMs have improved compared to the dense PCBM. In addition, the application of pressure on the filtration system also helped to increase the water flux. 2AP1CP porous PCBM showed superior performance as 39.73 L $m^{-2}hr^{-1}$ of UP water flux can be obtained

when 4 bar (g) filtration pressure was applied. The UP water flux is approximately 2 times more than the UP water flux that was obtained by the 2A1CP dense PCBM.

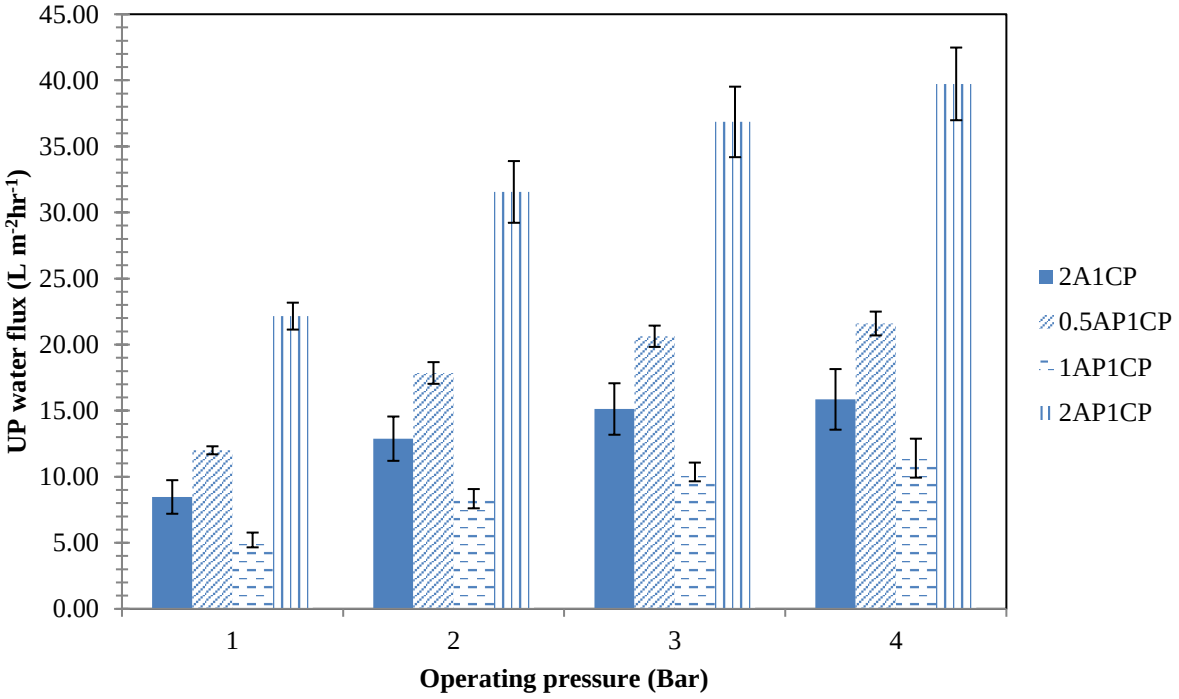

Figure 4.18. UP water flux of different pressure

The higher water flux is closely related to the swelling ratio and the MWCO of the 2AP1CP porous PCBM. The ability to retain more water due to exposure of more hydrophilic functional groups and also having slightly larger pores allows better passage of water through the porous PCBM. Despite having larger MWCO, the 0.5AP1CP porous PCBM was not able to exceed the production of UP water flux by 2AP1CP porous PCBM due to lower concentration of Alg in the membrane structure.

On the other hand, the 1AP1CP's dense layer at the surface of the Alg caused the UP water flux obtained to be lower than the 2A1CP dense PCBM. Although there are pores at some parts of the Alg layer of the 1AP1CP porous PCBM, the blending of PEG to the Alg network caused reduced

availability of carboxyl and hydroxyl groups that could help in the water uptake. Therefore, there is no significant increase in the UP water flux even when higher pressures were applied to the filtration system installed with the 1AP1CP porous PCBM.

Based on the results obtained so far, the significant increase in the UP water flux obtained using the 2AP1CP porous PCBM is desirable as higher volume of permeate can be generated even when only slightly pressurized. This allows reduction of energy consumption when processing high amount of greywater. However, there is a need to ensure that the greywater treatment efficiency is not compromised due to the larger MWCO of the porous PCBMs.

4.3.2 Greywater treatment efficiency

i. Pollutants removal

Table 4.7 lists the treatment efficiency after greywater filtration using porous PCBMs. It is evident that the porous PCBMs are superior in terms of TSS and turbidity removal as the effluent obtained were consistently < 1 ppm and < 1 NTU respectively, meeting the greywater reuse guidelines. This achievement is possible because the particle size that contributes to TSS and turbidity falls in the range that is way larger than the MWCO of the porous PCBMs (10 μm to 100 μm) (Jefferson & Palmer et al., 2004). Despite the increase in MWCO, the membrane also maintained its capability to remove COD from greywater, where more than 80% of COD can be removed using porous PCBMs. Therefore, it is evident that the 7.4% - 19% increase in MWCO does not have much impact on the contaminant removal efficiency of the porous PCBMs.

Table 4.7. Pollutants removal efficiency using dense and porous PCBMs

	Dense PCBM	Porous PCBM		
Parameters	**2A1CP**	**0.5AP1CP**	**1AP1CP**	**2AP1CP**
pH	6.99	6.84	6.94	6.99
Turbidity (%)	99.9	99.5	99.5	99.8
TSS (%)	100.0	97.8	99.0	99.5
COD (%)	85.5	80.7	89.2	81.5
BOD_5 (%)	86.6	37.0	73.6	96.9
***E. coli* (LRV)**	3.09	2.40	3.34	2.60
Other coliforms (LRV)	3.38	4.73	3.22	2.93

It was observed that the BOD_5 removal increased with the increase in the Alg/ PEG concentration. The complex porous structure of dual layer membrane played an important role to resist microorganisms and organic matters from passing through the PCBM, into the treated greywater. The BOD_5 removal percentage was found to be highest when using 2AP1CP membrane as this membrane has the thickest Alg/ PEG layer that exhibit highest resistance towards penetration of organic pollutants.

On the other hand, treated greywater effluent using porous PCBMs contained 0 CFU 100 mL^{-1} of *E. coli*. The respective *E. coli* log removal values (LRV) are 2.40-log using 0.5AP1CP, 3.40-log using 1AP1CP, 2.60-log using 2AP1CP. Besides, the porous PCBMs was found to be able to remove up to 4.73-log of coliforms bacteria. It could also be observed that, despite the higher MWCO of 0.5AP1CP and 1AP1CP as compared to 2A1CP membrane, the complex porous structure of the two membranes hindered the passage of these bacteria and resulted in high disinfection rate. In contrast, 2AP1CP membrane was found to have slightly lower overall LRV as compared to other PCBMs. It was deduced that the formation of PEC using high concentration of Alg/ PEG (eg. 2 wt%) involved higher degree of ionic crosslinking, causing a higher reduction in the functional groups of CS that are responsible for the anti-microbial property towards gram-positive and gram-negative bacteria (Kong & Chen et al., 2010).

4.3.3 Greywater flux decline

During greywater filtration, the membrane flux was found to decline with time. As a result, the greywater flux was recorded to evaluate the degree of membrane flux decline due to the clogging of pollutants. Figure 4.19 depicts the normalized flux of greywater permeate using different porous PCBMs and 2A1CP dense PCBM. The flux of dense PCBM 2A1CP was found to experience the most severe flux reduction. The membrane flux reduced approximately 57% from its UP water flux during greywater filtration. On the other hand, 1AP1CP had the flux decline of 32%, which is the most severe amongst porous PCBMs but still displayed better performance compared to the 2A1CP dense PCBM. The more severe flux decline of 1AP1CP porous PCBM compared to the other porous PCBMs was attributed to the smaller MWCO of 1AP1CP PCBM (3325 Da) and complex dense-porous structure due to the difficulty of removing P-6000 from the Alg layer. Meanwhile, the flux decline of 0.5AP1CP and 2AP1CP were relatively lower, as the MWCO of 0.5AP1CP and 2AP1CP were slightly higher than 1AP1CP. The greywater flux declined approximately 18% and 20% from its initial fluxes with the use of 0.5AP1CP and 2AP1CP membranes respectively.

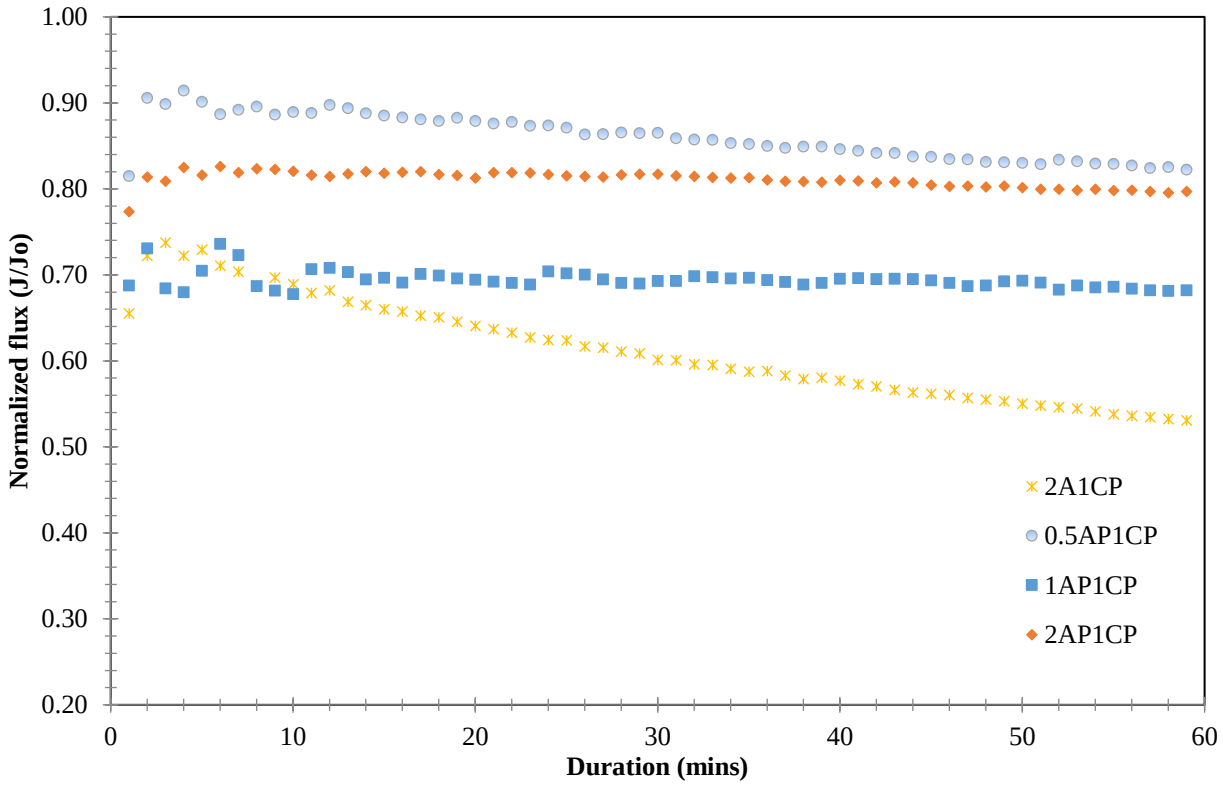

Figure 4.19. Normalized flux declined of greywater filtration using various membranes

Based on the result of normalized flux, it can be deduced that dense Alg layer is a crucial factor in contributing to severe flux decline, as shown in the result of 2A1CP dense PCBM. The dense layer contributed to high mass transfer resistance to water molecules, which eventually led to high flux reduction during greywater filtration. In addition, this membrane was found to have smaller pore size (3.08 kDa) as compare to other porous PCBMs. As the membrane foulants are mainly pollutants with sizes of 3 nm to 20 nm (Lee & Amy et al., 2004), these small pollutants could easily deposit in the small pores of 2A1CP to cause flux reduction (Field, 2010). Thus, it could be concluded that the size of the pollutants, membrane structure and MWCO of the membrane are closely related and these are the major factors contributing to flux decline.

2AP1CP membrane produced approximately 60% more UP water permeate as compared to the 2A1CP dense PCBM. On the other hand, the slight increase in the MWCO of 2AP1CP porous

PCBM was found to have limited effect on greywater treatment efficiency. Furthermore, the moderate flux decline as compared to other PCBMs could reduce frequency of membrane cleaning and replacement. Hence, this makes 2AP1CP porous PCBM to be an appropriate membrane for application in greywater treatment. However, the BOD_5 of the treated greywater did not meet the desired standard using the 2AP1CP porous membrane. As a consequence, the next phase will involve modification of 2AP1CP porous PCBM to enhance the disinfection efficiency that will contribute to improve BOD_5 removal efficiency of the membrane during greywater treatment.

4.4 Phase III: Incorporation of AgNP in porous PCBM: Effect on disinfection efficiency and flux decline evaluation

4.4.1 Phase overview

Results from Phase II highlighted the improvement of membrane water flux with the incorporation of PEG in the Alg layer. 2AP1CP membrane was found to produce the highest UP water flux (39.73 L $m^{-2}hr^{-1}$) with moderate flux decline while maintaining its ability in removing physical and chemical pollutants during greywater treatment. However, due to the presence of trace amount of microorganisms in the treated greywater, AgNP was proposed to be loaded into the 2AP1CP to improve the disinfection rate. This phase of the study thoroughly investigates the performance of the 2AP1CP membrane incorporated with AgNP on greywater filtration and the fouling mechanisms of the membrane.

4.4.2 Membrane characterizations

i. Swelling ratio

As the concentration of AgNP (0.02 % to 0.05 % of the total membrane weight) loaded in the Alg layer is very low as compared to other components in the membrane (eg. CS and Alg), the changes in the molecular structure of the membrane were not detected using the FTIR. Thus, swelling ratio was used to identify the changes of membrane structure when AgNP was loaded. As AgNP was loaded in the 2AP1CP porous PCBM, it was observed the swelling of the membrane became lower as compared to the membrane without AgNP.

As tabulated in Figure 4.20, the swelling ratio of the three AgNP PCBMs tested fall in the narrow range of 224% to 235%, as compared to 267% for 2AP1CP. The significant reduction of swelling ratio could be attributed to the formation of hydrogen bonding and static interaction between AgNP

and Alg polymer chain (eg. carboxyl and hydroxyl groups). As a result, the hydrophilic functional groups in the membrane decreased and contributed to the lower swelling ratio as compared to the 2AP1CP porous PCBM. In addition, the knot-tying effect of AgNP in polymers network was also reported in previous study by Yadollahi et al. (2015). It was found that the knot-tying effect could result in lower swelling ratio as the polymers chains formed knots and led to reduction of possible sites to pick up more water molecules (Yadollahi & Farhoudian et al., 2015).

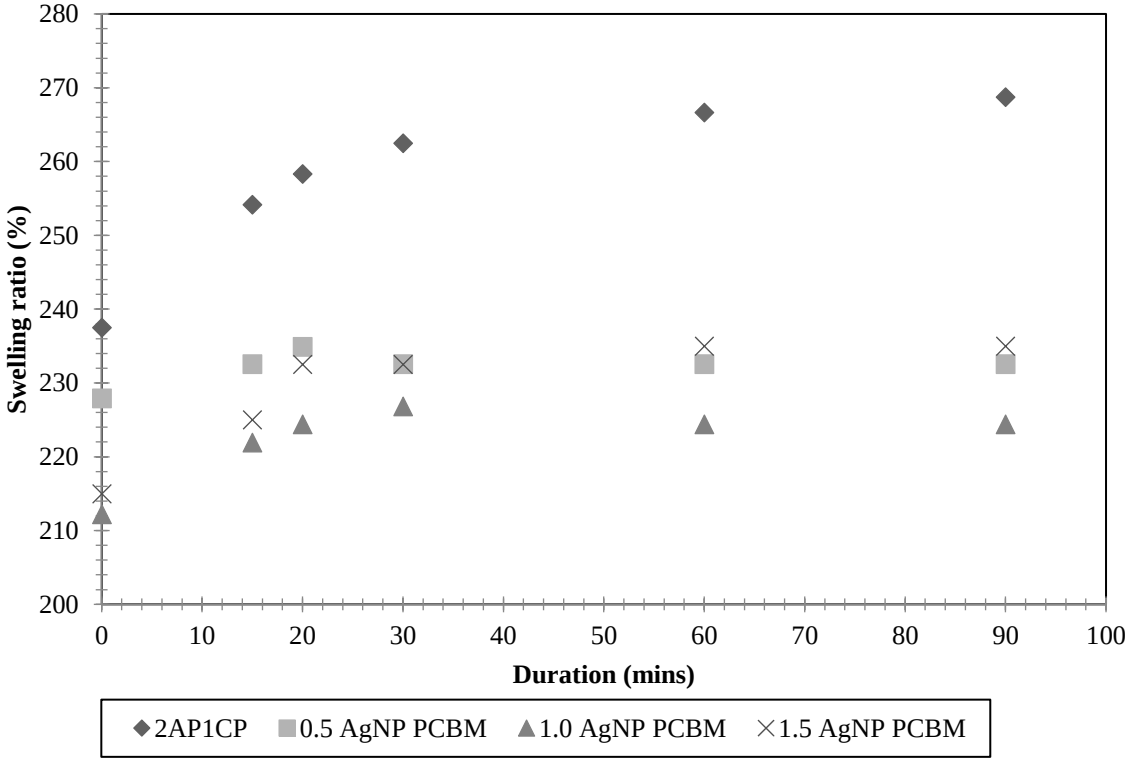

Figure 4.20. Swelling profiles of AgNP PCBM

ii. Thermagravimetry analysis (TGA)

To further justify the presence of AgNP in the AgNP PCBM, a few membranes (1CP, 2AP1CP, 1.5 AgNP PCBM) were subjected to thermal decomposition from 0°C to 800°C. The weight percentage and derivative weight loss of the samples tested were recorded. The thermal decomposition curves (Figure 4.21) showed that, 1CP and 2AP1CP membrane had two-stage

thermal degradation. The first weight change for 1CP happened in the temperature range of 22°C to 115°C due to water loss (Zhen & Xiaoxu et al., 2010). Subsequently, a second rapid change was observed at the region from 268°C to 351°C where the weight loss corresponded to the CS in the single layer membrane. The weight of the sample tested eventually smoothens out after the second drop and reached 1.07 mg at 700°C.

On the other hand, a more significant weight change was observed for 2AP1CP within the range of the temperature tested (0 °C to 800 °C), indicating the presence of Alg/ PEG in the membrane network. In addition, the weight loss of water content from 22°C to 115°C was observed to be higher than the 1CP membrane sample. This indicated that higher amount of water was retained in the membrane due to the presence of porous Alg/ PEG layer. Similarly, the gradient of the weight loss at 268°C to 351°C temperature region was also greater as compared to 1CP membrane. A total of 67% weight decline was observed for 2AP1CP, while only 61% total weight loss observed for 1CP membrane.

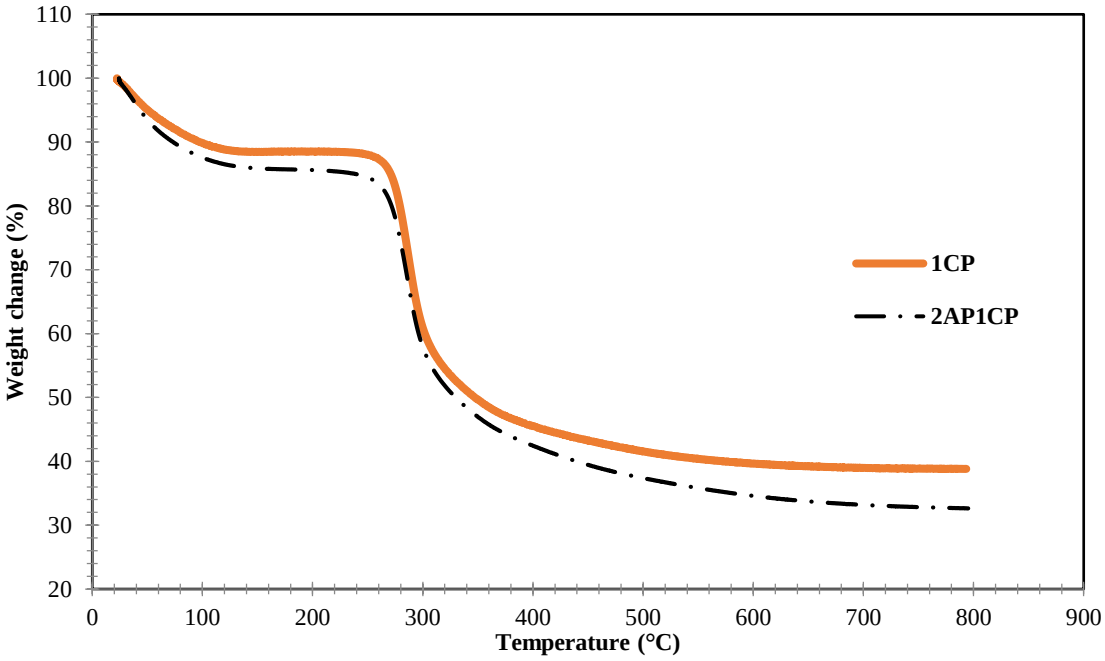

Figure 4.21. TGA curve of 1CP and 2AP1CP

Figure 4.22 illustrates the derivative weight curve of 1.5 AgNP PCBM. The graph indicated fours weight decline phases as the temperature increased from 0 °C to 800 °C. After the initial stage of weight decline due to evaporation of water content, the next decline was observed at 268°C is concurrent to the weight loss of 1CP and 2AP1CP. This indicated the presence of CS in the 1.5 AgNP PCBM. Thereafter, a third decline was detected at 321°C due to the Alg content in the membrane network and the last decline at 422°C corresponds to the AgNP content in the membrane. Besides, the total weight loss of 1.5 AgNP PCBM sample was observed to be 65%, which is higher than 61% in 1CP membrane but slightly lower than the 67% in 2AP1CP. The phenomena was reported due to the presence of AgNP that could not be completely degraded and the residue of AgNP in the tested sample resulted in the higher end weight (Abdul kareem & Anu kaliani, 2011). Hence, the TGA curves confirmed the presence of CS, Alg and AgNP in the 1.5 AgNP PCBM.

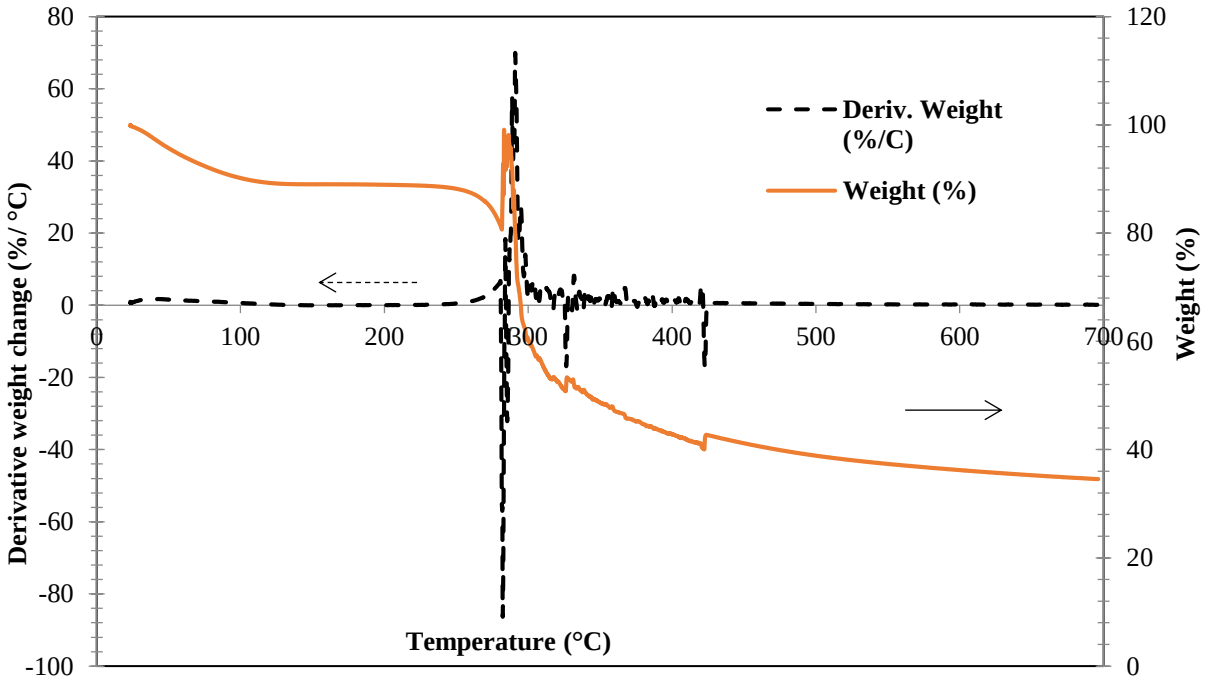

Figure 4.22. Derivatives weight change (%/C) and weight percentage of 1.5 AgNP PCBM

iii. Molecular weight cut-off (MWCO)

As the knot-tying effect of AgNP was found to have an impact on membrane swelling ratio, the effect could also cause reduction to the MWCO of AgNP PCBMs. As a matter of fact, the MWCO of the AgNP PCBMs was found to be relatively lower as compared to 2AP1CP (Figure 4.23 (a – d)). The MWCO of AgNP PCBM was found to range between 2766 Da to 2871 Da, which is approximately 14% lower than 2AP1CP (3342 Da). As the MWCO of the AgNP PCBMs reduced due to the formation of dense polymer network, the UP water flux should be affected by the reduction in MWCO of these membranes.

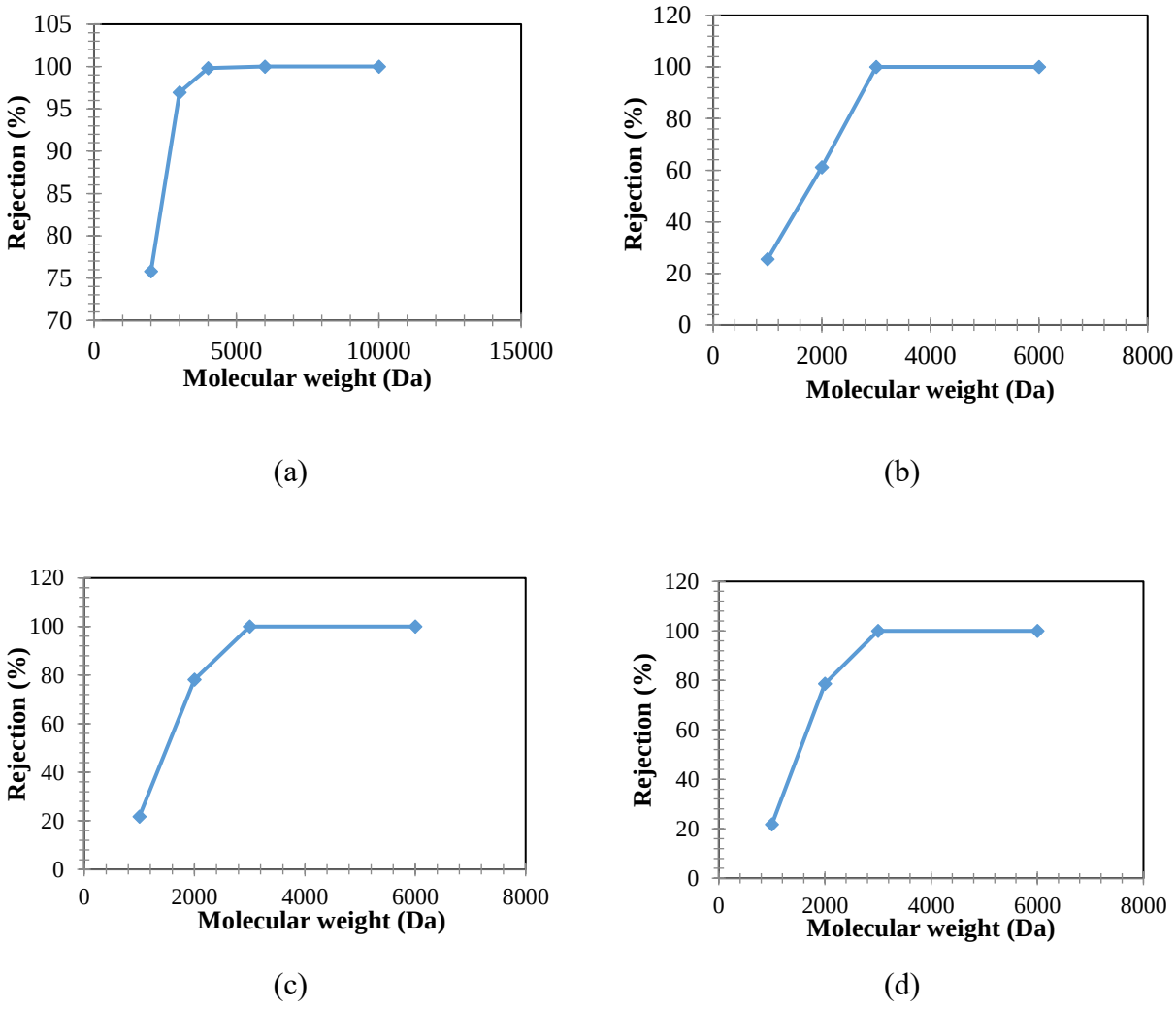

Figure 4.23. MWCO of (a) 2AP1CP; (b) 0.5 AgNP PCBM; (c) 1.0 AgNP PCBM and (d) 1.5 AgNP PCBM

iv. UP water flux of various AgNP PCBM

Figure 4.24 (a – d) shows the UP water flux of AgNP PCBM that was recorded from 1 bar (g) to 4 bar (g) filtration pressure. In general, there is a trend of reduced UP water flux when AgNP was incorporated into the 2AP1CP porous PCBM. The results agreed with the trend of the swelling profiles and MWCO of various AgNP PCBMs. It was observed that the recorded UP water flux for 0.5 AgNP PCBM was the lowest and ranged between 12.9 L $m^{-2}hr^{-1}$ to 22.8 L $m^{-2}hr^{-1}$ as filtration pressure was varied. As the concentration of AgNP increased, the repulsive interaction between AgNP resulted in higher voids, leading to higher UP water flux when AgNP concentration was increased. Amongst AgNP PCBMs, 1.5 AgNP PCBM showed highest UP water flux, which ranged from 17.9 L $m^{-2}hr^{-1}$ to 33.6 L $m^{-2}hr^{-1}$ for 1 bar (g) to 4 bar (g) filtration pressure. Despite the high UP water flux obtained from the usage of 1.5 AgNP PCBM, the UP water collected from the 1.5 AgNP PCBM was not as ample as 2AP1CP due to the presence of AgNP in the membrane. The UP flux of 1.5 AgNP PCBM was found to be 11% to 16% lower than 2AP1CP at various filtration pressures. Despite the slight reduction in UP water flux, the decrease of MWCO should contribute to better greywater treatment efficiency. At the same time, the anti-microbial effect of the membrane should be enhanced with the presence of AgNP.

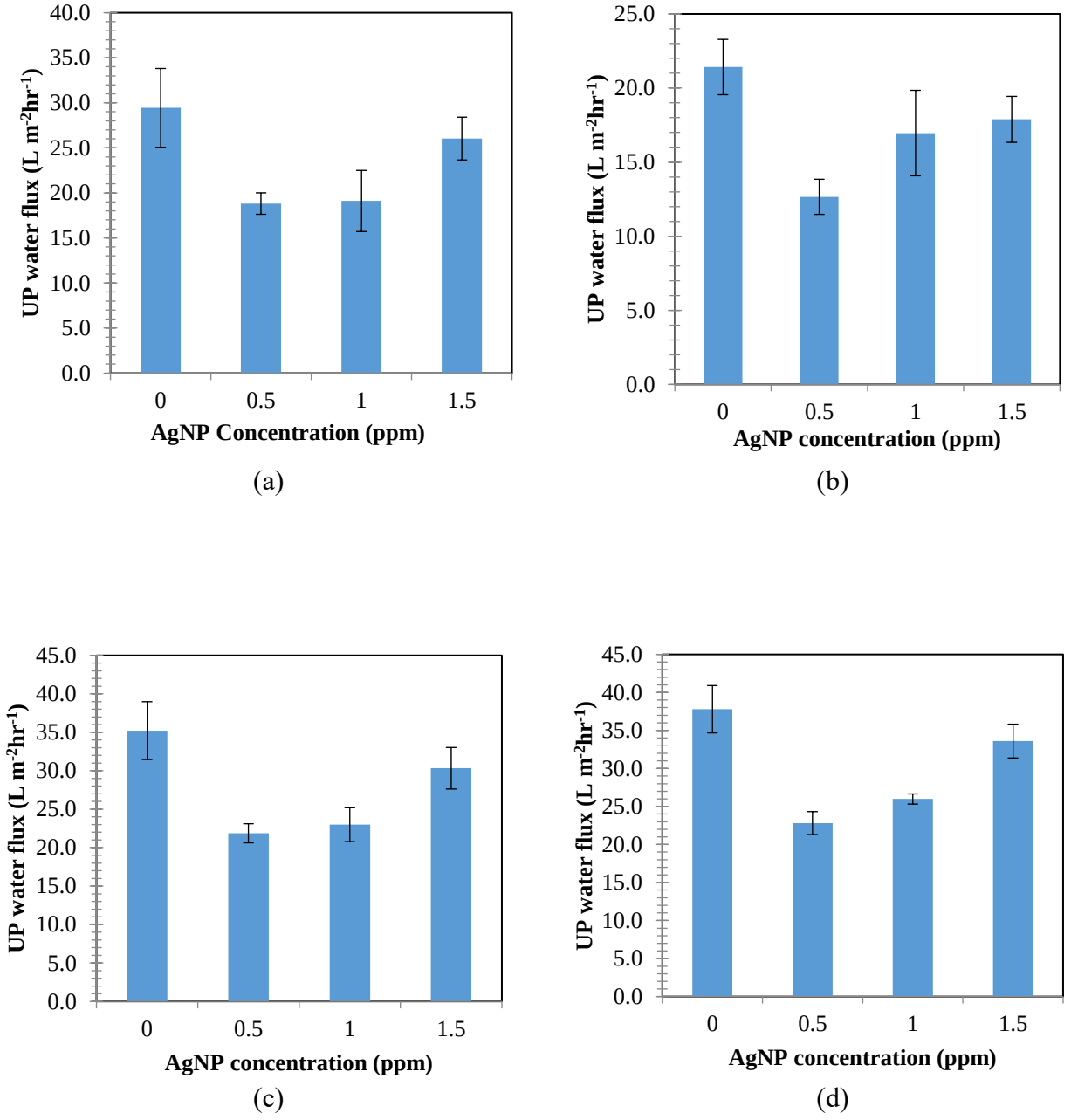

Figure 4.24. UP water flux of various AgNP PCBM at (a) 1 bar (g); (b) 2 bar (g); (c) 3 bar (g) and (d) 4 bar (g)

4.4.3 Greywater treatment efficiency

Based on Table 4.8, AgNP PCBMs were seen to retain the excellent performance of 2AP1CP porous PCBM in the removal of turbidity and TSS. The AgNP PCBMs were capable of removing 99.8% to 99.9% of turbidity, producing treated greywater with 0.2 - 0.35 NTU turbidity. Besides that, only < 1 ppm of TSS was detected in the treated greywater which corresponds to 99.6% to 100% removal of TSS. Meanwhile, COD removal by the AgNP PCBMs ranged from 79.7% to 82.5%, showing similar characteristic as 2AP1CP porous PCBM. This is mainly attributed to the small shift in the MWCO of approximately 14%. The particle sizes of COD generally fall in finer region (< 220nm). As such, the reduced MWCO of the AgNP PCBMs does not affect the COD removal performance of the membranes.

Table 4.8. Greywater treatment efficiency of 2AP1CP and AgNP PCBMs

Parameters	**2AP1CP**	**0.5 AgNP PCBM**	**1.0 AgNP PCBM**	**1.5 AgNP PCBM**
pH	6.99	7.14	6.9	7.1
Turbidity (%)	99.8	99.8	99.9	99.9
TSS (%)	99.5	100.0	99.6	100.0
COD (%)	81.5	80.9	79.7	82.5
BOD_5 (%)	96.9	67.0	46.7	82.6
***E. coli* (LRV)**	2.60	1.3	2.3	3.6
Other coliforms (LRV)	2.93	3.3	4.0	3.7

On the other hand, BOD_5 removal efficiency was enhanced when the concentration of AgNP loaded in the Alg/ PEG layer increased from 0.5 ppm to 1.5 ppm, peaking at 82.6% BOD_5 removal. However, BOD_5 removal using 1.0 AgNP PCBM was found to be relatively lower as compared to other AgNP PCBM, with only 47% removed from the greywater. This could be attributed to reduced exposure and contact of AgNP with the bacteria in the greywater at 1ppm AgNP concentration. By referring to the swelling profile in Figure 4.20, the 1.0 AgNP PCBM had the lowest swelling ratio due to the strong knots forming ability of 1 ppm AgNP with Alg polymer, causing reduced contact of

AgNP with the bacteria in greywater. As the concentration was further increased to 1.5 ppm of AgNP, the repulsive interaction between higher concentrations of AgNP resulted in higher spaces between AgNP and Alg polymer. This led to higher exposure of AgNP to the bacteria in greywater, resulting in higher BOD_5 removal using 1.5 AgNP PCBM.

Meanwhile, treated greywater from AgNP PCBM showed 100% removal of *E. coli* and coliforms bacteria. It can be postulated that biocides, such as AgNP, could interrupt the respiratory system, permeability of the cell membrane, cellular oxidation and enzymatic activity of the bacteria (Dror-Ehre & Mamane et al., 2009). As such, when the *E. coli* is in contact with AgNP, the silver ions could disrupt the phosphate and sulphur group in the bacteria cell membrane, which leads to bacteria cell fatality (Dror-Ehre & Mamane et al., 2009). Furthermore, the LRV of both *E. coli* and other coliform also showed an increasing trend with the AgNP concentration in the membrane. As shown in Table 4.8, when the AgNP concentration increase from 0.5 ppm to 1.5 ppm, the LRV of *E. coli* increased from 1.3-log to a maximum of 3.6-log, while LRV of coliforms increased from 3.3-log to 3.7-log. It was deduced that the increasing concentration of AgNP provides higher surface area and probability of bacteria to collide with AgNP. The result is concurrent with the finding of Dror-Ehre & Mamane et al. (2009) and Ping & Juan et al. (2005), in which these studies have indicated that higher AgNP concentration could lead to higher bacteria inactivation.

4.4.4 Membrane flux decline

The study of membrane flux decline mechanisms was conducted based on Hernia's model. By fitting the experimental data to the four different models of flux decline, the model with highest regression (R^2) value was selected as the best fit model for the prediction of membrane fouling. Constant and R^2 values of the fitted models were shown in Table 4.9. In general, the flux decline data of 2AP1CP porous membrane could fit the four flux decline models with high R^2 values that ranged

from 0.9744 to 0.9783. Due to the fact that the sizes of the pollutants in greywater were scattered over a wide range, the R^2 values obtained were quite close to each other. Of all the four models, it was found that cake formation and intermediate pore blocking models have better fit to all the membranes that were investigated for flux decline mechanism, with R^2 value as high as 0.9996. This indicated that cake formation and intermediate pore blocking were the two most predominant mechanisms to cause flux decline of the membranes.

Cake formation is one of the prevalent mechanisms of flux decline as greywater contains pollutants that have larger size than the pores. As the greywater is being filtered, there will be accumulation of these large sized pollutants on the surface of the membrane, forming a thick layer of filtered cake. This would have eventually resulted in high resistance for transportation of water molecules and led to membrane flux reduction (Salahi & Abbasi et al., 2010). Similarly, the data fitted for intermediate pore blocking also suggested that the membrane pores was clogged by pollutants of sizes similar to the membrane pore size (Salahi & Abbasi et al., 2010). This would have been made possible since greywater has pollutants with variety of sizes.

Amongst the two flux decline mechanisms identified, cake formation is regarded as the least severe fouling mechanism, as the foulant could be easily removed from the membrane via membrane washing or changing the flow configuration to crossflow filtration (Field, 2010; Skouteris & Hermosilla et al., 2012). However, there is a need to minimize the occurrence of intermediate pore blocking to avoid the deposition of pollutants in the membrane pores, which can cause irreversible fouling (Field, 2010; Skouteris & Hermosilla et al., 2012). As a result, it is suggested that routine membrane cleaning or replacement is required when the membrane is clogged. Other than that, mitigation step such as pre-filtering pollutants can be considered to reduce the frequency of such occurrences during the operation.

Table 4.9. Constants and regression for models fitting

	Slope (m)	C	R^2
2AP1CP			
Complete pore blocking	-0.138	3.5224	0.9744
Standard pore blocking	0.0121	0.1718	0.9764
Intermediate pore blocking	0.0042	0.0295	0.9771
Cake formation	0.0003	0.0009	0.9783
0.5 AgNP PCBM			
Complete pore blocking	-0.629	3.9551	0.9927
Standard pore blocking	0.0471	0.1385	0.9956
Intermediate pore blocking	0.0001	0.0191	0.9977
Cake formation	0.0006	0.0004	0.9996
1.0 AgNP PCBM			
Complete pore blocking	-0.4293	3.2155	0.9898
Standard pore blocking	0.0453	0.2002	0.9898
Intermediate pore blocking	0.0191	0.04	0.9917
Cake formation	0.0017	0.0016	0.9939
1.5 AgNP PCBM			
Complete pore blocking	-0.6762	3.3585	0.9911
Standard pore blocking	0.0684	0.1861	0.9946
Intermediate pore blocking	0.0277	0.0345	0.9971
Cake formation	0.0023	0.0012	0.9994

In phase III, AgNP was successfully loaded to improve the disinfection efficiency. The treated greywater generated from 1.5 AgNP PCBM was characterized and it was found that the quality of the treated greywater met the greywater reused standard of turbidity < 5NTU, BOD_5 < 20 ppm, non-detectable *E. coli* and other coliforms. In addition, the study of the flux decline of the membranes indicated that cake formation is the main fouling factor, followed by intermediate pore blocking.

4.5 Phase IV: Design and performance evaluation of a decentralized greywater treatment system (DGTS)

4.5.1 Phase overview

Previous phases emphasized on the characterization of membranes and greywater filtration performance without focus on long period operations. It is crucial to ensure that the membrane is able to last for multiple cycles to ensure applicability of such system in the commercial scale. Therefore, a 20 L DGTS was designed for the purpose of studying the long term operating performance of the 1.5 AgNP PCBM on greywater filtration.

4.5.2 Membrane characterizations

1.5 AgNP PCBM was selected for this study from Phase III as it produced considerable amount of water flux with treated greywater quality that met the greywater reuse standards. In Phase IV, 1.5 AgNP PCBM was fabricated with similar fabrication procedures in Phase III, except the diameter of the membrane was enlarged to 20 cm (membrane active area 113.1 cm^2) to meet the treatment capacity required by the DGTS.

Swelling ratio of the 1.5 AgNP PCBM for this study was found to be relatively higher as compared to the small 1.5 AgNP PCBM that was casted on the plastic petri dish. This is mainly attributed to the change on the casting surface from plastic petri dish to glass petri dish. When the membrane was dried on the glass petri dish with the same temperature, the solvent could evaporate faster due to the low specific heat of glass (840 J $kg^{-1}°C^{-1}$) as compared to polystyrene (1300 – 1500 J $kg^{-1}°C^{-1}$) (The Engineering Toolbox, 2016). As a result, the structure of the membrane in Phase IV had higher voids as compared to those casted on plastic petri dish. From Figure 4.25, it could be observed that that the

swelling curve of 1.5 AgNP PCBM in Phase IV is 16 % higher than the 1.5 AgNP PCBM in Phase III and also 4% higher than 2AP1CP at 60 mins.

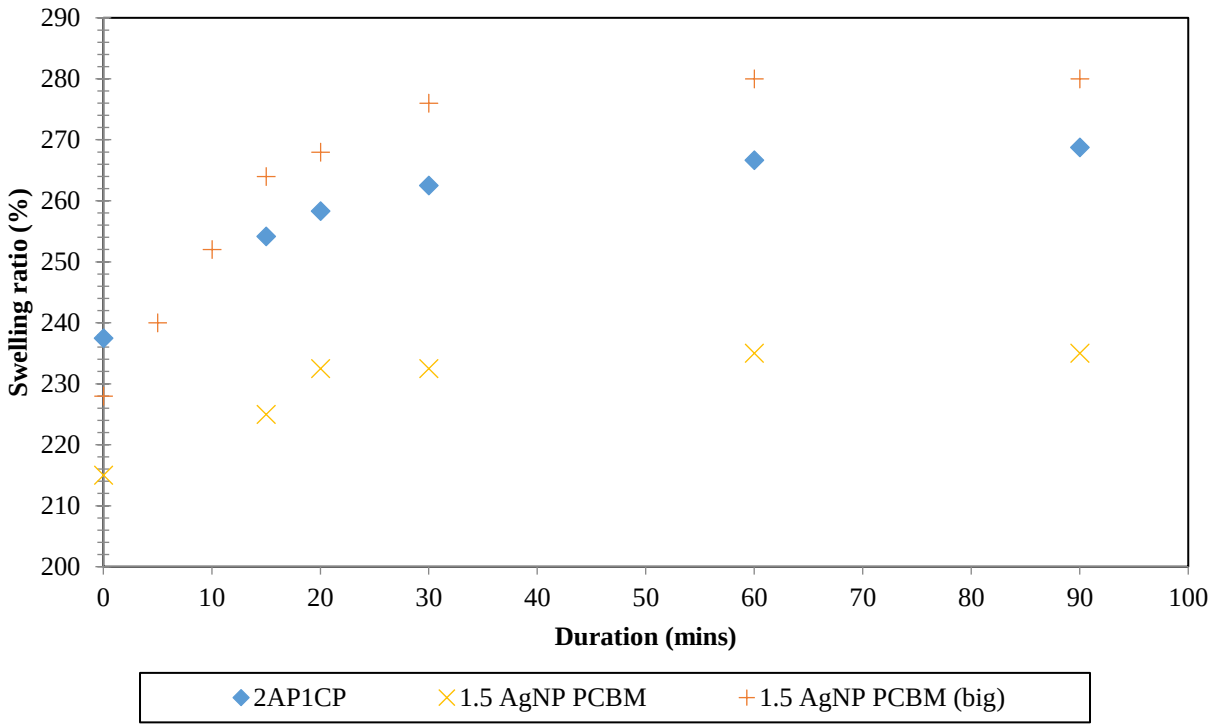

Figure 4.25. Swelling ratio of 2AP1CP, 1.5 AgNP PCBM (small) and 1.5 AgNP PCBM (big)

As the swelling ratio of 1.5 AgNP PCBM in Phase IV was found to increase, the change of casting surface to glass also caused the MWCO of the 1.5 AgNP PCBM in Phase IV to increase slightly. As shown in Figure 4.26, the MWCO of 1.5 AgNP PCBM in Phase IV was found to be 2991 Da, which is 7.5% higher than 1.5 AgNP PCBM in Phase III (MWCO = 2766 Da).

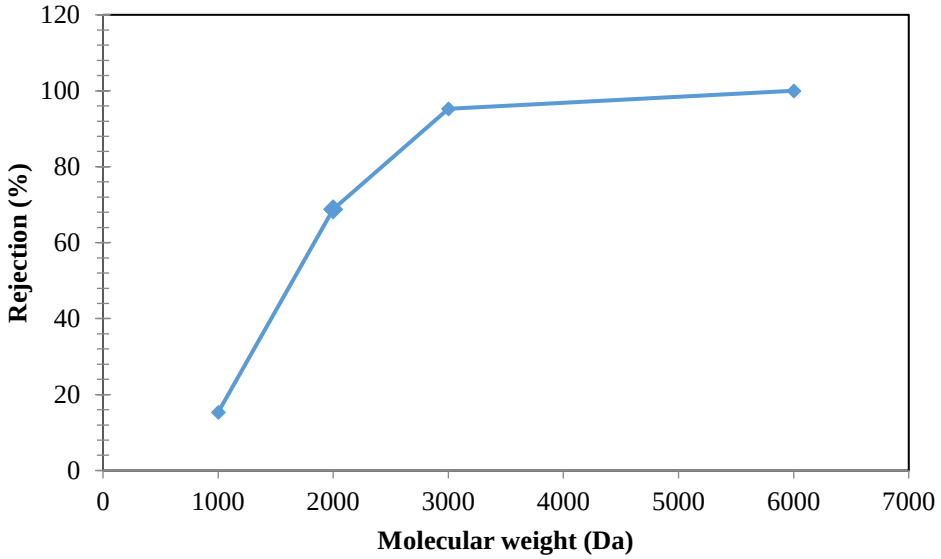

Figure 4.26. MWCO of big 1.5 AgNP PCBM

The increase in swelling ratio and MWCO of the membrane resulted in an increase of UP water flux of the 1.5 AgNP PCBM in Phase IV. From the study of using filtration pressure of 3 bar (g), the UP water flux of 1.5 AgNP PCBM (Phase IV) was found to be 49.5 L $m^{-2}hr^{-1}$ (Figure 4.27), while only 30.3 L $m^{-2}hr^{-1}$ (Figure 4.27) UP water flux was obtained using 1.5 AgNP PCBM from Phase III. Subsequently, the following section will study the effect of membrane properties changes on the greywater filtration efficiency using DGTS.

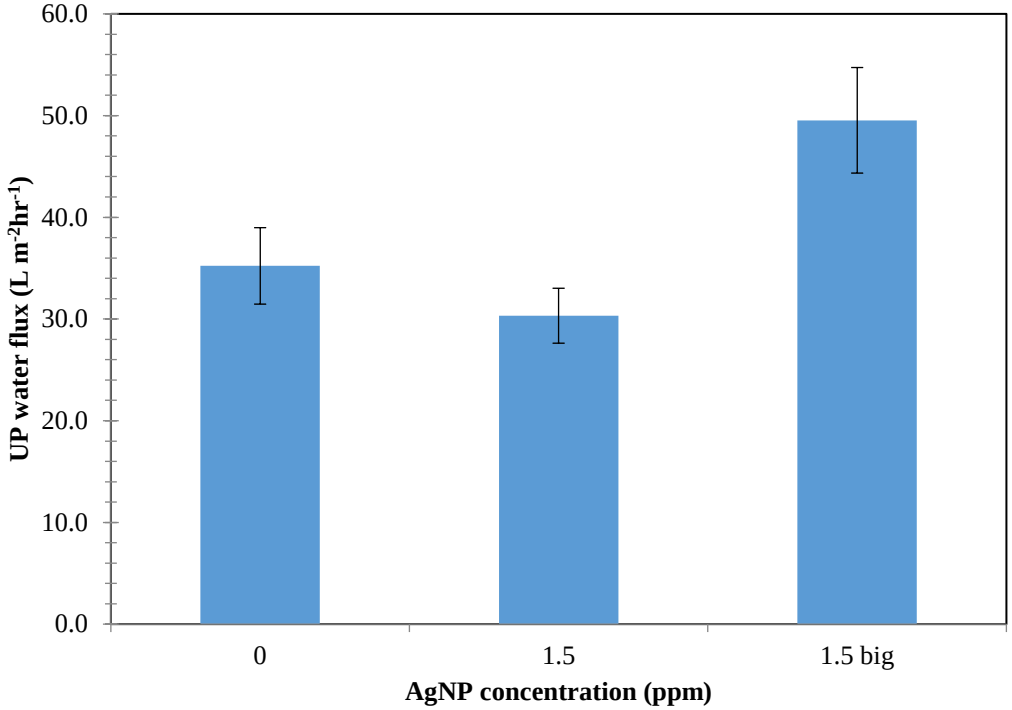

Figure 4.27. UP water flux at 3 bar (g)

4.5.3 Start-up of the system

Prior to carrying out the study, the pump was first calibrated to obtain its flow rate corresponding to its stroke number. The calibration curve is shown in Figure 4.28, in which, the volumetric flow rate of the pump could be obtained with the equation: $y = 1.1689x – 0.2$, where y is the volumetric flow rate (mL min^{-1}) and x is the stroke number. In addition, the membrane unit (as shown in Figure 3.5) was also subjected to leakage test prior greywater treatment. The leakage test is crucial to avoid the escape of pollutants from the membrane unit into the treated greywater tank. Any leakage from the unit has to be rectified prior to operation. Based on Table 4.10, the volume of UP water collected from the DGTS during the leakage test was similar to the volume collected from dead-end stirred cell filtration unit using 1.5 AgNP PCBM. This indicated that the membrane unit has no leakage and it is ready to be utilized for greywater filtration.

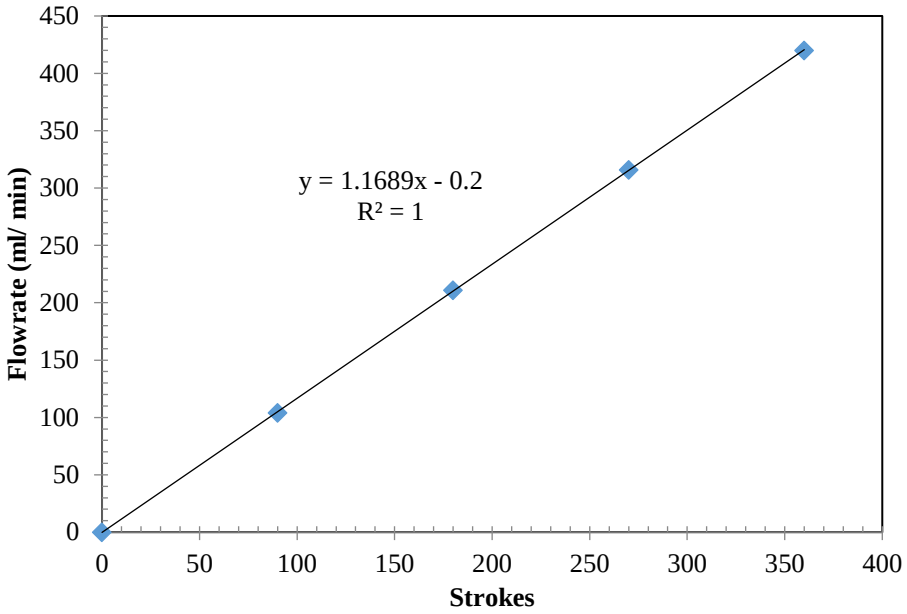

Figure 4.28. Pump flow rate calibration curve

Table 4.10. UP water volume collected in 30 mins from dead-end stirred cell filtration unit (HP 4750) and DGTS

Pressure (Bar (g))	UP water volume collected from DGTS (mL)	UP water volume collected from HP 4750 (mL)	Percentage Difference (%)
1	143.5	157.8	9.06
2	235.8	232.9	-1.21
3	285.0	279.4	-2.00
4	318.8	300.1	-6.21

4.5.4 Greywater treatment performance

During greywater treatment, the greywater was initially pressurized and maintained at 3 bar (g) for 30 mins. Thereafter, the pump was turned off and the water was allowed permeate out of the membrane with the remaining pressure in the membrane unit for 2 hours. The greywater flux was recorded to be at 46.86 L $m^{-2}hr^{-1}$ (as shown in Figure 4.29) when it was first filtered through the fresh membrane with an operating pressure of 3 bar (g). When the pump was switched off, the water flux

declined to approximately 18.57 L $m^{-2}hr^{-1}$. This was expected as the driving force to force the water through the membrane has declined. However, the flux did not improve but reduced slightly from the previous flux reading without pumping to 17.68 L $m^{-2}hr^{-1}$ on the second pressurized run. The decline in the greywater flux was mainly attributed to the accumulation of the pollutants on the surface of the fresh membrane. Based on the flux decline results in Section 4.4.4, the flux decline of the membrane is mainly due to cake formation and intermediate pore blocking on the membrane. As the study progressed with more cycles, it could be observed that the rate of the flux decline starts to reduce. It was found that from fourth cycle onwards, the greywater flux remained rather consistent as compared to the first 3 treatment cycles. An average of 0.19 L hr^{-1} per cycle of treated greywater was generated from fourth cycle to tenth cycle. Comparing to the 0.029 L hr^{-1} treated greywater obtained using dead-end stirred cell filtration unit (1.5 AgNP PCBM), the volume of treated greywater increased by 85% with the DGTS. Despite the vast improvement in the volume of treated greywater produced, the lab scale DGTS is still insufficient to process high amount of greywater. As such, the area of the membrane can be expanded or different membrane configurations (eg. tubular) can be adopted to further shorten the treatment duration while increasing the volume of treated greywater.

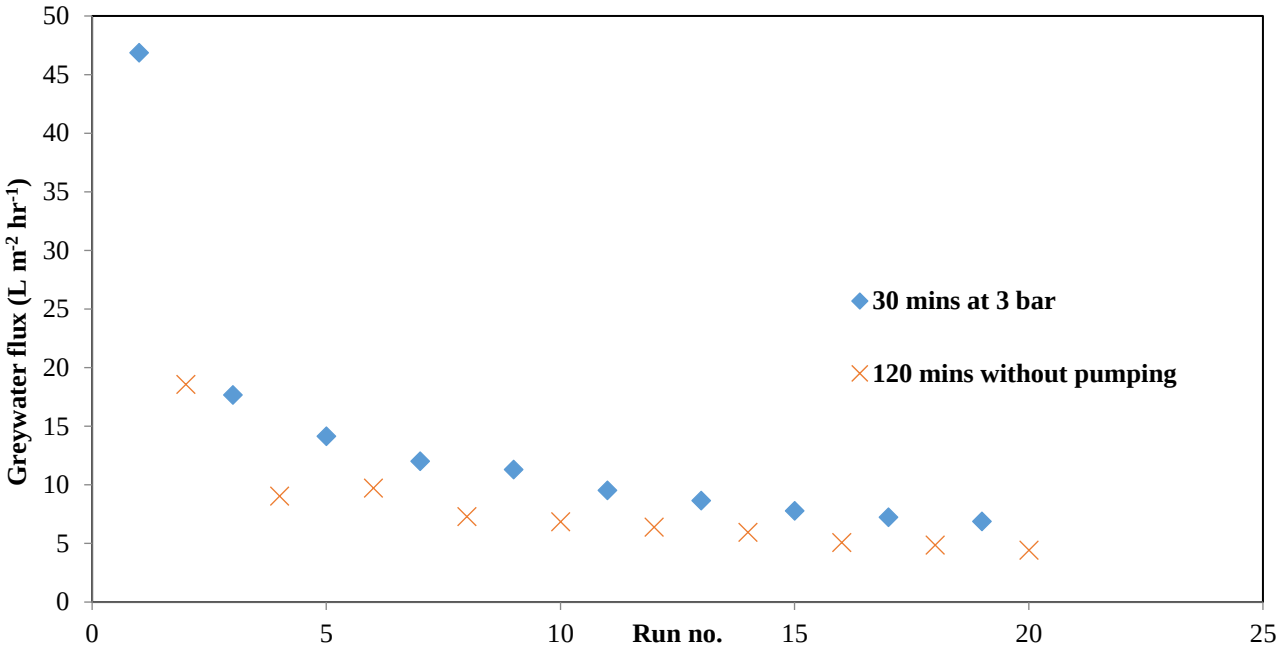

Figure 4.29. Greywater treatment flux in DGTS

Thereafter, the treated greywater from the first pressurized run was analysed and removal percentage was tabulated in Table 4.11. The results of the treated greywater reflected that the treatment performance of the greywater was consistent with the treatment performance evaluated using the dead-end stirred cell filtration unit. Similarly, the membrane also produced treated greywater that is free of turbidity and TSS. Moreover, the COD of the treated greywater was well below 100 ppm, which is lower than the allowable limits. The filtration was also found to be able to effectively remove *E. coli* and other coliforms bacteria, achieving 100% removal.

Table 4.11. Greywater treatment performance of 3 bar (g) filtration

Parameters	Unit	Percentage removal	LRV
pH	**%**		
Turbidity	**%**	99.8	
TSS	**%**	100.0	
COD	**%**	69.2	
BOD_5	**%**	50.2	
E. coli	**%**	100.0	1.875
Coliform Bacteria	**%**	100.0	3.352

When the system was in operation, random samples of the treated greywater were extracted and analysed to ensure that the membrane is functioning normally during the operation. Table 4.12 indicated that the membrane was still functional after 21 runs to produce treated greywater that is free of TSS and turbidity. The COD removal efficiency also improved over the duration of the treatment. This is attributed to the accumulation of pollutants of the surface of the membrane that led to greater resistance for the organic matters to pass through the membrane. Results from runs 17 and 21 have shown that the removal efficiency of the membrane remained consistent over the duration of the treatment process. However, the greywater flux continued to reduce as the excessive pollutants clogged the surface of the membrane. This implies that washing of membrane is required or a back flush system could be introduced to remove the accumulated pollutants on the membrane surface. Based on the current set up, it is suggested that the maintenance of the membrane is required at least twice in a month to retain the treatment flux of the system.

Table 4.12. Treatment efficiency and final concentration of treated greywater of various treatment cycles

Run no.		**17**	**21**
Parameters	Unit		
Turbidity	**%/ ppm**	99.95/ 0.17	98.70/ 0.42
TSS	**%/ ppm**	100/ 0	98.27/ 1
COD	**%/ ppm**	87.59/ 25	89.08/ 22

4.5.5 Bacteria inactivation on the 1.5 AgNP PCBM

Earlier results have all indicated that the 1.5 AgNP PCBM has the ability to disinfect the greywater. Nevertheless, the bacteria removal mechanism for the DGTS has yet to be identified. The bacteria inactivation study was carried out to identify whether the membrane works based on the sieving effect or the bacteria dies when it comes in contact on the membrane surface containing AgNP. It is essential to investigate the bacteria removal mechanism, as there is a chance for bacteria to regrow or reactivate after maintenance, where bacteria adhered on the surface might be able to

escape through the pores once the membrane has been cleaned. For this purpose, PI dye was used to identify dead bacteria cell. PI emits fluorescence red color when it reacts with dead cells (Shi & Günther et al., 2007). As PI enter the bacteria cell, it will bind with bases in the cell DNA, resulting in 20 to 30 times increment in the fluorescence intensity (Stiefel & Schmidt-Emrich et al., 2015).

As shown in Figure 4.30, very low density of dead bacteria was detected in the greywater prior to membrane filtration. The detected spots were mainly due to adhesion of bacteria that was originally present in the atmosphere. Based on Figure 4.31 and Figure 4.32, higher density of fluorescence red spots was detected on the used membrane, indicating that bacteria were inactivated on the surface of the membrane. The area of fluorescence red spots was significantly greater for the 1.5 AgNP PCBM as compared to the 2AP1CP porous PCBM. Therefore, it can be postulated that the fatality of bacteria on the surface of the membrane is attributed to the anti-microbial properties of the polymers in the 1.5 AgNP PCBM. The presence of AgNP on the surface of the membrane could remove bacteria from the greywater via sieving effect and at the same time, inactivating them on the surface of the membrane. The finding was concurrent with the study conducted by Sondi & Salopek-Sondi (2004) , where it was found that when the AgNP is in contact with the bacteria, it resulted in pits that are lethal to bacteria cell. As a result, after the treatment using 1.5 AgNP PCBM, the bacteria could not regrow in the treated greywater even if it escaped from the membrane.

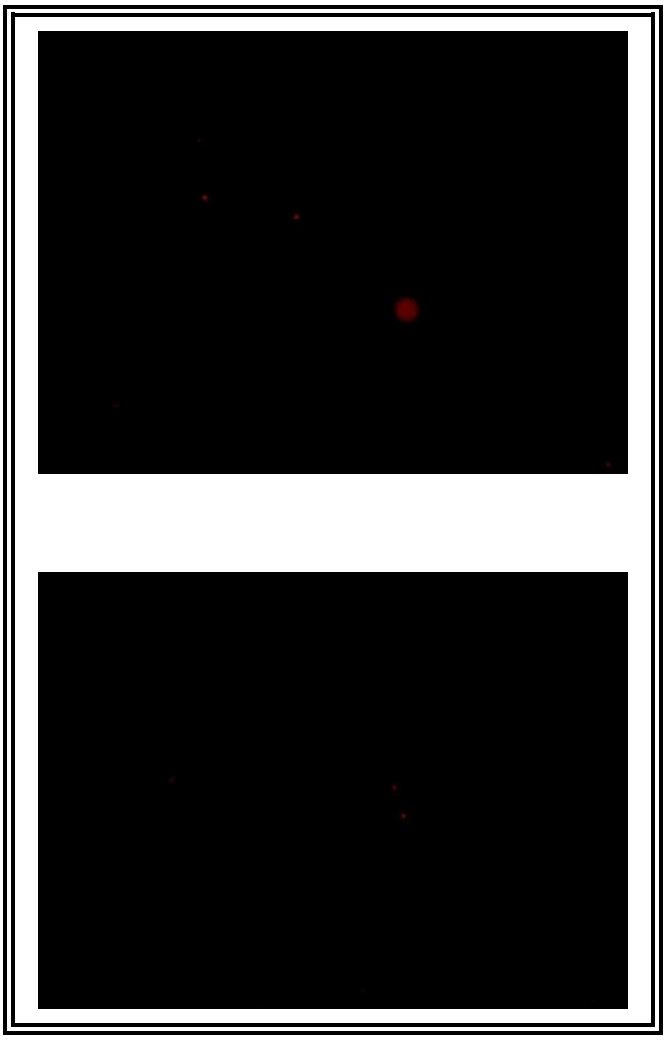

Figure 4.30. PI treated greywater before filtration

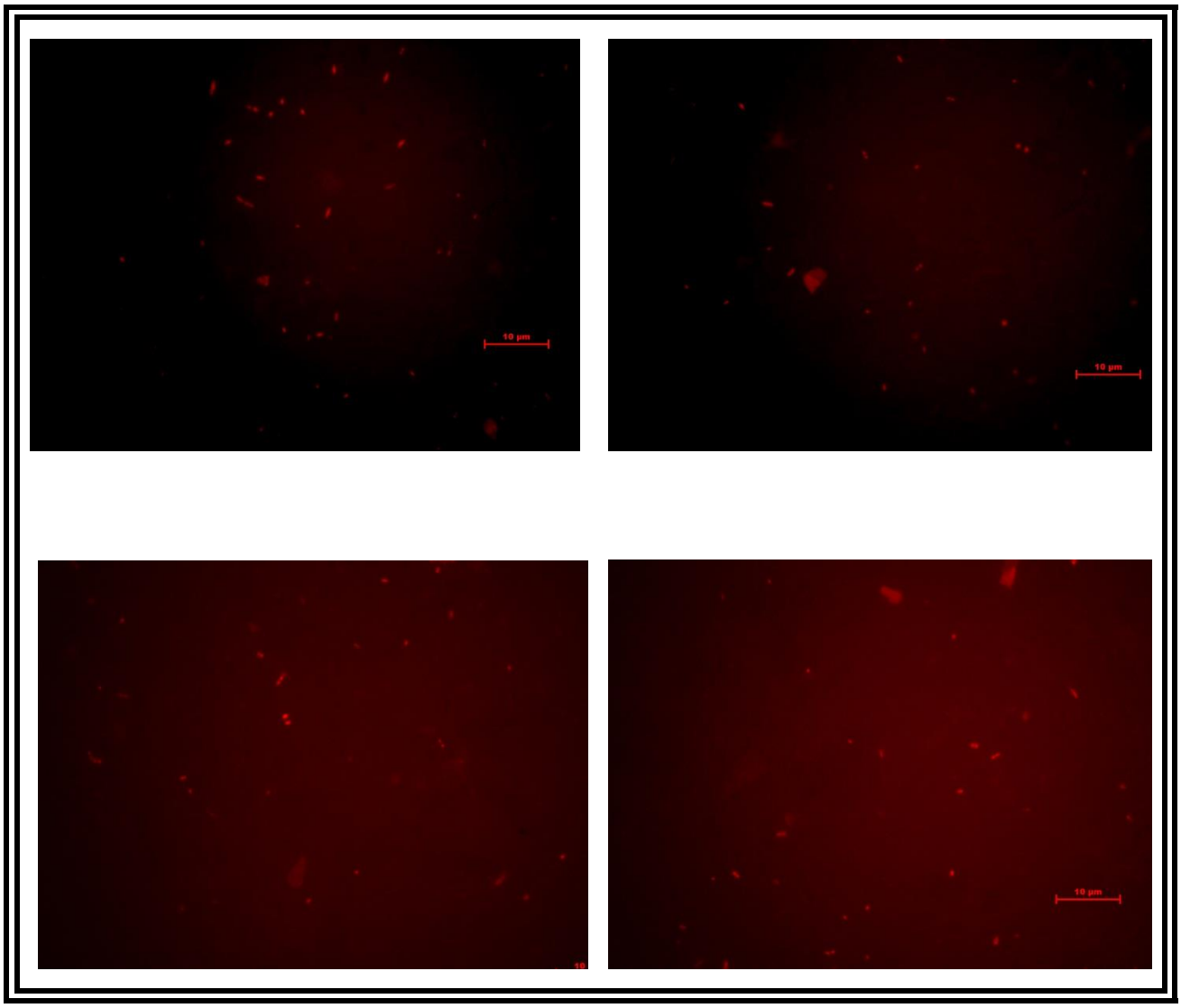

Figure 4.31. PI treated 2AP1CP

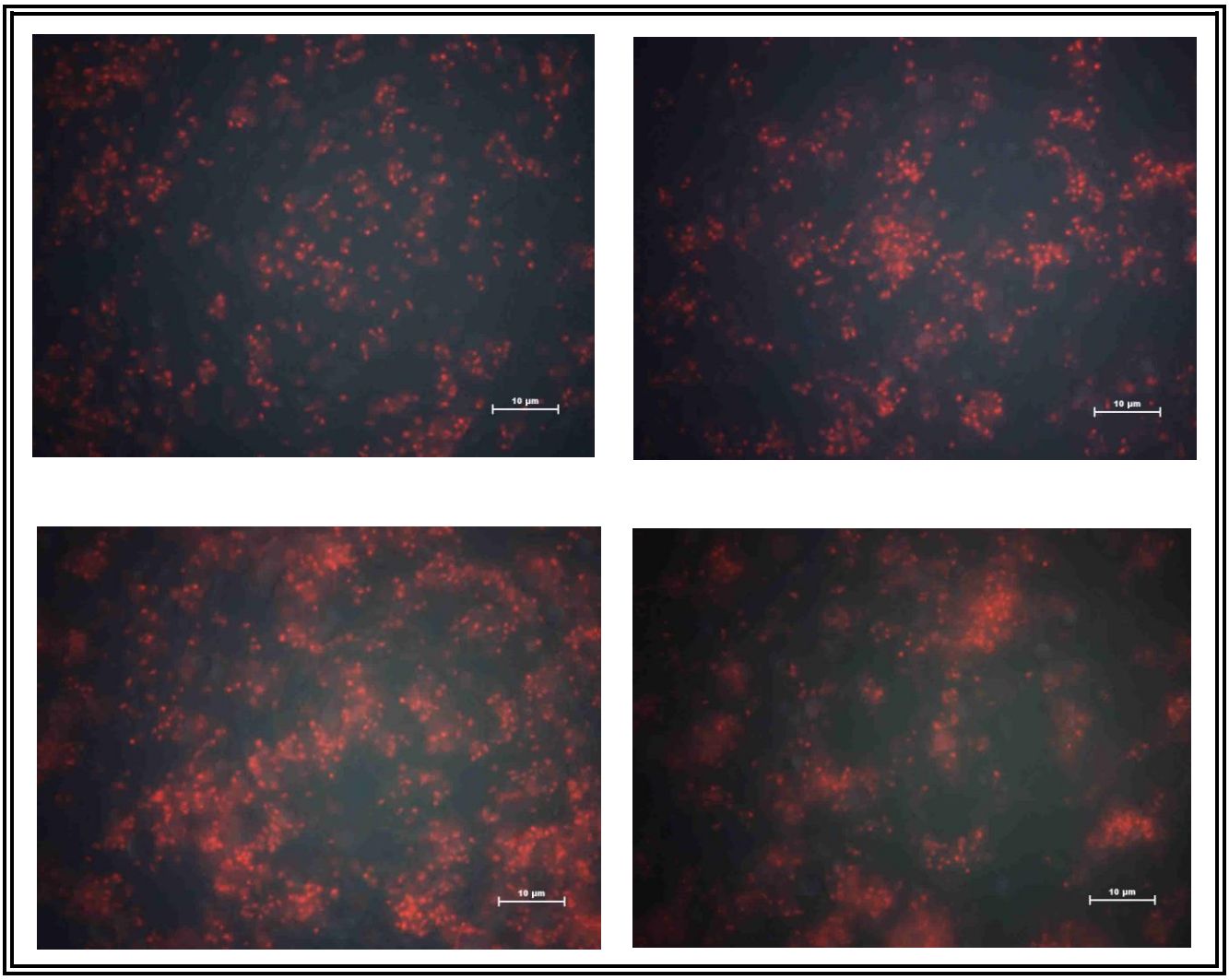

Figure 4.32. PI treated 1.5 AgNP PCBM after greywater filtration

4.5.6 Comparison LCA of AgNP PCBM and Nylon membrane fabrication

Up to this stage, a membrane specifically for greywater treatment has been developed using renewable polymers (eg. CS and Alg) and AgNP. Despite the fact that materials fabricated by renewable materials are usually considered as sustainable products, it might not be true in some circumstances, where the raw materials involved or the manufacturing process could be harmful to the environment (Piccinno & Hischier et al., 2015). Therefore, LCA becomes a crucial indicator that has to be considered to evaluate the environmental impacts during production of 1.5 AgNP PCBM. In this study, a conventional nylon 66 membrane was used as a comparison to the 1.5 AgNP PCBM. The filtration process using both the nylon 66 and 1.5 AgNP PCBM was not considered in the scope of LCA since the operational strategy for both systems will be the same.

In the LCA study, due to lack of information on the fabrication of nylon 66 membrane, a few assumptions were made to conduct the analysis. First, it was assumed that the duration and energy involved in the membrane fabrication process are the same for both the cases (Figure 4.33 and Figure 4.34) as both processes required the use of energy for the stirring of solutions, overnight drying of membranes and hot water treatment of membranes. Due to the fact that both membranes were assumed to be casted manually, thus, no energy input was considered for the casting process. Last but not least, 100% of the used membranes (both nylon 66 and AgNP PCBM) were assumed to be disposed and landfilled.

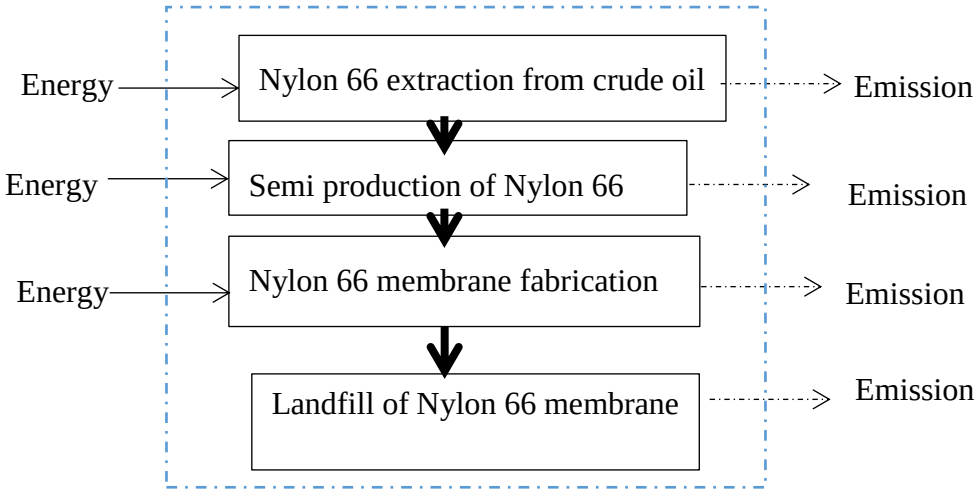

Figure 4.33. LCA system boundary for Nylon 66 membrane

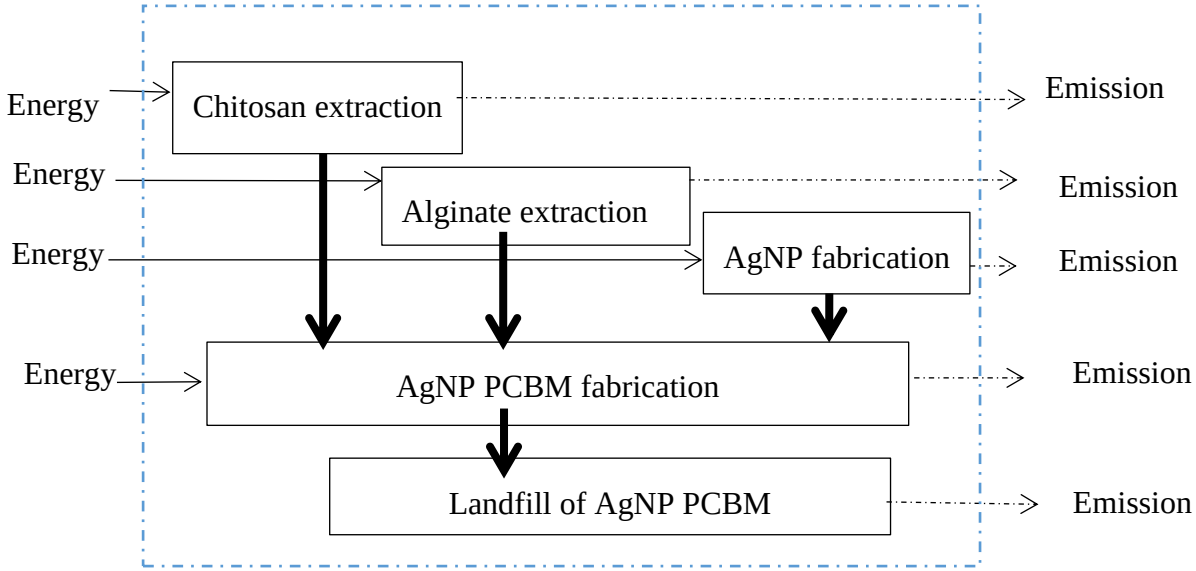

Figure 4.34. LCA system boundary for 1.5 AgNP PCBM

Based on the LCA results, it is evident that nylon 66 contributes to greater environmental impact in many of the categories compared to 1.5 AgNP PCBM. However, it was found that global warming potential (GWP), resources depletion (water), acidification and photochemical ozone are the four categories of environmental impact that were most severely affected by the production and landfill of both membranes.

Due to the fact that GWP associated with the fabrication of both membranes (Nylon 66 and AgNP PCBM) was most severe as compared to other impact categories, it was tabulated separately in Figure 4.35. As a FU, it was found that nylon 66 fabrication contributed to GWP of 47.7 kg-CO_2 eq, which is 9% higher than 1.5 AgNP PCBM (43.3 kg-CO_2 eq). From the detailed LCA of nylon 66 production, GWP emissions were found to be emitted from the usage of electricity or thermal energy during extraction and semi-production stage of nylon 66. In particular, the extraction of 1 kg of nylon 66 from crude oil required 30.81 kWh of energy and 33.88 kWh of energy was required during the semi-production stage. In contrast, the extraction 1 kg of CS and Alg only required 1.953 kWh and 7.763 kWh of energy respectively.

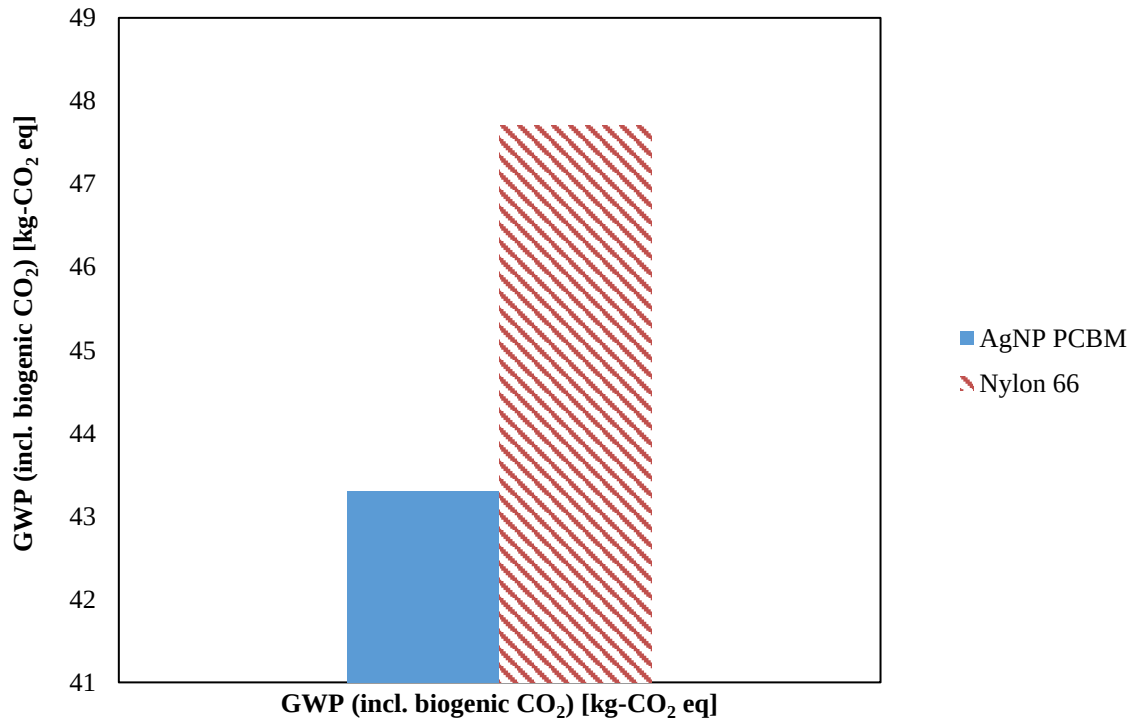

Figure 4.35. GWP of Nylon membrane and AgNP PCBM fabrication

On the other hand, the fabrication of nylon 66 membrane also caused serious resources depletion in terms of both water and mineral, fossils and renewable resources. Based on Figure 4.36,

an average of 0.837 m^3 of water was depleted during the fabrication of a FU of nylon 66 membrane, in which 0.0313m^3 eq. of water was consumed during the extraction process of nylon 66 from crude oil and 0.0334 m^3 eq. of water is used during the semi-production of nylon 66. In contrast, only 0.772 m^3 of water was required for the fabrication of 1.5 AgNP PCBM. Besides, it was found that fabrication of nylon 66 membrane contributed to 7.22×10^{-6} kg-Sb eq. resources depletion in term of mineral, fossils and renewables, which is 0.0388×10^{-6} kg-Sb eq. more than the fabrication of 1.5 AgNP PCBM (6.62×10^{-6} kg-Sb eq.). This is due to the fact that crude oil was consumed during the extraction of nylon 66, unlike 1.5 AgNP PCBM that does not involve crude oil consumption during extraction of raw materials. Thus, this study showed that more resources were depleted to fabricate nylon 66 membrane, as compared to 1.5 AgNP PCBM.

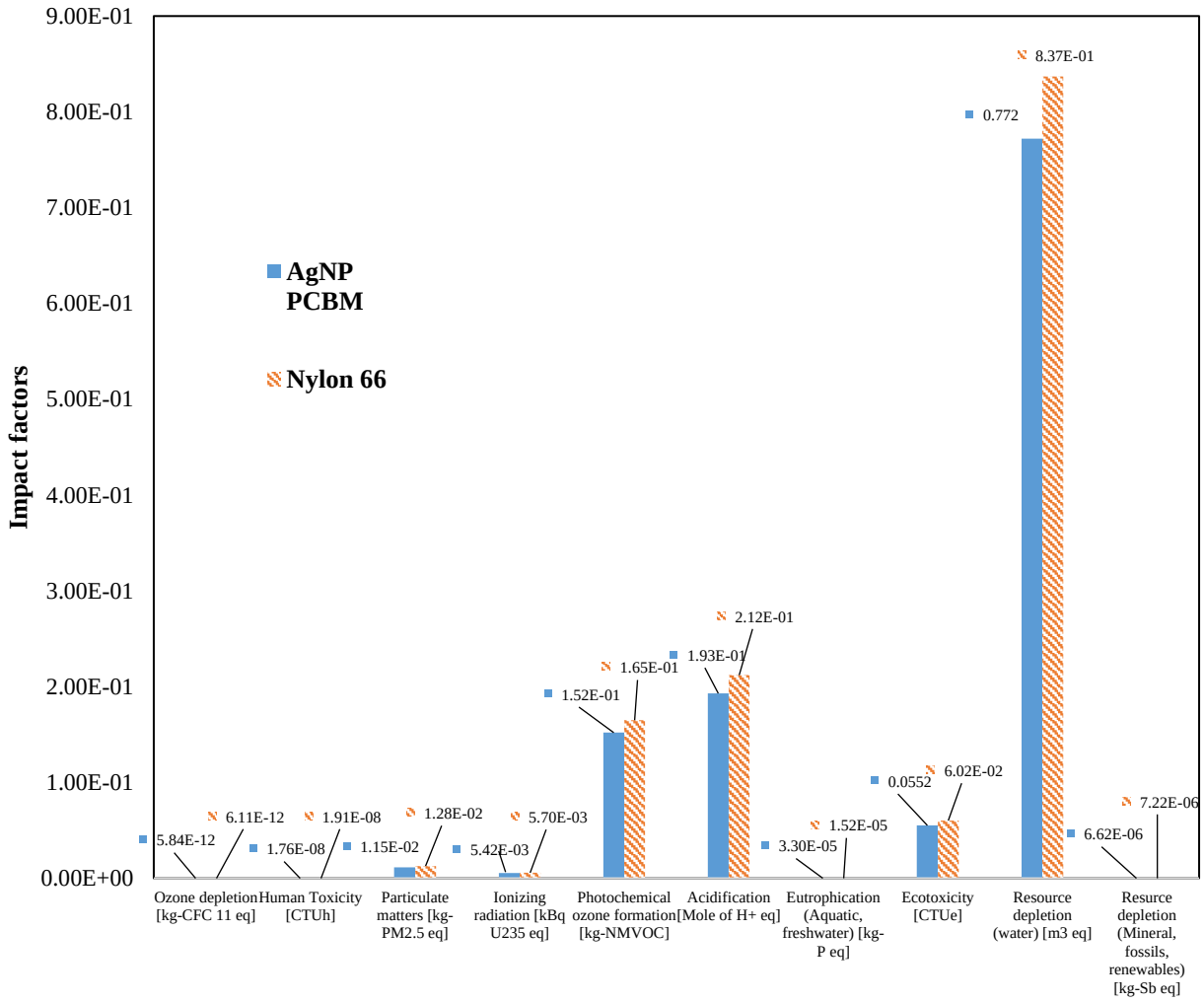

Figure 4.36. Impacts associated with production and landfill of **1.5** AgNP PCBM and nylon 66

In addition, acidification potential of both nylon 66 and 1.5 AgNP PCBM was found to be the third highest impact category. 0.212 mole of H^+ eq. is emitted during the production of nylon 66 membrane and 0.193 mole of H^+ eq. is released during the production of 1.5 AgNP PCBM. Acidification potential is mainly caused by the combustion of fossil fuels and processes that involved nitrogen oxides, sulphur oxides, hydrochloric acids and ammonia (Baumann & Tillman, 2004). Since the production of nylon 66 required higher amount of energy, it has led to higher emission of H^+ ions to the surrounding. The extraction of nylon 66 from crude oil resulted in the emission of 0.0078 mole

of H^+ eq. and semi production of nylon 66 released 0.0082 mole of H^+ eq, while 0.193 mole of H^+ eq. is associated with the nylon 66 membrane's fabrication process. In contrast, the acidification potential associated to the extractions of CS, Alg and AgNP were negligible. The main contributor of the acidification potential of 1.5 AgNP PCBM is mainly contributed by the membrane fabrication process, in which it resulted in 0.193 mole H^+ eq. of acidification potential. It is crucial to monitor and minimize the potential acidification pollutants, as the released of these pollutants could spread out to a large area and causes severe effect to the environment, such as acid rain. Therefore, 1.5 AgNP PCBM is preferred as the fabrication process released lesser pollutants that could cause acidification on the environment. In addition, steps to reduce use of fossil fuel to power machineries for fabrication process can be implemented. For example, more energy efficient equipment can be used and renewable energy source can be used to replace the use of fossil fuels during the fabrication process.

As high amount of energy is utilized in both the extraction and fabrication process of nylon 66 and 1.5 AgNP PCBM, the combustion of fuel releases nitrogen oxides and volatile organic compounds (VOCs) that has led to significant contribution towards photochemical ozone formation. In overall, the production of nylon 66 membrane releases 0.165 kg – NMVOC eq. photochemical ozone formation potential. At the same time, 0.152 kg – NMVOC eq. is emitted from the production 1.5 AgNP PCBM. The release of high concentration of sulphur oxides and VOCs to the surrounding could result in ozone formation with the presence of sunlight (Derwent & Jenkin et al., 2003). Despite the importance of ozone in UV protection, high concentration ozone in low attitude could cause negative impacts to the crops and results in severe negative health issues, such as respiratory issues (Elshorbany & Kleffmann et al., 2009).

Ecotoxicity is another crucial impact category that requires extensive attention, as selecting a membrane that uses less toxic chemicals in the fabrication process could avoid severe impacts on the

ecosystem. Based on this consideration, the comparison LCA indicated that 1.5 AgNP PCBM is a suitable membrane for greywater treatment, as it comprises of lesser toxic compounds. It was analysed that 0.0502 CTUe of ecotoxicity equivalent is associated with 1.5 AgNP PCBM production and 0.0602 CTUe was corresponded to nylon 66 membrane production. Moreover, landfilling 1.5 AgNP PCBM leads to 22% less ecotoxicity as compared to landfilling nylon 66 membrane. The detail evaluation showed that 0.000819 CTUe of ecotoxicity potential is contributed by landfilling 1.5 AgNP PCBM, whilst 0.00105 CTUe associated with landfill of nylon 66 membrane.

Besides that, production of nylon 66 membrane also showed higher emission of particulate matters (kg – PM 2.5 eq.), ozone depletion (kg – CFC 11eq.), human toxicity (CTUh) and ionizing radiation (kBq U235 eq.) as compared to 1.5 AgNP PCBM production. Results from LCA indicted 0.0128 kg – PM 2.5 eq., 6.11×10^{-6} kg – CFC 11 eq., 1.91×10^{-8} CTUh and 5.7×10^{-3} kBq U235 eq. were released during the production of nylon 66 membrane. In contrast, only 0.0115 kg – PM 2.5, 5.84×10^{-12} kg – CFC 11 eq., 1.76×10^{-8} CTUh and 5.42×10^{-3} kBq U235 eq were emitted from the production of 1.5 AgNP PCBM. These emissions of particulate matters, ozone depletion, ionizing radiation and human toxicity are mainly due to the emission of pollutants from the electricity grid during the production of membranes.

Despite lower impacts observed in most of the impact categories for 1.5 AgNP PCBM, eutrophication potential in freshwater were found to be slightly higher for 1.5 AgNP PCBM. In overall, 3.30×10^{-5} kg – P eq. is caused by production and landfilling 1.5 AgNP PCBM, while 1.52×10^{-5} kg – P eq. is incurred for nylon 66 membrane. A detail analysis of the process indicated that the high eutrophication associated with 1.5 AgNP PCBM is mainly due to the decompositions of biodegradable materials, such as CS and Alg. Generally, eutrophication could be caused by the increased in the carbon dioxide, sun light and nutrients in the water body, that eventually led to

excessive plant growth in water (Chislock & Doster et al., 2013). Despite the decomposition of biodegradable materials is non-toxic, the end products of decomposition of the membrane could be the nutrients for algae or other organisms in the water body that leads to the high eutrophication potential. As such, proper management in the disposal facility is essential to control the leaching of nutrients caused by storm water runoff from the disposal facility (US EPA, 2016). Another approach to resolve the issue is via biomanipulation to control the food web and restore the health of the water body (Chislock & Doster et al., 2013).

In view of the outcomes of this comparison LCA, it is deduced that producing 1.5 AgNP PCBM from biodegradable raw materials caused lower environmental impacts as compared to production of nylon 66 membrane from fossils. Consequently, when utilizing the membrane greywater recycling system in a wider scale, the adoption of 1.5 AgNP PCBM in the recycling system could compliment the environment by resulting in reduced environmental footprints.

4.5.7 Cost analysis

In order to assess the economical sustainability of greywater recycling, cost saving and payback period of implementing the system in a local family with 5 members was evaluated. In this analysis, the capital cost was roughly quoted to be ranging from USD 112 to USD 450 (MYR 500 to MYR 2000 equivalent, exchange rate of USD 1 to MYR 4.45, retrieved on 13 March 2017) based on the price of the local outdoor filtration systems (Water Filter Malaysia, 2017). In the current recycling system, one pump is required for the filtration, with the power consumption estimated to be 0.024 kWh (IWAKI, Model: EHN-C21VC3R). As a result, it led to electricity utility of USD 0.42 per month. Assuming, minor maintenance work such as changing of membrane is required every 3 months by the owner of the system and major servicing required every 6 month by the trained

technician, the total operating and maintenance cost, including 4 membranes replaced, was USD 50.76 per annum.

Based on the estimation of total amount of greywater (97.18 L/person/day) being recycled from this family, a total of 14.6m^3 of freshwater could be conserved every month. Thus, the freshwater consumption of this family could be reduced from 406.8 m^3 per annum to 231.93 m^3 per annum. As shown in Table 4.13, this reduction in freshwater consumption could lead to a total water utility bill reduction of USD 64.45 per annum. Taking into consideration of the capital cost of the recycling system, operational and maintenance cost and water utility bill savings, the payback period (without discounted rate) of this greywater recycling system is approximately 8.2 years to 16.4 years (Figure 4.37) with the capital of USD 112 to USD 224. It was found that when the capital cost higher than USD 224, this system is unable to break even within 20 years period. This indicates that the variation in capital cost of the greywater recycling system plays an important role on whether the system could be successfully implemented in Malaysia. For instance, if a subsidiary of USD 100 is provided for this family to install the greywater recycling system, this will reduce the payback period significantly to only 0.89 years. Thus, in order to encourage greywater recycling to help relief the water stress level and shorten the payback period, the local authority could provide subsidiary for the installation of the greywater recycling system.

Table 4.13. Cost involves in installation and operating the greywater recycling system (USD 1 to MYR 4.45 (adopted on 13 March 2017))

Cost	**MYR**	**USD**	**USD/ year**
Capital Cost (Treatment system and installation)	500 - 2000	112 – 450	112 - 450
Operating cost			
1. Pump (0.024kWh) estimating 30	0.16/ month	0.035	0.42

Cost	MYR	USD	USD/ year
operating days a month			
Maintenance cost			
2. Membrane replacement (four times a year)	40/ piece	9.21	36.9
3. Major service (twice a year)	30/ time	6.74	13.48
Freshwater saving			
1. Freshwater consumption without recycling	33.9 m^3/month		
2. Freshwater consumption with recycling	19.3 m^3 /month		
3. Water utility saved	23.9/ month	5.37/ month	64.45

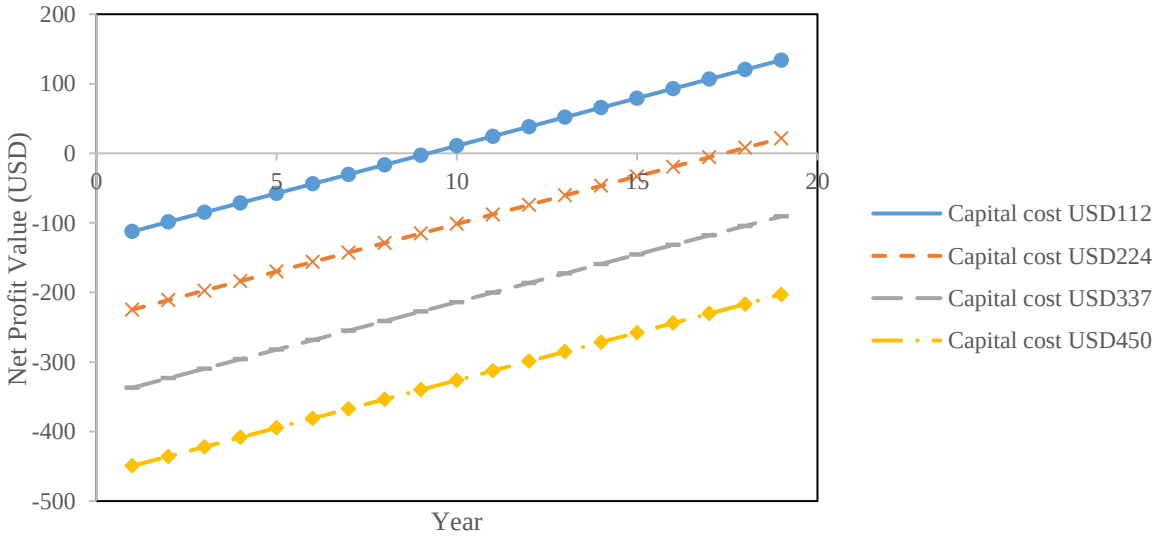

Figure 4.37. NPV and payback period of greywater recycling system

Chapter 5

5 Conclusion

A dual-layer biopolymeric membrane consisting of chitosan, alginate and AgNP was successfully fabricated and tested for greywater treatment. Conclusions for different stages of this study are as listed below:

1. CS membranes were fabricated with various PEG concentrations, and highest water flux (24.34 L $m^{-2}hr^{-1}$) could be achieved with 1wt% CS and CS: PEG weight ratio of 1: 1 at operating pressure of 3.2 bars (g). The 1% wt CS/ PEG membrane was found to be able to remove 94.37% turbidity, 100% TSS, 60.93% COD, 61.54% BOD_5 and 100% pathogenic bacteria (*E. coli* and other coliforms were not present in the raw greywater). The low COD and BOD removal efficiency made a cause for the need to integrate alginate to form PEC with chitosan membrane.
2. On the other hand, the formation of PEC reduced the MWCO of CS membrane from 242 kDa to 3080 Da with the 2A1CP PCBM and 3800 Da with the 2AP1CP PCBM. Greywater treatment using 2A1CP PCBM was found to be able to achieve removal of 99.9% turbidity, 100% TSS, 85.5% COD, 86.6% BOD_5, 99.9% *E. coli*, 100% other coliforms in greywater due to the lower MWCO, while 2AP1CP PCBM could remove up to 99.8% turbidity, 99.5% TSS, 81.5% COD, 96.9% BOD_5, 2.6-log of *E. coli* and 2.93–log of other coliforms in greywater.
3. In order to ensure complete removal of bacteria, silver nanoparticles was loaded onto the alginate layer. The loading of 1.5ppm AgNP in the 2AP1CP membrane enhanced the greywater disinfection efficiency and resulted in the removal of 3.6-log *E. coli* and 3.7-log other coliforms. The elimination of bacteria from greywater was found to be attributed by the

combination of size exclusion effect and contact-killing mechanism of 1.5 AgNP PCBM. Greywater treatment using 1.5 AgNP PCBM also showed removal of 99.9% turbidity, 100% TSS, 82.5% COD and 82.6% BOD_5.

4. Quality of the treated greywater produced by 1.5 AgNP PCBM met the greywater reuse standard of turbidity < 5 NTU, 5-days biological oxygen demand (BOD_5) < 20 ppm and non-detectable level of *E. coli* and coliform bacteria.
5. The scaled up 1.5 AgNP PCBM in decentralized greywater treatment system showed consistent greywater treatment efficiency across 10 days of operation. The fresh 1.5 AgNP PCBM could produce 1125 L $m^{-2}day^{-1}$ at 3 bar (g) and 446 L $m^{-2}day^{-1}$ without pumping. The membrane flux reduced over the two weeks period of operating the system. Study showed that flux decline was mainly attributed to intermediate pore blocking and cake formation mechanisms.
6. Results from LCA indicated that production of 1.5 AgNP PCBM from its raw materials causes lower environmental impacts as compared to conventional nylon 66 membrane. Last but not least, recycling greywater in 1.5 AgNP PCBM decentralized greywater treatment system could vastly reduce freshwater consumption and eventually contributes to sustainable development of a community.

Chapter 6

6 Future recommendations

1. The current scale of decentralized dead-end filtration system might not be suitable for application in highly dense buildings (i.e.: apartments and commercial buildings). Therefore, there is a need to develop an automated system and more efficient filtration setup (ability to handle higher wastewater flux) that can be installed and tested in highly densed buildings.
2. Due to the fact that bathroom greywater is the only wastewater source in the current PCBM treatment system, treatment performance on other source of wastewaters (eg. laundry greywater and rainwater) remains unknown. Thus, the future study could be further extended to investigate on the usability of PCBM treatment system in the recycling other sources or a combination of sources of wastewaters to further reduce freshwater consumption.
3. The greywater filtration flux of the current membrane could be further increased to reduce the energy required to filter greywater. As such, the overall structure of the membrane could be modified to enhance its hydrophilicity and water permeability while not compromising on the treated effluent quality.
4. The current membrane is fabricated with simple flat sheet configuration. The future study could be extended to evaluate the possibility of modifying the membrane configurations (eg. hollow fibers, spiral, and cross-flow) and conduct studies on the more sophisticated membrane configuration on greywater flux, treatment efficiency and membrane life span.

References

Abdul kareem, T., & Anu kaliani, A. (2011). Synthesis and thermal study of octahedral silver nano-plates in polyvinyl alcohol (PVA). *Arabian Journal of Chemistry, 4*(3), 325-331.

Abu Ghunmi, L., Zeeman, G., Fayyad, M., & Lier, J. B. v. (2010). Grey water treatment in a series anaerobic – Aerobic system for irrigation. *Bioresource Technology, 101*(1), 41-50.

Ageev, E., Matushkina, N., & Vikhoreva, G. (2007). Pervaporation properties of thermally modified chitosan films. *Colloid Journal, 69*(3), 272-277.

Ahamed, M., AlSalhi, M. S., & Siddiqui, M. K. J. (2010). Silver nanoparticle applications and human health. *Clinica Chimica Acta, 411*(23–24), 1841-1848.

Al-Jayyousi, O. R. (2003). Greywater reuse: towards sustainable water management. *Desalination, 156*(1–3), 181-192.

Alkhatib, R., Roesner, L., & Marjoram, C. (2006). An Overview of Graywater Collection and Treatment Systems. *World Environmental and Water Resource Congress 2006@ sExamining the Confluence of Environmental and Water Concerns* (pp. 1-10): ASCE.

Almeida, M. R., Alves, R. S., Nascimbem, L. B. L. R., Stephani, R., Poppi, R. J., & de Oliveira, L. F. C. (2010). Determination of amylose content in starch using Raman spectroscopy and multivariate calibration analysis. *Analytical and Bioanalytical Chemistry, 397*(7), 2693-2701.

Ames, W. (1952). The conversion of collagen to gelatin and their molecular structures. *Journal of the Science of Food and Agriculture, 3*(10), 454-463.

Anthemidis, A. N., Zachariadis, G. A., & Stratis, J. A. (2002). On-line preconcentration and determination of copper, lead and chromium(VI) using unloaded polyurethane foam packed column by flame atomic absorption spectrometry in natural waters and biological samples. *Talanta, 58*(5), 831-840.

Antoniewski, M. N., Barringer, S., Knipe, C., & Zerby, H. (2007). Effect of a gelatin coating on the shelf life of fresh meat. *Journal of food science, 72*(6), E382-E387.

Atasoy, E., Murat, S., Baban, A., & Tiris, M. (2007). Membrane bioreactor (MBR) treatment of segregated household wastewater for reuse. *CLEAN–Soil, Air, Water, 35*(5), 465-472.

Australian Capital Territory. (2004). Greywater Use: Guidelines for residential properties in Canberra. In A. C. Territory (Ed.). Australia: Canberra.

Azad, A. K., Sermsintham, N., Chandrkrachang, S., & Stevens, W. F. (2004). Chitosan membrane as a wound-healing dressing: Characterization and clinical application. *Journal of Biomedical Materials Research Part B: Applied Biomaterials, 69*(2), 216-222.

Balmayor, E. R., Tuzlakoglu, K., Marques, A. P., Azevedo, H. S., & Reis, R. L. (2008). A novel enzymatically-mediated drug delivery carrier for bone tissue engineering applications: combining biodegradable starch-based microparticles and differentiation agents. *Journal of Materials Science: Materials in Medicine, 19*(4), 1617-1623.

Bayer, C. L., Herrero, É. P., & Peppas, N. A. (2011). Alginate films as macromolecular imprinted matrices. *Journal of Biomaterials Science, Polymer Edition, 22*(11), 1523-1534.

Berger, J., Reist, M., Mayer, J., Felt, O., Peppas, N., & Gurny, R. (2004). Structure and interactions in covalently and ionically crosslinked chitosan hydrogels for biomedical applications. *European Journal of Pharmaceutics and Biopharmaceutics, 57*(1), 19-34.

Birch, N. P., & Schiffman, J. D. (2014). Characterization of self-assembled polyelectrolyte complex nanoparticles formed from chitosan and pectin. *Langmuir, 30*(12), 3441-3447.

Birks, R., Colbourne, J., Hills, S., & Hobson, R. (2004). Microbiological water quality in a large in-building, water recycling facility. *Water Science & Technology, 50*(2), 165-172.

Bitton, G. (2005). *Wastewater microbiology*. Wiley. com.

Bodlund, I. (2013). Coagulant Protein from plant materials: Potential Water Treatment Agent. KTH.

Boland, M. (1989). Extraction of proteins from animal tissue using multiphase aqueous systems. *Bioseparation, 1*(3-4), 293-304.

Boyjoo, Y., Pareek, V. K., & Ang, M. (2013a). A review of greywater characteristics and treatment processes. *Water Science & Technology, 67*(7), 1403-1424.

Boyjoo, Y., Pareek, V. K., & Ang, M. (2013b). A review of greywater characteristics and treatment processes. *Water science and technology, 67*(7), 1403-1424.

Burke, A., Yilmaz, E., & Hasirci, N. (2000). Evaluation of chitosan as a potential medical iron (III) ion adsorbent. *Turkish Journal of Medical Sciences, 30*(4), 341-348.

Burridge, K., Johnston, J., & Borrmann, T. (2011). Silver nanoparticle-clay composites. *Journal of Materials Chemistry, 21*(3), 734-742.

Casey, P., Moore, M., & Pask, D. (2000). Pipeline: Decentralized Wastewater Treatment Systems. (Vol. 11): National Small Flows Clearinghouse, West Virginia University.

Chaillou, K., Gérente, C., Andrès, Y., & Wolbert, D. (2011). Bathroom greywater characterization and potential treatments for reuse. *Water, Air, & Soil Pollution, 215*(1-4), 31-42.

Chan, N. (2005). Water Resources Management in Malaysia: NGO. *Perspectives, Paper presented during MENGO's Sustainable Development Conference PWTC, Kuala Lumpur, Malaysia*, 9.

Chang, J.-J., Lee, Y.-H., Wu, M.-H., Yang, M.-C., & Chien, C.-T. (2012). Electrospun anti-adhesion barrier made of chitosan alginate for reducing peritoneal adhesions. *Carbohydrate Polymers, 88*(4), 1304-1312.

Chen, J. P., Mou, H., Wang, L. K., Matsuura, T., & Wei, Y. (2008). Membrane separation: Basics and applications. *Membrane and Desalination Technologies* (pp. 271-332): Springer.

Chen, P., Hwang, Y., Kuo, T., Liu, F., Lai, J., & Hsieh, H. (2007). Improvement in the properties of chitosan membranes using natural organic acid solutions as solvents for chitosan dissolution. *Journal of Medical and Biological Engineering, 27*(1), 23.

Chen, T. K., Tien, Y. I., & Wei, K. H. (2000). Synthesis and characterization of novel segmented polyurethane/clay nanocomposites. *Polymer, 41*(4), 1345-1353.

Chen, Z., Ngo, H. H., & Guo, W. (2012). A critical review on sustainability assessment of recycled water schemes. *Science of The Total Environment, 426*(0), 13-31.

Chen, Z., Ngo, H. H., & Guo, W. (2013). A critical review on the end uses of recycled water. *Critical Reviews in Environmental Science and Technology, 43*(14), 1446-1516.

Chislock, M. F., Doster, E., Zitomer, R. A., & Wilson, A. (2013). Eutrophication: causes, consequences, and controls in aquatic ecosystems. *Nature Education Knowledge, 4*(4), 10.

Choong, M. Y. (2011). Malaysia faces looming water crisis. *The Star Online*. Malaysia.

Christova-Boal, D. (1995). Installation and evaluation of domestic greywater reuse systems. Victoria University of Technology.

Coates, J. (2000). Interpretation of infrared spectra, a practical approach. *Encyclopedia of analytical chemistry*.

Couto, E. d. A. d., Calijuri, M. L., Assemany, P. P., Santiago, A. d. F., & Lopes, L. S. (2014). Greywater treatment in airports using anaerobic filter followed by UV disinfection: an efficient and low cost alternative. *Journal of Cleaner Production*(0).

Couto, E. d. A. d., Calijuri, M. L., Assemany, P. P., Santiago, A. d. F., & Lopes, L. S. (2015). Greywater treatment in airports using anaerobic filter followed by UV disinfection: an efficient and low cost alternative. *Journal of Cleaner Production, 106*, 372-379.

Crini, G. (2005). Recent developments in polysaccharide-based materials used as adsorbents in wastewater treatment. *Progress in Polymer Science, 30*(1), 38-70.

Crini, G., & Badot, P.-M. (2008). Application of chitosan, a natural aminopolysaccharide, for dye removal from aqueous solutions by adsorption processes using batch studies: A review of recent literature. *Progress in Polymer Science, 33*(4), 399-447.

Cui, D., Szarpak, A., Pignot-Paintrand, I., Varrot, A., Boudou, T., Detrembleur, C., Jérôme, C., Picart, C., & Auzély-Velty, R. (2010). Contact-Killing Polyelectrolyte Microcapsules Based on Chitosan Derivatives. *Advanced Functional Materials, 20*(19), 3303-3312.

de-Bashan, L. E., Moreno, M., Hernandez, J.-P., & Bashan, Y. (2002). Removal of ammonium and phosphorus ions from synthetic wastewater by the microalgae Chlorella vulgaris coimmobilized in alginate beads with the microalgae growth-promoting bacterium Azospirillum brasilense. *Water Research, 36*(12), 2941-2948.

de Alvarenga, E. S. (2011a). Characterization and properties of chitosan. *BIOTECHNOLOGY OF BIOPOLYMERS*, 91.

de Alvarenga, E. S. (2011b). Characterization and properties of chitosan. *Biotechnology of biopolymers, 24*, 364.

Derwent, R. G., Jenkin, M. E., Saunders, S. M., Pilling, M. J., Simmonds, P. G., Passant, N. R., Dollard, G. J., Dumitrean, P., & Kent, A. (2003). Photochemical ozone formation in north west Europe and its control. *Atmospheric Environment, 37*(14), 1983-1991.

Dhepe, P. L., & Fukuoka, A. (2008). Cellulose Conversion under Heterogeneous Catalysis. *ChemSusChem, 1*(12), 969-975.

Dixon, A., Butler, D., & Fewkes, A. (1999). Water saving potential of domestic water reuse systems using greywater and rainwater in combination. *Water science and technology, 39*(5), 25-32.

Domene, E., & Saurí, D. (2006). Urbanisation and water consumption: Influencing factors in the metropolitan region of Barcelona. *Urban Studies, 43*(9), 1605-1623.

Domènech, L., & Saurí, D. (2010). Socio-technical transitions in water scarcity contexts: Public acceptance of greywater reuse technologies in the Metropolitan Area of Barcelona. *Resources, Conservation and Recycling, 55*(1), 53-62.

Donati, I., Vetere, A., Gamini, A., Skjåk-Bræk, G., Coslovi, A., Campa, C., & Paoletti, S. (2003). Galactose-substituted alginate: preliminary characterization and study of gelling properties. *Biomacromolecules, 4*(3), 624-631.

Donner, E., Eriksson, E., Revitt, D. M., Scholes, L., Lützhøft, H. C. H., & Ledin, A. (2010). Presence and fate of priority substances in domestic greywater treatment and reuse systems. *Science of The Total Environment, 408*(12), 2444-2451.

Dror-Ehre, A., Mamane, H., Belenkova, T., Markovich, G., & Adin, A. (2009). Silver nanoparticle–E. coli colloidal interaction in water and effect on E. coli survival. *Journal of Colloid and Interface Science, 339*(2), 521-526.

Elshorbany, Y. F., Kleffmann, J., Kurtenbach, R., Rubio, M., Lissi, E., Villena, G., Gramsch, E., Rickard, A. R., Pilling, M. J., & Wiesen, P. (2009). Summertime photochemical ozone formation in Santiago, Chile. *Atmospheric Environment, 43*(40), 6398-6407.

Environment Agency. (2011). Greywater for Domestic Users: an Information Guide. (Vol. 2015).

Eriksson, E., Auffarth, K., Henze, M., & Ledin, A. (2002). Characteristics of grey wastewater. *Urban Water, 4*(1), 85-104.

Fakhru'l-Razi, A., Pendashteh, A., Abdullah, L. C., Biak, D. R. A., Madaeni, S. S., & Abidin, Z. Z. (2009). Review of technologies for oil and gas produced water treatment. *Journal of hazardous materials, 170*(2), 530-551.

Fane, A. T., Wang, R., & Jia, Y. (2008). Membrane Technology: Past, Present and Future. *Membrane and Desalination Technologies* (pp. 1-45): Springer.

Fazilah, A., Maizura, M., Abd Karim, A., Bhupinder, K., Rajeev, B., Uthumporn, U., & Chew, S. (2011). Physical and mechanical properties of sago starch–alginate films incorporated with calcium chloride. *International Food Research Journal, 18*(3), 1027-1033.

Fenoradosoa, T. A., Ali, G., Delattre, C., Laroche, C., Petit, E., Wadouachi, A., & Michaud, P. (2010). Extraction and characterization of an alginate from the brown seaweed Sargassum turbinarioides Grunow. *Journal of Applied Phycology, 22*(2), 131-137.

Field, R. (2010). Fundamentals of fouling. *Membranes for water treatment, 4*, 1-23.

FOMCA. (2010). MALAYSIANS waste a lot of water - Wat-er waste. Malaysia.

Freitas, R. M., Spin-Neto, R., Spolidório, L. C., Campana-Filho, S. P., Marcantonio, R. A. C., & Marcantonio Jr, E. (2011). Different Molecular Weight Chitosan-Based Membranes for Tissue Regeneration. *Materials, 4*(2), 380-389.

Friedler, E., Kovalio, R., & Galil, N. (2005). On-site greywater treatment and reuse in multi-storey buildings. *Water science and technology, 51*(10), 187-194.

Friedrich, J., Zalar, P., Mohorčič, M., Klun, U., & Kržan, A. (2007). Ability of fungi to degrade synthetic polymer nylon-6. *Chemosphere, 67*(10), 2089-2095.

Gander, M., Jefferson, B., & Judd, S. (2000). Aerobic MBRs for domestic wastewater treatment: a review with cost considerations. *Separation and Purification Technology, 18*(2), 119-130.

Geise, G. M., Lee, H. S., Miller, D. J., Freeman, B. D., McGrath, J. E., & Paul, D. R. (2010). Water purification by membranes: the role of polymer science. *Journal of Polymer Science Part B: Polymer Physics, 48*(15), 1685-1718.

Geisinger, D., & Chartier, G. (2005). Managed Onsite/Decentralized Wastewater Systems as Long-Term Solutions. *Clearwaters, 35*, 6-11.

Ghaee, A., Shariaty-Niassar, M., Barzin, J., & Ismail, A. (2013). Chitosan/polyethersulfone composite nanofiltration membrane for industrial wastewater treatment. *International Journal of Nanoscience and Nanotechnology, 9*(4), 213-220.

Gilboa, Y., & Friedler, E. (2008). UV disinfection of RBC-treated light greywater effluent: Kinetics, survival and regrowth of selected microorganisms. *Water Research, 42*(4–5), 1043-1050.

Gross, A., Shmueli, O., Ronen, Z., & Raveh, E. (2007). Recycled vertical flow constructed wetland (RVFCW)—a novel method of recycling greywater for irrigation in small communities and households. *Chemosphere, 66*(5), 916-923.

Gross, R. A., & Kalra, B. (2002). Biodegradable polymers for the environment. *Science, 297*(5582), 803-807.

Gu, Z., Xue, P., & Li, W. (2001). Preparation of the porous chitosan membrane by cryogenic induced phase separation. *Polymers for advanced technologies, 12*(11-12), 665-669.

Guebitz, G. M., & Cavaco-Paulo, A. (2008). Enzymes go big: surface hydrolysis and functionalisation of synthetic polymers. *Trends in Biotechnology, 26*(1), 32-38.

Guibal, E. (2004). Interactions of metal ions with chitosan-based sorbents: a review. *Separation and Purification Technology, 38*(1), 43-74.

Guo, L., & Santschi, P. H. (2007). Ultrafiltration and its applications to sampling and characterisation of aquatic colloids. *IUPAC Series on Analytical and Physical Chemistry of Environmental Systems, 10*, 159.

Ha, T. L. B., & Quan, T. M. (2013). Naturally Derived Biomaterials: Preparation and Application.

Haering, K. C., Evanylo, G. K., Benham, B., & Goatley, M. (2009). Water Reuse: Using Reclaimed Water for irrigation. In V. S. University (Ed.). *Virginia Cooperative Extension*.

Hasan, J., Crawford, R. J., & Ivanova, E. P. (2013). Antibacterial surfaces: the quest for a new generation of biomaterials. *Trends in Biotechnology, 31*(5), 295-304.

Heckele, M., & Schomburg, W. K. (2004). Review on micro molding of thermoplastic polymers. *Journal of Micromechanics and Microengineering, 14*(3), R1.

Ho, S. C. (1996). Vision 2020: Towards an environmentally sound and sustainable development of freshwater resources in Malaysia. *GeoJournal, 40*(1-2), 73-84.

Hocaoglu, S. M., Atasoy, E., Baban, A., & Orhon, D. (2013). Modeling biodegradation characteristics of grey water in membrane bioreactor. *Journal of Membrane Science, 429*, 139-146.

Homayoni, H., Ravandi, S. A. H., & Valizadeh, M. (2009). Electrospinning of chitosan nanofibers: Processing optimization. *Carbohydrate Polymers, 77*(3), 656-661.

Hophmayer-Tokich, S. (2006). Wastewater Management Strategy: centralized v. decentralized technologies for small communities. *Twente Centre for Studies in Technology and Sustainable Development*.

Hourlier, F., Masse, A., Jaouen, P., Lakel, A., Gerente, C., Faur, C., & Cloirec, P. (2010). Membrane process treatment for greywater recycling: investigations on direct tubular nanofiltration.

Huang, R., Pal, R., & Moon, G. (2000). Pervaporation dehydration of aqueous ethanol and isopropanol mixtures through alginate/chitosan two ply composite membranes supported by poly (vinylidene fluoride) porous membrane. *Journal of Membrane Science, 167*(2), 275-289.

IWK. (2016). Sewage Treatment System. (Vol. 2016). Malaysia: Indah Water Konsortium Sdn Bhd (211763-P).

Jacob, M., Guigui, C., Cabassud, C., Darras, H., Lavison, G., & Moulin, L. (2010). Performances of RO and NF processes for wastewater reuse: Tertiary treatment after a conventional activated sludge or a membrane bioreactor. *Desalination, 250*(2), 833-839.

Jefferson, B., Palmer, A., Jeffrey, P., Stuetz, R., & Judd, S. (2004). Grey water characterisation and its impact on the selection and operation of technologies for urban reuse. *Water Science & Technology, 50*(2), 157-164.

Jeon, Y.-J., & Kim, S.-K. (2000). Production of chitooligosaccharides using an ultrafiltration membrane reactor and their antibacterial activity. *Carbohydrate Polymers, 41*(2), 133-141.

JM, B., JL, T., & L, S. (2002). Primary Structure: Amino Acids Are Linked by Peptide Bonds to Form Polypeptide Chains. *Biochemistry*. New York: W H Freeman.

Jose Ruben, M., Jose Luis, E., Alejandra, C., Katherine, H., Juan, B. K., Jose Tapia, R., & Miguel Jose, Y. (2005). The bactericidal effect of silver nanoparticles. *Nanotechnology, 16*(10), 2346.

Jury, W. A., & Vaux, H. J. (2007). The emerging global water crisis: managing scarcity and conflict between water users. *Advances in agronomy, 95*, 1-76.

Kajitvichyanukul, P., Hung, Y.-T., & Wang, L. (2008). Membrane Technologies for Point-of-Use and Point-of-Entry Applications. In L. K. Wang, J. P. Chen, Y.-T. Hung & N. K. Shammas (Eds.). *Membrane and Desalination Technologies* (Vol. 13, pp. 603-638): Humana Press.

Kaur, I., & Gautam, N. (2010). Starch Grafted Polyethylene Evincing Biodegradation Behaviour. *Malaysian Polymer Journal, 5*(1), 26-38.

Keoleian, G., Miller, S., Kleine, R. D., Fang, A., & Mosley, J. (2012). Life Cycle Material Data Update for GREET Model. In C. f. S. Systems (Ed.). Michigan: University of Michigan, Ann Arbor.

Khor, E., & Lim, L. Y. (2003). Implantable applications of chitin and chitosan. *Biomaterials, 24*(13), 2339-2349.

Khulbe, K., & Matsuura, T. (2000). Characterization of synthetic membranes by Raman spectroscopy, electron spin resonance, and atomic force microscopy; a review. *Polymer, 41*(5), 1917-1935.

Kim, J. S., Kuk, E., Yu, K. N., Kim, J.-H., Park, S. J., Lee, H. J., Kim, S. H., Park, Y. K., Park, Y. H., Hwang, C.-Y., Kim, Y.-K., Lee, Y.-S., Jeong, D. H., & Cho, M.-H. (2007). Antimicrobial effects of silver nanoparticles. *Nanomedicine: Nanotechnology, Biology and Medicine, 3*(1), 95-101.

Kim, M.-J., Sea, B., Youm, K.-H., & Lee, K.-H. (2006). Morphology and carbon dioxide transport properties of polyurethane blend membranes. *Desalination, 193*(1–3), 43-50.

Kishino, H., Ishida, H., Iwabu, H., & Nakano, I. (1996). Domestic wastewater reuse using a submerged membrane bioreactor. *Desalination, 106*(1-3), 115-119.

Kong, M., Chen, X. G., Xing, K., & Park, H. J. (2010). Antimicrobial properties of chitosan and mode of action: a state of the art review. *International journal of food microbiology*, *144*(1), 51-63.

Kulig, D., Zimoch-Korzycka, A., Jarmoluk, A., & Marycz, K. (2016). Study on Alginate–Chitosan Complex Formed with Different Polymers Ratio. *Polymers*, *8*(5), 167.

Lafuma, A., & Quéré, D. (2003). Superhydrophobic states. *Nature materials*, *2*(7), 457-460.

Laing, W., & Christeller, J. (2004). Extraction of proteins from plant tissues. *Current Protocols in Protein Science*, 4.7. 1-4.7. 7.

Lee, B.-B., Chan, E.-S., Ravindra, P., & Khan, T. A. (2012). Surface tension of viscous biopolymer solutions measured using the du Nouy ring method and the drop weight methods. *Polymer Bulletin*, *69*(4), 471-489.

Lee, K. Y., & Mooney, D. J. (2012). Alginate: properties and biomedical applications. *Progress in Polymer Science*, *37*(1), 106-126.

Lee, L. Y., Ong, S. L., & Ng, W. J. (2004). Denitrification of nitrate wastewater using packed-bed columns. *Water environment research*, *76*(5), 388-393.

Lee, N., Amy, G., Croué, J.-P., & Buisson, H. (2004). Identification and understanding of fouling in low-pressure membrane (MF/UF) filtration by natural organic matter (NOM). *Water Research*, *38*(20), 4511-4523.

Lee, S. B., Lee, Y. M., Song, K. W., & Park, M. H. (2003). Preparation and properties of polyelectrolyte complex sponges composed of hyaluronic acid and chitosan and their biological behaviors. *Journal of applied polymer science*, *90*(4), 925-932.

Lendlein, A., & Kelch, S. (2002). Shape-memory polymers. *Angewandte Chemie International Edition*, *41*(12), 2034-2057.

Levine, A. D., Tchobanoglous, G., & Asano, T. (1991). Size distributions of particulate contaminants in wastewater and their impact on treatability. *Water Research*, *25*(8), 911-922.

Li, F., Behrendt, J., Wichmann, K., & Otterpohl, R. (2008). Resources and nutrients oriented greywater treatment for non-potable reuses. *Water science and technology*, *57*(12), 1901-1907.

Li, F., Wichmann, K., & Otterpohl, R. (2009). Review of the technological approaches for grey water treatment and reuses. *Science of The Total Environment*, *407*(11), 3439-3449.

Li, J., Sanderson, R., & Jacobs, E. (2002). Ultrasonic cleaning of nylon microfiltration membranes fouled by Kraft paper mill effluent. *Journal of Membrane Science*, *205*(1), 247-257.

Li, Q., Mahendra, S., Lyon, D. Y., Brunet, L., Liga, M. V., Li, D., & Alvarez, P. J. (2008). Antimicrobial nanomaterials for water disinfection and microbial control: potential applications and implications. *Water Research*, *42*(18), 4591-4602.

Lim, S.-H., & Hudson, S. M. (2004). Synthesis and antimicrobial activity of a water-soluble chitosan derivative with a fiber-reactive group. *Carbohydrate Research*, *339*(2), 313-319.

Lin, S., Huang, R., Cheng, Y., Liu, J., Lau, B. L. T., & Wiesner, M. R. (2013). Silver nanoparticle-alginate composite beads for point-of-use drinking water disinfection. *Water Research*, *47*(12), 3959-3965.

Lin, Y.-S. E., Vidic, R. D., Stout, J. E., & Yu, V. L. (1996). Individual and combined effects of copper and silver ions on inactivation of< i> Legionella pneumophila</i>. *Water Research, 30*(8), 1905-1913.

Liu, C., Bai, R., & Nan, L. Sodium Tripolyphosphate (TPP) Crosslinked Chitosan Membranes and Application in Humic Acid Removal.

Liu, N., Chen, X.-G., Park, H.-J., Liu, C.-G., Liu, C.-S., Meng, X.-H., & Yu, L.-J. (2006). Effect of MW and concentration of chitosan on antibacterial activity of< i> Escherichia coli</i>. *Carbohydrate Polymers, 64*(1), 60-65.

Liu, R., Huang, X., Chen, L., Wen, X., & Qian, Y. (2005). Operational performance of a submerged membrane bioreactor for reclamation of bath wastewater. *Process Biochemistry, 40*(1), 125-130.

Liu, S., Butler, D., Memon, F. A., Makropoulos, C., Avery, L., & Jefferson, B. (2010). Impacts of residence time during storage on potential of water saving for grey water recycling system. *Water Research, 44*(1), 267-277.

Lu, D., Xiao, C., & Xu, S. (2009). Starch-based completely biodegradable polymer materials. *Express Polym Lett, 3*(6), 366-375.

Madihally, S. V., & Matthew, H. W. (1999). Porous chitosan scaffolds for tissue engineering. *Biomaterials, 20*(12), 1133-1142.

Massoud, M. A., Tarhini, A., & Nasr, J. A. (2009). Decentralized approaches to wastewater treatment and management: applicability in developing countries. *Journal of Environmental Management, 90*(1), 652-659.

Masuelli, M., Marchese, J., & Ochoa, N. A. (2009). SPC/PVDF membranes for emulsified oily wastewater treatment. *Journal of Membrane Science, 326*(2), 688-693.

Mehrabzadeh, M., & Rezaie, D. (2002). Impact modification of polyacetal by thermoplastic elastomer polyurethane. *Journal of applied polymer science, 84*(14), 2573-2582.

Mehta, S., & Gaur, J. (2005). Use of algae for removing heavy metal ions from wastewater: progress and prospects. *Critical Reviews in Biotechnology, 25*(3), 113-152.

Mello, R. S., Bedendo, G. C., Nome, F., Fiedler, H. D., & Laranjeira, M. C. (2006). Preparation of chitosan membranes for filtration and concentration of compounds under high pressure process. *Polymer Bulletin, 56*(4-5), 447-454.

Memon, F. A., Zheng, Z., Butler, D., Shirley-Smith, C., Lui, S., Makropoulos, C., & Avery, L. (2007). Life Cycle Impact Assessment of Greywater Recycling Technologies for New Developments. *Environmental Monitoring and Assessment, 129*(1), 27-35.

Méricq, J. P., Mendret, J., Brosillon, S., & Faur, C. (2015). High performance PVDF-TiO2 membranes for water treatment. *Chemical Engineering Science, 123*, 283-291.

Merz, C., Scheumann, R., El Hamouri, B., & Kraume, M. (2007). Membrane bioreactor technology for the treatment of greywater from a sports and leisure club. *Desalination, 215*(1), 37-43.

Meyssami, B., & Kasaeian, A. B. (2005). Use of coagulants in treatment of olive oil wastewater model solutions by induced air flotation. *Bioresource Technology, 96*(3), 303-307.

MHC. (2010). Canadian Guidelines for Domestic Reclaimed Water for Use in Toilet and Urinal Flushing. In M. o. H. Canada (Ed.). Ottawa, Ontario.

Millward, D. J. (1999). The nutritional value of plant-based diets in relation to human amino acid and protein requirements. *Proceedings of the Nutrition Society, 58*(2), 249-260.

Mohammad, T. A., Megat Johari, M. M. N., & Abdul Ghani, L. (2009). Preliminary evaluation of a hydrophilic microfiltration membrane in treating high strength wastewater. *Desalination and Water Treatment, 10*(1-3), 272-280.

Moon, G. Y., Pal, R., & Huang, R. Y. (1999). Novel two-ply composite membranes of chitosan and sodium alginate for the pervaporation dehydration of isopropanol and ethanol. *Journal of Membrane Science, 156*(1), 17-27.

Moore, C. J. (2008). Synthetic polymers in the marine environment: A rapidly increasing, long-term threat. *Environmental Research, 108*(2), 131-139.

Mutamim, N. S. A., Noor, Z. Z., Hassan, M. A. A., Yuniarto, A., & Olsson, G. (2013). Membrane bioreactor: applications and limitations in treating high strength industrial wastewater. *Chemical Engineering Journal, 225*, 109-119.

Naylor, T., Moglia, M., Grant, A. L., & Sharma, A. K. (2012). Self-reported judgements of management and governance issues in stormwater and greywater systems. *Journal of Cleaner Production, 29–30*, 144-150.

Ngah, W., & Fatinathan, S. (2010). Adsorption characterization of Pb (II) and Cu (II) ions onto chitosan-tripolyphosphate beads: Kinetic, equilibrium and thermodynamic studies. *Journal of Environmental Management, 91*(4), 958-969.

Ngah, W. S. W., Ab Ghani, S., & Kamari, A. (2005). Adsorption behaviour of Fe(II) and Fe(III) ions in aqueous solution on chitosan and cross-linked chitosan beads. *Bioresource Technology, 96*(4), 443-450.

Nguyen, L. N., Hai, F. I., Kang, J., Price, W. E., & Nghiem, L. D. (2012). Removal of trace organic contaminants by a membrane bioreactor–granular activated carbon (MBR–GAC) system. *Bioresource Technology, 113*(0), 169-173.

Ní Mhurchú, J. (2008). Dead-end and crossflow microfiltration of yeast and bentonite suspensions: experimental and modelling studies incorporating the use of artificial neural networks. Dublin City University.

Nitiyanontakit, S., Varanusupakul, P., & Miró, M. (2013). Hybrid flow analyzer for automatic hollow-fiber-assisted ionic liquid-based liquid-phase microextraction with in-line membrane regeneration. *Analytical and bioanalytical chemistry, 405*(10), 3279-3288.

Nolde, E. (2005). Greywater recycling systems in Germany results, experiences and guidelines. *Water Science & Technology, 51*(10), 203-210.

Norton, J. W. (2009). Decentralized Systems. *Water Environment Research, 81*(10), 1440-1450.

O'Neill, C., Hawkes, F. R., Hawkes, D. L., Esteves, S., & Wilcox, S. J. (2000). Anaerobic–aerobic biotreatment of simulated textile effluent containing varied ratios of starch and azo dye. *Water Research, 34*(8), 2355-2361.

Oh, K. S., Poh, P. E., Chong, M. N., Chan, E. S., Lau, E. V., & Saint, C. P. (2016). Bathroom greywater recycling using polyelectrolyte-complex bilayer membrane: Advanced study of membrane structure and treatment efficiency. *Carbohydrate Polymers, 148*, 161-170.

Ong, S., Hu, J., Lee, L., Ng, W., & Song, L. (2002). Packed bed columns for high rate nitrogen and carbon removals. *Water science and technology, 46*(11-12), 57-62.

Otis, R. J., Wright, A., & Bakalian, A. (1996). Guidlnies for the Design of Simplified Sewers, in:. In D. M. (Ed.) (Ed.). *Low-Cost Sewerage*: Chichester: John Wiley & Sons.

Pandey, J. K., Raghunatha Reddy, K., Pratheep Kumar, A., & Singh, R. P. (2005). An overview on the degradability of polymer nanocomposites. *Polymer Degradation and Stability, 88*(2), 234-250.

Paris, S., & Schlapp, C. (2010). Greywater recycling in Vietnam — Application of the HUBER MBR process. *Desalination, 250*(3), 1027-1030.

Parvin, F., Rahman, M., Islam, J. M., Khan, M. A., & Saadat, A. (2010). Preparation and characterization of starch/PVA blend for biodegradable packaging material. *Advanced Materials Research, 123*, 351-354.

Pham, T. T. N., Ngo, H. H., Guo, W., Dang, H. P. D., Mainali, B., Johnston, A., & Listowski, A. (2011). Responses of community to the possible use of recycled water for washing machines: A case study in Sydney, Australia. *Resources, Conservation and Recycling, 55*(5), 535-540.

Phan, N. H., Rio, S., Faur, C., Le Coq, L., Le Cloirec, P., & Nguyen, T. H. (2006). Production of fibrous activated carbons from natural cellulose (jute, coconut) fibers for water treatment applications. *Carbon, 44*(12), 2569-2577.

Piccinno, F., Hischier, R., Seeger, S., & Som, C. (2015). Life cycle assessment of a new technology to extract, functionalize and orient cellulose nanofibers from food waste. *ACS Sustainable Chemistry & Engineering, 3*(6), 1047-1055.

Pidou, M., Avery, L., Stephenson, T., Jeffrey, P., Parsons, S. A., Liu, S., Memon, F. A., & Jefferson, B. (2008). Chemical solutions for greywater recycling. *Chemosphere, 71*(1), 147-155.

Pidou, M., Memon, F. A., Stephenson, T., Jefferson, B., & Jeffrey, P. (2007). Greywater recycling: treatment options and applications. *Proceedings of the ICE-Engineering Sustainability, 160*(3), 119-131.

Pillai, C. K. S., Paul, W., & Sharma, C. P. (2009). Chitin and chitosan polymers: Chemistry, solubility and fiber formation. *Progress in Polymer Science, 34*(7), 641-678.

Ping, L., Juan, L., Changzhu, W., Qingsheng, W., & Jian, L. (2005). Synergistic antibacterial effects of β-lactam antibiotic combined with silver nanoparticles. *Nanotechnology, 16*(9), 1912.

Poletto, P., Duarte, J., Thürmer, M. B., Santos, V. d., & Zeni, M. (2011). Characterization of Polyamide 66 membranes prepared by phase inversion using formic acid and hydrochloric acid such as solvents. *Materials Research, 14*(4), 547-551.

Pourzahedi, L., & Eckelman, M. J. (2015). Comparative life cycle assessment of silver nanoparticle synthesis routes. *Environmental Science: Nano, 2*(4), 361-369.

Prabhu, S., & Poulose, E. K. (2012). Silver nanoparticles: mechanism of antimicrobial action, synthesis, medical applications, and toxicity effects. *International Nano Letters, 2*(1), 1-10.

Pramanik, B., Fatihah, S., Shahrom, Z., & Ahmed, E. (2012). Biological aerated filters (BAFs) for carbon and nitrogen removal: a review. *Journal of Engineering Science and Technology, 7*(4), 428-446.

Prathapar, S. A., Jamrah, A., Ahmed, M., Al Adawi, S., Al Sidairi, S., & Al Harassi, A. (2005). Overcoming constraints in treated greywater reuse in Oman. *Desalination, 186*(1–3), 177-186.

Qi, L., Xu, Z., Jiang, X., Hu, C., & Zou, X. (2004). Preparation and antibacterial activity of chitosan nanoparticles. *Carbohydrate Research, 339*(16), 2693-2700.

Rai, M., Yadav, A., & Gade, A. (2009). Silver nanoparticles as a new generation of antimicrobials. *Biotechnology Advances, 27*(1), 76-83.

Ramona, G., Green, M., Semiat, R., & Dosoretz, C. (2004). Low strength graywater characterization and treatmentby direct membrane filtration. *Desalination, 170*(3), 241-250.

Regiel, A., Irusta, S., Kyzioł, A., Arruebo, M., & Santamaria, J. (2012). Preparation and characterization of chitosan–silver nanocomposite films and their antibacterial activity against Staphylococcus aureus. *Nanotechnology, 24*(1), 015101.

Regiel, A., Irusta, S., Kyzioł, A., Arruebo, M., & Santamaria, J. (2013). Preparation and characterization of chitosan–silver nanocomposite films and their antibacterial activity against Staphylococcus aureus. *Nanotechnology, 24*(1), 015101.

Ren, J., & Wang, R. (2008). Preparation of polymeric membranes. *Membrane and desalination technologies* (pp. 47-100): Springer.

Rhim, J.-W. (2004). Physical and mechanical properties of water resistant sodium alginate films. *LWT - Food Science and Technology, 37*(3), 323-330.

Richardson, S. D., & Postigo, C. (2012). Drinking water disinfection by-products. *Emerging Organic Contaminants and Human Health* (pp. 93-137): Springer.

Rosenberger, S., Krüger, U., Witzig, R., Manz, W., Szewzyk, U., & Kraume, M. (2002). Performance of a bioreactor with submerged membranes for aerobic treatment of municipal waste water. *Water Research, 36*(2), 413-420.

Roy, D., Semsarilar, M., Guthrie, J. T., & Perrier, S. (2009). Cellulose modification by polymer grafting: a review. *Chemical Society Reviews, 38*(7), 2046-2064.

Ryan, A. M., Spash, C. L., & Measham, T. G. (2009). Socio-economic and psychological predictors of domestic greywater and rainwater collection: Evidence from Australia. *Journal of Hydrology, 379*(1), 164-171.

Sæther, H. V., Holme, H. K., Maurstad, G., Smidsrød, O., & Stokke, B. T. (2008). Polyelectrolyte complex formation using alginate and chitosan. *Carbohydrate Polymers, 74*(4), 813-821.

Salahi, A., Abbasi, M., & Mohammadi, T. (2010). Permeate flux decline during UF of oily wastewater: Experimental and modeling. *Desalination, 251*(1), 153-160.

Schiffman, J. D., & Schauer, C. L. (2007). Cross-linking chitosan nanofibers. *Biomacromolecules, 8*(2), 594-601.

Semikina Anna, L., & Skulacher Vladimr, P. (1990). Submicromolar Ag+ increases passive Na+ permeability and inhibits the respiration supported formation of Na+ gradient in Bacillus FTU vesicles. Elsevier Science publishers (biomedical division) FEBS.

Seyfarth, F., Schliemann, S., Elsner, P., & Hipler, U. C. (2008). Antifungal effect of high- and low-molecular-weight chitosan hydrochloride, carboxymethyl chitosan, chitosan oligosaccharide and N-

acetyl-d-glucosamine against Candida albicans, Candida krusei and Candida glabrata. *International Journal of Pharmaceutics, 353*(1–2), 139-148.

Shahriari, T., & NabiBidhendi, G. (2012). Starch Efficiency in Water Turbidity Removal. *Asian Journal of Natural & Applied Sciences, 1*(2).

Sharma, S., Sanpui, P., Chattopadhyay, A., & Ghosh, S. S. (2012a). Fabrication of antibacterial silver nanoparticle-sodium alginate-chitosan composite films. *Rsc Advances, 2*(13), 5837-5843.

Sharma, S., Sanpui, P., Chattopadhyay, A., & Ghosh, S. S. (2012b). Fabrication of antibacterial silver nanoparticle—sodium alginate–chitosan composite films. *Rsc Advances, 2*(13), 5837-5843.

Shi, L., Günther, S., Hübschmann, T., Wick, L. Y., Harms, H., & Müller, S. (2007). Limits of propidium iodide as a cell viability indicator for environmental bacteria. *Cytometry Part A, 71*(8), 592-598.

Shirazi, M., Kargari, A., Bazgir, S., Tabatabaei, M., Shirazi, M., Abdullah, M. S., Matsuura, T., & Ismail, A. F. (2013). Characterization of electrospun polystyrene membrane for treatment of biodiesel's water-washing effluent using atomic force microscopy. *Desalination, 329*, 1-8.

Shrestha, R., Joshi, D. R., Gopali, J., & Piya, S. (2009). Oligodynamic action of silver, copper and brass on enteric bacteria isolated from water of Kathmandu Valley. *Nepal Journal of Science and Technology, 10*, 189-193.

Siddaramaiah, & Mruthyunjaya Swamy, T. (2007). Studies on miscibility of sodium alginate/polyethylene glycol blends. *Journal of Macromolecular Science, Part A: Pure and Applied Chemistry, 44*(3), 321-327.

Sionkowska, A. (2011). Current research on the blends of natural and synthetic polymers as new biomaterials: Review. *Progress in Polymer Science, 36*(9), 1254-1276.

Siracusa, V., Rocculi, P., Romani, S., & Dalla Rosa, M. (2008). Biodegradable polymers for food packaging: a review. *Trends in Food Science & Technology, 19*(12), 634-643.

Skouteris, G., Hermosilla, D., López, P., Negro, C., & Blanco, Á. (2012). Anaerobic membrane bioreactors for wastewater treatment: a review. *Chemical Engineering Journal, 198*, 138-148.

Sondi, I., & Salopek-Sondi, B. (2004). Silver nanoparticles as antimicrobial agent: a case study on E. coli as a model for Gram-negative bacteria. *Journal of Colloid and Interface Science, 275*(1), 177-182.

Stiefel, P., Schmidt-Emrich, S., Maniura-Weber, K., & Ren, Q. (2015). Critical aspects of using bacterial cell viability assays with the fluorophores SYTO9 and propidium iodide. *BMC microbiology, 15*(1), 1.

Svensson, A., Nicklasson, E., Harrah, T., Panilaitis, B., Kaplan, D. L., Brittberg, M., & Gatenholm, P. (2005). Bacterial cellulose as a potential scaffold for tissue engineering of cartilage. *Biomaterials, 26*(4), 419-431.

Swatloski, R. P., Spear, S. K., Holbrey, J. D., & Rogers, R. D. (2002). Dissolution of Cellose with Ionic Liquids. *Journal of the American Chemical Society, 124*(18), 4974-4975.

Syarikat Bekalan Air Selangor Sdn. Bhd. (2017). Water Tariff. Malaysia.

Tchobanoglous, G., & Burton, F. L. (1991). Wastewater engineering. *Management, 7*, 1-4.

Tchobanoglous, G., L. Burton, F., & Stensel, H. D. (2004). *Wastewater Engineering, Treatment and reuse*. Metcalf & Eddy, Inc (New York): McGraw-Hill Education

Tenaga Nasional Berhad. (2017). Tariff rate. (Vol. 2017). Malaysia.

Thakur, S., & Chauhan, M. (2013). Grey water recycling.

The Engineering Toolbox. (2016). Specific Heat of common Substances.

US EPA. (2004). Guidelines for Water Reuse. In U. S. E. P. Agency (Ed.). *EPA/625/R-04/108*. Washington, DC

US EPA. (2016). Nutrient Policy and Data. *Causes and Prevention* (Vol. 2016).

van Voorthuizen, E. M., Zwijnenburg, A., & Wessling, M. (2005). Nutrient removal by NF and RO membranes in a decentralized sanitation system. *Water Research, 39*(15), 3657-3667.

Vasilenko, A. P., Guzenko, N. V., Nosach, L. V., & Voronin, E. F. (2010). Effects of modification of highly disperse silica with polyvinylpyrollidone on gelatin adsorption. *Pharmaceutical Chemistry Journal, 44*(2), 81-84.

Verma, A., & Verma, A. (2013). Polyelectrolyte complex-an overview. *International Journal of Pharmaceutical Sciences and Research, 4*(5), 1684.

Vimala, K., Mohan, Y. M., Sivudu, K., Varaprasad, K., Ravindra, S., Reddy, N. N., Padma, Y., Sreedhar, B., & MohanaRaju, K. (2010). Fabrication of porous chitosan films impregnated with silver nanoparticles: a facile approach for superior antibacterial application. *Colloids and Surfaces B: Biointerfaces, 76*(1), 248-258.

Wang, B.-L., Liu, X.-S., Ji, Y., Ren, K.-F., & Ji, J. (2012). Fast and long-acting antibacterial properties of chitosan-Ag/polyvinylpyrrolidone nanocomposite films. *Carbohydrate Polymers, 90*(1), 8-15.

Wang, L. K. (2011). *Membrane and desalination technologies*. Springer.

Wang, X., Chen, R., Zhang, Q., & Li, K. (2008). Optimized plan of centralized and decentralized wastewater reuse systems for housing development in the urban area of Xi'an, China. *Water science and technology, 58*(5), 969-975.

Wang, Z., & Pinnavaia, T. J. (1998). Nanolayer Reinforcement of Elastomeric Polyurethane. *Chemistry of Materials, 10*(12), 3769-3771.

Water Filter Malaysia. (2017). Water filter malaysia- Outdoor and Indoor filter. (Vol. 2017).

Wei, D., Sun, W., Qian, W., Ye, Y., & Ma, X. (2009). The synthesis of chitosan-based silver nanoparticles and their antibacterial activity. *Carbohydrate Research, 344*(17), 2375-2382.

Widiastuti, N., Wu, H., Ang, M., & Zhang, D.-k. (2008). The potential application of natural zeolite for greywater treatment. *Desalination, 218*(1–3), 271-280.

Yadollahi, M., Farhoudian, S., & Namazi, H. (2015). One-pot synthesis of antibacterial chitosan/silver bio-nanocomposite hydrogel beads as drug delivery systems. *International journal of biological macromolecules, 79*, 37-43.

Young Moon, G., Pal, R., & Huang, R. Y. (1999). Novel two-ply composite membranes of chitosan and sodium alginate for the pervaporation dehydration of isopropanol and ethanol. *Journal of Membrane Science, 156*(1), 17-27.

Yu, D., Wu, L. L., Wang, J. F., Tao, Y. W., Shen, Y. T., Liang, B. Y., & Wang, H. (2013). Preparation of β-Cyclodextrin/Chitosan Membranes and its Application in the Wastewater Treatment of Acid Dyes. *Advanced Materials Research, 726*, 2558-2562.

Yuan, H., Nie, J., Gu, L., & Zhu, N. (2013). An effective method for decentralized wastewater treatment: addition of polyurethane foam to subsurface wastewater infiltration system. *Desalination and Water Treatment*(ahead-of-print), 1-9.

Yuan, Y., & Lee, T. R. (2013). Contact angle and wetting properties. *Surface science techniques* (pp. 3-34): Springer.

Zeng, M., & Fang, Z. (2004). Preparation of sub-micrometer porous membrane from chitosan/polyethylene glycol semi-IPN. *Journal of Membrane Science, 245*(1–2), 95-102.

Zeng, M., Fang, Z., & Xu, C. (2004). Novel method of preparing microporous membrane by selective dissolution of chitosan/polyethylene glycol blend membrane. *Journal of applied polymer science, 91*(5), 2840-2847.

Zhang, M., Li, X. H., Gong, Y. D., Zhao, N. M., & Zhang, X. F. (2002). Properties and biocompatibility of chitosan films modified by blending with PEG. *Biomaterials, 23*(13), 2641-2648.

Zhang, Q., Zhang, S., Zhang, Y., Hu, X., & Chen, Y. (2013). Preparation of PVDF/PVC composite membrane for wastewater purification. *Desalination and Water Treatment, 51*(19-21), 3854-3857.

Zhen, H., Xiaoxu, Y., Xi, P., Yulong, Z., Meifen, F., & Qiang, Z. (2010). Thermal degradation study of sodium alginate-zeolite 4A composites. *Proc. 17th IAPRI World Conf. on Packag* (pp. 406-409).

Zhou, Y., Zhao, H., Bai, H., Zhang, L., & Tang, H. (2012). Papermaking Effluent Treatment: A New Cellulose Nanocrystalline/Polysulfone Composite Membrane. *Procedia Environmental Sciences, 16*(0), 145-151.

Appendix

A1. Phylogenetic trees for strian S1 and strain S2 mentioned in chapter 4, section 4.1.2 viiii.

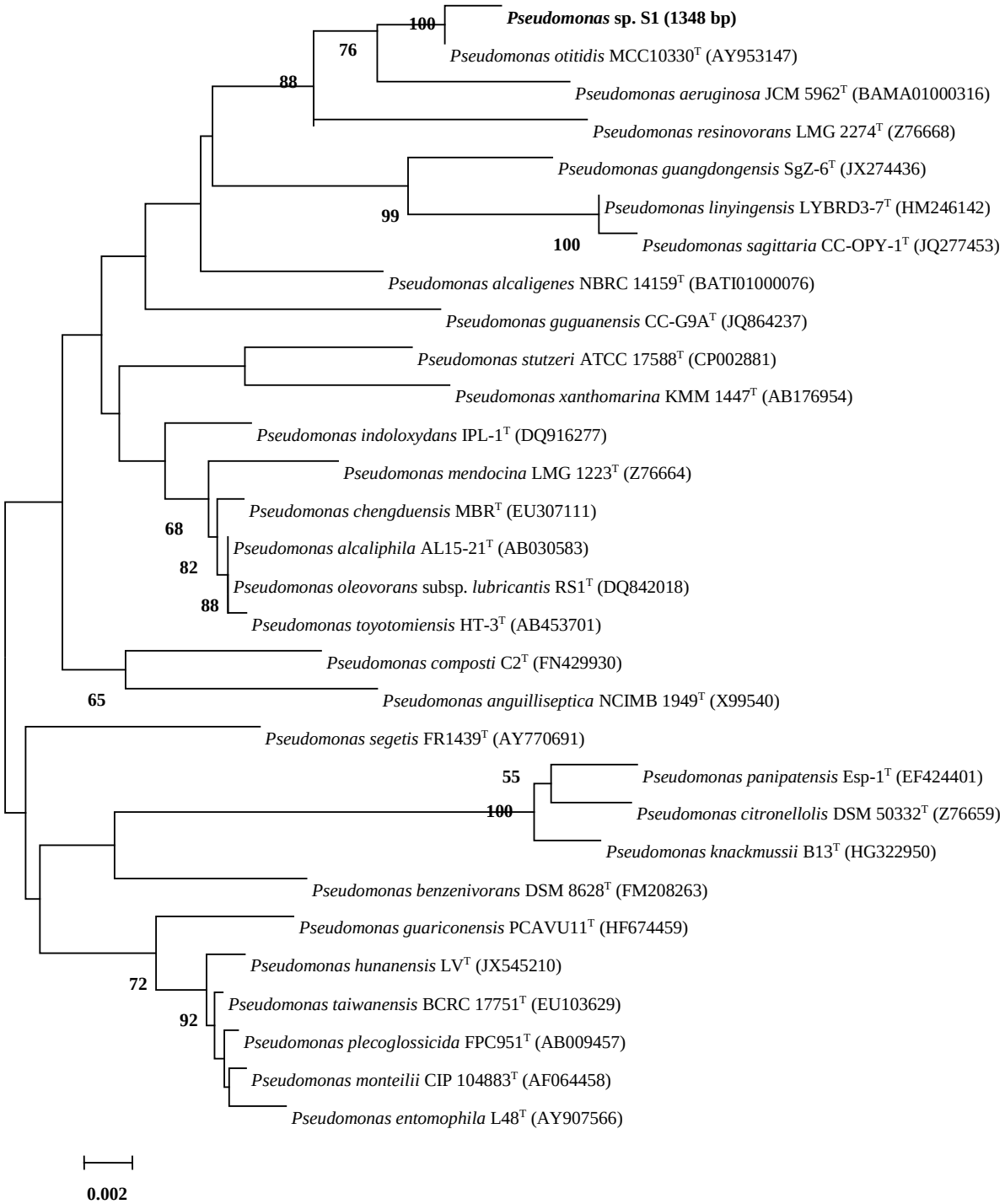

Figure A1. Neighbour-joining tree based on 16S rRNA sequences showing relationship between strain S1 and representatives of some other related taxa. Bootstrap values (>50%) based on 1000 resampled datasets are shown at branch nodes. Bar, 2 substitutions per 1000 nucleotide positions.

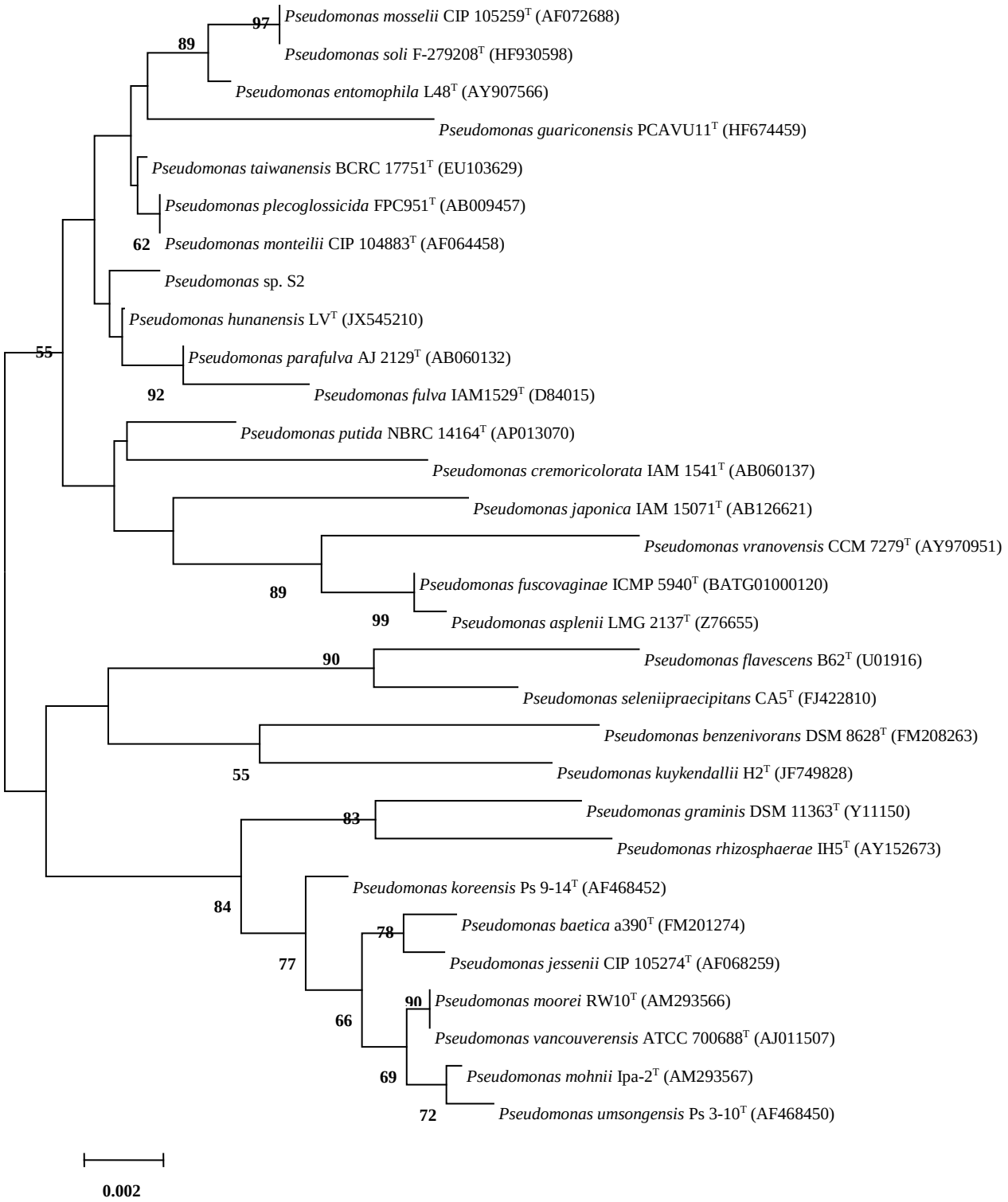

Figure A2. Neighbour-joining tree based on 16S rRNA sequences showing relationship between strain S2 and representatives of some other related taxa. Bootstrap values (>50%) based on 1000 resampled datasets are shown at branch nodes. Bar, 2 substitutions per 1000

Sample calculations

A2. Membrane swelling ratio

Table A. 1. 2AP1CP membrane weigh immersed in UP water

Duration (sec)	Weigh (g)
0	0.0048
5	0.0162
10	0.0168
15	0.0168
20	0.017
25	0.0172
30	0.017
60	0.0174
90.0	0.0176
120	0.0177

Swelling ratio of first 5 mins (%) = $\frac{W_{wet}-W_{dry}}{W_{dry}} \times 100$

$= \frac{0.0162-0.0048}{0.0048} \times 100$

= 237.5%

A3. Equilibrium Moisture Content

Table A. 2. Weigh of 1CP membrane after 24 hours immersed in UP water

Duration (hour)	1CP
0	0.0246
24	0.1006

EMC (%) = $(W_{wet} - W_{dry}) / W_{wet} \times 100$

$= \frac{0.1006 - 0.0246}{0.1006} \times 100$

= 75.5%

A4. Tensile strength

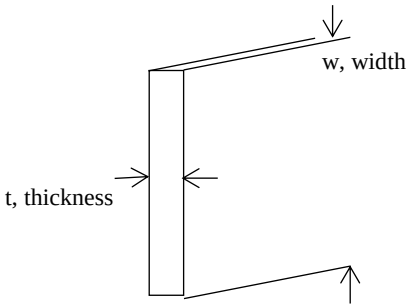

Figure A 3. Cross-section of membrane sample

Tensile strength (MPa) = $\frac{F_l}{A}$ = $\frac{F_l}{t \times \mathrm{w}}$

= 415.5 N/ (0.025 m ×0.0004 m)

= 41.55 MPa

A5. Water flux

For instance, at 3 bar (g) pressure, 2AP1CP membrane produced 26.18 g of UP water at 30 mins.

Effective area, A_e of dead-end stirred cell filtration unit = 0.00146 m^2

Flux, J ($^{g}/_{m^2hr}$) = $M_{permeate} / (A_e \times t)$

= 26.85 g / (0.00146 m^2 × 0.5 hour)

= 36777.4 $^{g}/_{m^2hr}$

A6. MWCO of membrane

Table A. 3. PEGs rejection by 2AP1CP PCBM

PEG (Da)	Initial conc. (ppm)	Final conc. (ppm)	Removal (%)
1000	57.787	52.645	8.90
2000	60.33	14.59	75.82
4000	52.20	0.11	99.80
6000	54.00	0.00	100.00
10000	50.17	0.00	100.00

Rejection (%) = $\frac{C_i - C_f}{C_i} \times 100$

= $\frac{57.787 - 52.645}{57.787} \times 100$

= 8.9%

By interpolating between PEG 2000 and PEG 4000 to obtain the MWCO at 95% PEG removal.

MWCO = 4000 - [($\frac{4000-2000}{99.8-75.82}$) × (99.8 – 95)]

The MWCO of 2AP1CP was found to be 3352 Da

A7. Normalized flux and flux decline percentage

Greywater flux of 2AP1CP = 29421.92 $^{g}/_{m^2hr}$

UP water flux at 3 bar (g) = 36777.4 $^{g}/_{m^2hr}$

Normalized flux = J/ J_o

= 29421.92 $^{g}/_{m^2hr}$ / 36777.4 $^{g}/_{m^2hr}$

= 0.8

Flux decline percentage = $(1 – J/ J_o) \times 100\%$

= $(1 – 0.8) \times 100\%$

= 20%

A8. BOD_5

Table A. 4 Dissolved oxygen reading for greywater sample

Dissolved oxygen value	Day 1 (ppm)	8.17
	Day 5 (ppm)	5.15

4 mL of greywater sample was pipetted into the 300 mL BOD bottle,

BOD_5 of greywater sample = $\frac{DO_i - DO_f}{P}$

= $\frac{8.17-5.15}{4/300}$

= 226.5 ppm

A9. Treatment efficiency/ Removal percentage

Table A. 5. Characteristic of greywater and treated greywater

	Unit	Greywater	Treated greywater
pH		6.6	7.1
Turbidity	NTU	188.8	0.2
TSS	ppm	199.6	0.0
COD	ppm	550.0	94.5
BOD_5	ppm	228.3	54.0
E. coli	CFU mL^{-1}	2840.0	0.0
Other coliform	CFU mL^{-1}	5223.3	0.0

Treatment efficiency/ Removal percentage (%) = $\frac{C_i - C_f}{C_i} \times 100$

Turbidity removal (%) = $\frac{C_i - C_f}{C_i} \times 100$

$= \frac{188.8 - 0.2}{188.8} \times 100$

= 99.9%

A10. Log Removal value

Based on Table A. 5,

LRV of *E. coli* = log (2840) – 0

= 3.45-log

LRV of *other coliforms* = log (5223) – 0

= 3.71-log

A11. Sample calculation for functional units

Table A. 6. Materials require to fabricate 1.5 AgNP PCBM and nylon 66 membrane

Membrane	Polyamide (g)	HCl (g)	CS (g)	Alg (g)	Ac (g)	NaOH (g)	AgNP (g)	PEG (g)
Nylon 66	67.1	124.1	-	-	-	-	-	-
AgNP PCBM	-	-	94.1	47.4	188.2	141.0	0.013	141.1

Nylon 66

The membranes materials were first assumed to be fabricated according to the membrane area of the decentralized greywater treatment unit.

Membrane area = 0.0113 m^2

Thickness of the nylon 66 were in accordance to the Poletto et al. (2011), = 0.0003 m

Thus, volume of polyamide needed to cast = 0.0113 m^2 × 0.0003 m

= 3.39×10^{-6} m^3 = 3.393 mL

Concentration of the polyamide solution were 20 wt% and 37% HCl ,

Thus, polyamide needed = 3.393 mL × 20 /100

= 0.6786 g needed to make 0.0113 m^2 membrane

HCl needed = 3.393 mL × 37 /100

= 1.26 g needed to make 0.0113 m^2 membrane

As a result, to scale up the membrane to the FU, 1.12 m^2 of nylon 66 is needed for the production of 17.9 L of UP water, thus,

Polyamide needed = 0.6786 g × 1.12 m^2/0.0113 m^2

= 67.13 g

HCl needed = 1.26 g × 1.12 m^2/0.0113 m^2

= 124.18 g

1.5 AgNP PCBM

For 1.5 AgNP PCBM, it was assumed to fabricate with the size of 0.01131 m^2.

The materials needed are:

CS/ PEG 1wt% = 106.4 mL

Alg/ PEG 2wt% = 26.6 mL

AgNP 0.02 mg/mL = 7.5 mL

NaOH, 2wt% = 79.76 mL

Therefore, CS needed to fabricate 0.0113 m^2 membrane = 106.4 mL × 1 g/ 100 mL

= 1.064 g

Alg needed to fabricate 0.0113 m^2 membrane = 26.6 mL × 2 g/ 100 mL

= 0.532 g

AgNP needed to fabricate 0.0113 m^2 membrane = 7.5 mL × 0.02 mg/mL

= 0.00015 g

NaOH needed to fabricate 0.0113 m^2 membrane = 79.76 mL × 2 g/ 100 mL

= 1.60 g

PEG needed to fabricate 0.0113 m^2 membrane = 1.064 g + 0.532 g

= 1.60 g

Ac needed to fabricate 0.0113 m^2 membrane = 106.4 mL× 2 g/ 100 mL

= 2.128 g

Thus, in order to fabricate 1.5 AgNP PCBM per FU, 1m^2 of 1.5 AgNP PCBM is needed for the production of 17.9 L of UP water, thus

CS needed = 1.064 g × 1 m^2/ 0.0113 m^2

= 94.1 g

Alg needed = 0.532 g × 1 m^2/ 0.0113 m^2

= 47.4 g

AgNP needed = 0.00015 g × 1 m^2/ 0.0113 m^2

= 0.013 g

NaOH needed = 1.60 g × 1 m^2/ 0.0113 m^2

= 141.0 g

Ac needed = 2.128 g × 1 m^2/ 0.0113 m^2

= 188.2 g

PEG needed = 1.60 g × 1 m^2/ 0.0113 m^2

= 141.0 g